

Syracuse University

SURFACE

Dissertations - ALL

SURFACE

1-1-2015

Controlling Microbial Multicellular Behaviors With Saccharide Derivatives

NISCHAL SINGH
Syracuse University

Follow this and additional works at: <https://surface.syr.edu/etd>



Part of the [Physical Sciences and Mathematics Commons](#)

Recommended Citation

SINGH, NISCHAL, "Controlling Microbial Multicellular Behaviors With Saccharide Derivatives" (2015).
Dissertations - ALL. 317.
<https://surface.syr.edu/etd/317>

This Dissertation is brought to you for free and open access by the SURFACE at SURFACE. It has been accepted for inclusion in Dissertations - ALL by an authorized administrator of SURFACE. For more information, please contact surface@syr.edu.

Abstract

Microbial multicellular behaviors like biofilm formation and swarming motility are known to increase their tolerance against antimicrobials. From microbial standpoint, nonmicrobicidal agents that do not impede growth are tolerable and therefore, there is a lower propensity to develop resistance against such agents as compared to microbicidal ones (antibiotics). This study describes a new antibiofilm approach of using nonmicrobicidal saccharide derivatives for controlling the multicellular behaviors of gram-negative bacteria, *Pseudomonas aeruginosa* and fungus, *Candida albicans*.

Pseudomonas aeruginosa is known to secrete rhamnolipids, a class of biosurfactants that plays an important role in maintaining the architecture of its biofilm and promoting its swarming motility. Here we show the ability of certain synthetic nonmicrobicidal disaccharide derivatives (DSDs) to mimic the biofunctions of rhamnolipids. The *rhlA* mutant of *P. aeruginosa* is incapable of synthesizing rhamnolipids and also unable to swarm on semi-solid agar gel. When the natural ligands, rhamnolipids were externally added into the semi-solid agar gel in a concentration dependent manner, the swarming of the *rhlA* mutant reactivated at lower concentrations (10 μM) and then at relatively higher concentrations (15 μM), the swarming reactivation was reversed. When some active synthetic DSDs were tested on the *rhlA* mutant, the bacterial swarming first reactivated and then the activation reversed at higher DSD concentrations, similar to the effect of externally added rhamnolipids. Previously, a known bacterial signalling molecule has been shown to exhibit a similar concentration dependent activation and then activation reversal for light simulation by *Vibrio fischeri*. Some DSDs having disaccharide stereochemistries (cellobiose or maltose) and a bulky aliphatic tail (3, 7, 11-

trimethyl-dodecanyl) caused swarming reactivation of the *rhlA* mutant at concentrations lower than that caused by the externally added rhamnolipids.

The synthetic nonmicrobicidal DSDs were also very effective at inhibiting the adhesion of *P. aeruginosa* to polystyrene surface, and at inhibiting the bacterial biofilm formation. These DSDs were also potent dispersers of pre-formed biofilm of *P. aeruginosa*. The potent antibiofilm (inhibition and dispersion) activities were observed for those DSDs that possessed a disaccharide (cellobiose or maltose) stereochemistry and a bulky aliphatic chain such as 3, 7, 11-trimethyl-dodecanyl. These potent DSDs had half-maximal inhibitory concentrations for biofilm inhibition (IC₅₀) and dispersion (DC₅₀) comparable to those of known potent antibiofilm agents against *P. aeruginosa*. Gene-reporting assays indicate that the mechanism of action of such DSDs is not via the known *las* or *rhl* quorum sensing systems of *P. aeruginosa* but that the adhesin protein, pilin maybe a likely target of such molecules.

Biofilms formed under natural settings are usually formed by both bacteria and fungus that co-reside in the same microenvironment. Therefore, agents that can prevent mixed biofilms are desirable from a therapeutic standpoint. Despite being nonmicrobicidal to both fungal blastospores and hyphae, the synthetic DSDs were able to inhibit the biofilm formation of fungus *Candida albicans*. Microscopic evaluation showed that most DSDs did not prevent the blastospores-to-hyphae morphogenesis. The DSDs were effective at inhibiting biofilm formation of *Candida albicans* when applied within five minutes of seeding the test surface with fungal cells. Using a surface based assay it was shown that one DSD dramatically reduced the surface adhesion of *Candida albicans* hyphae. The antibiofilm activity of such DSDs against *Candida albicans* is probably due to their ability to prevent hyphae surface adhesion.

Controlling Microbial Multicellular Behaviors With
Saccharide Derivatives

by

Nischal Singh

M. Phil. (Chemistry), Syracuse University, 2011

M.Sc. (Chemistry), University of Mumbai, Mumbai, India, 2008

B.Sc. (Chemistry), University of Mumbai, Mumbai, India 2006

Dissertation

Submitted in partial fulfillment of the requirements for the degree of
Doctor of Philosophy in *Chemistry*

Syracuse University

August 2015

Copyright © Nischal Singh 2015

All Rights Reserved

Acknowledgements

Earnest gratitude to both my PhD advisors, Dr. Yan-Yeung Luk and Dr. Michael B. Sponsler for laying down the path, guiding me through the journey, encouraging me when I failed, applauding me when I met success and believing in my abilities throughout this PhD study. I am grateful to Dr. Luk for much of my scientific discourse, training and learning. Dr. Luk's training has prepared me to face the scientific community on my own. I am grateful to Dr. Sponsler for graciously agreeing to read the contents of this PhD dissertation.

I am grateful to all the committee members, Dr. Melissa Pepling (committee chair), Dr. James Hougland, Dr. Mark Braiman and Dr. Joseph Chaiken who on very short notice agreed to serve on my PhD defense committee. I really appreciate the committee's thoughtful review of this dissertation. Their inputs has improved the overall scientific quality of this dissertation. I also acknowledge the kindness of Dr. Ivan Korendovych and Dr. James Houghland for generously allowing me to use their laboratory space and analytical instruments.

I am indebted to great colleagues both at Luk laboratory, Dr. Gauri S. Shetye, Dr. Nisha Varghese, Dr. Debjyoti Bandopadhyay, Dr. Deepali Prashar and Dr. Sijie Yang and at Sponsler laboratory, Dr. Amanda Lashua and Dr. Andrew Basner who helped me evolve scientifically as well as socially. Heartfelt thanks to my friends and colleagues at Syracuse University including, Raghuvaran Iyer, Arijit Adhikari, Pallavi Gosavi and Dr. Rabeka Alam. Special thanks to Elizabeth Raymond (Korendovych laboratory) for helping me with peptide synthesis.

I am grateful to the staff at SU's Chemistry Office and at The Lillian & Emanuel Slutzker Center for International Services for their constant support and help.

To my best friends back in India, Deepti Potey, Kiran Machi and Devanand Bagdure, thanks for always being around. A special mention of Dr. Nandini Pai (Ex-Chair, Department of Chemistry, Ruparel College, Mumbai) for her constant motivation and guidance.

The most wonderful thing that happened to me during my PhD days was my marriage to my best friend, colleague and my love, Gauri Shetye. Marriage bestowed upon me the love and support of the entire Shetye family. Thanks to my father-in-law, Mr. Shirish Shetye for believing in me. Thank you to my generous and loving mother-in-law, Mrs. Sheetal Shetye for her kindness and her unconditional support. Thanks to my brother-in-law, Mr. Raj Shetye for constantly reminding me that no matter what the situation, life is fulfilled and one should live it to the fullest.

I will never forget the relentless sacrifices, unending love and support that my dad, Mr. Jagjit Singh & my mother, Mrs. Bhupender Kaur have bestowed upon me throughout their life. Dear mom and dad, if I were to relive my childhood again, there is not a thing I would change. Thanks to my elder brother, Mr. Navtej Singh for his endless support and for partly bearing the cost of my undergraduate studies in chemistry. I am grateful to Mrs. Seema Kaur (bhabhi) for always being by my elder brother's side and raising the world's sweetest nephew and niece, Samartej and Shanaiya. My sister, Mrs. Avinashi Singh has shaped me by always believing in my abilities. Dear Avinashi and her daughter, Katyayani, I will always be by your side.

Finally, my beloved wife, Gauri, thank you for being a part of my life since the year 2005. Your companionship is happiness! Thanks to you, I appreciate my work, and enjoy painting, watching movies, listening to music, cooking, eating and travelling. You teach me about culture and tradition. You are the reason, I will continue fighting our life battles for.

Nischal Singh

Table of content	Page
Chapter 1	
Introduction	
1.1 Treating microbial infections - two different approaches.....	1
1.2 Two different kinds of lifestyles that bacteria adopt: Unicellular and multicellular	2
1.3 Sessile and motile multicellular behaviors	3
1.3.1 Formation of biofilm is a developmental process: A sessile group behavior	3
1.3.2 Five stage differentiation of bacterial biofilms.....	4
1.3.3 Numerous medical and industrial problems are associated with formation of biofilms.....	6
1.3.4 Common antibiofilm strategies	8
1.3.4.1 Quorum sensing inhibitors.....	8
1.3.4.2 Bacteriophages that degrade biofilm matrix.....	8
1.3.4.3 Surface modifications can prevent bio-fouling	9
1.3.4.4 Antibiofilm enzymes	9
1.3.4.5 Small molecular chemical dispersers of preformed biofilms	10
1.3.4.6 Physical methods for treating biofilms	10
1.3.5 Swarming on surfaces: A motile group behavior.....	10
1.4 Synopsis of Chapters 2 & 3	11
1.5 Synopsis of Chapter 4	12

Chapter 2

Saccharide Derivatives Modulate the Swarming Motility of *Pseudomonas aeruginosa*

Abstract.....	13
2.1 Introduction.....	14
2.1.1 Types of bacterial motility.....	14
2.1.2. Swarming motility is a multicellular phenomenon.....	16
2.1.3 Understanding the cell-to-cell communication process.....	18
2.1.4 Components of a typical gram negative quorum sensing gene circuitry	21
2.1.5. Swarming in <i>P. aeruginosa</i>	22
2.1.5.1 Swarming in <i>P. aeruginosa</i> requires flagella	23
2.1.5.2 Alteration in gene expression of <i>P. aeruginosa</i> during swarming	24
2.1.5.3 The <i>LasI-LasR</i> and <i>RhlI-RhlR</i> Quorum Sensing Systems of <i>P. aeruginosa</i> are homologous to the <i>LuxI/LuxR</i> system found in <i>Vibrio fischeri</i>	25

2.1.5.4 Quorum sensing regulates synthesis of biosurfactant rhamnolipids	27
2.1.6 Concentration dependent activity reversal phenomenon previously reported for bacterial cell-signaling molecule	32
2.2 Results and discussion	33
2.2.1 Design of synthetic saccharide derivatives library	33
2.2.1. 1 Synthesis of saccharide derivatives (SDs).....	36
2.2.1. 2 Synthesis of oligosaccharide derivative	37
2.2.2. All saccharide derivatives (SDs) were nontoxic to the growth of planktonic bacteria	37
2.2.3 The nonswarming mutant <i>rhlA</i> was used to screen swarming agonists and the wild type <i>P. aeruginosa</i> brought forward the swarming antagonists	39
2.2.4 Disaccharide derivatives and rhamnolipids exhibit dual functions of activating and inhibiting swarming motility of <i>Pseudomonas aeruginosa</i>	41
2.2.5 Disaccharide derivatives and rhamnolipids exhibited "activity reversals" that transitioned from swarm-activating to swarm-inhibiting as the concentration was increased.....	45
2.2.6 Disaccharide derivatives, SF β C (12), SF β M (14) and D β C (4) dominated rhamnolipids at inhibiting the swarming motility of PAO1	51
2.2.7 Competition assays indicated SF β C (12) to be a stronger swarming inhibitor than D β C (4).....	53
2.3 Conclusion	55
2.4 Materials and methods	56

Chapter 3

Disaccharide derivatives Inhibit and Disperse Biofilm of *P. aeruginosa*

Abstract	134
3.1 Introduction.....	135
3.1.1 <i>P. aeruginosa</i> is a prominent pathogen associated with medical bacterial infections	135
3.1.2 Motile and sessile multicellular behaviors in <i>P. aeruginosa</i> are inversely regulated	136
3.1.3 Apart from being critical during swarming, rhamnolipids are important biomolecules secreted by <i>P. aeruginosa</i> during biofilm formation	138
3.1.4 Bacteria employ surface proteins known as adhesins to recognize and bind carbohydrate epitopes found on host cells	139
3.2 Results and Discussion	141
3.2.1 Effect of generic surfactants on biofilm formation	144
3.2.2 Structure-activity relationship (SAR) for biofilm inhibition	145

3.2.3 Antibiofilm ability of certain DSDs were qualitatively assessed by performing a confocal microscopy assay	149
3.2.4 Rhamnolipids antibiofilm activity increases and then decreases with increasing doses exhibiting an “activity reversal”	150
3.2.5 Strong biofilm inhibitors were also good biofilm dispersers	152
3.2.6 The potent DSDs strongly dispersed the preformed biofilm of <i>P. aeruginosa</i> while rhamnolipids could not	153
3.2.7 Some DSDs and even rhamnolipids reduce the initial adhesion of bacteria to a polystyrene surface.....	155
3.2.8 Bioactivities of DSDs depend on structural details	156
3.2.9 A more stringent structural requirement on DSD is needed for controlling biofilm formation than for controlling swarming motility	157
3.2.10 DSDs do not interfere with the known <i>las</i> and <i>rhl</i> quorum sensing circuits of <i>P.aeruginosa</i> ...	159
3.2.11 Competitive biofilm inhibition assay with one DSD and synthetic pili peptide reduced antibiofilm potency of the DSDs	160
3.2.12 Mechanistic understanding	162
3.3 Conclusion	163
3.4 Materials and methods	164

Chapter 4

Synthetic Disaccharide Derivatives Inhibit the Biofilm Formation of *Candida albicans* by Preventing Hyphal Adhesion

Abstract	170
4.1 Introduction.....	171
4.1.1 Biofilm development in <i>Candida albicans</i> involves morphogenesis	171
4.1.2 Farnesol is the key quorum sensing molecule.....	173
4.1.3 Interspecies interactions between fungus and bacteria can be cooperative as well as uncooperative.....	174
4.1.4 Three broad classes of fungicidal agents against <i>Candida albicans</i>	174
4.1.5 Antibiofilm strategies developed so far	175
4.2 Results and Discussions	177
4.2.1 Structural design of disaccharide derivatives (DSDs) selected for biofilm inhibition of <i>Candida albicans</i>	177
4.2.2 None of the DSDs were toxic to the growth of <i>Candida albicans</i> blastospores.....	178

4.2.3 The disaccharide derivatives (DSDs) were not fungicidal	179
4.2.4 Most DSDs did not inhibit <i>Candida albicans</i> hyphae formation	180
4.2.5 DSDs were screened for biofilm inhibition potencies at 170 μ M using a semi-quantitative XTT-dye based assay.....	182
4.2.6 Dose response assays brought forward potent DSDs	183
4.2.7 DSD prevent surface adhesion of <i>Candida albicans</i> hyphae	184
4. 3 Conclusion	187
4.4 Materials and Methods.....	187

Chapter 5

5.1 Future Directions	199
References.....	199

Chapter 1

Figure 1.1 Different stages of biofilm development and dispersion. Inset-Criteria for developing antibiofilm strategies include interfering with one or multiple biofilm developmental stages. [Reprinted with permission from Citation: 6

Chapter 2

Figure 2.1 Bacteria perform both unicellular and multicellular movements. (a) Swarming is multicellular movement of bacteria on a surface; (b) Individual bacteria are able to move in aqueous media by beating their flagella, known as swimming motility; (c) Twitching is a unicellular bacteria movement on a surface that is facilitated by extension of the pili; (d) Gliding movement is also a unicellular movement that proceeds through formation of focal-adhesion points; (e) Sliding is passive movement across the surface that occurs due to the growth of bacterial population. The arrows in the diagram indicates the direction of movement. 15

Figure 2.2 Chemical signals or autoinducers employed by bacteria for cell-to-cell communication process. The figure shows the chemical structure of an autoinducer and the corresponding bacterial species that secretes the signal (a) Example of acyl-homoserine lactone (AHL) based autoinducers used by some Gram-negative bacteria (also known as AI-I); (b) Autoinducing peptides (AIP) deployed by some Gram-positive bacteria to achieve cellular communication; (c) The butyrolactone based autoinducer secreted by the *Streptomyces* species; (d) The borate diester (AI-2) type of autoinducer (AI-II) used during inter-cellular communication by some gram negative bacteria. 20

Figure 2.3 The components and the representation of a typical quorum sensing process performed by Gram-negative bacteria 22

Figure 2.4 Biosynthesis of rhamnolipids by *P. aeruginosa*. The two-component LasI-LasR/RhlI-RhlR quorum sensing circuit of *P. aeruginosa* controls expression of various virulence genes, including biofilms formations, swarming and rhamnolipids biosynthesis 26

Figure 2.5 Swarming pattern of either wild type PA14 or its *rhlA* mutant. Wild type PA14 inoculated on agar plates containing discs of either di-rhamnolipids, monorhamnolipids or HAA (a, b, and c, respectively). Swarm plates containing either dirhamnolipids or monorhamnolipids or HAAs or no agent inoculated with either wild type PA14 (d, e, f and g, respectively) or the *rhlA* mutant (h, i, j and k, respectively) 30

Figure 2.6 (a) Diffusion rate for di-rhamnolipids and HAA on agar plates. (b) Positive concentration gradient of di-rhamnolipids/HAA mainatins tendril pattern 31

Figure 2.7 Dose-response curve for simulation of light production with increasing concentration of acyl homeserine lactone (AHL). Bioluminescence increased over the range 0.003-3 µg/mL and then decreased at higher concentrations.

Figure 2.8. Structures of synthetic saccharide based derivatives that include maltose, cellobiose, lactose, glucose, rhamnose, and β-cyclodextrin stereochemistries; and hydrocarbons derived

from farnesyl and “saturated” farnesyl molecules. The structures of di-rhamnolipid and mono-rhamnolipid are also shown.

Figure 2.9 Growth curve (24 h) of PAO1 with or without agents to confirm that the effects on swarming and biofilm formation are not due to toxic effects. Resultant concentration of each agent within wells ~ 170 μ M. ^aConcentration of agent ~ 110 μ M.....38

Figure 2.10 Images of swarm agar plates inoculated with either PAO1 (Control) or the *rhlA* mutant containing various generic surfactants. (a) Control swarm plate with no surfactants inoculated with PAO1; Swarm plate inoculated with the *rhlA* mutant containing; (b) No agent; (c) D β M (1); (d) DTAC; (e) SDS and (f) C12EG4OH. Concentration of the generic surfactants in the swarm plates ~ 110 μ M..... 40

Figure 2.11 Four different types of swarming motility behaviors exhibited by wild type PAO1 and the *rhlA* mutant on semisolid gel (~0.5 % agar, M8 media) in presence of various DSDs (at ~85 μ M), except for ^aDe β C (2) (160 μ M), and ^bRhamnolipids (30 μ M for PAO1) and (10 μ M for *rhlA*). Controls are without added agents in the gel. Images were taken 24 h after inoculation with bacteria..... 45

Figure 2.12 Semisolid gels (~0.5 % agar) with 0 (no agent) or 85 μ M concentration of De β C (2) or 160 μ M concentration of F β C (11) inoculated at the center with either *wt* PAO1 (row 1) or *rhlA* mutant (row 2). Images were taken 24 h after inoculation with bacteria. 45

Figure 2.13 Images of swarming motilities of the *rhlA* mutant (left) and PAO1 (right) on semisolid gel (~0.5 % agar) containing increasing concentrations of DSDs and rhamnolipids. The concentrations are indicated above the images, and the identities of the agents are shown to the left. Red boxes highlight the swarming patterns that reveal the dominance of DSDs over rhamnolipids at comparable concentrations..... 49

Figure 2.14 Swarm agar plates with additional concentrations of D β C (4) or T β C (5) for their effects on the swarming of the *rhlA* mutant. Both the DSDs caused swarming “activity reversal.....50

Figure 2.15 Plot of the *rhlA* mutant’s swarm area (after 24 h) versus increasing concentrations of rhamnolipids, D β C (4), T β C (5), SF β M (14), D β G (8) and SF β C (12) in the semisolid gel (~ 0.5% agar). Insert shows the curves that had low transition concentrations from swarm-activating to swarm-inhibiting. (Also see Materials and Methods, Figure S1)..... 53

Figure 2.16 Images of the *rhlA* mutant inoculated on semisolid surface (~0.5 % agar) containing 40 μ M of D β C (4) and increasing concentrations of SF β C (12). The images were taken 24 hours after inoculation of the surface with bacteria..... 55

Figure 2S1. Plot of the *rhlA* mutant’s swarm area (after 24 h) versus increasing concentrations of rhamnolipids and SF β M (14) in the semisolid gel (~ 0.5% agar). The experiment was repeated on three different plates. The error bars are obtained from the mean of the three different experiments..... 79

Chapter 3

Figure 3.1 Inverse regulation of swarming and biofilm formation.....	137
Figure 3.2. Structures of synthetic saccharide based derivatives that include maltose, cellobiose, lactose, glucose, rhamnose, and β -cyclodextrin stereochemistries; and hydrocarbons derived from farnesyl and “saturated” farnesyl molecules. The structures of di-rhamnolipid and mono-rhamnolipid are also shown.	143
Figure 3.3 Inhibition of <i>P. aeruginosa</i> (PAO1) biofilm by 110 μ M of generic surfactants	144
Figure 3.4 Biofilm inhibition potencies of DSDs and rhamnolipids quantified by CV-dye based assay.....	149
Figure 3.5 Biofilm inhibition activities of DSDs was also validated qualitatively by a confocal fluorescence based biofilm assay.....	150
Figure 3.6 Disaccharide derivatives' (DSDs) and rhamnolipids' dose-response curves for <i>P. aeruginosa</i> (PAO1) biofilm inhibition.	152
Figure 3.7 Biofilm dispersion potencies of DSDs and rhamnolipids quantified by CV-dye based assay.....	153
Figure 3.8 Disaccharide derivatives' (DSDs) and rhamnolipids' dose-response curves for dispersion of 24-h old <i>P. aeruginosa</i> (PAO1) biofilms.....	154
Figure 3.9 Percent bacterial adhesion inhibition potencies of the various DSDs and rhamnolipids.	156
Figure 3.10 Gene-reporter assay with two reporter strains of <i>Pseudomonas aeruginosa</i> , PAO1/plasI-LVAgfp and PAO1/prhII-LVAgfp, showed that DSDs did not interfere with either the las or the rhl quorum sensing systems.	160
Figure 3.11 Crystal violet (CV) stained PAO1 biofilm within the wells of the microtiter plate after biofilm was allowed to develop for 24 hours in LB-media without any agents and in LB-media that is supplemented with SF α C (13) \sim 85 μ M; SF α C (13) \sim 85 μ M + Pili peptide \sim 85 μ M; SF α C (13) \sim 85 μ M + Scrambled pili peptide \sim 85 μ M; Pili peptide \sim 85 μ M; Scrambled pili peptide \sim 85 μ M.....	162

Chapter 4

Figure 4.1 Dimorphic nature of <i>Candida albicans</i> where both blastospores and hyphae co-exist is evident in both (a) in vitro and (b) in vivo biofilm.	172
Figure 4.2 Synthetic disaccharide derivatives (DSD) used in this study.....	177
Figure 4.3 <i>Candida albicans</i> growth curves in YPD medium. Growth was monitored in the presence (340 μ M) or in absence of various DSDs by measuring the optical density of the culture at 600 nm (OD600) over 24 hours.....	179

Figure 4.4 Microbroth dilution antifungal susceptibility assays. Images of micotiter plate wells inoculated with <i>Candida albicans</i> in 1640-RPMI media YPD supplemented with various concentrations of different DSDs. The images were taken 48 hours after	180
Figure 4.5 Optical micrograph images of <i>Candida albicans</i> grown in RPMI-1640 media with (at 340 or 40 μ M) or without (0 μ M; control) DSDs.....	181
Figure 4.6 <i>Candida albicans</i> percent biofilm inhibition caused by various DSDs with two different seeding times (5 minutes & 4-hours).....	183
Figure 4.7. Analysis of antiadhesive property of DSD, SF α C (5) against <i>Candida albicans</i> blastospores and hyphae. Phase contrast optical micrographs of <i>Candida albicans</i> grown in medium supporting either blastospores (left box) or hyphae (right box) growth in presence (170 μ M) or in absence of DSD, SF α C (5).	186
Figure 4S1. Schematic depicting XTT-dye based biofilm assay for <i>Candida albicans</i> with two different seeding times (5 minutes and 4 hours).....	192
Figure 4S2. Dose-response curves for inhibition of <i>Candida albicans</i> biofilms by various disaccharide derivatives (DSDs).....	193

Table	Page
Chapter 1	
Table 1.1 Biofilm forming pathogen and the corresponding associated medical condition	7
Chapter 2	
Table 2.1. Transition concentrations of DSDs that exhibit activity reversal from activating to inhibiting swarming motilities of the rhlA mutant and PAO1.....	50
Chapter 3	
Table 3.1. Transition concentrations of DSDs that exhibit activity reversal from activating to inhibiting swarming motilities of the rhlA mutant and PAO1, and IC ₅₀ and DC ₅₀ of DSDs for PAO1 biofilm inhibition and dispersion. Antibiofilm activities (inhibition & dispersion) at 160 μM of various agents.	158
Chapter 4	
Table 4.1. Half-maximal inhibitory concentrations (IC ₅₀) for inhibition of <i>Candida albicans</i> biofilm by various DSDs. DSDs were immediately added after seeding the microtiter plate wells with <i>Candida albicans</i> cells (1 X 10 ⁵ cell/mL) for 5 minutes.	184

Scheme	Page
Chapter 2	
Scheme 2.1 Synthesis of saccharide derivatives (SDs) (i) AcBr/AcOH, rt or 60 °C, ~ 1h; (ii) ROH, FeCl ₃ or Hg(CN) ₂ , MeCN, rt, 1h; (iii) ROH, FeCl ₃ , MeNO ₂ , rt, 1h; (iv) MeONa/MeOH, 12h, H ⁺ amberlite resin, Neutralize, (pH ~6.5).....	37
Scheme 2.2 Synthesis of β-cyclodextrin (βCD) based saccharide derivative (i) CH ₃ (CH ₂) ₁₁ NH ₂ , THF, -78 ⁰ C, ~ 12h; (ii) DMF, acetone, rt, 4days	37

Chapter 1

Introduction

1.1 Treating microbial infections - two different approaches

The existence of strains exhibiting multidrug resistance (MDR) for many species of bacteria is a matter of grave concern and enormous magnitude in today's healthcare settings.¹⁻⁵ The result is that, infections from many nonlife threatening species are often being cured by the most potent drugs only. To add to the woes, the pace at which newer microbicidal agents or antibiotics are being discovered and approved has been sluggish with only oxazolidinones and lipopeptides being inducted as potent new drugs in the recent years.⁶⁻¹⁰ Bacteria use at least three strategies to invoke MDR. These include, ability to destroy the activity of the drug compound, to undergo mutations that lead to expression of altered target proteins that do not recognize the antagonistic drug, and to deploy efflux pump mechanisms that lower cellular concentration of the drug at the active site.¹¹⁻¹³ Another problem associated with bacteria is that they possess the ability to spread drug resistant genes to other species through a phenomenon known as horizontal gene transfer (HGT).¹⁴⁻¹⁶ The occurrence of HGT has ensured that over time, drug resistant genes have been disseminated from strain to strain and from species to species, resulting in strains exhibiting MDR.¹⁷

Taking a step back and assessing the conventional approach towards treating microbial infections, brings forward the underlying common principle, "microbicidal action of drugs".^{18,19} Antibiotics target the cellular processes that are essential for bacterial survival; therefore bacteria employ the three strategies in their survival pack to overcome the effects of such microbicidal agents.²⁰⁻²² From the human perspective, the "fightback" by microbes to our invasive

microbicidal agents has generated strains that are now sturdier and resistant to the action of most antibiotics and the occurrence of such resistant strains are on the increase due to easy transfer of genetic elements amongst strains.^{3,23} Therefore agents that prevent microbial infections without affecting their growth will have lower propensity to invoke drug resistance.²⁴ To summarize, the two main problems associated with the conventional microbicidal strategies for treating bacterial infections are; (i) Antibiotics enhance the chances of inducing drug resistance in bacteria,^{3,25,26} (ii) Antibiotics work better when bacteria exist as unicellular organisms.^{27,28}

Alternatively, the newer strategies to treat bacterial infections should address the above mentioned problems associated with conventional antibacterial strategies. The issue of invoking drug resistance can be overcome or reduced with the use of nonmicrobicidal agents that do not impede bacterial cellular activities. In the present day, the notion that bacteria exist both as unicellular planktonic cells and as multicellular organisms has been widely acknowledged by the scientific community.²⁹⁻³¹ Bacterial multicellular processes are known to be associated with most infections but are less important for bacterial survival.³² Employing strategies that look beyond bacteria as simple unicellular organisms necessitates an understanding of why and when bacteria switch between the two lifestyles.³³

1.2 Two different kinds of lifestyles that bacteria adopt: Unicellular and multicellular

Despite some earlier observations of coordinated activities, bacteria until recently were regarded as archetypal unicellular organisms.^{34,35} But advances in microbiology have since focused on why and when do bacteria choose a multicellular lifestyle over remaining loners.^{31,33} The evolutionary benefits that have been identified as being important for establishing multicellularity in bacteria include resistance from predators and better management of

nutrients.^{30,36} To achieve these benefits, bacteria associate to form adherent clusters that give rise to various kinds of communities, both sessile and motile having different superficial morphologies.³⁷⁻⁴⁰ The formation of both kinds of multicellular communities is known to be initiated by different types of chemical signals that bacteria secrete, receive and interpret.⁴¹⁻⁴³ The signal transduction alters bacterial gene expression and sets into motion a series of changes that eventually leads to formation of multicellular communities.⁴⁴ Once multicellularity is established, the resulting communities either create sessile complex 3-dimensional architectures or motile 2-dimensional patterns that ensure division of labor and coordination of nutrients.³⁶

1.3 Sessile and motile multicellular behaviors

Bacteria are able to perform at least two distinct multicellular processes; (i) Formation of biofilm, a sessile lifestyle and (ii) Swarming, a motile lifestyle . While both of these processes have distinct characteristics, where one is a stationary phenomenon and the other is a motile one, there exists evidence that both these processes are intertwined and have mechanistic intermingling.^{38,45}

1.3.1 Formation of biofilm is a developmental process: A sessile group behavior

Biofilms are highly hydrated surface attached microbial communities having structural and metabolic division of labor and where microbes reside within a matrix of secreted extra polymeric substances (EPS).⁴⁶⁻⁴⁸ The choice of planktonic bacteria to harbor themselves within multicellular communities confers many advantages (i) Biofilm architecture and framework allows easy flow and supply of nutrients. (ii) The formation of sturdy biofilms creates a protective barrier against physical and chemical assaults. (iii) Formation of biofilms renders the

community a thousand-fold more resistant to the action of antibiotics. (iv) Different kinds of species can inhabit the same matrix as nutrient requirements for specific species are easily met by slow diffusion of small molecules across the matrix. (v) Because many species or strains reside within the same scaffold, interspecies or inter-strain transfer of genetic material can occur to spread competitive advantages against particular environmental challenges.^{49,50}

1.3.2 Five stage differentiation of bacterial biofilms

In early reports, a biofilm was thought to be an unstructured slime of polymeric matrix which bore embedded bacteria.⁵¹ During these early years, it was not clear how such deeply embedded bacteria have access to nutrients or even oxygen. Later, with the use of confocal laser scanning microscopy (CLSM), Costerton and coworkers were the first to report that the three dimensional architecture of biofilms consists of matrix enclosed bacterial microcolonies that have voids or water-channels (Figure 1.1).^{47,52,53}

The formation of biofilm is a developmental process involving five key stages (Figure 1.1).⁵⁴ The first stage of biofilm development is the "reversible attachment" of bacteria to a surface. The planktonic bacteria at this stage are open to both mobile or sedentary lifestyle, and once environmental cues are favorable, the bacteria commit to a sessile lifestyle. Once attached onto surfaces the bacteria begin a second stage of multicellularity by secreting EPS and establishing "irreversible attachment".^{55,56} The composition of EPS secreted by microbes is quite diverse and varies from species to species but common elements include polysaccharides, nucleic acids, proteins and phospholipids.^{57,58} The matrix created by secretion of EPS helps "glue" cells together to initiate microcolony formation.⁵²

The surface adhered bacteria then secrete chemical signals known as autoinducers into the surrounding environment to perform cell-to-cell communication, a process usually referred to as quorum sensing.⁵⁹⁻⁶³ Quorum sensing is carried out by bacteria to assess the cellular density of other bacteria in the environment.^{42,64} The assessment of cellular density is achieved by detection of secreted bacterial chemical signals in the environment.⁴³ The increase in concentration of chemical signals in the environment is correlated with the cellular density of the bacteria. Once a threshold concentration for the chemical signals is achieved, individual bacteria transduce the signal and initiate a cascade of signaling pathways that eventually alter bacterial gene expression to initiate the third stage of biofilm formation which is the shift from planktonic lifestyle to a multicellular commune.⁶⁵⁻⁶⁸

The sessile communities formed exhibit a fourth development stage of "maturation" where the biofilm takes complex shapes along with redistribution of bacterial cells for distinct roles and formation of water channels.⁶⁹ One important change during the fourth stage is the alteration in the level of expression of many genes that are different from the genetic expression amongst planktonic bacteria.^{47,70}

Formation of biofilm is a lifestyle change with the underlining principle of ensuring bacterial survival and propagation.⁷¹ Therefore, like other sessile communities, biofilms too have evolved dispersive strategies to colonize new surfaces.⁷² This is the final stage of biofilm development that includes both passive and active dispersal strategies.^{73,74} In passive dispersal, chunks of the existing biofilm may erode away due to fluid shear and move to newer uncolonized surfaces. On the other hand, active dispersal, also known as seeding dispersal, of free swimming planktonic bacteria from the mature biofilms is thought to be under the control of complex cellular signaling. The mechanism by which microorganisms manipulate cellular

dispersal from biofilms is still poorly understood but the concept finds broad applications in the field of antibiofilm strategies.⁴⁹

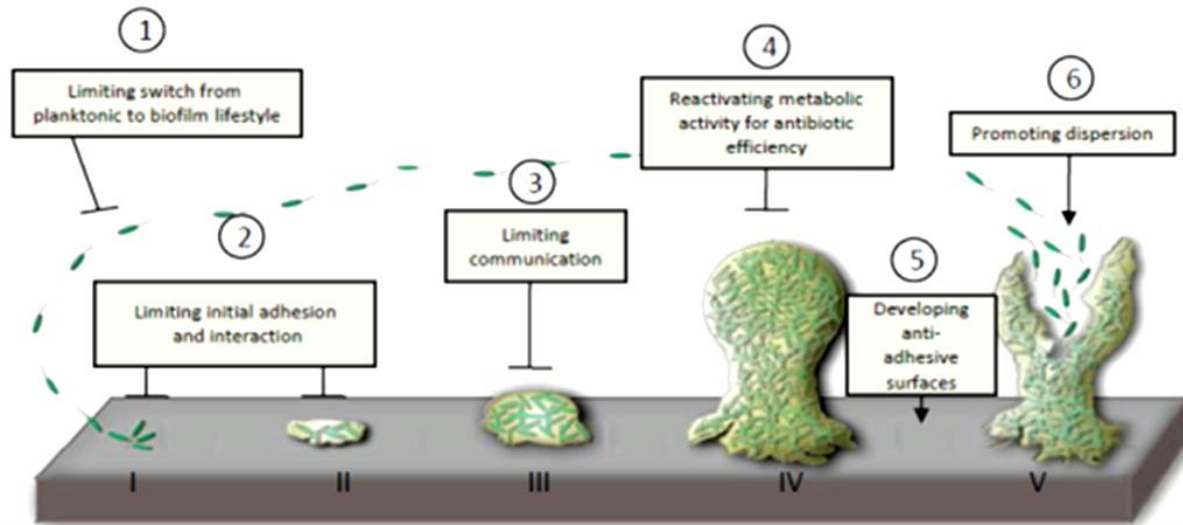


Figure 1.1 Different stages of biofilm development and dispersion. Insert-Criteria for developing antibiofilm strategies include interfering with one or multiple biofilm developmental stages.

[Reprinted with permission from Citation:40 Bordi and de Bentzmann (2011) Hacking into bacterial biofilms: a new therapeutic challenge. *Annals of intensive care*, 2011, 1: 19.

doi:10.1186/2110-5820-1-19; Image Credit: de Bentzmann; Copyright: © 2011 Bordi and de Bentzmann; licensee Springer. This is an open-access article distributed under the terms of the Creative Commons Attribution License, which permits unrestricted use, distribution and reproduction in any medium, provided the original author and source are cited.

1.3.3 Numerous medical and industrial problems are associated with formation of biofilms

Until three decades ago, bacteria were primarily regarded as unicellular entities, but since then the view about bacteria has evolved to appreciate that formation of biofilms may be a preferred bacterial lifestyle. The formation of biofilms by bacteria on both biotic and abiotic

surfaces causes immense monetary losses to both medical as well as industrial setups.

Pseudomonas aeruginosa is the primary microbial dweller in the lungs of cystic fibrosis patients, where the bacteria's preferred mode of living is by forming biofilms. Bacteria are known to reside within oral cavities, form dental plaques and known to colonize a wide variety of medical devices by forming biofilms.⁴⁸ Common diseases associated with formation of bacterial biofilms include burn wound infections, otitis media and bacterial endocarditis.⁷⁵ (Table 1.1). Two important issues associated with formation of bacterial biofilms are enhanced resistance to antimicrobials and lack of strategies that can completely eradicate colonization.

Table 1.1 Biofilm forming pathogen and the corresponding associated medical condition

Organism	Biofilm-associated diseases
<i>Pseudomonas aeruginosa</i>	Cystic fibrosis lung infection
<i>Burkholderia cepacia</i>	Cystic fibrosis lung infection
<i>Acinetobacter baumannii</i>	Burn wound, trauma infection
<i>Helicobacter pylori</i>	Gastrointestinal infection
<i>Escherichia coli</i>	Urinary, catheter infection
<i>Haemophilus influenzae</i>	Otitis media
<i>Bordetella pertussis</i>	Respiratory infection
<i>Legionella pneumophila</i>	Legionnaires disease
<i>Staphylococcus aureus</i>	Burn wound, catheter, trauma infection
<i>Staphylococcus epidermidis</i>	Sepsis, catheter infection
<i>Streptococcus mutans</i>	Dental plaques, gingivitis
<i>Vancomycin-resistant enterococci (VRE)</i>	Nosocomial infection

The National Institute of Health (NIH) has estimated that 65-80% percent of bacterial infections in humans are associated with microbial multicellularity.^{76,77} It has been reported that formation of biofilm renders the bacteria about one thousand times more resistant to the action of antibiotics.⁷⁸⁻⁸⁰ From a monetary standpoint, microbial multicellularity is causes huge losses both in medical as well as industrial set-ups. The cost of treating biofilm related infections in the United states can be upward of US \$ 1 billion.^{46,71} Until recently, treating microbial infections

had been directed towards bacteria as an unicellular entity. But, since the appreciation of multicellularity being associated with persistent microbial infections, alternative strategies to treat such infections have been explored.

1.3.4 Common antibiofilm strategies

Since biofilm formation is a developmental process, the antibiofilm strategies developed mainly aim to arrest various stages of colonization (**Figure 1.1**). The antibiofilm strategies use both chemical and physical methods.

1.3.4.1 Quorum sensing inhibitors

Quorum sensing is the communication process that facilitates both inter and intra species cell-to-cell signaling that ultimately results in altered microbial gene expression leading to biofilm formation. The use of both synthetic and naturally occurring antagonists that interfere with the cell-to-cell chemical signaling in bacteria is a popular strategy to treat biofilms.⁸¹⁻⁸³ These antagonists are nonmicrobicidal and hence considered to be generally safe for use as they possess lesser propensity to induce drug resistance.^{77,80}

1.3.4.2 Bacteriophages that degrade biofilm matrix

Bacteriophages have co-evolved within bacterial biofilms and can replicate within their host cells.⁸⁴ Although bacteriophages are structurally larger than chemical antibiotics, they are still comparatively much smaller than bacterial cells and therefore do infect microbes within biofilms.⁸⁴⁻⁸⁷ Such bacteriophages secrete depolymerizing enzymes that reduce biofilm content by eliminating bacteria that produce the components of the biofilm matrix like EPS etc.⁸⁸⁻⁹⁰ Bacteriophages can also reside within persister cells without causing any damage to the

metabolically inactive host cells, and when such such cells became active, the bacteriophages are able to use the host genetic cycle, multiply and cause biofilm elimination.⁸⁴

1.3.4.3 Surface modifications can prevent bio-fouling

The use of chemicals to create modified bio-inert surfaces that resist bio-fouling is another viable antibiofilm strategy.⁹¹⁻⁹⁷ Such strategies are directed towards blocking of initial bacterial adhesion and hence prevent early stages of biofilm development. The surface chemical modifications make include coating with antibiotics,⁹⁶ changing hydrophobicity or hydrophilicity,^{98,99} changing surface texture/roughness,^{100,101} and coating with polyethyleneglycol (PEG) derivatives.¹⁰² The Type I pili of *E. Coli* are important adhesin proteins that are recognize mannose moieties presented by host cells. Therefore, mannoside derivatives have been deployed as agents that interfere with the natural binding process of Type I pili to mannose epitopes present on host cells.¹⁰³⁻¹⁰⁶

1.3.4.4 Antibiofilm enzymes

While prevention of biofilm formation is difficult, it is still relatively easier than disrupting biofilms that have already formed, which is normally the problem on medical devices. Multiple enzymes have been used to degrade the components of the biofilm matrix, such as polysaccharide, eDNA and proteins. One such study has demonstrated the use of dispersin B to degrade the components of *S. epidermidis* biofilm EPS.¹⁰⁷ One component of biofilm matrices is secreted extracellular DNA (eDNA), and hence Izano *et al* showed that DNAase I could be used to degrade the biofilm of *S. aureus*.¹⁰⁸ Chaignon *et al* showed that proteases such as Proteinase K and trypsin degrade the biofilm formed by *S. aureus*.¹⁰⁹

1.3.4.5 Small molecular chemical dispersers of preformed biofilms

A D-amino acid extracted from dispersing cells of *B. subtilis* was shown to degrade the existing biofilm and also prevent the formation of biofilm by *S. aureus* and *P. aeruginosa*.¹¹⁰ Another molecule isolated from *B. subtilis*, Norspermidine, was demonstrated to break down biofilm by targeting the exopolysaccharides.¹¹¹ Nitric oxide (NO) is known to trigger biofilm dispersal in mature biofilms.¹¹² Therefore, the use of low-dose of NO synergistically with an antibiotic was shown to reduce the colonization of *P. aeruginosa* in the lungs of cystic fibrosis patients.^{113,114} Apart from these agents, many of the small molecules used to prevent bacterial cell-to-cell communications (quorum sensing inhibitors) have been used effectively to disperse preformed biofilms of *P. aeruginosa*.^{80,115,116}

1.3.4.6 Physical methods for treating biofilms

Apart from using chemicals to treat biofilms, many physical and mechanical techniques are also employed to treat or prevent biofilm related infections, especially in the food industry. Ultrasonication is used to decontaminate food. Decontamination of food and food containers is often done with the use of electrolyzed water. Sometimes, prevention of adhesion or removal of adhered biofilm on surfaces is done with the use of electrical techniques.

1.3.5 Swarming on surfaces: A motile group behavior

While sessile lifestyle (biofilm formation) is critical, bacterial motility also plays an important role in microbial pathogenesis. There are different kinds of bacterial motilities that planktonic cells or a group of cells can perform. Among the various surface associated bacterial motilities, swarming is the fastest and is a coordinated multicellular phenomenon. Swarming is usually observed in both Gram-positive as well as Gram-negative bacterial strains that possess

flagella, including *Salmonella*, *Vibrio*, *Yersinia*, *Serratia*, *Proteus* and *Pseudomonas*. Apart from possession of flagella, the swarming phenomenon is also dependent on surface nutrients and surface "wettability" (surface tension). As a result of all the physico-chemical cues, the swarmer cells become hyperflagellated, elongated and undergo gene expression alteration as compared to vegetative cells. The differentiation of vegetative cells into swarmer cells suggests that swarming does not merely represent physical changes in the bacterial behavior but a more complex motile lifestyle adaptation. Swarming colonies have distinct resistance to action of antibiotics.

1.4 Synopsis of Chapters 2 & 3

This thesis brings forward a new way to modulate the two kinds of microbial multicellular behaviors; swarming (motile) and biofilm formation (sessile). Chapter 2 describes a study in which saccharide derivatives were used for modulating the swarming motility of a Gram-negative opportunistic bacterium, *Pseudomonas aeruginosa*. Some saccharide derivatives were able to mimic the functions of a naturally secreted biosurfactant, rhamnolipids, that *Pseudomonas aeruginosa* secrete. The most potent saccharide derivatives seemed to dominate the effect that the natural biosurfactant had on swarming motility of *Pseudomonas aeruginosa*. Chapter 3 demonstrates how the nonmicrobicidal saccharide derivatives can also prevent *Pseudomonas aeruginosa* biofilm formation, adhesion and cause biofilm dispersal. The antibiofilm (biofilm inhibition and dispersion) half-maximal inhibitory concentrations (IC₅₀s) of the most potent saccharide derivatives were comparable to the most potent known nonmicrobicidal antibiofilm agents. Overall, Chapters 2 & 3 bring forward certain saccharide derivatives as modulators of *Pseudomonas aeruginosa* multicellular behaviors and also suggest

that the secreted biosurfactant, rhamnolipids may have more than just a physical significance in the bacterial lifecycle.

1.5 Synopsis of Chapter 4

Prokaryotes (bacteria) are not the only organisms that exhibit biofilm formation; Biofilm formation is a common way of colonization in eukaryotes (fungus) like *Candida albicans*. In addition to the various effects of DSDs on bacterium *Pseudomonas aeruginosa*, Chapter 4 encompasses a study that demonstrates the versatility of saccharide derivatives to also inhibit the biofilm formed by fungus *Candida albicans*. Surface-chemistry experiments show how the antibiofilm activity of these nonmicrobicidal agents against *Candida albicans* is through their ability to prevent hyphal adhesion to surfaces.

Chapter 2

Saccharide Derivatives Modulate the Swarming Motility of *Pseudomonas aeruginosa*

Abstract

Secretion of biosurfactant rhamnolipids by Gram-negative bacteria, *Pseudomonas aeruginosa* has been previously reported to be important for assisting swarming motility and for maintaining the architecture of water channels within the biofilm. In this chapter, the control of bacterial swarming by synthetic saccharide derivatives that function as rhamnolipids analogues has been reported. Few synthetic disaccharide derivatives (DSDs) were shown to be much more effective than both the naturally secreted and the externally added rhamnolipids at activating swarming of a nonswarming *P. aeruginosa* mutant. The study also brought forward a dose-response phenomenon where the activation of swarming in a nonswarming *P. aeruginosa* mutant, *rhlA* by some DSDs and also rhamnolipids first increases with increasing doses and after a threshold dose, the swarming activation is reversed. Previously, a bacterial cell signaling molecule, N-(3-oxohexanoyl)-3-aminodihydro-2(3H)-furanone has been shown to exhibit a similar dose-response “activity reversal” phenomenon for a different multicellular behavior, i.e light simulation. It is therefore predicted that production and secretion of rhamnolipids by *P. aeruginosa* probably has a greater biological significance than mere physical impact on multicellularity.

2.1 Introduction

Multicellularity offers at least three different advantages over planktonic lifestyle:^{38,117} (i) Increased tolerance to antagonists; (ii) Good management of limited nutrients, and (iii) Morphological differentiation helps in division of labor. The way free-living bacteria colonize a surface depends upon the immediate physio-chemical environment surrounding the bacterial population^{29,42,45,64,118-121} and as a consequence, multicellularity in bacteria can be manifested through either a sessile^{29,34,35,46-48,64,71,75,77,115} or a motile lifestyle.^{38,45,117,119,121-125} This chapter is dedicated to the study of how a class of small molecules modulate bacterial swarming motility.

2.1.1 Types of bacterial motility

It is important to make clear distinctions of the various types of motilities that bacteria exhibit and why amongst these motilities, swarming is unique and important from an infection standpoint.^{38,122} The first classification of bacterial translocation was done by J. Henrichsen, where movements by hundreds of bacterial strains were classified into five main categories: swimming, swarming, gliding, twitching and sliding (Figure 2.1).^{122,126-133}

While swimming motility is a flagellar dependent planktonic behavior of the bacteria in liquid medium (Figure 2.1a), swarming is a surface translocation that a group of thousands of bacteria perform in coordination (Figure 2.1b).^{117,122} The presence of flagella is known to be essential for the occurrence both swimming^{132,133} and swarming¹²³ motilities. The direction of the rotation of the flagella decides the trajectory of the motility movement. While counterclockwise rotation ensures smooth linear trajectories with speeds of up to 40 $\mu\text{m/s}$, a clockwise rotation creates a random tumbling effect (0.1 $\mu\text{m/s}$).^{38,117} Swarming bacterial cells are generally multi-flagellated and longer than vegetative counterparts.^{38,117,122} Although swarming is the movement of choice under natural colonization on surfaces, under laboratory settings swarming is usually

observed on the semisolid gels of agar (0.5 to 1 %) that contain energy rich solid media.¹²² Since, within a swarmer colony, each cell can move with a speed between 2 to 10 $\mu\text{m/s}$, swarming is considered the fastest mode of bacterial surface translocation.¹¹⁷

The extension and retraction of type IV pili is known to drive the slow surface associated twitching motility exhibited by planktonic bacteria (Figure 2.1c).¹²⁷ In addition to this, gliding is a surface associated motility that bacteria perform without the use of flagella or pili (Figure 2.1d).¹²⁸ Beside the various models like, repulsion by macromolecule, movement of outer membrane or formation of focal adhesion complexes, no one model clearly explains the gliding movement of bacteria.¹¹⁷ Apart from this, the passive outward movement as a consequence of colonial growth on a surface is known as sliding motility (Figure 2.1e).¹²⁹⁻¹³¹ The reduction of surface tension by secretion of surfactant has been observed during sliding movement.¹²²

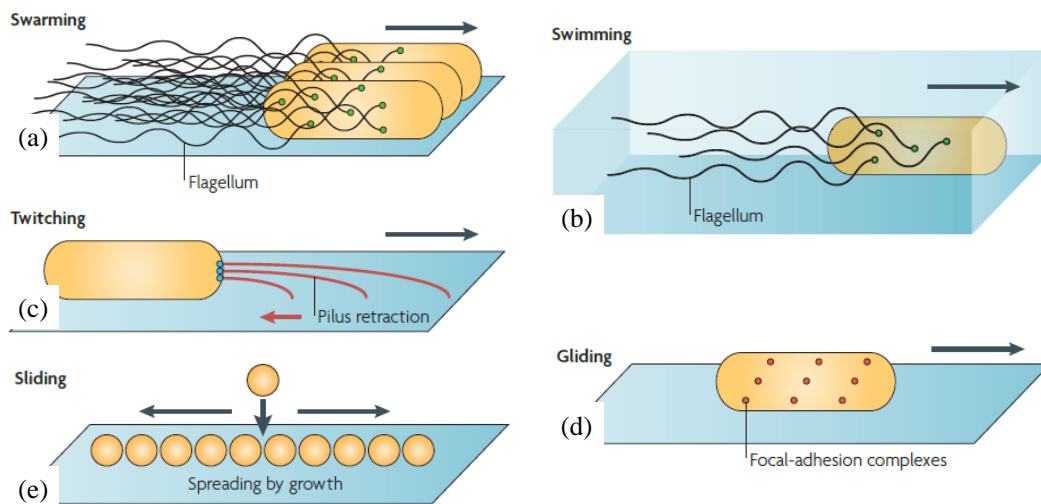


Figure 2.1 Bacteria perform both unicellular and multicellular movements. (a) Swarming is multicellular movement of bacteria on a surface; (b) Individual bacteria are able to move in aqueous media by beating their flagella, known as swimming motility; (c) Twitching is a unicellular bacteria movement on a surface that is facilitated by extension of the pili; (d) Gliding

movement is also a unicellular movement that proceeds through formation of focal-adhesion points; (e) Sliding is passive movement across the surface that occurs due to the growth of bacterial population. The arrows in the diagram indicates the direction of movement. [Reprinted with permission from Citation¹²²: Kearns, D. B. *et al*, A field guide to bacterial swarming motility. *Nat. Rev. Microbiol.* **2010**, 8, (9), 634-644.

2.1.2. Swarming motility is a multicellular phenomenon

Both swarming and biofilm formation are bacterial multicellular behaviors that contribute to the overall survival of the microbes in the environment and therefore are essential for maintaining virulence.^{30,34,118} A switch to swarming lifestyle will generally require a coordinated merger of many chemical and physical cues.¹²² Also, a certain cell density is requisite for this multicellular behavior to be initiated.¹²³ The swarming phenomenon has been observed both in gram negative as well as gram positive bacterial species.¹¹⁷ So far swarming has been observed in three bacterial families including gamma-proteobacteria, alpha-proteobacteria and firmicutes.^{122,134} Under laboratory settings, the water content of the agar gel is critical for observing swarming. Under laboratory settings, while some bacteria can swarm on gels composed of a wide variety of agar concentrations, usually most bacteria swarm on gels above 0.5% and below 1% agar.¹³⁵ A concentration of below 0.5% agar is usually deemed suitable for swimming motility,¹³² while concentration above 1.5% is known to inhibit swarming.¹³⁶

In general the key features important for ensuring that swarming occurs include: presence of flagella, cell-to-cell communication and biosynthesis of surfactants.^{122,123}

A number of studies have shown that mutations that reduce flagellar biosynthesis also abolish or reduce swarming motility.^{123,125} Contrary to this, enhanced expression of flagella

increases swarming in certain mutant species.¹³⁷⁻¹³⁹ Therefore, it is not surprising that most swarmer cells have a peritrichous arrangement of flagella.^{122,137,140,141} Bacteria form a bundle with these multiple flagella and the rotation of such a bundle powers the bacteria to move on a viscous media.^{142,143} Some bacteria like *Pseudomonas aeruginosa* synthesize a lateral flagella in addition to the existing polar flagella to move on a viscous surface.^{123,136,141,144}

The number of cells are critical to initiate the swarming process and therefore many swarming processes are linked to the cell-to-cell communication process known as quorum sensing.^{123,145} The *swr* quorum sensing system in *Serratia liquefaciens* which is homologous to the *lux* system of *Vibrio fischeri* has been shown to control the swarming of *Serratia liquefaciens*.¹⁴⁵ Autoinducers, N-acylhomoserine lactones (AHLs) are known to control the biosynthesis of a biosurfactant necessary for the swarming of a *P. aeruginosa*,¹²³ and *S. marcescens*;¹⁴⁶ and peptides autoinducers control surfactant synthesis in *B. subtilis*.^{147,148} One important aspect of swarming is cellular collaboration manifested through the formation of "rafts" where bacteria move side by side as groups.^{122,137,140,145,149-151} To the present date it is not exactly clear why the formation of rafts is necessary during swarming but it is appreciated that such a process would require communication between cells.¹²²

Secretion of surfactants by bacteria is commonly observed during the swarming process.^{121,123,137,140} Surfactants, being amphiphilic molecules, reduce the surface tension between the bacterial cells and the substrate, hence allowing easy translocation. Under laboratory conditions, most bacteria swarm on moist semi-solid gels containing 0.5-1.0 % agar. However, some bacteria species like *Proteus*,¹⁵² *Vibrio*,¹⁵³ *Rhodospirillum*,¹⁵⁴ and *Azospirillum*¹²⁶ possess the ability to swarm effectively on solid agar gels that normally inhibit swarming, i.e >1.5 % agar.¹²⁶ Such bacterial species are known to secrete surfactants like polysaccharides to achieve

lower surface tension and create a more conducive micro environment for swarming.^{134,152}

Surfactants and polysaccharides are the major components of the slime that normally surround swarmer colonies.¹³⁴ Production of surfactin, a surface active agent secreted by *B. subtilis* is critical for its swarming.¹³⁷ While *B. subtilis* mutants that lacked surfactin biosynthesis lacked the ability to swarm, when externally added surfactin was introduced, the mutants were able to swarm again.¹³⁷ *P. aeruginosa* is known to secrete a class of lipopolysaccharide based molecules, known as rhamnolipids that have been shown to be critical for its swarming process.¹²³

2.1.3 Understanding the cell-to-cell communication process

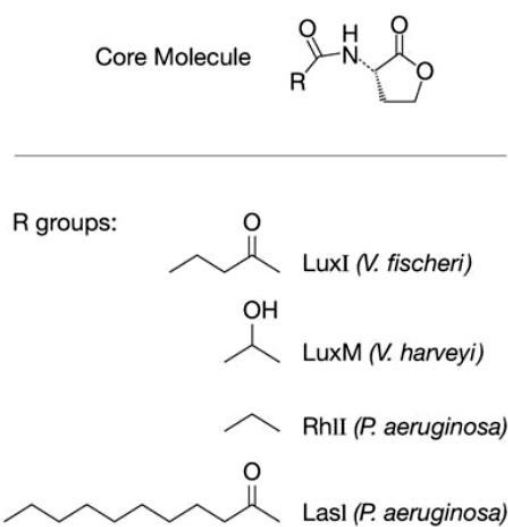
Bacteria perform cell-to-cell communication with the use of unique chemical signals known as autoinducers (AI) that they produce and secrete out into their environment.^{41,43,64,147,155-157} The accumulation of these chemical signals increases in proportion to the bacterial cell density and upon reaching a threshold concentration such signals are able to bind to the cognate receptors thereby altering population wide gene expression and inducing multicellular behaviors.^{29,31,43,64,118,147,155,158} This chemical cellular communication process also known as quorum sensing has features that are conserved amongst various species while at the same time each species has elements that are unique to its system.^{29,43,64,118,147,155,158-160}

The common elements amongst the various quorum sensing systems are;^{29,147} (i) Each system is able to synthesize a chemical signaling molecule that is secreted out and upon reaching a threshold concentration such molecules are detected and induce a response. (ii) The receptors for such signals may either exist in the cytoplasm or on cell surface membranes and signal transduction activates cooperative behaviors. (iii) Additionally, signal transduction causes autoinduction of the originally secreted chemical signal. The uniqueness of each quorum sensing

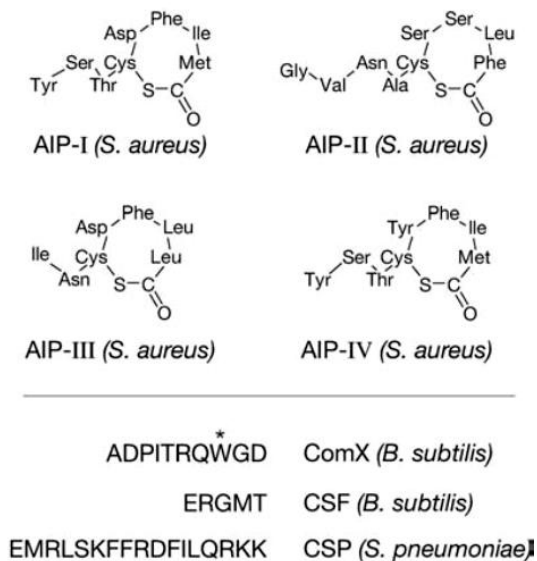
systems is manifested through the existence of signals and receptors that are structurally different for different systems but specific for each signal-receptor pair.

The Gram-negative bacteria use small molecular autoinducers that are either acyl homoserine lactones (AHL or AI-1) or furanosyl borate diester (AI-2)^{29,64,147,155,157} (Figure 2.2 (a & d)). Contrary to the small molecular autoinducer signals of the Gram-negatives, the autoinducers secreted by the gram positive bacteria are oligopeptides known as autoinducing peptides (AIP)^{29,64,147,155,157,161} (Figure 2.2b). The secreted AIPs are able to bind to cognate membrane bound histidine kinase receptors and the binding causes a phosphorylation cascade that ultimately results in alteration of gene expression.¹⁶¹⁻¹⁶³ Certain Gram positive species like *Streptomyces* employ γ -butyrolactones (Figure 2.2c) for regulation of antibiotic production and morphological differentiation.^{155,164}

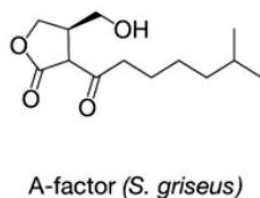
a **cyl-homoserine lactones (AHL)**



b **Oligopeptide autoinducers**



c **Streptomyces γ -butyrolactones**



d **AI-2 family**

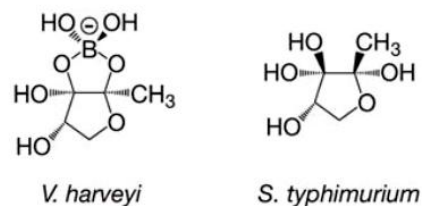


Figure 2.2 Chemical signals or autoinducers employed by bacteria for cell-to-cell communication process. The figure shows the chemical structure of an autoinducer and the corresponding bacterial species that secretes the signal (a) Example of acyl-homoserine lactone (AHL) based autoinducers used by some Gram-negative bacteria (also known as AI-I); (b) Autoinducing peptides (AIP) deployed by some Gram-positive bacteria to achieve cellular communication; (c) The butyrolactone based autoinducer secreted by the Streptomyces species; (d) The borate diester (AI-2) type of autoinducer (AI-II) used during inter-cellular communication by some gram negative bacteria. [Reprinted with permission from Citation:¹⁵⁵

Quorum Sensing: Cell-to-Cell Communication in Bacteria Christopher M. Waters and Bonnie L. Bassler

2.1.4 Components of a typical gram negative quorum sensing gene circuitry

All known quorum sensing systems described for gram negative bacteria are homologous to the LuxI/LuxR type quorum sensing system first described in *Vibrio fischeri* (Figure 2.3).^{147,155,156,158,165-167} In the LuxI/LuxR quorum sensing system the LuxI homologue is the AI synthase that couples the acyl group from specific donor proteins to the methionine on S-adenosyl methionine (SAM) and produces AHLs.^{156,168} The synthesized AHLs are secreted out of the cell and as the cellular population of bacteria in the milieu increases, the concentration of secreted AHLs also increases proportionally.¹⁶⁹ When the external AHL concentration reaches a specific threshold, the binding of AHLs to the cognate LuxR type protein becomes effective.⁶⁴ The LuxR-AHL binding results in the stabilization of the LuxR type protein and the ligand-receptor complex eventually activates the transcription of genes including the ones that control the production of virulence factors like biofilm formation, swarming, biosurfactant, pyocyanine, elastate B, and bioluminescence.¹⁷⁰

The quorum sensing systems in more than hundred Gram-negative bacteria species are known to be typified by the LuxI/LuxR type quorum sensing of *Vibrio fischeri*.^{42,147,155,156,158,159,165,166,171-173} The differences are that the AHL secreted by these systems are unique and are distinguished by different lengths of side chains (between C-4 to C-18) or different functional group (hydroxyl or carbonyl) decoration on the side chains (Figure 2.2a).^{42,118,147,155,156,158,159,166,171,173} Chemical diversity of the AHL chemical signals is matched by occurrence of corresponding homologous LuxR type receptor proteins.^{42,118,147,155,156,158,159,166,171,173} For each species the binding of the AHL signal to its

corresponding LuxR type protein is highly specific and critical for achieving intra species cell-to-cell communication. Some Gram-negative bacteria species like *P. aeruginosa* use more than one LuxI/LuxR type quorum sensing systems in tandem to carry out cell-to-cell communication.^{64,156,174}

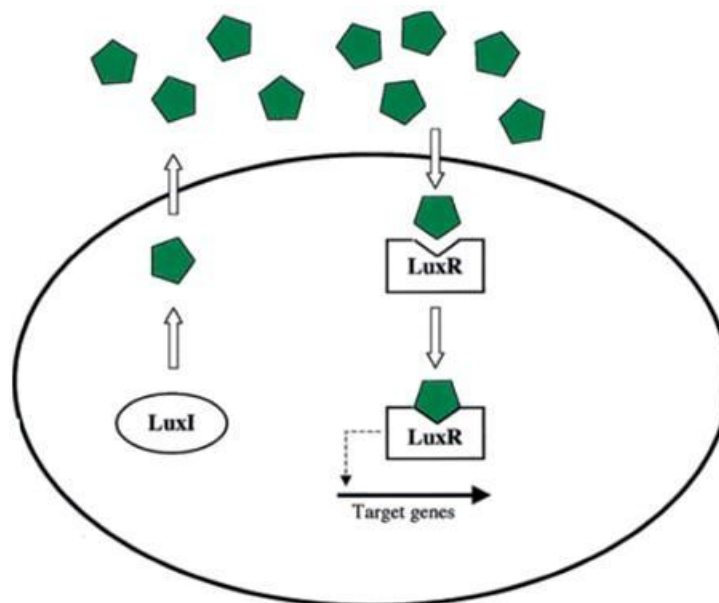


Figure 2.3 The components and the representation of a typical quorum sensing process performed by Gram-negative bacteria [Reprinted with permission from Citation:¹¹⁸ Bassler, B. L. *et al*, The Languages of Bacteria. *Genes Dev.* **2001**, 15, (Copyright (C) 2012 American Chemical Society (ACS). All Rights Reserved.), 1468-1480.

2.1.5. Swarming in *P. aeruginosa*

Pseudomonas aeruginosa is a gram-negative bacteria and is the primary pathogen that colonizes the lungs of cystic fibrosis patients.¹⁷⁵⁻¹⁷⁹ *P. aeruginosa* uses many techniques for movement through either solution or on surfaces.^{122,123,132,134,136,144,180} Generally, the single flagellated planktonic *Pseudomonas aeruginosa* propels through aqueous media with regular "beating" of the flagella.^{132,133,136} Under laboratory conditions too, *P. aeruginosa* is able to

employ flagellar propulsion to swim in low-agar (<0.4 %) medium.^{119,123,132,133,181} Apart from using flagella, *P. aeruginosa* is known to use the extension and retraction of pilus filament to move on surfaces.¹⁸² The type-IV pili in *Pseudomonas aeruginosa* are also important for attachment to both epithelial cells and abiotic surfaces.¹⁸³ However, the fastest mode of surface translocation that *P. aeruginosa* performs is swarming.¹²²

The swarming colonies formed by *P. aeruginosa* (PA14) are typified by having an appearance of tendrils originating from the center point of inoculation.¹²³ (Figure 2.5g) Other strains like PAO1 swarm by forming a circular colony with not very conspicuous tendril formation.¹³⁵ Like other bacteria, the important features necessary for swarming of *P. aeruginosa* are presence of flagella and pili, quorum sensing dependent gene-regulation and the secretion of biosurfactants.¹²³

2.1.5.1 Swarming in *P. aeruginosa* requires flagella

Under the swarming mode the monotrichious *Pseudomonas aeruginosa* vegetative cells usually become elongated and acquire a second polar flagella.¹³⁶ Kohler and coworkers reported that a mutant strain *Pseudomonas aeruginosa* PAO1, *fliC* that did not synthesize any flagellum had impaired swarming.¹²³ These investigators also discovered that another surface appendage which is responsible for twitching motility, type-IV pili was essential for swarming in strains PT623 and PT612 of *P. aeruginosa*. The mutant strains of both PT623 and PT612, that is *pilA* and *pilR*, respectively were complete nonswarmers. Swarming was however partially restored in mutant *pilR* when a plasmid encoding for expression of pili was introduced.¹²³

2.1.5.2 Alteration in gene expression of *P. aeruginosa* during swarming

Overhage and coworker were first to report that swarming is a bacterial lifestyle adaptation under a viscous environment.¹⁸⁰ In adapting to a motile lifestyle, *P. aeruginosa* have been reported to up-regulate certain genes related to virulence and antibiotic resistance.^{180,184} On comparing swimming with swarming cells, they observed that there was a major shift in gene expression of virulence regulated genes like those encoding for Type-III secretion systems, extracellular proteases and iron transport.^{180,184} Amongst the up-regulated virulence genes, Overhage and coworkers showed that *lasB* and *pvdQ* were required for swarming motility in *P. aeruginosa*.¹⁸⁴ The comparison of swimmer and swarmer cells also showed that the latter were more resistant to the action of at least three antibiotics, polymyxin B, gentamicin, and ciprofloxacin.¹⁸⁰

Deziel and coworkers compared the gene expression of nonswarming *Pseudomonas aeruginosa* PA14 cells to cells both at the center and at the tendril tips of a swarming colony.¹²⁴ Deziel and co-workers' screening showed the over-expression of 20 genes and down regulation of 121 genes by bacteria at tip of the tendril in comparison with bacteria in the swarm center of the swarming pattern. Using gene microarray they obtained transcriptomic profiles to show that a minority of the genes, including those for energy metabolism and transport of small molecules, were upregulated in cells found at the swarming tips. In contrast, they reported that genes responsible for virulence were repressed in cells found at the swarm edges as compared to the cells at the swarm center. This report of down regulation of virulence genes at swarming edges was distinct from the work of Overhage, where upregulation of virulence genes in cells at the swarming edge was reported in a direct comparison to cells found in broth.^{124,180} The work by Deziel and coworkers highlighted the existence of a bacterial subpopulation within a swarming

colony, a population of metabolically hyperactive swarmer cells ("hyperswarming") found at the edges and population of cells at the center of the colony that are more virulent ("hyposwarming").

Bacterial multicellularity is initiated by quorum sensing and ultimately results in altered gene expression. Since swarming motility has also been shown to exhibit altered gene expression, it is important to establish a link between quorum sensing and swarming.

2.1.5.3 The LasI-LasR and RhII-RhIR Quorum Sensing Systems of P. aeruginosa are homologous to the LuxI/LuxR system found in Vibrio fischeri

In *P. aeruginosa*, there exist a hierarchical system of two LuxI/LuxR type quorum sensing circuits known as LasI/LasR and RhII/RhIR, respectively that work in tandem to control group behavior of a population (Figure 2.4).^{160,165,172,185,186} The LasI/LasR system functions similar to the homologous LuxI/LuxR QS-system of *Vibrio fischeri*. The LasI is the AHL synthase that catalyzes the synthesis of autoinducer N-(3-oxododecanoyl) homoserine lactone (PAI-1).¹⁶⁷ At a particular higher cellular density, the concentration of secreted PAI-1 is sufficient to exhibit effective binding to its cognate receptor protein, LasR.^{167,171} The LasR-PAI-1 complex initiates a signaling cascade that induces transcription of genes (like *lasB*, *lasA*, *apr*, and *toxA*) responsible for production of virulence factors.^{156,165,166,172,187,188} The LasR-PAI-1 complex also auto regulates the *lasI* gene and directs it to synthesize more PAI-1, thus the name autoinducer is assigned to the N-acyl homoserine lactone (PAI-1) molecule.^{156,165,166,172,187,188} Additionally, the LasR-PAI-1 complex also activates the expression of *rhII* and *rhIR* genes.¹⁸⁹ The gene product of *rhII*, RhII catalyzes the synthesis of a second autoinducer, N-(butanoyl) homoserine lactone (PAI-2), which upon binding its cognate receptor protein, RhIR activates additional specific

target genes including *rhlAB* (Figure 2.4).¹⁸⁹ The *rhlAB* operon encodes for the synthesis of rhamnolipids, a class of biosurfactants crucial for swarming motility.¹⁸⁹ Therefore, the LasI-LasR/RhlI-RhlR two component quorum sensing system in *P. aeruginosa* regulates a cell density dependent expression of various virulence genes. The expression of such virulence genes includes secretion of toxins such as exotoxin A and exoenzyme S, proteases such as elastase, LasA protease, secretion of alginate, formation of biofilm, induction of swarming and production of surface wetting agents such as rhamnolipids.

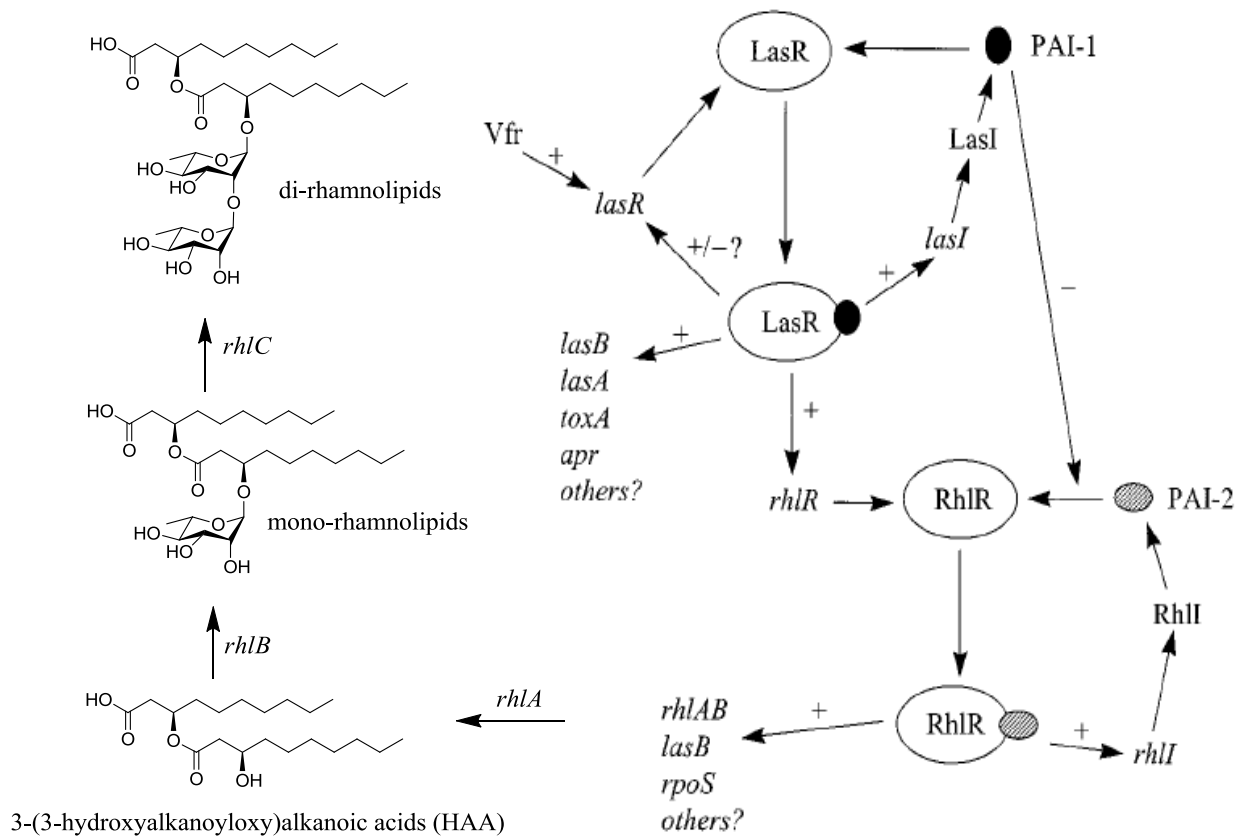


Figure 2.4 Biosynthesis of rhamnolipids by *P. aeruginosa*. The two-component LasI-LasR/RhlI-RhlR quorum sensing circuit of *P. aeruginosa* controls expression of various virulence genes, including biofilms formations, swarming and rhamnolipids biosynthesis

[Adapted and modified with permission from Citation:¹⁷¹ E C Pesci, (1997), "Regulation of *las*

and *rhl* quorum sensing in *Pseudomonas aeruginosa*” *Journal of Bacteriology* (179), 3127-3132; Copyright: 1997, American Society for Microbiology.]

2.1.5.4 *Quorum sensing regulates synthesis of biosurfactant rhamnolipids*

Rhamnolipids are glycolipid biosurfactants secreted by *P. aeruginosa*. These molecules play crucial role in maintaining biofilm architecture and assisting swarming.^{123,190,191} The PAI-2/RhlR complex activates the genes in the *rhlAB* operon.¹⁷⁴ The gene product of *rhlA*, RhlA catalyses the synthesis of 3-(3-hydroxyalkanoxy)alkanoic acids (HAA).^{174,189} RhlB is the rhamnosyltransferase protein encoded by the *rhlB* gene which catalyses the reaction between dTDP-L-rhamnose and HAA to yield monorhamnolipids. A second rhamnosyltransferase RhlC encoded by the *rhlC* gene adds the second dTDP-L-rhamnose moiety to mono-rhamnolipids, thereby synthesizing di-rhamnolipids (Figure 2.4).¹⁹² The composition of the biosurfactant released by *P. aeruginosa* during swarming is usually a mixture of the different congeners that include di-rhamnolipids, mono-rhamnolipids and their intermediate precursor HAA.

2.1.5.4.1 *Role of biosurfactant rhamnolipids in swarming*

Multiple scientific reports indicate that rhamnolipids secreted by *P. aeruginosa* play an important role in the two social activities displayed by bacteria, i.e swarming^{121,123,181} and biofilm formation.¹⁹¹ Scientific work elaborating the role of rhamnolipids in swarming is presented in this chapter, whilst work highlighting rhamnolipids' role in biofilm formation will be discussed in the next chapter (chapter 3, Section 3.1.3)

Kohler and coworkers used isogenic derivatives of wild type *P. aeruginosa* strain PT5 in which either of the four crucial quorum sensing genes were inactivated i.e, *lasI*, *lasR*, *rhlI*, or *rhlR*.¹²³ Their findings revealed that the mutants having inactivated *lasI* and *lasR* exhibited

reduced swarming after prolonged incubation on semisolid swarm gels (0.5-0.7 % agar) where as *rhlI* and *rhlR* mutants were completely unable to swarm. Kohler and coworkers findings led them to hypothesize that certain factors under the control of quorum sensing genes was crucial for swarming. Since rhamnolipids have surface activity properties that could be crucial in the surface motility, and since production of rhamnolipids is directly under the control of the *rhl* cell-to-cell signaling system, Kohler and coworkers further studied the surface motility of mutant *rhlA*. The mutant *rhlA* strain PT712 which is deficient in the production of rhamnolipids but can synthesize the quorum sensing signaling molecule, N-(butanoyl) homoserine lactone (PAI-2) was completely incapable of swarming on semisolid gel. Co-inoculating the *rhlA* mutant strain PT712 with wild type strain PT5 that can synthesize rhamnolipids, reinstated the swarming in the mutant strain. By this experiment, Kohler and coworkers identified the presence of rhamnolipids as being crucial for swarming motility in *P. aeruginosa*.

The unique feature that a population of swarming *P. aeruginosa* cells exhibit is the formation of a fractal-like pattern on the swarm plate, where many tendrils formed by the bacterial population exude out from the central point of inoculation (Figure 2.5g). O' Toole and coworkers were the first to demonstrate that the production of rhamnolipids were important for maintaining tendril formation and preventing colonization between tendrils.¹¹⁹ They observed that tendrils from two different swarming colonies avoided each other and when a nonmotile mutant of *P. aeruginosa*, *flgK* was placed in the course of a wild type swarm colony, the tendrils of the swarmer colony proximal to *flgK* mutant radiated away suggesting that both the wild type and *flgK* mutant secrete extracellular factors that cause repulsion between two colonies. Also, they observed that when wild type strain was inoculated onto a swarm plate containing spent supernatant prepared from a *rhlA* colony, the wild type strain swarmed normally, but when

grown with supernatant from a wild type colony, there was no swarming. The *rhlA* mutant is unable to synthesize di-rhamnolipids, its precursor mono-rhamnolipids and HAA and is also a nonswarming strain (Figure 2.5 k). To evaluate the effect of each component on swarming, they further constructed mutants *rhlB* and *rhlC* lacking the rhamnosyltransferase necessary to generate mono-rhamnolipid and di-rhamnolipid, respectively. The swarming patterns of wildtype had a radial array of fine tendrils, where as both *rhlB* and *rhlC* swarmed with short, thick and irregular tendrils, suggesting that di-rhamnolipids were important for pattern formation. They further showed that when both wild type and *flgk* mutant (nonswarming control) were co-inoculated on plates containing spent supernatant from either *rhlB* or *rhlC* mutant, the wild type did exhibit swarming with *rhlC* supernatant but no swarming with supernatant from *rhlB* mutant. With their study, O' Toole and coworkers reported that since the *rhlC* mutant can produce mono-rhamnolipids and *rhlB* mutant cannot, monorhamnolipids are the minimum component to cause swarming inhibition of wild type.

Deziel and coworkers made a deeper analysis of the role of each component from rhamnolipids biosynthesis (i.e HAA, mono-rhamnolipids and di-rhamnolipids) in creating swarm patterns of *Pseudomonas aeruginosa*.¹²¹ Deziel *et al* isolated and used pure HAA, mono-rhamnolipids and di-rhamnolipids in their experiments. They reported that the tendrils of a wild type *Pseudomonas aeruginosa* (PA14) swarmer colony get attracted to a paper disk soaked with di-rhamnolipids and move away from a disk soaked with HAA (Figure 2.5 a & c). Further Deziel *et al* exogenously added drops of either di-rhamnolipids, mono-rhamnolipids or HAA on the center of swarm plates and then inoculated these plates with either wild type strain or the *rhlA* mutant. Their experiments showed that HAA inhibited the swarming of wild type and caused no restoration of swarming in the *rhlA* mutant (Figure 2.5 f & j, respectively). Mono-rhamnolipids

facilitated the formation of tendrils in wild type and dispersion of bacteria away from the swarm center and no biomass accumulation at the center for the *rhlA* mutant (Figure 2.5 e & i, respectively). Contrary to HAA, di-rhamnolipids promoted formation of fine tendrils and biomass accumulation at the swarm center for both wildtype and the *rhlA* mutant (Figure 2.5 d & h, respectively). With these experiments, Deziel and coworkers concluded that, with respect to the active swarming cells, di-rhamnolipids act as attractants, HAA act as repellants and that mono-rhamnolipids are mere surface wetting agents (Figure 2.5b).

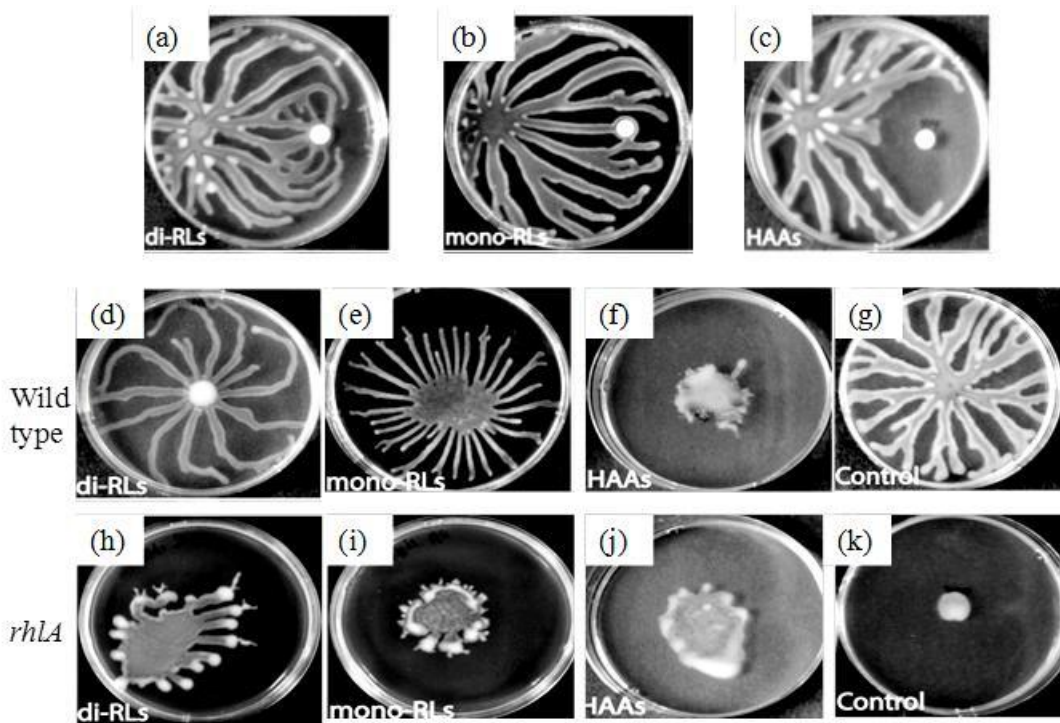


Figure 2.5 Swarming pattern of either wild type PA14 or its *rhlA* mutant. Wild type PA14 inoculated on agar plates containing discs of either di-rhamnolipids, monorhamnolipids or HAA (a, b, and c, respectively). Swarm plates containing either dirhamnolipids or monorhamnolipids or HAAs or no agent inoculated with either wild type PA14 (d, e, f and g, respectively) or the *rhlA* mutant (h, i, j and k, respectively) [Adapted and modified with permission from Citation:¹²¹ Deziel, E., Self-produced extracellular stimuli modulate the *Pseudomonas aeruginosa* swarming

motility behavior. *Environ. Microbiol.* **2007**, 9, (Copyright (C) 2013 American Chemical Society (ACS). All Rights Reserved.), 2622-2630.

In order to postulate a theory for the formation of tendrils by swarming *Pseudomonas aeruginosa* cells, Deziel and coworkers further tested the rate of diffusion for di-rhamnolipids and HAA on agar plates. The results indicated that di-rhamnolipids diffuse faster and further on the agar plate as compared to HAA. Hence when swarmer cells are present at the center of an agar plate, the continuous secretion of di-rhamnolipids and HAA creates a positive concentration gradient of di-rhamnolipids/HAA. Since di-rhamnolipids diffuses faster in the agar and is an attractant for active swarming cells, there is a positive drive to move away from the slower diffusing repellent HAA. The occurrence of this positive concentration gradient creates tendrils which become more and more distinct as the cells migrate outward under continuously evolving di-rhamnolipids/HAA concentration gradient (Figure 2.6).

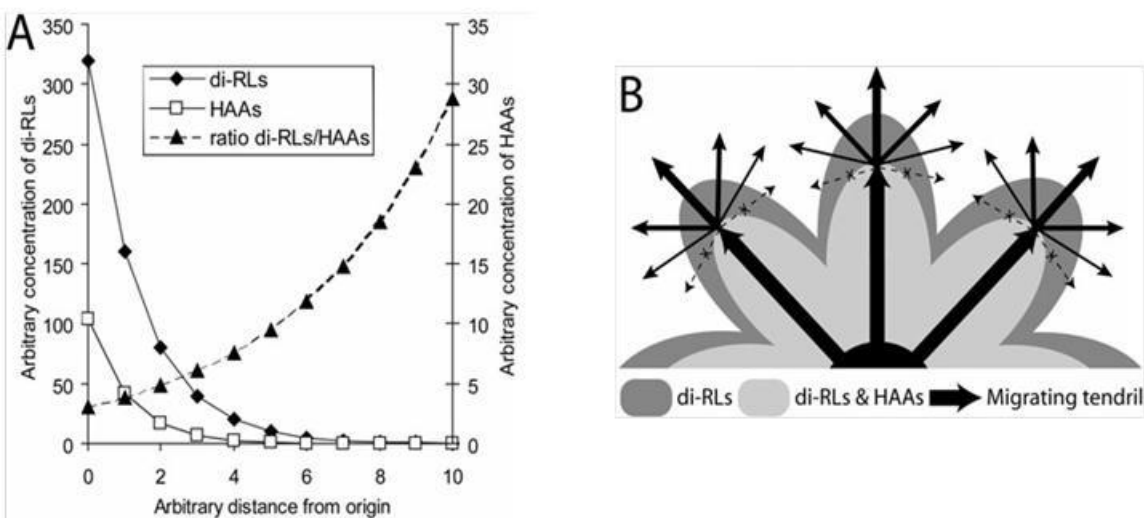


Figure 2.6 (a) Diffusion rate for di-rhamnolipids and HAA on agar plates. (b) Positive concentration gradient of di-rhamnolipids/HAA maintains tendril pattern [Reprinted with permission from Citation:¹²¹ Deziel, E., Self-produced extracellular stimuli modulate the

Pseudomonas aeruginosa swarming motility behavior. *Environ. Microbiol.* **2007**, 9, (Copyright (C) 2013 American Chemical Society (ACS). All Rights Reserved.), 2622-2630.

2.1.6 Concentration dependent activity reversal phenomenon previously reported for bacterial cell-signaling molecule

Photobacterium fischeri is a marine bacteria that can emit visible light through a biochemical process known as bioluminescence.^{120,193} The bioluminescence in *Photobacterium fischeri* is controlled by the luciferase enzyme which is under the control of the quorum sensing system LuxI-LuxR.^{29,118,147,155} The LuxI-LuxR quorum sensing system is in turn activated by the cell-signaling molecules (AHLs) whose production increases in proportion to bacterial population. Upon activation, the luciferase enzyme catalyzes the oxidation of a long-chain aldehyde (RCHO) and reduced flavin mononucleotide (FMNH₂)¹⁹³ resulting in the release of excess free energy in the form of blue-green light at 490nm.

Eberhard and coworkers in the classical paper isolate and characterize N-(3-oxohexanoyl)-3-aminodihydro-2(3H)-furanone (acyl homoserine lactone, AHL) as the cell signaling molecule that controls the quorum sensing of *Photobacterium fischeri*.¹²⁰ In this work, Eberhard and coworkers demonstrated that both natural and synthetic AHLs molecules were able to simulate light production in *Photobacterium fischeri*. They also performed a dose-dependent study to understand effect of AHL concentration on light production. On doing a dose-response curve with synthetic AHLs, the bioluminescence increased over the range 0.003-3 µg/mL and then decreased at higher concentrations (Figure 2.7).¹²⁰ The vague explanation the authors provided to describe this "activity reversal" is that the production of luciferase enzyme probably decreases as the bacteria reach the stationary phase. However, since it was first reported, the mechanism of how such an "activity reversal" operates appears to have been overlooked.

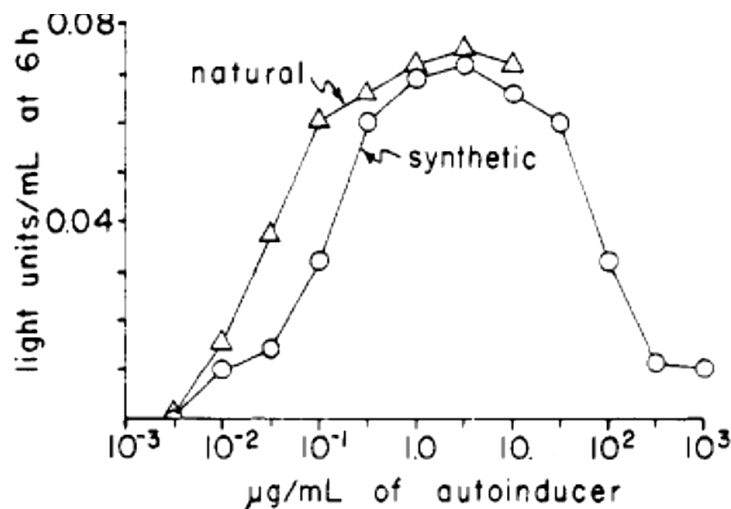


Figure 2.7 Dose-response curve for simulation of light production with increasing concentration of acyl homoserine lactone (AHL). Bioluminescence increased over the range 0.003-3 µg/mL and then decreased at higher concentrations. [Reprinted with permission from Citation:¹²⁰ Eberhard, A.; Burlingame, A.; Eberhard, C.; Kenyon, G.; Nealson, K.; Oppenheimer, N., Structural identification of autoinducer of *Photobacterium fischeri* luciferase. *Biochemistry* **1981**, 20, (9), 2444-2449.

2.2 Results and discussion

2.2.1 Design of synthetic saccharide derivatives library

The initial thought was to investigate if rhamnolipids exhibit a mere physical effect on swarming or whether their secretion is correlated with a more complex biological process. Rhamnolipids and its congeners are glycolipids biosurfactants and the amphiphiles have a disaccharide polar head group and greasy aliphatic tail. Due to the amphiphilic structure of rhamnolipids the initial inclination was to evaluate the effect of different types of generic surfactants (anionic, cationic, and nonionic) on bacterial swarming.¹⁹⁴ The generic surfactants that were used included two non ionic surfactants, dodecyl-β-maltoside (**DβM, 1**) and

tetra(ethylene glycol) monododecyl ether (**C₁₂EG₄OH**), one anionic surfactant, sodium dodecyl sulfate (**SDS**), and one cationic surfactant, dodecyl trimethylammonium chloride (**DTAC**). Since microbes possess the ability to recognize a diverse range of saccharide stereochemistries,¹⁹⁵⁻¹⁹⁹ the chemical library also included amphiphiles that had a stereochemistry other than rhamnose and an aliphatic chain different from rhamnolipids (Figure 2.8). The chemical library included three disaccharide stereochemistries, cellobiose (Glc β (1 \rightarrow 4)Glc β), maltose (Glc α (1 \rightarrow 4)Glc β) and lactose (Gal β (1 \rightarrow 4)Glc β), two monosaccharide stereochemistries, glucose (Glc β), and rhamnose (Rha α) and one large cyclic hepta-saccharide, β -cyclodextrin (β CD). The disaccharide derivatives (DSDs) comprising of maltose (Glc α (1 \rightarrow 4)Glc β)-based stereochemistry included dodecyl- β -maltoside (**D β M**), **1**; saturated farnesyl- β -maltoside (**SF β M**), **14**; and those comprised of cellobiose (Glc β (1 \rightarrow 4)Glc β)-based stereochemistry included dodecyl- β -cellobioside (**D β C**), **4**; decyl- β -cellobioside (**De β C**), **2**; undecyl- β -cellobioside (**U β C**), **3**; tridecyl- β -cellobioside (**T β C**), **5**; dodecyl- α -cellobioside (**D α C**), **6**; undecylenyl- β -cellobioside (**UD β C**), **10**; farnesyl- β -cellobioside (**F β C**), **11**; saturated farnesyl- β -cellobioside (**SF β C**), **12**; saturated farnesyl- α -cellobioside (**SF α C**), **13**; 2-octyl-dodecyl- β -cellobioside (**2-OD β C**), **16**; 2-octyl-dodecyl- α -cellobioside (**2-OD α C**), **17**; and that comprised of lactose (Gal β (1 \rightarrow 4)Glc β)-based stereochemistry included dodecyl- β -lactoside (**D β L**), **7**; saturated farnesyl- β -lactoside (**SF β L**), **15**. The monosaccharide derivatives (MSDs) included dodecyl- β -glucoside (**D β G**), **8**, and dodecyl- α -rhamnoside (**D α R**), **9**. To examine the effect of a large oligo-saccharide group, dodecyl- β -cyclodextrin (**D β CDS**), **18**, was synthesized. It is to be noted that the aliphatic derivatizations included derivatives with different length of hydrocarbons chains (**2**, **3**, **4**, **5**), different degree of aliphatic unsaturation (**10** and **11**), and possessing or lacking methyl branches

(1, 4, 6, 7, 12, 13, 14, 15). The methyl branched hydrocarbons were derived from hydrogenation of the farnesyl moiety to yield 3, 7, 11-trimethyl-dodecanyl group.

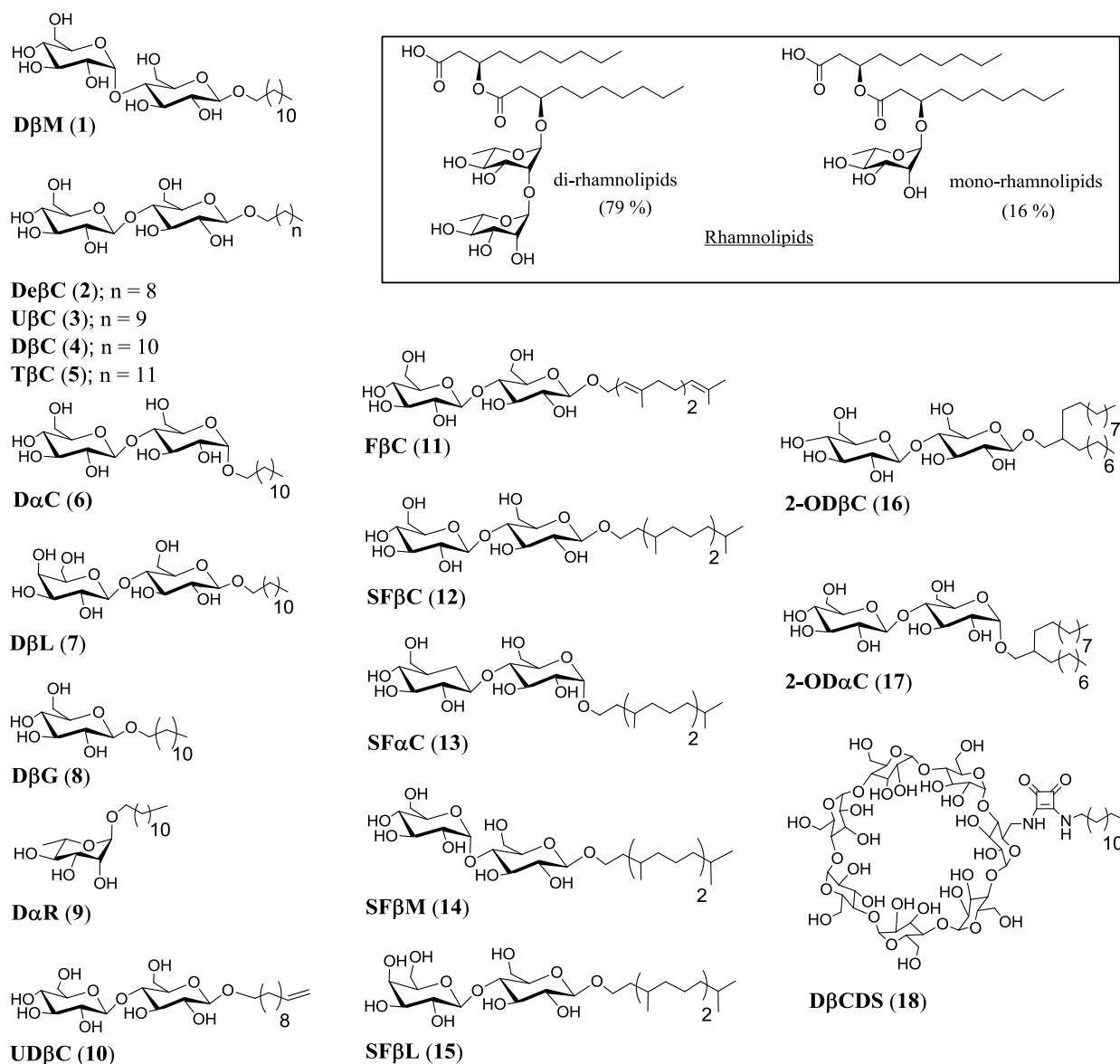
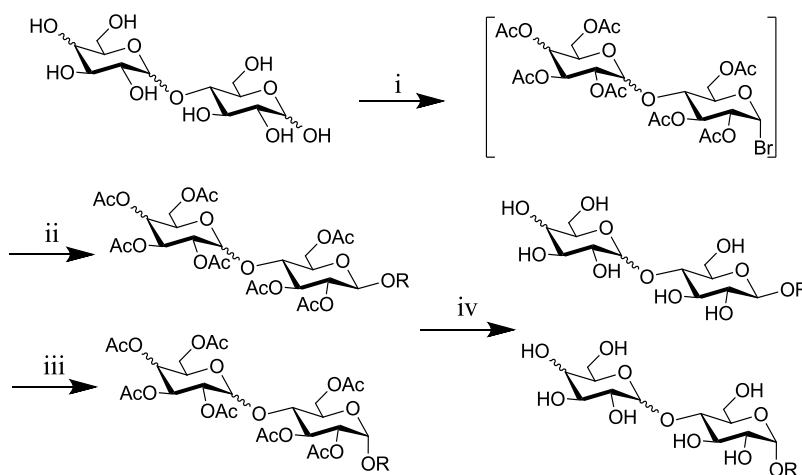


Figure 2.8. Structures of synthetic saccharide based derivatives that include maltose, cellobiose, lactose, glucose, rhamnose, and β -cyclodextrin stereochemistries; and hydrocarbons derived from farnesyl and “saturated” farnesyl molecules. The structures of di-rhamnolipid and mono-rhamnolipid are also shown.

2.2.1. 1 Synthesis of saccharide derivatives (SDs)

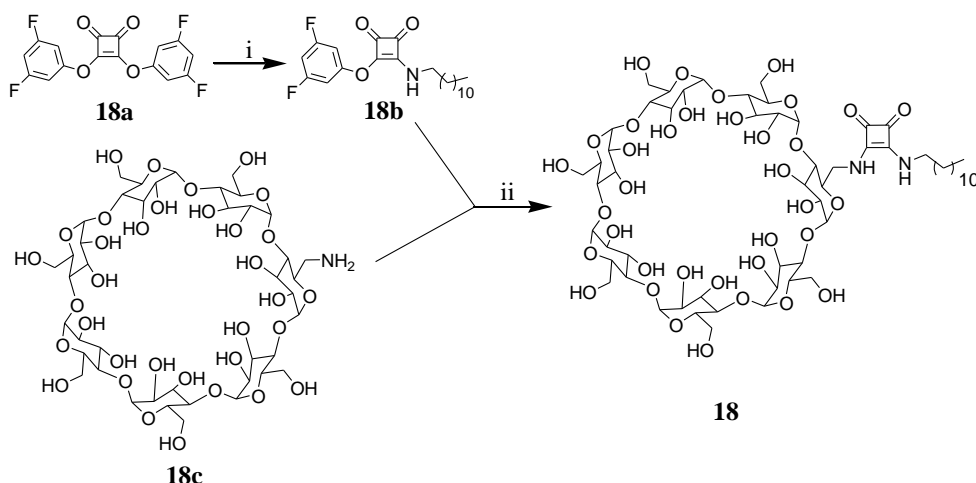
Most disaccharide and monosaccharide derivative were synthesized using the Fischer glycosylation and Zemplen deacetylation conditions mentioned in Scheme 2. 1.²⁰⁰ General synthetic route for the monosaccharide and the disaccharide derivatives involved the simultaneous peracetylation and monobromination at the anomeric position of desired sugar using a binary mixture of AcBr/AcOH, followed by Fischer glycosylation with either a synthetic or a commercially available alcohol in presence of Lewis acid catalyst. For obtaining β -anomer as the major glycosidation product, the solvent used was MeCN, where as substituting the solvent to MeNO₂ primarily gave α -anomer. The α/β anomers were purified with normal phase silica chromatography (β anomer usually eluted first). The per-acetylated saccharide-derivatives were deacetylated using Zemplen deacetylation conditions of methanolic sodium methoxide solution and neutralized further to pH ~6.5 with H⁺ ion-exchange amberlite resins.



Scheme 2.1. Synthesis of saccharide derivatives (SDs). (i) AcBr/AcOH, rt or 60 °C, ~ 1h; (ii) ROH, FeCl₃ or Hg(CN)₂, MeCN, rt, 1h; (iii) ROH, FeCl₃, MeNO₂, rt, 1h; (iv) MeONa/MeOH, 12h, H⁺ amberlite resin, Neutralize, (pH ~6.5).

2.2.1. 2 Synthesis of oligosaccharide derivative

The synthesis of the oligosaccharide derivative involved a longer six step convergent synthesis (Scheme 2.2). The intermediates **18a** and **18c** were synthesized via previously reported literature procedure.²⁰¹ Substituting one of the difluorophenoxy group on **18a** with dodecylamine yielded **18b**. Subsequently, the remaining difluorophenoxy group on **18b** was substituted with β CD-NH₂ over four days in a ternary solvent system comprising of water/DMF/acetone to yield D β CDS (**18**). The compound was purified by repeated precipitation from aqueous solution with acetone.



Scheme 2.2 Synthesis of β -cyclodextrin (β CD) based saccharide derivative

(i) CH₃(CH₂)₁₁NH₂, THF, -78^oC, ~ 12h; (ii) DMF, acetone, rt, 4days

2.2.2. All saccharide derivatives (SDs) were nontoxic to the growth of planktonic bacteria

At the onset it was necessary to establish that the observed impact of these molecules on swarming, and biofilm formation did not originate from the ability of these agents to impede bacterial growth. Also, establishing the nonmicrobicidal action was necessary to ascertain whether these SDs have the potential to change or control bacterial behavior with low or no propensity to invoke drug resistance.⁷⁷ Therefore, the initial test after synthesis of the SDs was to

check the toxicity of these agents on the growth of planktonic bacteria in culture media. The concentration (170 μM) of SDs chosen for the toxicity studies was either relatively higher than or equivalent to the highest concentrations at which all the other bioassays (swarming in this chapter, and inhibition of bacterial adhesion and biofilm formation in chapter 3) were done. At 170 μM none of the SDs inhibited the growth of planktonic wild type *Pseudomonas aeruginosa* (PAO1) in Luria-Bertani (LB) broth (Figure 2.9).

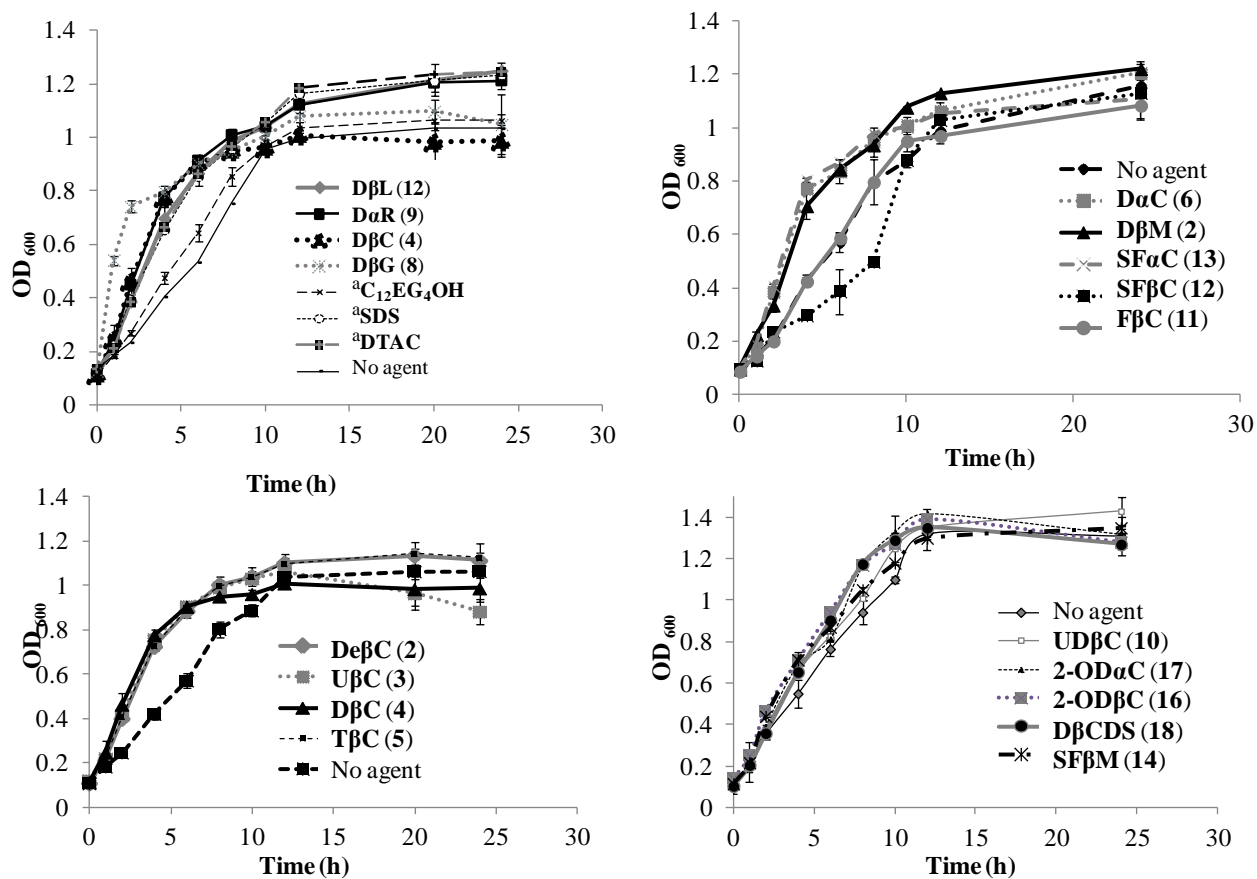


Figure 2.9 Growth curve (24 h) of PAO1 with or without agents to confirm that the effects on swarming and biofilm formation are not due to toxic effects. Resultant concentration of each agent within wells ~ 170 μM . ^aConcentration of agent ~ 110 μM .

2.2.3 The nonswarming mutant *rhlA* was used to screen swarming agonists and the wild type *P. aeruginosa* brought forward the swarming antagonists

Previously, in separate works both Deziel *et al*¹²¹ and O' Toole *et al*¹¹⁹ demonstrated that on supplementing the swarm agar plate (~0.5% agar) with exogenous rhamnolipids the swarming of the inoculated *rhlA* mutant was reactivated. These seminal works by others showed that either rhamnolipids were ligands for specific target proteins that control or activate swarming or that secretion of the biosurfactant rhamnolipids is simply required to reduce surface tension and enable swarming. To decipher what role rhamnolipids played in swarming (biological or physical) and to test whether the synthetic saccharide derivatives could mimic rhamnolipids, two kinds of swarming assays were constituted, swarming agonist and swarming antagonist.

A transposon mutation that impairs a gene in the rhamnolipids biosynthesis pathway of *P. aeruginosa* (PAO1) generates a rhamnolipids nonproducing and therefore a nonswarming mutant strain, *rhlA* (genotype, *rhlA*-E08::ISphoA/hah)^{123,202-204} Therefore, swarming agonist assays were constituted by adding various SDs into the swarm plates and then inoculating the plate with the *rhlA* mutant. Agents that can mimic the functions of rhamnolipids and thereby reactivate swarming in such a nonswarming mutant would therefore qualify as swarming agonists. Contrary to this, a swarming assay with wild type PAO1 where both the naturally secreted rhamnolipids and the externally added agent are present constitutes an antagonist assay because the wild type strain can inherently synthesize rhamnolipids,¹²³ therefore agents that have the ability to modulate swarming of such a strain will have to first compete with the natural ligand (rhamnolipids) for the putative receptor before exhibiting their effects. While inhibition of swarming by an added SD in such an antagonist swarming assay is a clear indicator of antagonistic behavior, a promotion of PAO1 swarming motility to form a bigger swarm ring is

more complex to interpret. Therefore, in the antagonist swarming assay, antagonistic behavior was primarily gauged by the ability to reduce or completely inhibit the swarming of wild type PAO1.

Firstly, the test of whether surface activity alone was critical for enabling swarming was performed by Shetye *et al* where, one anionic (**SDS**), one cationic (**DTAC**) and two nonionic (**C₁₂EG₄OH** and **DβM (1)**) generic surfactants were tested for their ability to reactivate swarming of the *rhlA* mutant, (screening for swarming agonists) (Figure 2.10a&b). The results indicated that when tested at 110 μM, three out of the four tested generic surfactants, anionic **SDS**, cationic **DTAC** and nonionic **C₁₂EG₄OH** were not able to reactivate the swarming of the *rhlA* mutant (Figure 2.10 d, e & f, respectively). However, when the disaccharide based nonionic surfactant, **DβM (1)** was added to the semisolid swarm gel at 110 μM, swarming of the inoculated *rhlA* mutant was fully restored and the swarm colony formed a pattern of radiating tendrils (Figure 2.10c).

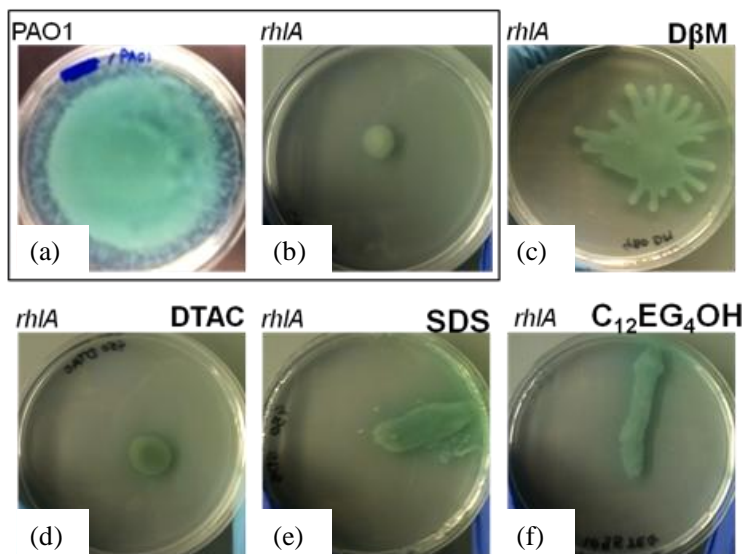


Figure 2.10 Images of swarm agar plates inoculated with either PAO1 (Control) or the *rhlA* mutant containing various generic surfactants. (a) Control swarm plate with no

surfactants inoculated with PAO1; Swarm plate inoculated with the *rhIA* mutant containing; (b) No agent; (c) D β M (1); (d) DTAC; (e) SDS and (f) C12EG4OH. Concentration of the generic surfactants in the swarm plates ~ 110 μ M. [Reprinted with permission from Citation:¹⁹⁴ Shetye, G. S.; Singh, N.; Jia, C.; Nguyen, C. D. K.; Wang, G.; Luk, Y.-Y., Specific Maltose Derivatives Modulate the Swarming Motility of Nonswarming Mutant and Inhibit Bacterial Adhesion and Biofilm Formation by *Pseudomonas aeruginosa*. *ChemBioChem* **2014**, 15, (10), 1514-1523.

2.2.4 Disaccharide derivatives and rhamnolipids exhibit dual functions of activating and inhibiting swarming motility of Pseudomonas aeruginosa

The antagonistic or agonistic effect of various SDs was initially screened at a constant concentration of 85 μ M, except for **D β C (4)** and rhamnolipids, for which results from 160 μ M and 30 μ M are shown, respectively (Figure 2.11). The commercially available rhamnolipids used in the swarming experiments contained two congeners of rhamnolipids, dirhamnolipids (79%) and monorhamnolipid (16%) (Figure 2.8). The average molecular weight of the rhamnolipids extract calculated by using the percent composition of each congener was 626 g/mol, and the rhamnolipids sample preparation for the swarming studies was done using this average molecular weight.

Based on the effects that the saccharide derivatives had on the swarming of both wt PAO1 and its *rhIA* mutant at 85 μ M, they can be classified into four groups (Figure 2. 11). Two SDs, **D β CDS (18)** and **UD β C (10)**, that exhibited no apparent effect on the swarming motility of both the wild type PAO1 and its *rhIA* mutant were categorized as group I. The two SDs that were categorized as group II, **De β C (2)** and **F β C (11)** showed weak swarming activation in *rhIA* mutant and slight promotion of the swarming motility in wild type PAO1. The results of one of the group II agents, **De β C (2)** shown in Figure 2.11 was the effect observable at a concentration

of 160 μM and at 85 μM , **De β C (2)** did not cause a noticeable effect on the swarming motility of either strains (Figure 2.12). It is noted that there was a complete abolition of bacterial growth (both PAO1 and *rhlA*) on the semisolid gel (~0.5 % agar) when **F β C (11)** was used at higher concentration of 160 μM (Figure 2.12). Contrary to the toxic effect on a swarm plate, there was no bacterial growth inhibition when planktonic PAO1 was grown in LB media containing 160 μM of **F β C (11)** (Figure 2.9).

All of the five disaccharide derivatives (DSDs) in group III, **D β M (1)**, **U β C (3)**, **D β C (4)**, **T β C (5)**, and **D α C (6)**, were able to cause significant tendrils formation in the swarm colony of the otherwise nontendrils forming wild type PAO1 strain.^{121,204,205} Without the presence of these five group III DSDs, the wild type PAO1 (control) swarms outward with a fairly circular front, but when the DSDs were added, the swarm pattern obtained contained protrusions that radially extended outward from the central spot of bacterial inoculation. The type of tendrils formed by wild type PAO1 in presence of these five DSDs also varied slightly. Two DSDs from group III, **D β M (1)** and **D β C (4)** created PAO1 swarm patterns having fine straight tendrils that protruded out from the center and these tendrils themselves did not branch out further. However, the three other DSDs in this group, **U β C (3)**, **T β C (5)** and **D α C (6)** caused the main radial tendrils to branch out and form a self-similar, fractal-like pattern (Figure 2.11). Among the DSDs in group III, three DSDs, **D β M (1)**, **U β C (3)** and **D β C (4)**, were able to fully reactivate the swarming of the *rhlA* mutant with a swarm area that was comparable to that of the wild type PAO1 without any agents (Control, Figure 2.11). The other two DSDs in group III, **T β C (5)** and **D α C (6)** at the tested concentration of 85 μM exhibited no apparent swarming activation of the *rhlA* mutant.

The group IV consisted of six DSDs, **D β G (8)**, **D α R (9)**, **SF β C (12)**, **SF α C (13)**, **SF β M (14)**, and **2-OD β C (16)** that at 85 μM were able to completely inhibit the swarming motility of

wild type PAO1 (Figure 2.11). Also, the six group IV DSDs at 85 μM concentration in the swarm plate exhibited no apparent effect on the inoculated *rhlA* mutant (Figure 2.11).

For the swarming studies done with the rhamnolipids extract at a concentration of 10 μM there was a ~38 % increase in the swarming area of the *rhlA* mutant. Also, when used at 30 μM , the rhamnolipids extract caused a ~51 % decrease in swarming area for wild type PAO1 (to see the calculation of how the swarming areas and percentage increase or decrease in areas were calculated, refer to Materials and Methods section). The change in percent swarming area was obtained by comparing the swarm area in presence of the agents to that by the wild type PAO1 under the same conditions with no added agents in the swarm plate (~0.5 % agar). Apart from changing the swarm pattern qualitatively, certain DSDs also had an impact on the swarm area of either or both PAO1 and the *rhlA* mutant. By measuring the increase in the swarming area, the DSDs grouped as II appear to promote swarming in both PAO1 and the *rhlA* mutant at 85 μM . The effect of group III DSDs was more complex because at 85 μM while they inhibit the swarming of PAO1 they seem to activate the swarming of the *rhlA* mutant. The DSDs in group IV at 85 μM drastically reduce the swarm area of PAO1 and have no apparent effect on the swarm area of the *rhlA* mutant (decrease in swarm area cannot be detected because the *rhlA* mutant is inherently nonswarming). Three DSDs, **DBL (7)**, **SF β L (15)** and **2-OD α C (17)** had poor water solubilities and therefore were not tested in the swarming agonist or antagonist assays.

Two important observations from the swarming studies done with various agents were (i) Rhamnolipids inhibit swarming of PAO1 at 30 μM whereas at 10 μM they activate or promote swarming of the *rhlA* mutant; (ii) The DSD **De β C (2)** seemed to promote swarming of PAO1 and activate swarming of the *rhlA* mutant only at relatively higher concentration (160 μM).

Because these two agents exhibited the dual functions of either activating or inhibiting swarming at different concentrations, it was speculated that the other SDs, in general would also possess these dual-functions, and may manifest different activities at different concentrations. Therefore, a concentration dependent study with selected SDs from various groups (II, III and IV) was done next.

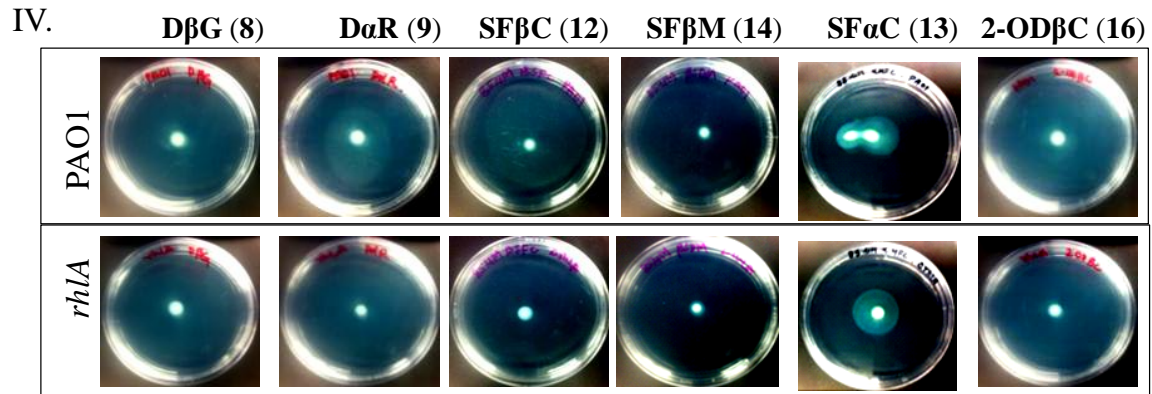
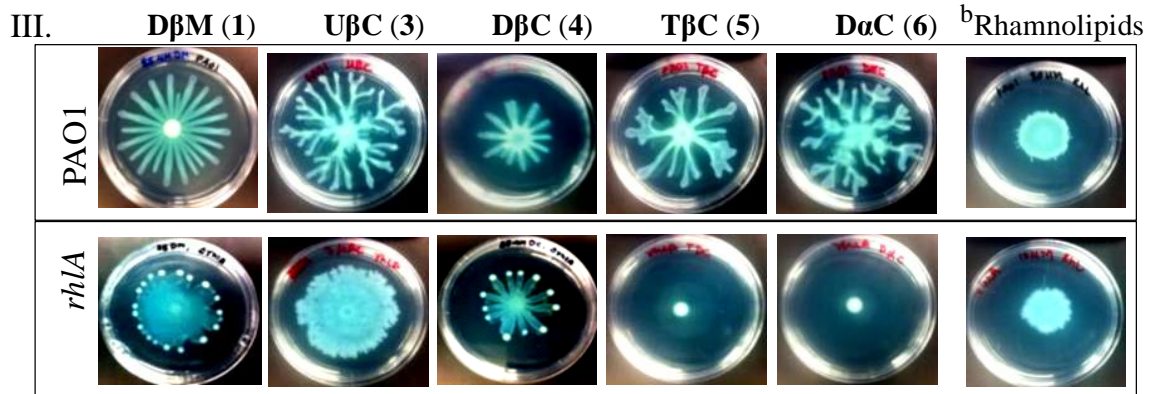
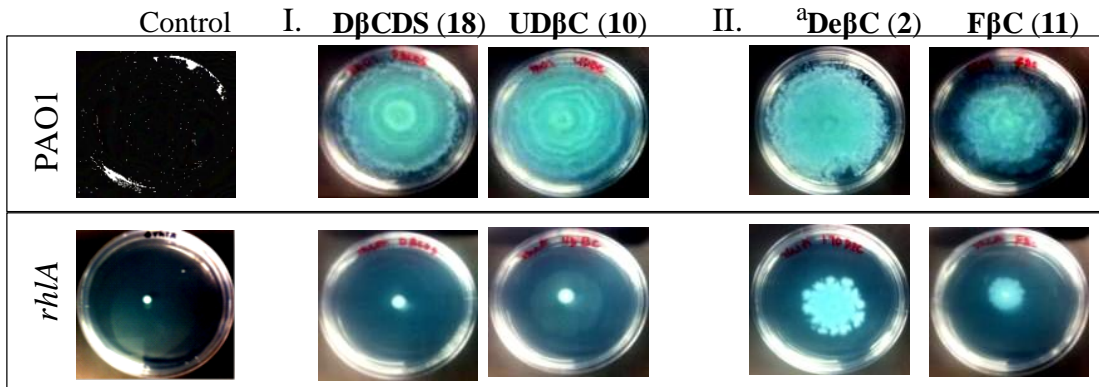


Figure 2.11 Four different types of swarming motility behaviors exhibited by wild type PAO1 and the *rhIA* mutant on semisolid gel (~0.5 % agar, M8 media) in presence of various DSDs (at ~85 μ M), except for ^aDe β C (2) (160 μ M), and ^bRhamnolipids (30 μ M for PAO1) and (10 μ M for *rhIA*). Controls are without added agents in the gel. Images were taken 24 h after inoculation with bacteria.

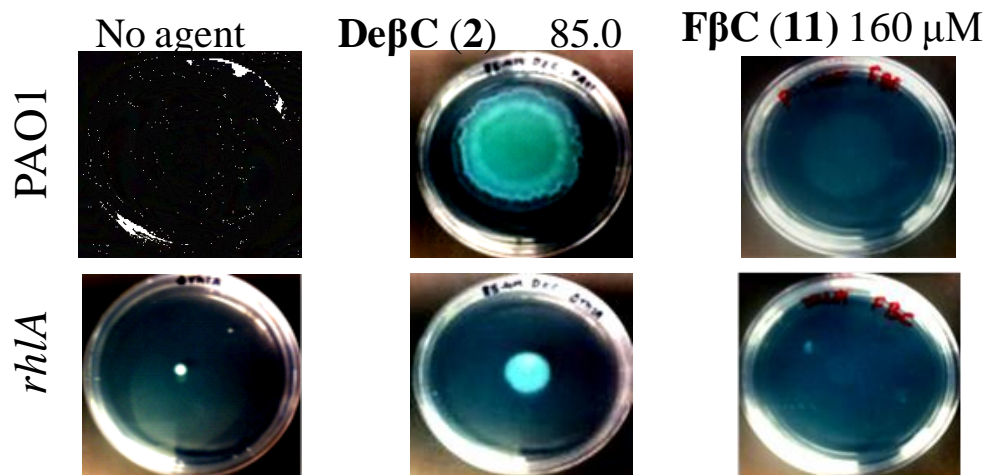


Figure 2.12 Semisolid gels (~0.5 % agar) with 0 (no agent) or 85 μ M concentration of De β C (2) or 160 μ M concentration of F β C (11) inoculated at the center with either *wt* PAO1 (row 1) or *rhIA* mutant (row 2). Images were taken 24 h after inoculation with bacteria.

2.2.5 Disaccharide derivatives and rhamnolipids exhibited “activity reversals” that transitioned from swarm-activating to swarm-inhibiting as the concentration was increased

The fact that concentration of the DSD determined the overall effect on swarming was clearly observable when a switch in **De β C (2)** concentration from 85 to 160 μ M increased the *rhIA* swarming area by ~38% with respect to swarming area of PAO1 without agents. The effect that different concentrations of either rhamnolipids or **De β C (2)** had on swarming of PAO1 and its *rhIA* mutant alluded to two opposites bioactivities – concentration dependent activation and

inhibition of swarming motilities. Comparison of the PAO1 swarm area on a plate with no added agent (~24 cm²) to a plate containing 85µM of DSD **DβC (4)** (~13 cm²), showed that swarm area decreased by a value of ~46 % (Figure 2.11). Therefore, intriguingly at 85µM, **DβC (4)** displayed the ability to both activate swarming in the *rhlA* mutant and at the same time cause an overall apparent inhibition for PAO1 swarming.

It has been reported before by Deziel and coworkers that the bacteria at the swarming tip are genetically different than bacteria in the swarm center (See section 2. 1. 5. 2).¹²⁴ The ability of certain group III DSDs, **DβM (1)**, **UβC (3)** and **DβC (4)** to activate the swarming of the *rhlA* mutant and also induce tendrils formation in PAO1 swarms suggested that newer bacterial phenotypes may be generated by different DSDs. It can be hypothesized that the tip of the tendril may be populated with swarming hyperactive and the stem of the tendril along with the center of the colony may be populated with hyposwarming phenotype, termed as "phenotypic bifurcation" here. To see if "phenotypic bifurcation" could be achieved by rhamnolipids and other DSDs and see if such an effect depends on the concentration of the agent in the plate, a dose-dependent study with rhamnolipids and selected DSDs from group II, III and IV was performed.

First, the concentration effect of the rhamnolipids extract on swarming of both PAO1 and its *rhlA* mutant was investigated. When the concentration of rhamnolipids in the swarm plate was increased from 0 to 5 µM, the swarming of the inoculated nonswarming *rhlA* mutant appeared to be reactivated; and the size of the PAO1 swarm ring appeared increase in area in comparison to the control (Figure 2.13, row 1). The trend in swarming reactivation for the *rhlA* mutant by rhamnolipids extract reversed at about 10 µM, at which concentration the size of the swarming ring was maximum (~9 cm²). The reversal in swarming activation beyond 10 µM ultimately

culminated with no observable swarming at 20 μM or higher by *rhlA* (swarm ring size was reduced to a dot). With PAO1, 10 and 15 μM of externally added rhamnolipids caused the swarming rings to appear larger than the control (with no added agents), but with 30 μM of added rhamnolipids, a significant reduction in the swarming ring was observed. Quantitatively, with 30 μM of rhamnolipids in the swarm plate, the wild type PAO1 covered an area of $\sim 11 \text{ cm}^2$ and with no rhamnolipids the swarm area was $\sim 24 \text{ cm}^2$. This observation indicated that, as the concentration of rhamnolipids is gradually increased, a shift from swarm-activation to swarm-inhibition occurs. The occurrence of an activity reversal with increasing ligand concentration has also been reported for another bacterial multicellular behavior, simulated light production by *Photobacterium fischeri* (section 2.1.6). In this classical work, Eberhard and coworkers had demonstrated that when the concentration of the AHL (ligand) is gradually increased, the production of light by *Photobacterium fischeri* first increases, reaches a threshold and ultimately decreases.

Similar to the effects that rhamnolipids extract had, the active DSDs (Group II, III and IV from Figure 2.11) also caused swarming promotion at lower concentration and swarming inhibition at relatively higher concentration. The dose-dependent swarming results with five DSDs using wild type PAO1 and its *rhlA* mutant are summarized in Figure 2.13. The images of swarming plates in Figure 2.13 containing various concentrations of DSDs clearly show the transitions from swarming activating to swarming inhibiting for both bacterial strains. For all the active DSDs, the concentrations at which the swarming transitioned from being activated or promoted to deactivated or inhibited for *rhlA* and PAO1, respectively were different. In general, the concentrations at which the swarming activity reversed (from activated to deactivated) for the *rhlA* mutant were slightly lower than the concentrations at which swarming of PAO1 were

inhibited (Table 2.1). Apart from this, the DSDs themselves could be classified into two categories; those that caused an early swarming "activity reversal" at lower concentration and those caused a late "activity reversal" at relatively higher concentrations (Figure 2.13 & Table 2.1). The low transition concentration agents included rhamnolipids, **SFβM (14)** and **SFβC (12)** that caused an activity reversal for the *rhlA* mutant at 10 μM, 10 μM and 8 μM; and swarming inhibition for PAO1 at 20-30 μM, 7-20 μM, 10-20 μM, respectively. The DSDs with high transition concentration, DSDs **DβC (4)**, **TβC (5)** and **DβG (8)** exhibited the activity reversal at 45-56 μM, 40 μM and 35 μM for the *rhlA* mutant; and swarming inhibition for PAO1 at 20-30 μM, 20-30 μM and 35-50 μM, respectively. As visible in the swarming images with *rhlA* mutant (Figures 2.13), the low transition agents, **SFβC (12)**, **SFβM (14)** and rhamnolipids created smaller swarming rings in comparison to the agents with high transition concentration, **DβC (4)**, **TβC (5)** and **DβG (8)**. These results imply that agents with poor swarming inhibition capabilities (for PAO1) were better swarming activators (for the *rhlA* mutant) than agents that had strong potencies to inhibit the swarming of PAO1. Another observation that the dose-response study brought forward was that certain DSDs beyond the transition concentration were able to induce tendrils formation while others were not. Amongst the plates inoculated with the *rhlA* mutant, only **DβC (4)** induced tendrils formation around ~56 μM (Figure 2.13); whereas for the plates inoculated with PAO1, tendrils formation was caused by **DβC (4)** at 20 μM, **TβC (5)** at ~30 μM, **SFβM (14)** at ~2 μM and **SFβC (12)** at ~1μM (Figure 2.13).

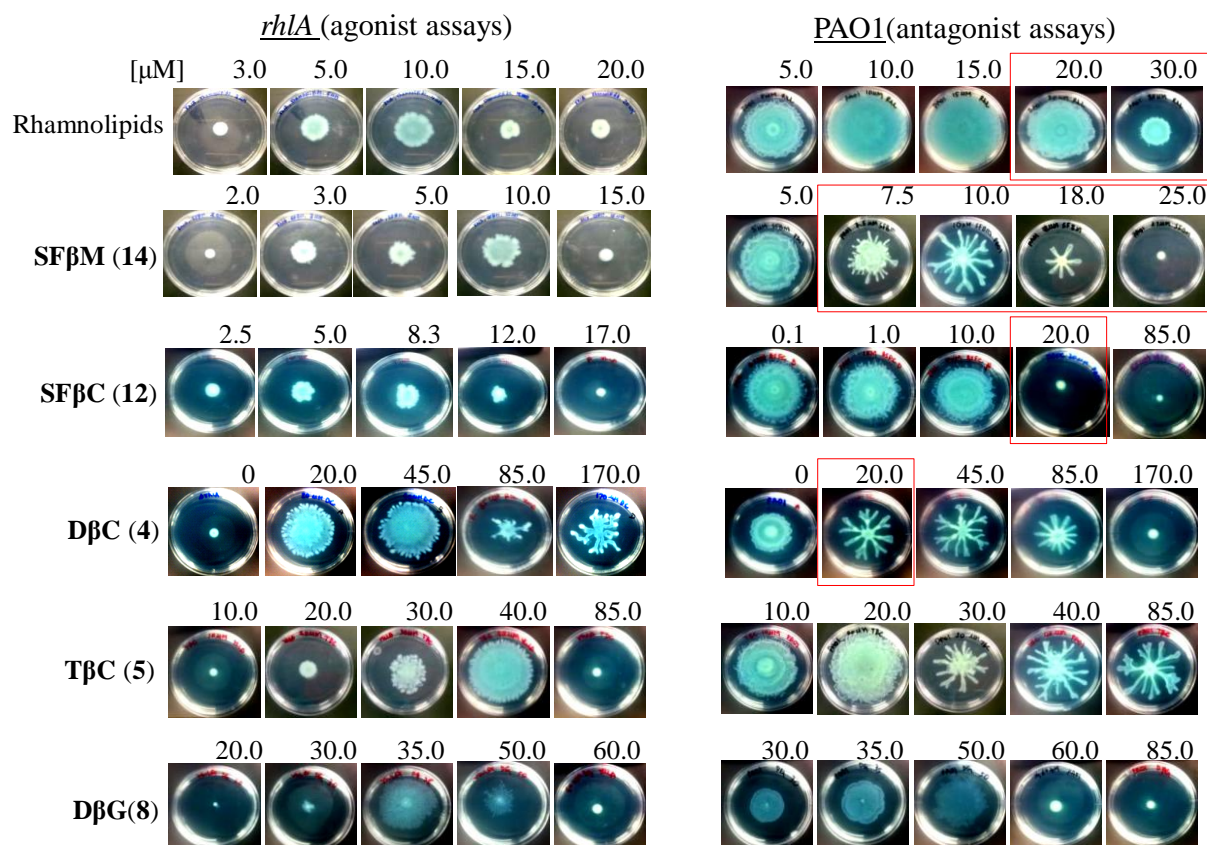


Figure 2.13 Images of swarming motilities of the *rhIA* mutant (left) and PAO1 (right) on semisolid gel (~0.5 % agar) containing increasing concentrations of DSDs and rhamnolipids. The concentrations are indicated above the images, and the identities of the agents are shown to the left. Red boxes highlight the swarming patterns that reveal the dominance of DSDs over rhamnolipids at comparable concentrations.

The swarming patterns of *rhIA* with additional concentrations of D β C (4), and T β C (5) apart from those included in Figure 2.13 are shown in Figure 2.14. Interestingly, quantitative measurement of the *rhIA* mutant's swarm areas with these two DSDs, D β C (4), and T β C (5), indicated that after the first activity reversal around 50 μM , there was a second increase in swarm area at a higher concentration of 160 μM (Figure 2.14). This increase, then decrease followed by another increase in swarming area of the *rhIA* mutant in response to the changing concentrations

of the two DSDs is indicative of an oscillatory response by the bacteria.²⁰⁶ Overall the dose-response study indicated that both rhamnolipids and the active DSDs possess the unique dual abilities to both activate swarming at lower concentration, an agonistic behavior as well as inhibit swarming at relatively higher concentrations, an antagonistic behavior.

Table 2.1. Transition concentrations of DSDs that exhibit activity reversal from activating to inhibiting swarming motilities of the *rhlA* mutant and PAO1.

Compound	^a Transition concentration (<i>rhlA</i>)	^b Transition concentration (PAO1)
Rhamnolipids	~10-15 μM	~20-30 μM
SFBM (14)	~10-15 μM	~7.5-25 μM
SFBC (12)	~8-12 μM	~10-20 μM
D β C (4)	^c ~45-56 μM	~20-30 μM
T β C (5)	~40 μM	~20-30 μM
D β G (8)	~35-50 μM	~50-60 μM
SF α C (13)	^c --	^c --

^aFrom activating to inhibiting swarming motility of the *rhlA* mutant. ^bFrom promoting to inhibiting swarming motility of PAO1; ^cNot determined.

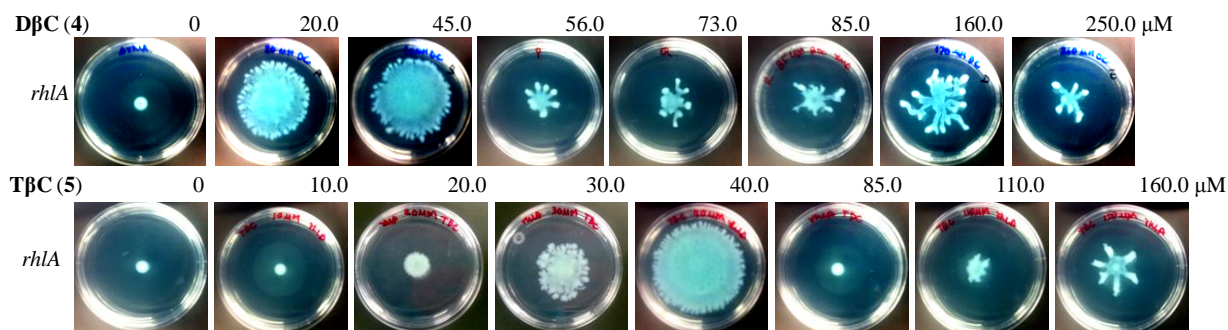


Figure 2.14 Swarm agar plates with additional concentrations of D β C (4) or T β C (5) for

their effects on the swarming of the rhlA mutant. Both the DSDs caused swarming “activity reversal.” Nonswarming mutant rhlA was inoculated at the center of the semisolid gels (~0.5 % agar). Pictures were taken 24 h after inoculation with bacteria.

2.2.6 Disaccharide derivatives, SFβC (12), SFβM (14) and DβC (4) dominated rhamnolipids at inhibiting the swarming motility of PAO1

The activation-to-inhibition “activity reversal” effect on swarming in response to concentration of both rhamnolipids and some DSDs suggests a regulatory response by PAO1 to such agents.¹²⁰ On evaluating the potencies of the active DSDs, two separate dominating effects over rhamnolipids seem to stand out. Firstly, the swarming motility of wild type PAO1 that is facilitated by *in situ* secretion of natural rhamnolipids was inhibited by all the five DSDs tested, i.e. **SFβC (12)**, **SFβM (14)**, **DβC (4)**, **TβC (5)**, and **DβG (8)**. The concentrations at which each of these DSDs dominated and inhibited the *in situ* produced rhamnolipids were different, with **SFβC (12)**, **SFβM (14)**, **DβC (4)**, being more potent than **TβC (5)** and **DβG (8)** (Figure 2.13, right column and Figure 2.15). Secondly, for PAO1, three DSDs, **SFβC (12)**, **SFβM (14)** and **DβC (4)** exhibited stronger swarming inhibition than externally rhamnolipids at the same concentrations. The dominance of **SFβC (12)** over externally added rhamnolipids is evident at 20 μM, where at this concentration **SFβC (12)** completely reduced the swarmer colony to a dot occupying an area of 1.2 cm² which is about 5% of the 24 cm² exhibited by PAO1 without any added agents; at this concentration, the external rhamnolipids caused no apparent swarming inhibition and the swarm area was equivalent to the control (i.e. 24 cm²) (Figure 2.13). Apart from this, as tendrils formation amounts to an overall reduction in swarming area, two other DSDs **SFβM (14)** and **DβC (4)** at concentrations lower than 20 μM exhibited stronger swarming inhibition of wild type PAO1 than externally added rhamnolipids. Additionally, the unique

characteristic of DSDs, **SFβM (14)** and **DβC (4)** to induce tendrils and cause phenotypic bifurcation of wild type PAO1 swarms was also not achieved by the externally added rhamnolipids at the tested concentration range (1-30 μM). A prominent activation dominance of DSD **SFβM (14)** over externally added rhamnolipids was also exhibited by the *rhIA* swarm colony. When the areas of swarm colonies at 10 μM of either **SFβM (14)** or external rhamnolipids were compared, the **SFβM (14)** caused swarming activation to generate a ring of ~38 cm² whereas only a 9 cm² ring was observed for rhamnolipids (Figure 2.13 and Figure 2.15). When viewed together, these results highlight that DSDs, **SFβC (12)**, **SFβM (14)** and **DβC (4)** are more potent than both the *in situ* produced (and secreted) and the externally added rhamnolipids. The *rhIA* swarming results with increasing concentrations of rhamnolipids and one DSD, **SFβM (14)** was repeated three times to obtain an error bar for swarming area at each concentration (see Materials and Methods, Figure S1).

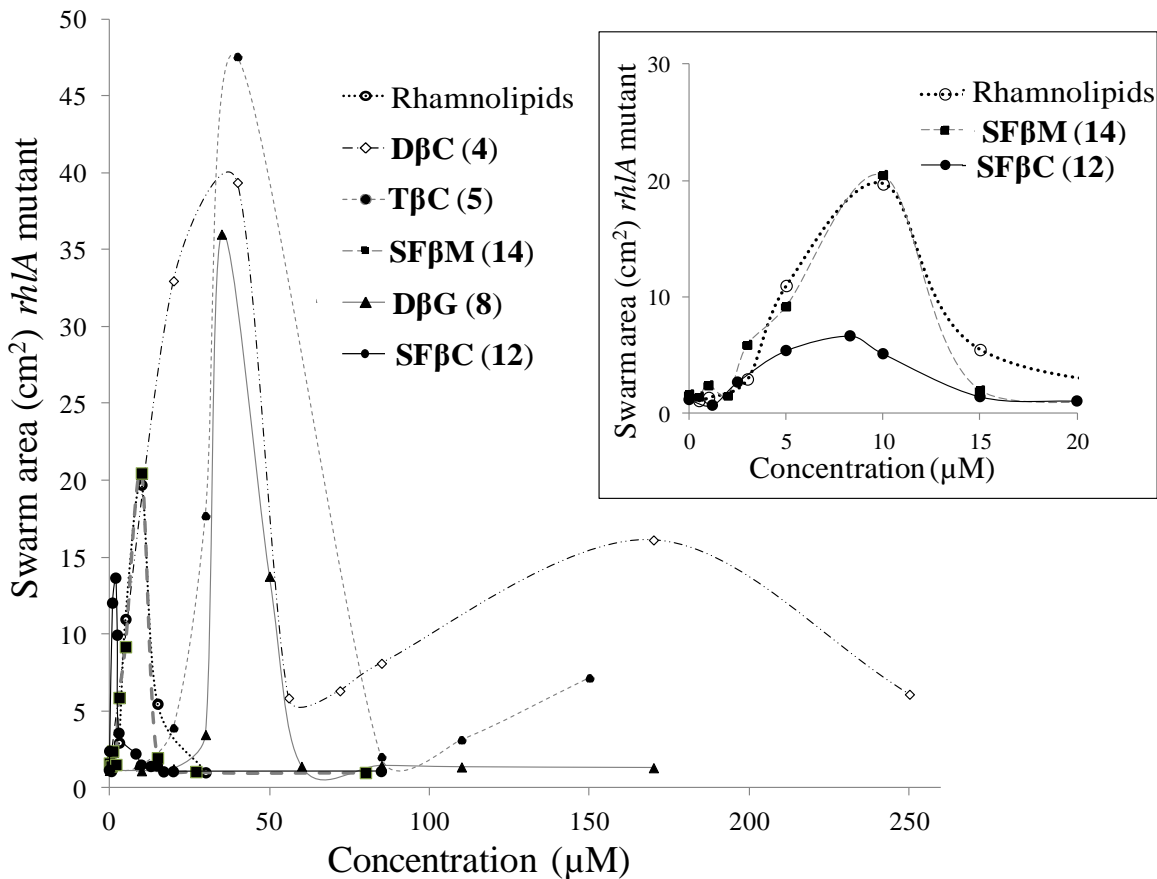


Figure 2.15 Plot of the *rhlA* mutant's swarm area (after 24 h) versus increasing concentrations of rhamnolipids, DβC (4), TβC (5), SFβM (14), DβG (8) and SFβC (12) in the semisolid gel (~ 0.5% agar). Insert shows the curves that had low transition concentrations from swarm-activating to swarm-inhibiting. (Also see Materials and Methods, Figure S1)

2.2.7 Competition assays indicated SFβC (12) to be a stronger swarming inhibitor than DβC (4)

While results indicate that both SFβC (12) and DβC (4) could activate and inhibit the swarming motility of *P. aeruginosa*, SFβC (12) had a lower transition (from activating to inhibiting) concentration than DβC (4) (Table 2.1). From the previous dose-dependence study (Figure 2.13), it was evident that 20 μM of SFβC (12) did not activate the swarming motility of the *rhlA* mutant. However, from these results it was difficult to speculate whether at this

concentration (20 μM), **SF βC (12)** had an inhibiting effect or whether it had no effect on the swarming of the *rhlA* mutant. **SF βC (12)** did inhibit the swarming motility of wild type PAO1 at 20 μM and hence there was some indication that the corresponding effect on the *rhlA* mutant may be primarily inhibition and not no effect. Contrary to the effect of **SF βC (12)**, the swarming activation of the *rhlA* mutant by 40 μM **D βC (4)** was quite unambiguous. Considering the results of these DSDs, it was hypothesized that the DSDs with low transition concentrations for the “activity reversal” dominated the DSDs with high transition concentrations. In order to validate this hypothesis, a competitive swarming assay was constructed where both **D βC (4)** and **SF βC (12)** were introduced into the swarming gel. For this swarming assay, the bacteria of choice was the *rhlA* mutant primarily because it lacks production of rhamnolipids and hence the swarming results would be unambiguous. In the competition swarming assay the concentration of **D βC (4)** was kept constant at 40 μM in all the plates, but the concentration of **SF βC (12)** was incrementally increased from 0.5 to 10, 20, and 40 μM (Figure 2.16) from one plate to another. The competition assay demonstrated that when 10 μM of **SF βC (12)** was added into the gel containing 40 μM of **D βC (4)**, there was no inhibition of *rhlA* swarming activation. But when the concentration of **SF βC (12)** was increased to 20 μM , the swarming activation brought about by 40 μM of **D βC (4)** was completely inhibited. Parallel to what was hypothesized, this result suggested that **SF βC (12)** (having low transition concentration) is a stronger antagonist than **D βC (4)** (having relatively higher transition concentration) for the putative swarming receptor. Also, the experiment confirmed that **SF βC (12)** has a dominating effect on swarming at high enough concentrations for both wild type PAO1 and its *rhlA* mutant.

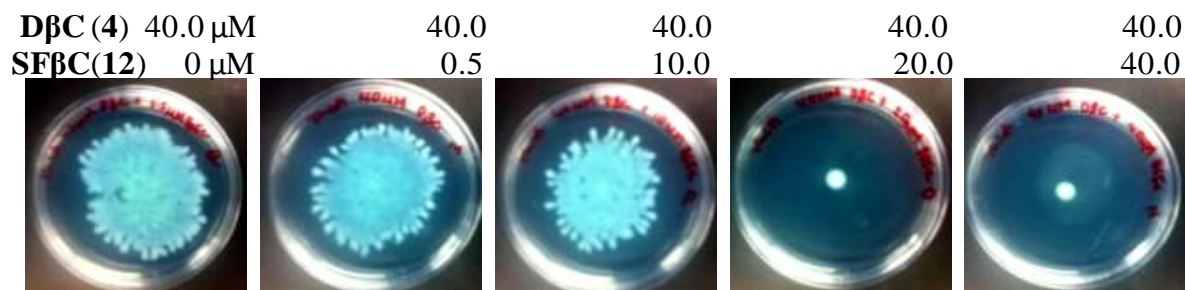


Figure 2.16 Images of the *rhlA* mutant inoculated on semisolid surface (~0.5 % agar) containing 40 μM of DβC (4) and increasing concentrations of SFβC (12). The images were taken 24 hours after inoculation of the surface with bacteria.

2.3 Conclusion

A surfactant having a saccharide head and an aliphatic tail, **DβM (1)** was the only generic surfactant that reactivated the swarming of the *rhlA* mutant. These swarming results with generic surfactants showed that while surface activity may be important for swarming, not any surfactant could instill swarming in the *rhlA* mutant. Amongst the saccharide derivatives (SDs), few specific structures showed the ability to activate and inhibit the swarming motility of both *P. aeruginosa* and its nonswarming mutant *rhlA*. For controlling swarming motility, all the active DSDs and the rhamnolipids extract exhibited a dual function that transitioned from swarm-activating at low concentrations to swarm-inhibiting at higher concentrations. Certain DSDs, **SFβC (12)**, **SFβM (14)** and **DβC (4)** were able to dominate the effect of both *in situ* produced (and secreted) and the externally added rhamnolipids. The dominance of these DSDs over rhamnolipids is probably a result of better binding to putative swarming receptor or the ability to bind effectively to an allosteric site on the receptor. Competition swarming assay revealed that a DSD with lower transition concentration (**SFβC (12)**) was a better antagonist than a DSD with higher transition concentration **DβC (4)**. Results implied that secretion of rhamnolipids is sensed

by the bacteria and the binding of these rhamnolipids to the putative swarming receptor relays a biological response. Results also demonstrated that certain DSDs are the functional analogues of rhamnolipids and that certain DSDs overpower the effects of rhamnolipids.

2.4 Materials and methods

General experimental information for synthesis

Standard solvents and reagents were purchased from commercial sources (Sigma-Aldrich, Fisher, Acros) and used as received. Solvents were removed *in vacuo* using Büchi rotary evaporator below 40°C. EMD silica gel 60 F254 pre-coated plates (0.25-mm thickness) were used for TLC. Unless otherwise stated, TLC visualization was done using ceric ammonium molybdate (CAM) stain. ¹H-NMR spectra were recorded in deuterated NMR solvents at 300 and 400 MHz (¹H-NMR) and 75 and 100 MHz (¹³C-NMR) Bruker instruments respectively. ¹H chemical shifts are reported in ppm relative to CDCl₃ δ 7.26, D₂O δ 4.80, or CD₃OD δ 3.31. ¹³C chemical shifts are reported relative to CDCl₃ δ 77.23 and CD₃OD δ 49.0. Couplings are reported in hertz (Hz). HRMS was obtained through positive ESI on Bruker 12 Tesla APEX-QE FTICR-MS with an Apollo II ion source, at Cosmic instrumentation center, Virginia. Unless otherwise stated, the % yield indicates the pure anomeric products that were successfully isolated by column chromatography resolution (the yield for mixture of anomers has not been accounted for). Anomeric configurations are assigned from the magnitude of J_{1,2} (7–9 Hz for the diaxial coupling, β-configuration; 2–4 Hz indicates equatorial-axial coupling, α-configuration).²⁰⁷

MALDI-TOF.²⁰¹ Matrix Assisted Laser Desorption Ionization Mass Spectrometry (MALDI-MS). A saturated solution of 2,4,6-trihydroxyacetophenone monohydrate (matrix) (10 mg) was prepared in acetonitrile (1 mL). The saturated βCD compound solution (in water) and matrix

solution in 1:1 ratio were spotted on a MTP 384 target ground steel plate (Bruker Daltonics, Billerica, MA). Mass spectra were obtained on a Bruker AutoFlex III instrument (Bruker Daltonics, Billerica, MA). Molecular ion peak was detected in positive ion linear mode.

Synthetic procedures and spectral data. The synthetic procedures and spectral data for the compounds used in this work are given below.

Synthesis of per-acetylated-bromo-sugars (Scheme 1). The synthesis of saccharide derivatives was done by using a reported literature procedure with some modifications.²⁰⁸ Briefly, to an oven dried round bottom flask, disaccharide (maltose, lactose and rhamnose) (1.0 g, 2.8 mmol), AcBr (~3.6 mL, 44.4mmol), and AcOH (19 mL) were added and stirred at room temperature (25 °C) for ~ 1 h. Reaction mixture was concentrated *in vacuo* at 35 °C and then co-evaporated three times with PhMe (2×10 mL, anhydrous). After removal of solvent, the flask was further heated *in vacuo* at 50 °C for 15min to give a foamy solid, aceto-bromo sugars. The crude aceto-bromo sugars were immediately used in next step without any further purification.

The synthesis of per-acetyl-bromo cellobiose was done under more vigorous conditions. In an oven dried round bottom flask cellobiose (1.0 g, 2.8 mmol), AcBr (~7.2 mL, 88.8 mmol), and AcOH (19 mL) were added and stirred at 60 °C for ~ 1 h. The work up of aceto-bromo cellobiose (**4b**) involved similar steps as done for aceto-bromo lactose/rhamnose to obtain crude as foamy solid. The crude aceto-bromo sugars were immediately used in next step without any further purification.

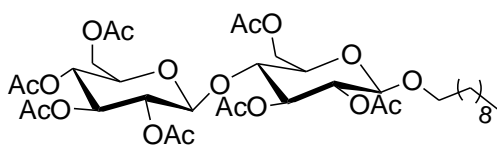
General synthesis of n-alkyl glycosides (cellobiosides, maltoside, rhamnoside and lactoside)

For obtaining β -anomer as major product, the crude aceto-bromo sugars were the dissolved in MeCN (10 mL) and various alcohols (5.6 mmol, 2 equiv) were added along with two equivalents

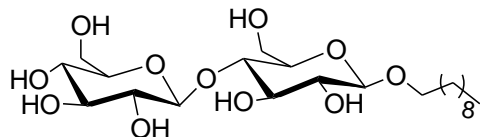
of FeCl_3 or $\text{Hg}(\text{CN})_2$. The α -anomers were obtained as major products by using MeNO_2 as solvent. The reaction mixture was stirred vigorously for about ~45-60 min at rt. After stirring at rt, aq KBr (10%, 25 mL) and then PhMe (60 mL) were added under stirring. The organic phase was washed twice with aq KBr (10%, 2 \times 25 mL), once with aq NaHCO_3 (5%, 25 mL) and twice with H_2O (2 \times 25 mL). The crude product was then purified by column chromatography using gradient elution (100 % hexane to 35 % ethyl acetate in hexane).

Zemplén deacetylation. For all acetylated sugar derivatives, the deprotection of acetyl groups were achieved by Zemplén deacetylation using MeONa/MeOH (10 mM solution) conditions followed by neutralization (pH ~6.5) over H^+ amberlite resins. The resins were filtered off and products dried under high vacuum overnight.

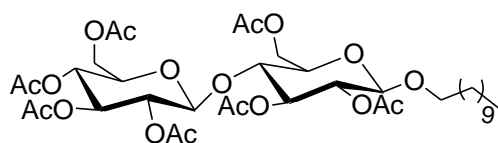
Spectral data



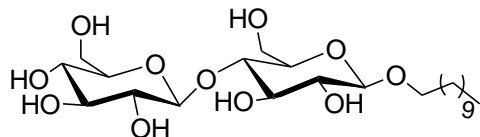
Acetylated decyl- β -cellobioside, ADef β C (2a) Colorless powder, 0.302 g, 19.7 % (2-step), $R_f =$ (0.30, 40 % EtOAc in Hexane). ^1H NMR (300 MHz, CDCl_3): δ 5.21 (m, 3H), 4.92 (q, $J_{1-2} = 8.4$ Hz, 2H), 4.54-4.43 (m, 3H), 4.39 (dd, $J_{1-3} = 12.9$ Hz, $J_{1-2} = 4.8$ Hz, 1H), 4.13-4.02 (m, 2H), 3.87-3.74 (m, 2H), 3.69-3.56(m, 2H), 3.44 (q, $J_{1-2} = 8.4$ Hz, 2H), 2.13-1.99 (s, 7 X 3H), 1.57-1.48 (m, 2H), 1.26 (br, s, 14 H), 0.88 (t, $J = 6.3$ Hz, 3H). ^{13}C NMR (75 MHz, CDCl_3): δ 170.0, 169.9, 169.8, 169.1, 168.8, 168.6, 100.3, 100.2, 72.5, 72.2, 72.1, 71.5, 71.2, 69.8, 67.3, 61.5, 61.1, 31.4, 29.1, 29.1, 28.9, 28.8, 28.8, 25.3, 22.2, 20.4, 20.1, 20.1, 13.6. HRMS (ESI) m/z : Calcd. ($\text{C}_{36}\text{H}_{56}\text{O}_{18}$) Na^+ : 799.3358; Found: 799.3339, Difference: -2.4 ppm.



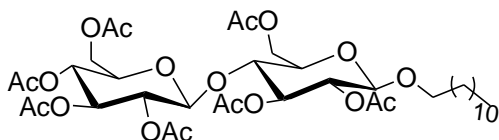
Decyl- β -cellobioside, De β C (2): Colorless powder, 0.025 g, 87 %. ^1H NMR (300 MHz, CD_3OD) δ : 4.36 (d, $J = 7.8$ Hz, 1H), 4.28 (d, $J = 7.8$ Hz, 1H), 3.87 (br, s, 4H), 3.69-3.47 (m, 4H), 3.40-3.31 (m, 4H, overlapping with MeOH), 3.27-3.18 (m, 2H), 1.68-1.56 (m, 2H), 1.30 (br, s, 14H), 0.91 (t, $J = 6.6$ Hz, 1H). ^{13}C NMR (75 MHz, CD_3OD): δ 102.8, 102.4, 78.9, 76.3, 76.0, 74.6, 73.1, 73.0, 69.5, 69.2, 60.6, 60.0, 31.3, 29.1, 29.0, 28.9, 28.9, 28.8, 28.7, 25.3, 21.9, 12.7. HRMS (ESI) m/z : Calcd. $(\text{C}_{22}\text{H}_{42}\text{O}_{11})\text{Na}^+$: 505.2619; Found: 505.2611, Difference: -1.5 ppm



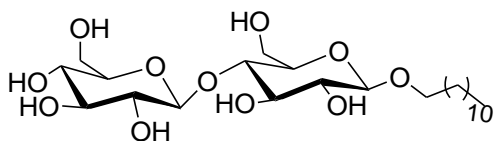
Acetylated undecyl- β -cellobioside, AU β C (3a): Colorless powder, 0.313 g, 13.5 % (2-step), $R_f = 0.52$, 1:1 Hexane:EtOAc). ^1H NMR (300 MHz, CDCl_3): δ 5.16-4.96 (m, 3H), 4.90-4.81 (m, 2H), 4.51-4.27 (m, 4H), 4.02 (t, $J = 13.2$, 2H), 3.84-3.67 (m, 2H), 3.65-3.49 (m, 2H), 3.46-3.24 (m, 1H), 2.07-1.89 (s, 7 x 3H), 1.57-1.31 (m, 2H), 1.20 (br, s, 16H), 0.82 (br, s, 3H). δ 170.0, 169.9, 169.8, 169.8, 169.81, 168.8, 168.5, 100.4, 95.1, 72.6, 71.4, 71.2, 71.1, 70.6, 69.3, 68.2, 67.6, 67.3, 61.1, 61.0, 31.4, 29.1, 28.8, 28.8, 28.7, 25.5, 25.3, 22.2, 20.4, 20.2, 20.1, 20.0, 13.6. HRMS (ESI) m/z : Calcd. $(\text{C}_{37}\text{H}_{58}\text{O}_{18})\text{Na}^+$: 813.3545; Found: 813.3496, Difference: -2.4 ppm



Undecyl- β -cellobioside, U β C (3): Colorless powder, 0.024 g, 84 %. ^1H NMR (300 MHz, MeOD) δ : 4.38 (d, $J = 7.8$, 1H), 4.25 (d, $J = 7.8$, 1H), 3.91 (br, s, 4H), 3.79-3.68 (m, 1H), 3.58-3.44 (m, 3H), 3.39-3.26 (m, 2H, overlapping with MeOD), 3.25-3.15 (m, 2H). ^{13}C NMR (75 MHz, CD_3OD): δ 102.8, 102.4, 78.9, 76.3, 76.0, 74.6, 73.1, 73.0, 69.5, 69.2, 60.6, 60.0, 31.3, 29.0, 29.0, 28.8, 28.7, 25.3, 22.0, 12.7. HRMS (ESI) m/z : Calcd. ($\text{C}_{23}\text{H}_{44}\text{O}_{11}$) Na^+ : 519.2776; Found: 519.276, Difference: -1.5 ppm

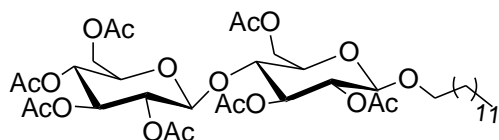


Acetylated dodecyl- β -cellobioside, AD β C (4a): Colorless powder, 0.330g, 14 % (2-step), $R_f =$ (0.47, 42% EtOAc in Hexane). ^1H NMR (300 MHz, CDCl_3): δ 5.19-5.01 (m, 3H), 4.90 (q, $J_{1-2} = 8.1$ Hz, 2H), 4.50-4.40 (m, 3H), 4.10-4.00 (m, 2H), 3.82-3.72 (m, 2H), 3.66-3.55 (m, 2H), 3.43 (q, $J_{1-2} = 2.7$ Hz, 1H), 2.10-1.96 (s, 7 X 3H), 1.50 (br, s, 2H), 1.23 (br, s, 18H), 0.86 (t, $J = 6.6$ Hz, 3H). ^{13}C NMR (75 MHz, CDCl_3): δ 170.1, 169.9, 169.8, 169.5, 169.2, 168.9, 168.7, 100.4, 100.3, 76.2, 72.5, 72.2, 72.1, 71.5, 71.2, 69.8, 67.3, 61.5, 61.1, 31.5, 29.3, 29.2, 29.2, 29.2, 29.0, 29.0, 28.9, 28.8, 28.7, 25.4, 22.3, 14.1. HRMS (ESI) m/z : Calcd. ($\text{C}_{38}\text{H}_{60}\text{O}_{18}$) Na^+ : 827.3672; Found: 827.3665, Difference: -1.0 ppm

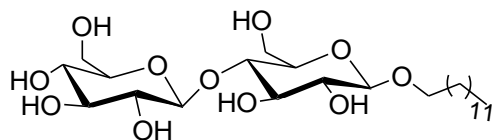


Dodecyl- β -cellobioside, D β C (4): Colorless powder, 0.082 g, 92.0 %. ^1H NMR (300 MHz, MeOD) δ 4.39 (d, $J = 7.5$ Hz, 1H), 4.26 (d, $J = 8.1$ Hz, 1H), 3.85 (br, s, 4H), 3.66-3.40 (m, 4H),

3.35-3.31 (m, 2H, overlapping with MeOD), 3.29-3.16 (m, 2H), 1.65-1.54 (m, 2H), 1.27-1.22 (br, s, 18 H), 0.88 (t, $J = 7.5$ Hz, 3H). ^{13}C NMR (75 MHz, CD_3OD): δ 102.8, 102.4, 78.9, 76.3, 76.0, 74.6, 73.1, 73.0, 69.5, 69.2, 60.6, 60.0, 31.3, 29.0, 28.9, 28.8, 28.7, 25.3, 21.9, 12.7. HRMS (ESI) m/z : Calcd. $(\text{C}_{24}\text{H}_{46}\text{O}_{11})\text{Na}^+$: 533.2932; Found: 533.2931, Difference: <-1.0 ppm

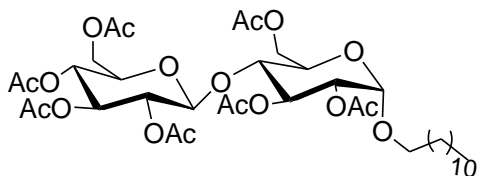


Acetylated tridecyl- β -cellobioside, AT β C (5a): Colorless powder, 0.345g, 14.4 % (2-step), $R_f = (0.50, 1:1$ Hexane: EtOAc). ^1H NMR (300 MHz, CDCl_3) δ 5.16-4.98 (m, 3H), 4.85 (q, $J_{1-2} = 8.4$ Hz, 2H), 4.48-4.29 (m, 4H), 4.06 - 3.97 (m, 2H), 3.82 - 3.69 (m, 2H), 3.66 -3.50 (m, 2H), 3.44 - 3.34 (m, 1H), 2.07-1.93 (s, 7 X 3H), 1.56 -1.32 (m, 2H), 1.20 (br, s, 20 H), 0.83 (t, $J = 8.7$ Hz, 3 H). ^{13}C NMR (75 MHz, CDCl_3): δ 170.1, 169.9, 169.8, 169.5, 169.2, 168.9, 168.7, 100.4, 100.3, 76.2, 72.5, 72.2, 72.1, 71.5, 71.2, 69.9, 67.3, 61.5, 61.1, 31.5, 29.3, 29.2, 29.1, 28.9, 25.4, 22.3, 20.5, 20.3, 20.2, 13.7. HRMS (ESI) m/z : Calcd. $(\text{C}_{39}\text{H}_{62}\text{O}_{18})\text{Na}^+$: 841.3828; Found: 841.3808, Difference: <-2.3 ppm

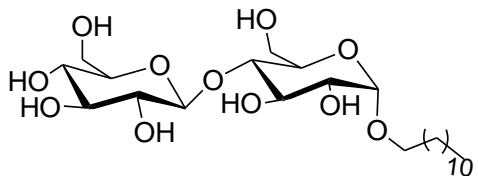


Tridecyl- β -cellobioside, T β C (5): Colorless powder, 0.052 g, 91.0 %. ^1H NMR (300 MHz, MeOD) δ 4.38 (d, $J = 7.8$ Hz, 1), 4.24 (d, $J = 7.8$ Hz, 1H), 3.83 (br, s, 4H), 3.62 (dd, $J_{1-3} = 12.0$ Hz, $J_{1-2} = 5.1$ Hz, 1H), 3.56-3.44 (m, 3H), 3.37-3.27 (m, 5H, overlapping with MeOD), 3.22-3.16 (m, 2H), 1.61-1.54 (m, 2H), 1.25 (br, s, 20 H), 0.86 (t, $J = 6.6$ Hz, 3H). ^{13}C NMR (75 MHz, CD_3OD): δ 102.8, 102.4, 78.9, 76.3, 76.0, 74.6, 73.1, 73.0, 69.5, 69.2, 60.6, 60.0, 31.3, 29.0,

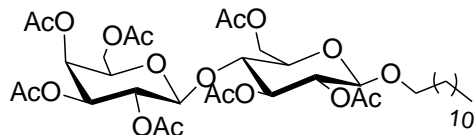
28.9, 28.8, 28.7, 25.3, 22.0, 12.7. HRMS (ESI) m/z: Calcd. (C₂₅H₄₈O₁₁)Na⁺: 547.3089; Found: 547.3080, Difference: <-1.5 ppm



Acetylated dodecyl- α -cellobioside, ADaC (6a): Colorless powder, 0.050 g, 2.1 % (2-step)}, R_f = (0.39, 42 % EtOAc in Hexane). ¹H NMR (300 MHz, CDCl₃): δ 5.46 (t, J = 8.4 Hz, 1H), 5.21 - 4.87 (m, 4H), 4.78 (dd, J_{1-3} = 10.8, J_{1-2} = 4.8, 1H), 4.56-4.34 (m, 3H), 4.16-3.87 (m, 4H), 3.73-3.63 (m, 3H), 3.44-3.35 (m, 1H), 2.13-1.99 (s, 7 x 3H), 1.65-1.56 (m 2H), 1.26 (br, s, 18 H), 0.88 (t, J = 7.2 Hz, 3H). HRMS (ESI) m/z: Calcd. (C₃₈H₆₀O₁₈)Na⁺: 827.3671; Found: 827.3663, Difference: -1.0 ppm. The spectroscopic data was consistent with a previously reported report.²⁰⁸

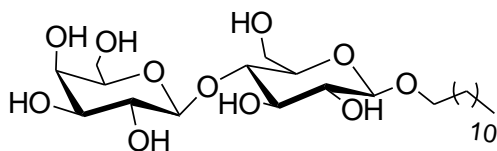


Dodecyl- α -cellobioside, DaC (6): Colorless powder, 0.010 g, 80.2 %. ¹H NMR (300 MHz, MeOD) δ 4.76 (d, J = 3.9, 1H), 4.39 (d, J = 7.8, 1H), 3.86 (t, J = 11.4, 2H), 3.79-3.76 (m, 1H), 3.71-3.63 (m, 2H), 3.60-3.43 (m, 3H), 3.40-3.31 (m, 5 H, overlapping with MeOD), 3.23 (t, J = 8.7, 1H), 1.72-1.56 (m, 2H), 1.29 (br, s, 18 H), 0.90 (t, J = 6.9, 3H). ¹³C NMR (75 MHz, CD₃OD): δ 100.4, 98.9, 72.4, 72.1, 71.3, 69.9, 69.6, 69.0, 68.0, 61.9, 61.1, 47.8, 31.5, 29.2, 29.0, 25.4, 22.3, 20.6, 20.5, 20.4, 13.7. HRMS (ESI) m/z: Calcd. (C₂₄H₄₆O₁₁)Na⁺: 533.2932; Found: 533.2931, Difference: <-1.0 ppm. The spectroscopic data was consistent with a previously reported report.²⁰⁸

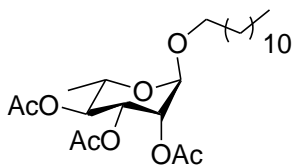


Acetylated dodecyl- β -lactoside, AD β L (7a): Colorless powder, 0.282 g, 12 % (2-step), Rf = (0.40, 1:1 Hexane:EtOAc). ^1H NMR (300 MHz, CDCl_3): δ 5.35 (d, $J = 0.6$ Hz, 1H), 5.34-5.08 (m, 2H), 4.97-4.85 (m, 2H), 4.46 (t, $J = 17.4$ Hz, 3H), 4.14-4.04 (m, 3H), 3.62-3.48 (m, 2H), 2.17-1.97 (s, 7 X 3H), 1.61-1.47 (m, 2H), 1.22 (br, s, 18 H), 0.88 (t, $J = 7.2$ Hz, 3H).

Spectroscopic data is consistent with reported literature.²⁰⁹ HR-MS: Calcd. $(\text{C}_{38}\text{H}_{60}\text{O}_{18})\text{Na}^+$: 827.3671; Found: 827.3677, Difference: < 1.0 ppm.

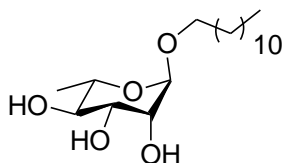


Dodecyl- β -lactoside, D β L (7): Colorless powder, 0.150 g, 85 %. ^1H NMR (300 MHz, CD_3OD): δ 4.29 (t, $J = 7.2$ Hz, 1H), 4.08 (t, $J = 6.6$ Hz, 1H), 3.92-3.78 (m, 3H), 3.75-3.66 (m, 5H), 3.55-3.44 (m, 5H), 3.41-3.32 (m, 2H overlapping with MeOD), 3.18 (dd, $J_{1-3} = 16.2$ Hz, $J_{1-2} = 3$ Hz, 2H), 1.66-1.55 (m, 2H), 1.29 (br, s, 18 H), 0.90 (t, $J = 7.2$ Hz, 3H). Spectroscopic data is consistent with reported literature.²⁰⁹ HRMS (ESI) m/z: Calcd. $(\text{C}_{24}\text{H}_{46}\text{O}_{11})\text{Na}^+$: 533.2932; Found: 533.2923, Difference: -1.7 ppm

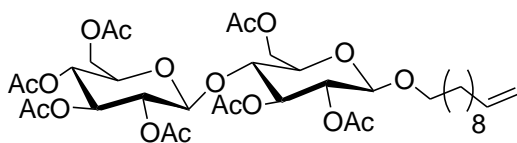


Acetylated dodecyl- α -rhamnoside, AD α R (9a): Colorless powder, 0.200 g, 7.3 % (2-step), Rf = (0.30, 40 %:EtOAc in Hexane). ^1H NMR (300 MHz, CDCl_3): δ 5.30 (dd, $J = 10.1, 3.7$ Hz, 1H),

5.23 (dd, $J = 3.7, 1.9$ Hz, 1H), 5.06 (t, $J = 9.9$ Hz, 1H), 4.71 (d, $J = 1.4$ Hz, 1H), 3.9–3.85 (m, 1H), 3.68–3.64 (m, 1H), 3.43–3.40 (m, 1H), 2.15–1.99 (s, 3 X 3H), 1.63–1.56 (m, 2H), 1.33–1.30 (m, 2H), 1.28 (br s, 16H), 1.22 (d, 3H), 0.88 (t, $J = 7.1$ Hz, 3H). Spectroscopic data is consistent with reported literature.²¹⁰

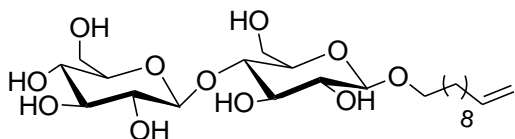


Dodecyl- α -rhamnoside, AD α R (9): Colorless powder, 0.03g, 12 % . ^1H NMR (300 MHz, CD_3OD): δ 4.62 (br, s, 1H), 3.76 (br, s, 1H), 3.67–3.52 (m, $\sim 3\text{H}$), 3.39–3.27 (m, 3H, overlapping with MeOD), 1.55–1.53 (m, 2H), 1.27 (br, s, 18 H), 1.24 (d, $J = 8$ Hz, 3H), 0.89 (t, $J = 6$ Hz, 3H). ^{13}C NMR (75 MHz, MeOD): δ 102.8, 102.4, 78.9, 76.3, 76.0, 74.6, 73.1, 73.0, 69.5, 69.2, 60.6, 60.0, 31.3, 29.0, 28.9, 28.8, 28.7, 25.3, 22.0, 12.7. ^{13}C NMR (100 MHz, CD_3OD): δ 104.2, 76.8, 76.5, 75.0, 74.9, 72.3, 71.8, 35.6, 33.3, 33.3, 33.3, 33.2, 33.1, 33.0, 29.9, 26.3, 20.5, 17.0. HRMS (ESI): Calcd. $(\text{C}_{19}\text{H}_{38}\text{O}_5)\text{Na}^+$ $\{[\text{M} + \text{Na}]^+ = 369.2611$; Found: 369.2610, Difference = < -1.0 ppm.



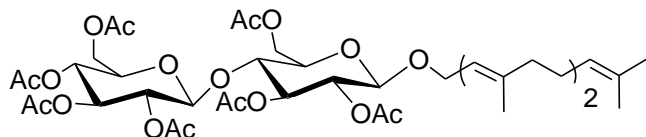
Acetylated undecylene- β -cellobioside, UD β C (10a): Colorless powder, 0.350g, 15.2 % (2-step), $R_f = (0.53, 60\%$ EtOAc in Hexane). ^1H NMR (300 MHz, CDCl_3): δ 5.88–5.74 (m, 1H), 5.21–5.02 (m, 4H), 4.95–4.86 (m, 3H), 4.52–4.42 (m, 3H), 4.37 (dd, $J_{1-3} = 12.3$ Hz, $J_{1-2} = 4.2$ Hz, 1H), 4.12–4.02 (m, 2H), 3.86–3.55 (m, 4H), 3.44 (q, $J_{1-2} = 6.6$ Hz, 1H), 2.13–1.98 (s, 7 x 3H), 1.57–1.40 (br, s, 2H), 1.34 (br, s, 12H). ^{13}C NMR (75 MHz, CDCl_3): δ 170.1, 169.9, 169.8,

169.4, 169.1, 168.9, 168.6, 138.7, 113.7, 100.3, 100.2, 72.5, 72.2, 72.1, 71.5, 71.2, 70.4, 69.9, 69.8, 67.3, 61.0, 33.3, 29.1, 29.0, 29.0, 28.9, 28.8, 28.7, 28.5, 25.3, 20.4, 20.2, 20.1, 20.1, 20.0.
 HRMS (ESI) m/z: Calcd. (C₃₇H₅₆O₁₈)Na⁺: 811.3359; Found: 811.3343, Difference: <-1.9 ppm

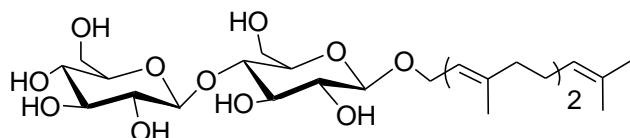


Undecylene- β -cellobioside, UD β C (10): Colorless powder, 0.200 g, 94.0 %. ¹H NMR (300 MHz, CD₃OD) δ 5.88-5.75 (m, 1H), 5.01 (d, J = 1.8 Hz, 1H), 4.96 (d, J = 1.8, 1H, overlapped with H₂O), 4.42 (d, J = 7.8, 1H), 4.29 (d, J = 7.8 Hz, 1H), 3.93-3.85 (m, 4H), 3.70-3.61 (m, 1H), 3.58-3.48 (m 3H), 3.41-3.31 (m 4H, overlapping with MeOD), 3.23-3.20 (m, 2H), 2.05(q, J_{1-2} = 6.6 Hz, 2H), 1.62 (q, J_{1-3} = 13.5 Hz, J_{1-2} = 6.6 Hz, 2H), 1.32 (br, s, 12H). δ ¹³C NMR (100 MHz, CD₃OD): δ 138.7, 113.3 103.2, 102.8, 79.3, 76.7, 75.1, 75.0, 73.5, 73.4, 70.0, 69.5, 61.0, 60.5, 33.5, 29.4, 29.3, 29.2, 29.1, 28.8, 28.7, 25.7. (ESI) m/z: Calcd. (C₂₃H₄₂O₁₁)Na⁺: 517.2619; Found: 517.2619, Difference: <-1.0 ppm

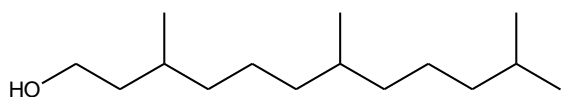
Acetobromo-cellobiose, AC (11a): Synthesis of acetobromo-cellobiose was done as reported earlier. Aceto-bromo cellobiose was purified using gradient elution (100 % hexane to 40 % ethyl acetate in hexane). R_f = 0.3 (40 % ethyl acetate in hexane). ¹H NMR (300 MHz, CDCl₃): 6.54 (d, J = 6.0 Hz, 1H), 5.55(t, J = 9.0Hz, 1H, 5.20-5.06(m, 2H), 4.96(t, J = 6.0 Hz, 1H), 4.78(dd, J_{1-3} = 9.0 Hz, J_{1-2} = 3.0 Hz, 1H), 4.57-4.53(m, 2H), 4.39(dd, J = 12.0 Hz, J = 3.0 Hz, 1H), 4.20-4.16(m, 2H), 4.07(d, J = 12.0 Hz, 1H), 3.85(t, J = 9.0 Hz, 1H), 3.71-3.67(m, 1H), 2.15-2.00(s, 7 X 3H).



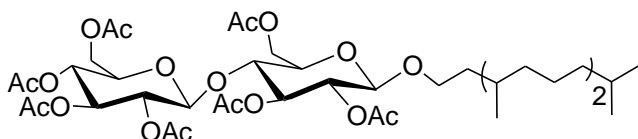
Acetylated farnesyl- β -cellobioside, AF β C (11b): Glycosylation of acetobromo cellobiose with farnesol was achieved by using Hg(CN)₂. To a round bottom flask acetobromo-bromo cellobiose (0.5 g, 7.0 mmol) and farnesol (0.158g, 7.0 mmol) were added and dissolved in benzene (10 mL). Hg(CN)₂ (0.182g, 7.15 mmol) was then added and the mixture was allowed to stir at 50 °C for ~ 2 hours. After 2 hours H₂O (25 mL) was added and the organic phase was extracted with ethyl acetate (2 X 15 mL). The combined organic phase were washed with brine and dried with Na₂SO₄ (anhydrous), and concentrated in vacuo. The product was purified using a gradient solvent system (100 % hexane to 40 ethylacetate in hexane). Colorless powder, 0.143 g, 23.8 %. R_f = (0.50, 60% EtOAc: Hexane). ¹H NMR (300 MHz, CDCl₃): δ 5.24 (br, s, 1H), 5.17-5.02 (m, 5H), 4.90 (q, J_{1-2} = 6.9 Hz, 2H), 4.46 (br, s, 3 H), 4.35-4.25 (m, 1H), 4.16 (br, s, 2H), 4.05 (t, J = 14.7 Hz, 2H), 3.75(t, J = 10.8 Hz, 1H), 3.66-3.63 (m, 1H), 3.57-3.56 (m, 1H), 2.11-1.97 (s, 7 x 3H), 1.66-1.59 (s, 4 x 3H). ¹³C NMR (75 MHz, CDCl₃): δ 170.9, 170.7, 170.6, 170.3, 170.0, 169.7, 169.5, 142.8, 135.9, 131.1, 124.7, 124.0, 119.5, 101.2, 99.0, 73.3, 73.1, 73.0, 72.3, 72.0, 71.9, 68.1, 65.6, 62.4, 61.9, 40.1, 40.0, 27.1, 26.7, 26.1, 21.2, 21.1, 21.1, 21.1, 21.0, 20.9, 18.1, 16.8, 16.4. HRMS (ESI) m/z: Calcd. (C₄₁H₆₀ O₁₈)Na⁺: 863.3671; Found: 863.3652, Difference: - 2.3 ppm



Farnesyl- β -cellobioside, F β C (11): The deprotection of acetylated-farnesyl cellobioside (**11b**) was done using Zemplén deacetylation conditions as reported above. Colorless powder, 0.020g, 95.3 %. ^1H NMR (300 MHz, CD_3OD): δ 5.39 (t, $J = 6.3$, 1H), 5.10 (q, $J_{1-2} = 6.9$ Hz, 2H), 4.24-4.21 (m, 4H), 3.91-3.85 (m, 3H), 3.69-3.47 (m, 3H), 3.40-3.19 (m, 7H overlapping with MeOD), 2.19-1.93 (m, 8H), 1.69 (s, 3H), 1.67 (s, 3H), 1.61 (s, 3H), 1.60 (s, 3H). ^{13}C NMR (75 MHz, CD_3OD): δ 140.9, 135.3, 131.1, 124.4, 124.1, 120.9, 103.6, 101.5, 79.7, 77.1, 76.8, 75.5, 75.4, 73.9, 73.8, 70.3, 65.3, 61.4, 60.8, 39.9, 39.7, 26.8, 26.4, 24.9, 16.8, 15.5, 15.1. HRMS (ESI) m/z : Calcd. ($\text{C}_{27}\text{H}_{46}\text{O}_{11}$) Na^+ : 569.2932; Found: 569.2926, Difference: -1.1 ppm.

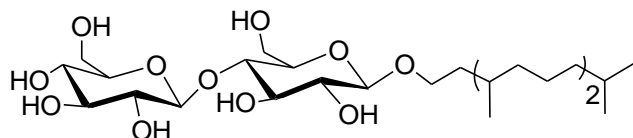


Saturated farnesol, SF (12b) The reduction of trans-trans farnesol was done using H_2 , Pd/C conditions using reported literature procedure (Scheme 3).²¹¹ Briefly, a flask containing farnesol (0.887g, 3.96 mmol) and Pd/C (10% Pd) (0.1 g) in 10 mL MeOH was evacuated and filled with H_2 gas. The reaction mixture was allowed to stir at room temperature for ~ 24 hours, following which Pd/C was filtered off and purification was done over silica column to obtain a viscous oil as product (0.300 g, 32.9%) ^1H NMR (300 MHz, CDCl_3): δ 3.63-3.73 (m, 2H), 1.49-1.62 (m, 4H), 1.05-1.38(m, 13H), 0.84-0.90 (m, 12H). Spectroscopic data is consistent with reported literature.²¹¹

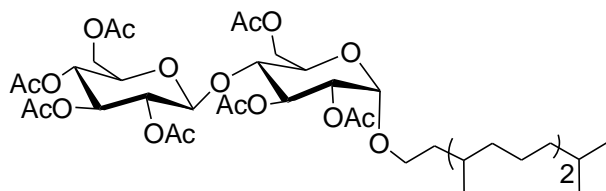


Acetylated saturated farnesyl- β -cellobioside, ASF β C (12a): Colorless powder, 0.080g, 21.0 % (2-step), $R_f = (0.53, 60\% \text{ EtOAc: Hexane})$. ^1H NMR (300 MHz, CDCl_3): δ 5.21-5.03 (m, 3H),

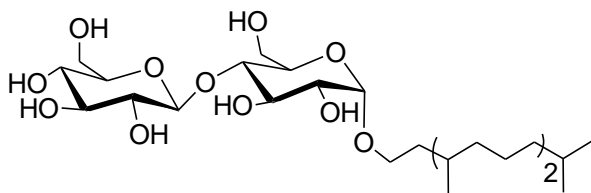
4.91 (q, $J_{1-2} = 7.8$ Hz, 2H), 4.52-4.49 (m, 2H), 4.44 (dd, $J_{1-3} = 8.1$ Hz, $J_{1-2} = 1.8$ Hz, 1H), 4.37 (dd, $J_{1-3} = 12.3$ Hz, $J_{1-2} = 4.2$ Hz, 1H), 4.06-4.02 (m, 2H), 3.92-3.83 (m, 1H), 3.77 (t, $J = 9.3$ Hz, 1H), 3.68-3.56 (m, 2H), 3.52-3.44 (m, 1H), 2.13-1.98 (s, 7 x 3H), 1.54-1.04 (m, 18 H), 0.88 (s, 3H), 0.86 (s, 3H), 0.85 (s, 3H), 0.83 (s, 3H). ^{13}C NMR (75 MHz, CDCl_3): δ 170.7, 170.6, 170.5, 170.1, 169.8, 169.5, 169.3, 101.8, 100.8, 76.8, 73.2, 72.9, 72.8, 72.7, 72.2, 71.9, 68.8, 68.8, 62.2, 61.8, 39.6, 37.7, 37.6, 37.5, 33.0, 30.0, 29.7, 28.2, 25.0, 24.6, 23.0, 22.9, 21.1, 20.9, 20.8, 20.7, 20.0, 19.9, 19.8, 19.7, 19.5. HRMS (ESI) m/z : Calcd. $(\text{C}_{41}\text{H}_{66}\text{O}_{18})\text{Na}^+$: 869.4141; Found: 869.4123, Difference: -2.1 ppm



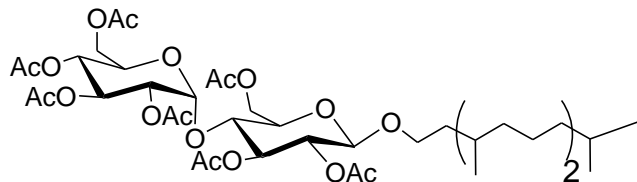
Saturated farnesyl- β -cellobioside, SF β C (12): Colorless powder, 0.034g, 85.7 % ^1H NMR (300 MHz, CD_3OD) δ 4.42 (d, $J = 7.8$ Hz, 1H), 4.29 (d, $J = 7.8$ Hz, 1H), 3.94 (br, s, 4H), 3.60-3.41 (m, 4H), 3.38-3.26 (m, 4H, overlapping with MeOD), 3.23 (t, $J = 5.7$ Hz, 2H), 1.75-1.13 (m, 18 H), 0.92-0.87 (s, 4 x 3H). ^{13}C NMR (75 MHz, CD_3OD): δ 103.6, 103.3, 79.7, 77.1, 76.8, 75.4, 73.9, 73.8, 70.3, 68.3, 61.4, 60.8, 39.5, 37.7, 37.5, 37.4, 33.0, 29.9, 28.1, 24.9, 24.5, 22.1, 19.2, 19.1, 19.0, 18.9. HRMS (ESI) m/z : Calcd. $(\text{C}_{27}\text{H}_{52}\text{O}_{11})\text{Na}^+$: 575.3401; Found: 575.3394, Difference: -1.3 ppm



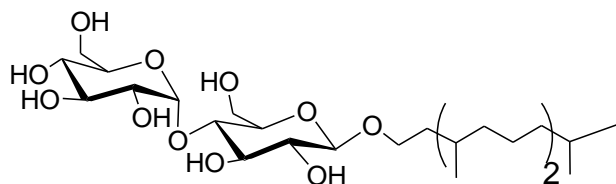
Acetylated Saturated farnesyl- α -cellobioside, ASF α C (13a): Colorless powder, 0.059 g, 21.0 % (2-step), Rf = (0.48, 60% EtOAc: Hexane). ^1H NMR (300 MHz, CDCl_3): δ 5.46 (t, $J = 10.2$, 1H), 5.19-5.05 (m, 2H), 4.99-4.91 (m, 2H), 4.78 (dt, $J_1 = 4.5$ Hz, $J_2 = 3.0$ Hz, 1H), 4.39 (dd, $J_{1-3} = 12.6$ Hz, $J_{1-2} = 4.8$ Hz, 1H), 4.17 (dd, $J_{1-3} = 12.3$ Hz, $J_{1-2} = 4.8$ Hz, 1H), 4.05 (dd, $J_{1-3} = 12.3$ Hz, $J_{1-2} = 2.4$ Hz, 1H), 3.96-3.89 (m, 3H), 3.42 (p, $J_{1-3} = 15.6$ Hz, $J_{1-2} = 7.8$ Hz, 1H), 2.14-1.99 (s, 7 x 3H), 1.57-1.00 (m, 18 H), 0.90-0.84 (s, 4 x 3H). ^{13}C NMR (75 MHz, CDCl_3): δ 170.9, 170.8, 170.8, 170.7, 169.7, 169.5, 101.3, 96.1, 95.9, 73.5, 72.3, 72.1, 72.1, 71.5, 71.4, 70.2, 68.5, 68.2, 62.3, 62.0, 39.7, 37.8, 37.7, 36.6, 33.2, 30.1, 28.4, 25.2, 24.8, 23.1, 23.0, 21.3, 21.1, 21.0, 21.0, 19.9, 19.8, 19.7. HRMS (ESI) m/z: Calcd. $(\text{C}_{41}\text{H}_{66}\text{O}_{18})\text{Na}^+$: 869.4141; Found: 869.4120, Difference: -2.4 ppm



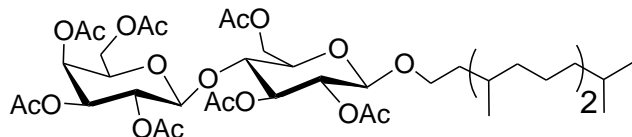
Saturated farnesyl- α -cellobioside, SF α C (13a): Colorless powder, 0.020g, 95.3 % ^1H NMR (300 MHz, CD_3OD): δ 4.77 (d, $J = 3.6$ Hz, 1H), 4.40 (d, $J = 8.1$ Hz, 1H), 3.92-3.88 (m, 2H), 3.81-3.63 (m 4H), 3.57-3.33 (m, 3H), 3.36-3.29 (m, 2 H, overlapping with MeOD), 3.23 (t, $J = 8.1$ Hz, 2H), 1.79-1.50 (m, 3H), 1.46-1.22 (m, 10 H), 1.21-1.03 (m, 5H), 0.92-0.86 (s, 4 x 3H). ^{13}C NMR (75 MHz, MeOD): δ 103.9, 99.0, 98.9, 79.8, 77.1, 76.9, 73.9, 72.5, 72.3, 71.1, 70.3, 61.4, 60.8, 39.6, 37.8, 37.5, 36.7, 33.0, 30.1, 28.2, 24.9, 24.4, 22.1, 22.0, 19.2, 18.9. HRMS (ESI) m/z: Calcd. $(\text{C}_{27}\text{H}_{52}\text{O}_{11})\text{Na}^+$: 575.3401; Found: 575.3395, Difference: -1.3 ppm



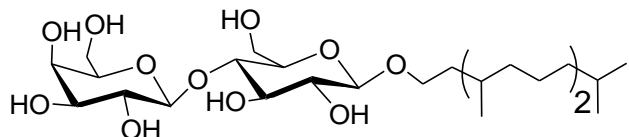
Acetylated saturated farnesyl- β -maltoside, ASF β M (14a): Colorless powder, 0.040g, 29.0 % (2-step), $R_f = (0.41, 60\% \text{ EtOAc: Hexane})$. $^1\text{H NMR}$ (300 MHz, CDCl_3): δ 5.43-5.36 (m, 2H), 5.25 (t, $J = 9.3$ Hz, 1H), 5.07 (t, $J = 4.5$ Hz, 1H), 4.97-4.79 (m, 2H), 4.53-4.42 (m, 2H), 4.29-4.20 (m, 2H), 4.07-3.85 (m, 4H), 3.70-3.65 (m, 1H), 3.53-3.44 (m, 1H), 2.14-2.01 (s, 7 x 3H), 1.66-1.16 (m, 18 H), 0.89 (br, s, 12H). $^{13}\text{C NMR}$ (75 MHz, CDCl_3): δ 169.5, 169.4, 169.2, 169.1, 169.0, 100.0, 99.8, 72.4, 72.3, 71.8, 71.6, 69.6, 68.9, 68.1, 67.6, 62.1, 61.1, 60.0, 37.1, 36.9, 32.4, 29.3, 27.5, 24.4, 23.9, 22.3, 22.2, 20.6, 20.5, 20.4, 20.3, 20.2, 19.3, 19.2, 19.1, 18.8, 13.8. HRMS (ESI) m/z : Calcd. $(\text{C}_{41}\text{H}_{66}\text{O}_{18})\text{Na}^+$: 869.4141; Found: 869.4130, Difference: -1.2 ppm



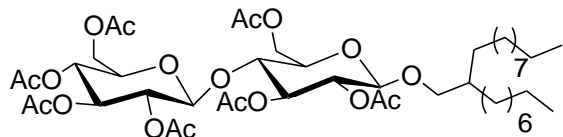
Saturated farnesyl- β -maltoside, SF β M (14): Colorless powder, 0.022g, 96.0 % $^1\text{H NMR}$ (300 MHz, CD_3OD): δ 5.17 (br, s, 1H), 4.27 (d, $J = 9$ Hz, 1H), 3.95-3.92 (m, 4H), 3.88-3.43 (m, 6H, overlap with CD_3OD peak), 3.27-3.20 (m, 4H), 1.79-1.13 (m, 18 H), 0.90 (s, 3H), 0.89 (s, 3H), 0.88 (s, 3H), 0.87 (s, 3H). $^{13}\text{C NMR}$ (75 MHz, CD_3OD): δ 102.6, 101.6, 79.5, 76.1, 74.8, 73.3, 72.9, 72.5, 72.4, 69.7, 67.5, 67.4, 60.9, 60.4, 38.7, 36.9, 36.7, 36.6, 32.2, 29.1, 27.4, 24.1, 23.7, 21.3, 21.2, 18.4, 18.3, 18.2, 18.2. HRMS (ESI) m/z : Calcd. $(\text{C}_{27}\text{H}_{52}\text{O}_{11})\text{Na}^+$: 575.3401; Found: 575.3399, Difference: < -1.0 ppm



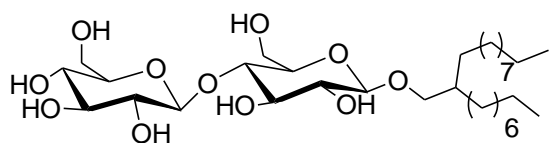
Acetylated saturated farnesyl- β -lactoside, ASF β L (15a): Colorless powder, 0.059 g, 21.0 % (2-step), Rf = (0.48, 60% EtOAc: Hexane). ^1H NMR (300 MHz, CDCl_3): δ 5.53-5.47 (m, 1H), 5.30-5.16 (m, 1H), 5.12-5.07 (m, 1H), 4.94-4.86 (m, 3H), 4.66-4.60 (m, 1H), 4.54-5.41 (m, 3H), 4.33-4.23 (m, 1H), 4.15-4.07 (m, 2H), 3.99-3.59 (m, 4H), 3.53-3.26 (m, 2H), 2.17-1.96 (s, 7 x 3H), 1.70-1.02 (m, 18 H), 0.88 (s, 3H), 0.85 (s, 3H), 0.84 (s, 3H), 0.82 (s, 3H). ^{13}C NMR (100 MHz, CDCl_3): δ 169.4, 169.0, 168.8, 168.5, 168.3, 168.1, 99.6, 98.3, 76.3, 76.2, 76.0, 75.7, 75.1, 72.6, 71.5, 70.8, 70.7, 70.0, 69.0, 68.4, 67.9, 67.4, 67.0, 66.2, 61.3, 61.0, 60.5, 47.1, 38.9, 36.4, 36.2, 35.3, 31.8, 28.7, 28.5, 27.0, 26.2, 23.8, 23.3, 21.7, 21.6, 20.0, 19.9, 19.9. HRMS (ESI) m/z: Calcd. ($\text{C}_{41}\text{H}_{66}\text{O}_{18}$) Na^+ : 869.4141; Found: 869.4135, Difference: < 1.0 ppm



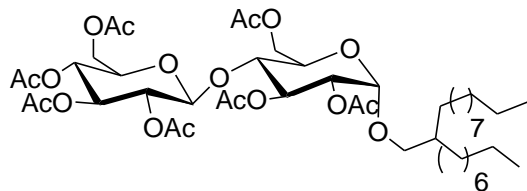
Saturated farnesyl- β -lactoside, SF β L (15): Colorless powder, 0.020g, 95.3 % ^1H NMR (300 MHz, CD_3OD): δ 4.41 (t, J = 6.8 Hz, 1H), 4.33-4.29 (m, 1H), 4.09-4.08 (m, 1H), 3.95-3.88 (m, 2H), 3.83-3.76 (m, 3H), 3.76-3.66 (m, 2 H), 3.56-3.32 (m, 6H), 3.31-3.21 (m, 1H), 3.17 (d, J = 5.2 Hz, 1H), 1.57-1.06 (m, 18 H), 0.92 -0.87 (s, 4 x 3H). ^{13}C NMR (75 MHz, CD_3OD): δ 103.9, 103.4, 79.6, 75.4, 74.9, 73.4, 73.1, 72.0, 67.9, 66.2, 60.4, 54.4, 48.2, 48.1, 47.9, 37.1, 37.0, 36.4, 32.6, 29.5, 29.0, 27.7, 24.5, 24.0, 21.6, 18.8, 18.7. HRMS (ESI) m/z: Calcd. ($\text{C}_{27}\text{H}_{52}\text{O}_{11}$) Na^+ : 575.3402; Found: 575.3403, Difference: < 1.0 ppm.



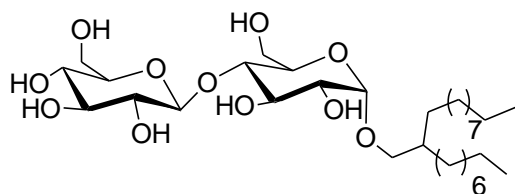
Acetylated-2-octyl-dodecyl- β -cellobioside, 2-AOD β C (16a): Colorless powder, 0.240g, 9.0 % (2-step), $R_f = (0.53, 60\% \text{ EtOAc in Hexane})$. $^1\text{H NMR}$ (300 MHz, CDCl_3): δ 5.21-5.03 (m, 3H), 4.92 (q, $J_{1-2} = 6.6 \text{ Hz}$, 2H), 4.53-4.50 (m, 2H), 4.43-4.34 (m, 2H), 4.07 (t, $J = 16.8$, 2H), 3.81-3.74 (m, 2H), 3.68-3.54 (m, 2H), 3.27 (t, $J = 6.3 \text{ Hz}$, 1H), 2.13-1.99 (s, 7 x 3H), 1.59-1.48 (m, 1H), 1.26 (br, s, 32H), 0.89 (t, $J = 6.3 \text{ Hz}$, 6H). HRMS (ESI) m/z : Calcd. $(\text{C}_{46}\text{H}_{76}\text{O}_{18})\text{Na}^+$: 939.4923; Found: 939.4910, Difference: -1.5 ppm



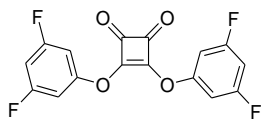
2-Octyl-dodecyl- β -cellobioside, 2-OD β C (16): Colorless powder, 0.05 g, 94.0 %. $^1\text{H NMR}$ (300 MHz, CD_3OD): δ 4.43 (d, $J = 7.8 \text{ Hz}$, 1H), 4.26 (d, $J = 9.9$, 1H), 3.93 (br, s, 3H), 3.84-3.78 (m, 4H), 3.70-3.49 (m, 3H), 3.42-3.31 (m, 5H, overlapping with MeOD), 3.29-3.21 (m, 2H), 1.69-1.57 (m, 1H), 1.31 (br, s, 32 H), 0.92 (t, $J = 6.3 \text{ Hz}$, 6H). $^{13}\text{C NMR}$ (75 MHz, CD_3OD): δ 102.8, 79.0, 76.3, 76.0, 74.7, 74.6, 73.1, 73.0, 72.3, 69.6, 60.6, 60.2, 37.6, 31.3, 30.4, 29.4, 29.4, 29.0 (8 carbons), 28.9, 28.9, 28.7, 26.1, 22.0, 12.7. HRMS (ESI) m/z : Calcd. $(\text{C}_{32}\text{H}_{62}\text{O}_{18})\text{Na}^+$: 645.4184; Found: 645.4179, Difference: <-1.0 ppm



Acetylated-2-octyl-dodecyl- α -cellobioside, 2-AOD α C (17a): Colorless powder, 0.040g, 1.5 % (2-step), Rf = (0.48, 60% EtOAc in Hexane). ^1H NMR (300 MHz, CDCl_3): δ 5.43 (t, $J = 9.3$ Hz, 1H), 5.11 (p, $J_{1-3} = 18.3$ Hz, $J_{1-2} = 9.0$ Hz, 2H), 4.96 -4.90 (m, 2H), 4.77 (dd, $J_{1-3} = 10.2$ Hz, $J_{1-2} = 3.3$ Hz, 1H), 4.52-4.45 (m, 2H), 4.38 (dd, $J_{1-3} = 12.6$ Hz, $J_{1-2} = 4.5$ Hz, 1H), 4.15-4.02 (m, 2H), 3.88-3.73 (m, 1H), 3.69-3.55 (m, 4H), 3.20 (t, $J = 6.3$ Hz, 1H), 2.13-1.98 (s, 7 X 3H), 1.62 -1.55 (m, 1H), 1.26 (br, s, 32H), 0.88 (t, $J = 6.6$ Hz, 3H). ^{13}C NMR (75 MHz, CDCl_3): δ 170.1, 169.9, 169.8, 169.8, 169.1, 168.8, 168.5, 100.5, 95.3, 76.8, 76.4, 72.6, 71.5, 71.3, 71.1, 70.8, 69.4, 67.6, 67.3, 61.4, 61.1, 37.3, 31.4, 30.8, 30.4, 29.6, 29.2, 29.2, 28.9, 26.3, 26.2, 22.2, 13.7. HRMS (ESI) m/z: Calcd. $(\text{C}_{46}\text{H}_{76}\text{O}_{18})\text{Na}^+$: 939.4923; Found: 939.4910, Difference: <-1.4 ppm

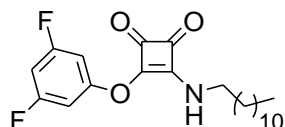


2-Octyl-dodecyl- α -cellobioside, 2-AOD α C (17): Colorless powder, 0.015 g, 83.5.0 % ^1H NMR (300 MHz, CD_3OD): δ 4.44 (t, $J = 3.6$ Hz, 1H), 4.27 (t, $J = 3.6$ Hz, 1H), 3.89 (br, s, 3H), 3.77-3.71 (m, 2H), 3.63-3.60 (m, 2H), 3.49-3.21 (m, 8H, overlapping with MeOD peak), 1.68-1.57 (m, 1H), 1.31 (br, s, 32H), 0.91 (m, 6H). ^{13}C NMR (75 MHz, MeOD): δ 102.8, 98.4, 79.2, 76.3, 76.0, 73.0, 71.6, 71.5, 70.7, 70.3, 69.5, 60.6, 59.9, 37.5, 31.2, 30.5, 30.5, 29.3, 29.3, 29.2, 28.9, 28.9, 28.7, 28.6, 28.6, 28.5, 26.1, 26.0, 26.0, 21.6, 13.0. HRMS (ESI) m/z: Calcd. $(\text{C}_{32}\text{H}_{62}\text{O}_{18})\text{Na}^+$: 645.4184; Found: 645.4178, Difference: -1.0 ppm



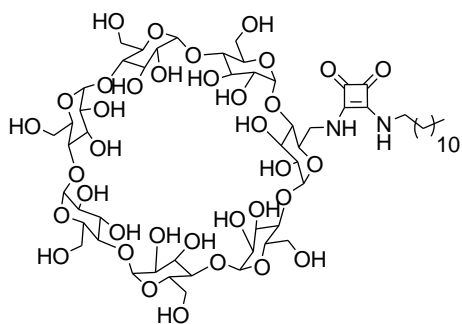
Difluoro phenoxy squarate, DPSq (18a) - (Scheme 2) Finely powdered 1, 2-Dihydroxycyclobutene-3,4-dione (1.10 g, 9.6 mmol), carbon tetrachloride (20 mL), and DMF (0.05mL), were introduced into a 50 mL round-bottomed flask previously filled with argon. The mixture was frozen by immersing in dry ice-acetone and oxalyl chloride (2.10 mL, 24 mmol) was introduced at once through the condenser's outlet. Then the flask was allowed to warm to room temperature, agitation started at 300 rpm, and the flask was then lowered into an oil bath thermostatted to 50-60 °C. Regular gas evolution started immediately and was no more apparent after 50 min. After heating further for 3 h the agitation was discontinued. The solvent was removed to give 1,2-dichlorocyclobutene-3,4-dione as yellow crystal. (Yield = 1.15 g, 80 %)

(1.15 g, 7.6 mmol) of 1,2-dichlorocyclobutene-3,4-dione was dissolved in benzene (50 mL), and the solution was cooled to 0°C. 3,5-Difluorophenol (2.0 g, 15.3 mmol) was added to the above solution in one portion, followed by slow addition of excess Et₃N (2.090 g, 20.674 mmol), and the reaction mixture was stirred at room temperature overnight. The reaction mixture was filtered, and the residue obtained was washed with benzene to yield a white solid. The solid obtained was purified using flash silica gel column (20% EtOAc in hexanes) to give 2 (0.80 g, 27%) as a white solid. R_f = 0.59 (20% EtOAc in hexanes). Yield = {white powder, 0.282 g, 12 % (2-step)}, R_f = (0.40, 1:1 Hexane:EtOAc). ¹H NMR (300 MHz, CDCl₃): δ 6.906.88 (m, 4H), 6.846.78 (m, 2H). Spectroscopic data are consistent with reported values.²¹²



Dodecylamine-phenoxy squarate, DPSq (18b): A round bottom flask was charged with difluoro-bis phenoxy squarate (0.04 g, 1.18 mmol) and THF (5 mL, anhydrous distilled over

CaH₂) was added. The solution was cooled to -78 °C in a dry-ice/acetone bath. Dodecyl amine (0.0153 g, 0.8 mmol) dissolved in THF (5 mL, anhydrous) was then added dropwise over 30 minutes. The mixture was stirred at -78 °C for 2 hours. Column chromatographic separation using a gradient of 100 % hexane to 30 % ethyl acetate in hexane yielded product as a viscous oil, 0.025 g, 54.3 % (R_f = 0.46 (30 % ethyl acetate in hexane)). ¹H NMR (400 MHz, CDCl₃): δ 6.92- 6.87 (m, 2H), 6.73-6.68 (m, 1H), 3.76-3.52 (m, 2H), 1.70-1.68 (m, 2H), 1.38-1.25 (m, 18H), 0.88 t, *J* = 6.0 Hz, 3H). ¹³C NMR (100 MHz, CDCl₃): δ 189.9, 180.2, 173.3, 171.8, 102.6, 102.5, 102.4, 102.3, 101.3, 101.0, 45.2, 31.9, 31.0, 29.6, 29.5, 29.4, 29.3, 29.1, 26.4, 26.3, 22.7, 14.1. HRMS (ESI) *m/z*: Calcd. (C₂₂H₂₉F₂NO₃)Na⁺: 416.2008; Found: 416.2005, Difference: <- 1.0 ppm.



Dodecyl βCD squarate, DβCDS (18b): Synthesis of βCD-NH₂ (18c) was done via a 3 step reported literature procedure.²¹² The synthesized βCD-NH₂ (0.028 g, 0.02 mmol) was dissolved in distilled water (2 mL). To this βCD-NH₂ solution was added dropwise a solution of phenoxy amino dodecyl squarate (0.02 mmol) dissolved in a binary solvent mixture of DMF (2 mL) and acetone (1 mL). The reaction mixture was allowed to stir at room temperature, monitoring with TLC to check for consumption of starting material squarate (~ 4 days) (TLC solvent system; 30 % ethyl acetate in hexane). Formation of new spot was also monitored using a polar TLC system (*i*-PrOH: EtOAc: H₂O: NH₄OH:: 5: 2: 3: 1, R_f = 0.7) followed by staining with Ceric

Ammonium Molybdate (CAM) stain. The product (D β CDS) (**14**) was precipitated by addition of excess of acetone (10 mL) and separated by centrifuging at 3000 rpm for 10 mins. The obtained white solid was washed several times with acetone followed by centrifugation. Colorless powder, yield 0.02 g, 56.0%). ¹H NMR (300 MHz, CD₃OD): 3.95-3.64 (m, 30 H), 3.57-3.38 (m, 14H), 1.92-1.88 (m, 1H), 1.22 (br, s, 12H), 0.89 (br, s, 3H). Analyzed by MALDI and matched on [C₅₈H₉₆N₂O₃₆]Na⁺ at 1420.37 Expected Mass of sodium adduct: 1420.37.

Biological assays

Materials and methods of biological assays. Rhamnolipids (R95; 79:16 percent ratio of di-rhamnolipids:mono-rhamnolipids, 95 % pure, average molecular weight 626 g/mole) was obtained from Agae technologies, Corvallis, OR and was used as received. Water was purified using a Millipore Analyzer Feed System. Flat-bottomed polystyrene 96-well microtiter plates (untreated) (Costar 3370, VWR) were used to perform antibiofilm assays (biofilm inhibition, biofilm dispersion). For measuring fluorescence for adhesion and gene reporter assays, flat-bottomed 96-well microtiter plates with black walls (μ Clear, Greiner-One 655096, Sigma Aldrich) were used. Measurement of absorbance at 600 nm (OD₆₀₀) for growth assay was performed with 200 μ L of culture-media in microtiter plate well on a Biotek ELx800TM absorbance microplate reader (BioTek Instruments, Inc., Winooski, VT), and the data was analyzed with Gen5TM data analysis software. Quantification of biofilm (inhibition and dispersion) was done using a crystal violet (CV) dye-based static-biofilm assay.²¹³ For quantifying fluorescence for adhesion and gene reporter assays, Synergy 2 multi-mode microplate reader (BioTek Instruments, Inc., Winooski, VT) with Gen5 data analysis software

was used to detect green fluorescent protein (GFP) signal at an excitation wavelength of 500 nm and emission wavelength of 540 nm. For biofilm inhibition and dispersion, bacterial adhesion, and gene reporter assays, controls contained the same volume of deionized water without any added agents. For each biological assay, at least 3 triplicates were conducted, and data shown are the average of readings from at least 4-replicates wells. Half maximal inhibitory concentration for both biofilm inhibition and dispersion (IC_{50} and DC_{50}) were calculated by fitting values into a logarithmic equation, $y = m \ln(x) + C$

Bacterial strains and plasmids. *Pseudomonas aeruginosa* strains PAO1 and PAO1-EGFP were obtained from Dr. Guirong Wang (Upstate Medical University). *Pseudomonas aeruginosa* transposon mutant strain PW6886 (rhIA-E08::ISphoA/hah) was obtained from two-allele library.²⁰² PAO1 (*plasI*-LVAgfp), PAO1 (*prhII*-LVAgfp) strains were prepared by literature reported protocol.²¹⁴ The plasmid *plasI*-LVAgfp and *prhII*-LVAgfp were obtained from Dr. Hiroaki Suga (The University of Tokyo) and were maintained by adding 300 $\mu\text{g}/\text{mL}$ of carbenicillin in culture media. Freezer stocks of all strains were stored at $-80\text{ }^{\circ}\text{C}$ in LB media with ~20% glycerol. All strains were grown at $37\text{ }^{\circ}\text{C}$ in a rotary-shaker (at 250 rpm) in Luria Bertaini (LB) media (10 g/L tryptone, 5 g/L yeast extract, and 10 g/L NaCl). All biofilm inhibition, dispersion and adhesion assays were performed in LB-media and plates were incubated at $37\text{ }^{\circ}\text{C}$ under static conditions.

Stock solution and delivery of disaccharide derivatives (DSDs). All but three saccharide derivatives were water-soluble. For the water soluble DSDs, no organic solvents were used to assist the mixing and delivery for all biological assays. Stock solution (~11.5 mM) of DSDs were prepared in autoclaved water and further sterilized by filtering through cellulose acetate syringe filter (0.2 μm pore size, GVS filter technology) into sterilized vials. The sterilized DSDs stock

solutions were stored at -20 °C and thawed prior to each use. Aliquots of DSD stock solutions were added to the cultures in wells. Sterile water (same volume as the DSD stock solution used) was used as positive controls (no agents) in all assays to eliminate the effect of water from the stock solution. Three agents **DβL (7)**, **SFβL (15)** and **2-ODαC (17)** exhibited low water solubility, and were prepared in mixed solution of sterile water (90%) and 200 proof EtOH (10%). Controls for these agents consisted of the same mixed water-ethanol solution.

Toxicity of disaccharide derivatives against planktonic bacteria. Overnight inoculum of PAO1 was sub-cultured to an OD₆₀₀ ~ 0.01 and the sub-culture was allowed to reach an OD₆₀₀ of ~0.1, from which 200 μL was aliquoted into the wells of a microtiter plate, followed by 3 μL of DSDs stocks (to achieve a final 160 μM). Wells without added agents were used as a positive control. The microtiter plate was shaken (250 rpm at 37 °C), and the optical density was measured after regular intervals of time over 24 h using Biotek ELx800TM absorbance microplate reader (BioTek Instruments, Inc., Winooski, VT). The OD₆₀₀ values were plotted against time to obtain a growth curve for planktonic growth with or without agents (see supporting information Figure S2).

Swarming assays. Semisolid gel for swarming assays were prepared using M8 medium supplemented with 0.2 % glucose, 0.5 % casamino acid, 1 mM MgSO₄ and 0.5 % Bacto agar.²⁰⁴ For each set of swarming experiment, the plates were poured from same batch of agar and allowed to dry for 1 h before inoculation of bacteria. Bacterial culture (3 μL) (wild type PAO1 or *rhlA* mutant) with OD₆₀₀ between ~0.4-0.6 was inoculated on the semisolid agar gel. These “swarm plates” were incubated at 37 °C for 12 h and then incubated for additional 12 h at room temperature. After a total 24 h period, pictures of the swarming plates were taken.

Swarm area measurement. To measure swarming area, images of “swarm plates” were adjusted to keep the diameters of all the petri dishes containing the semisolid gel to a constant 4.4 inches. The adjusted images were printed and the swarming patterns were cut and weighed. With 1 cm² square of the copy paper weighing 8.0 mg, the swarming areas were calculated.

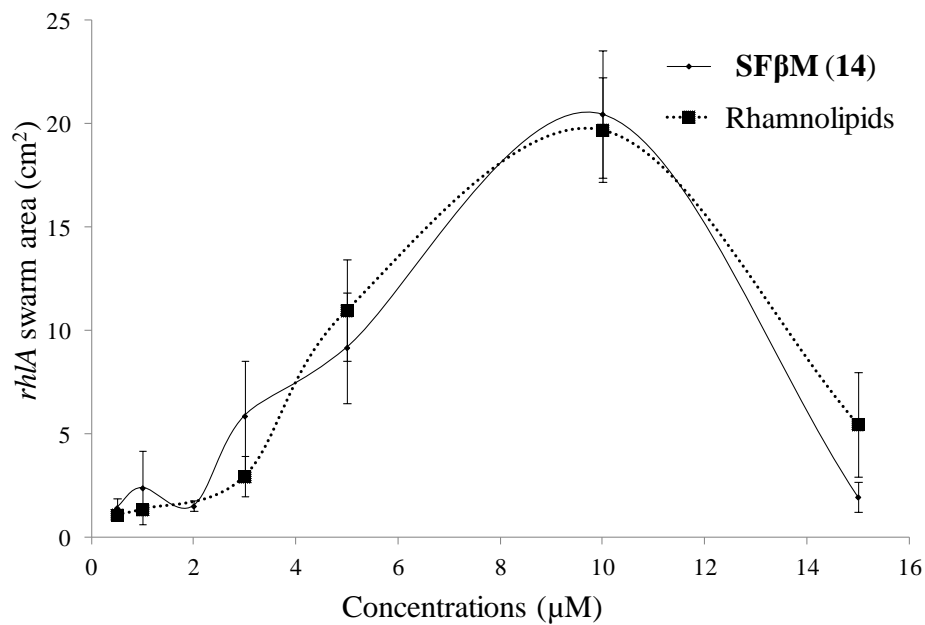
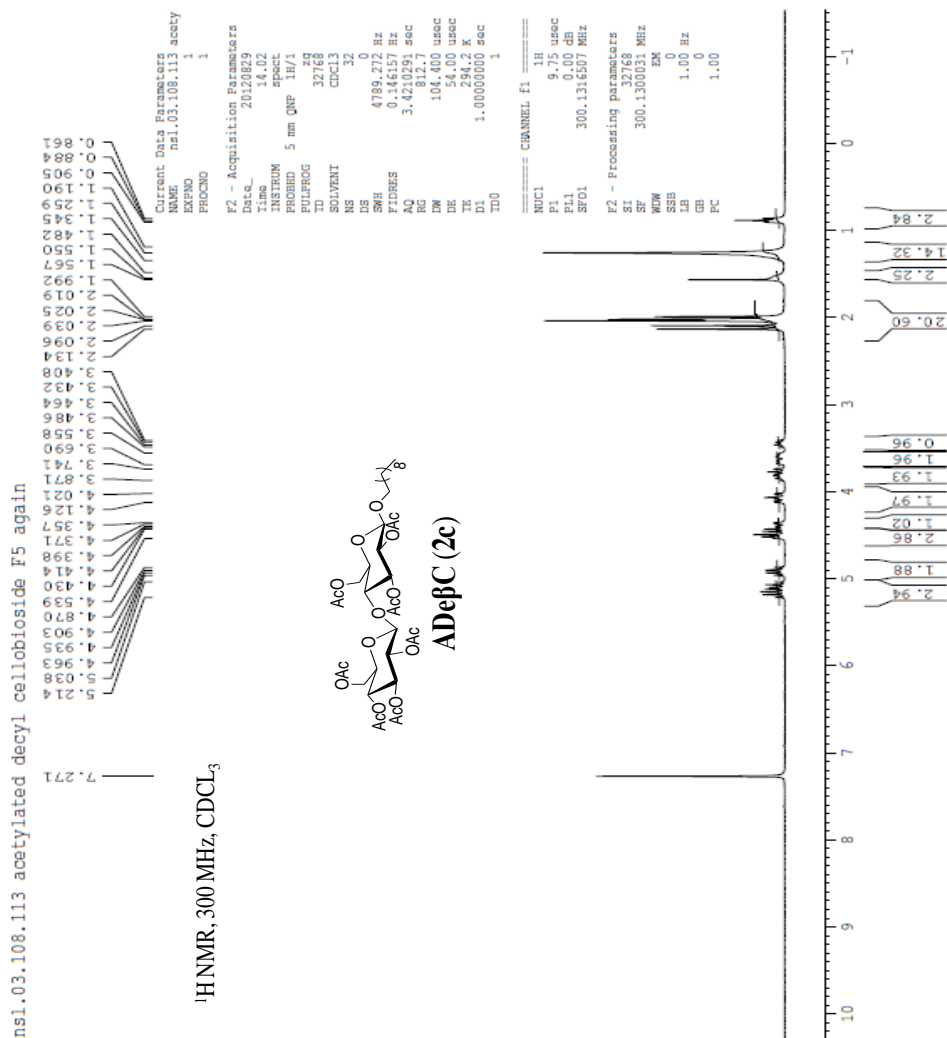
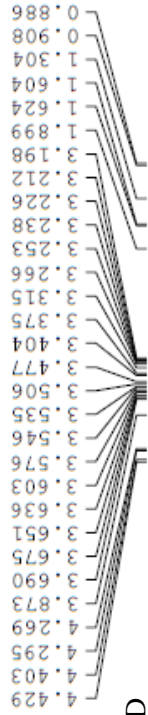


Figure 2S1. Plot of the rhlA mutant’s swarm area (after 24 h) versus increasing concentrations of rhamnolipids and SFβM (14) in the semisolid gel (~ 0.5% agar). The experiment was repeated on three different plates. The error bars are obtained from the mean of the three different experiments.

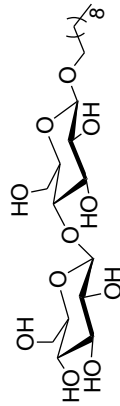
¹H and ¹³C NMR Spectra



nsl.03.109.114 decyl b cellobioside



¹H NMR, 300 MHz, CD₃OD



DeβC (2)

Current Data Parameters
NAME nsl.03.109.114 c
EXPNO 1
PROCNO 1

F2 - Acquisition Parameters
Date_ 20120830
Time 14.18
INSTRUM spect
PROBHD 5 mm QNP 1H/1
PULPROG zg
TD 32768
SOLVENT MeOH
NS 16
DS 0
SWH 4789.272 f
FIDRES 0.146157 f
AQ 3.4210291 s
RG 574.7
DW 104.400 u
DE 54.00 u
TE 294.2 K
D1 1.00000000 s
TD0 1

CHANNEL f1
NUC1 1H
P1 9.75 u
PL1 0.00 c
SFO1 300.1316507 M

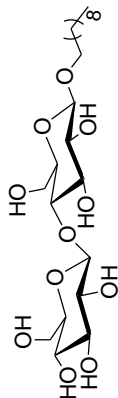
F2 - Processing parameters
SI 32768
SF 300.1300031 M
WDW EM
SSB 0

GB 1.00 f
PC 1.00

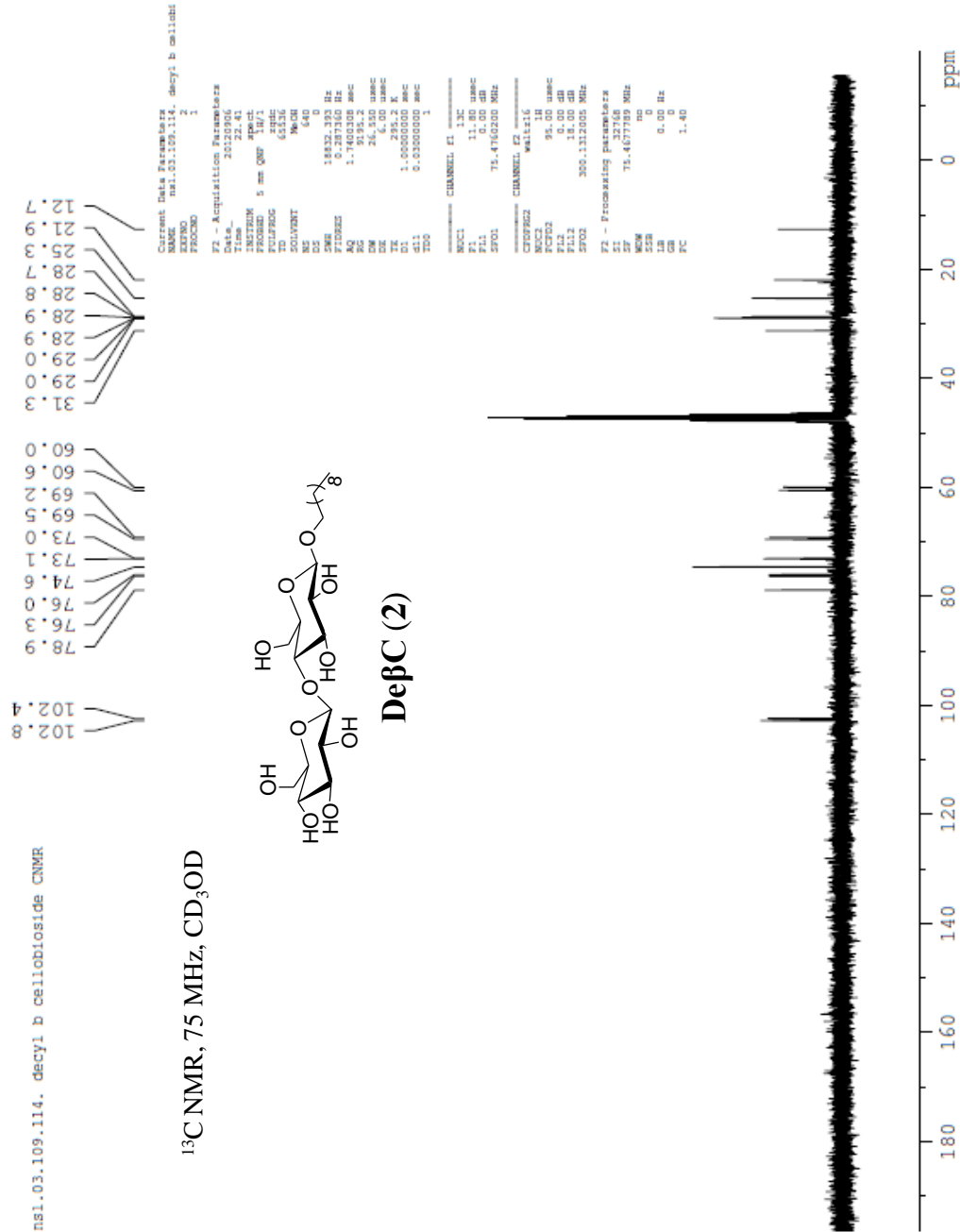


nsi.03.109.114. decyl b cellobioside CNMR

¹³C NMR, 75 MHz, CD₃OD

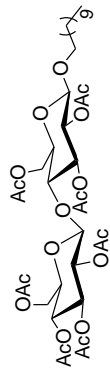
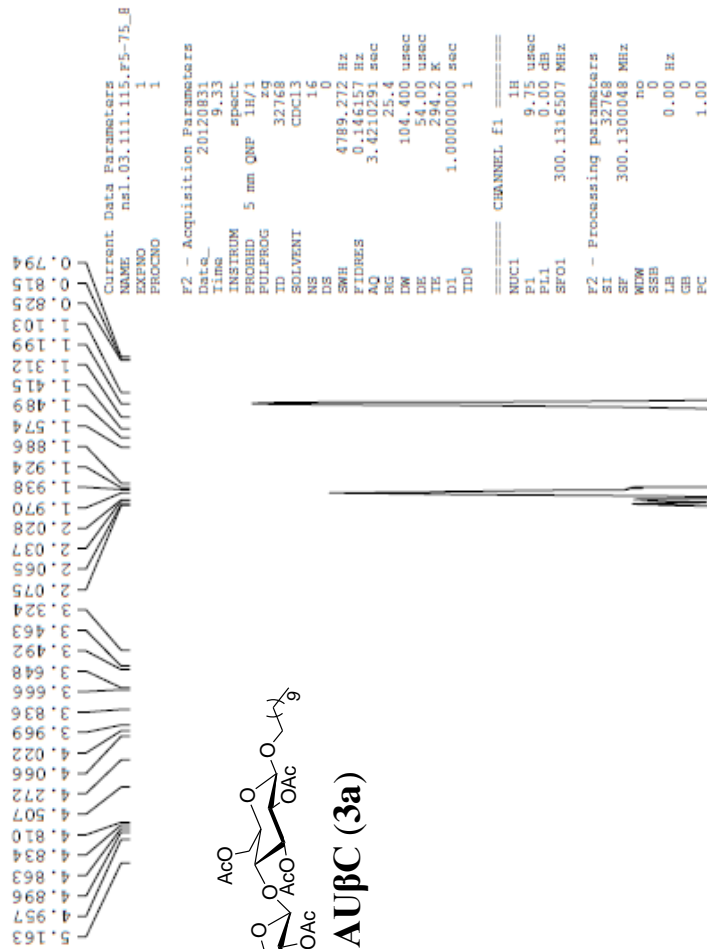


DefC (2)



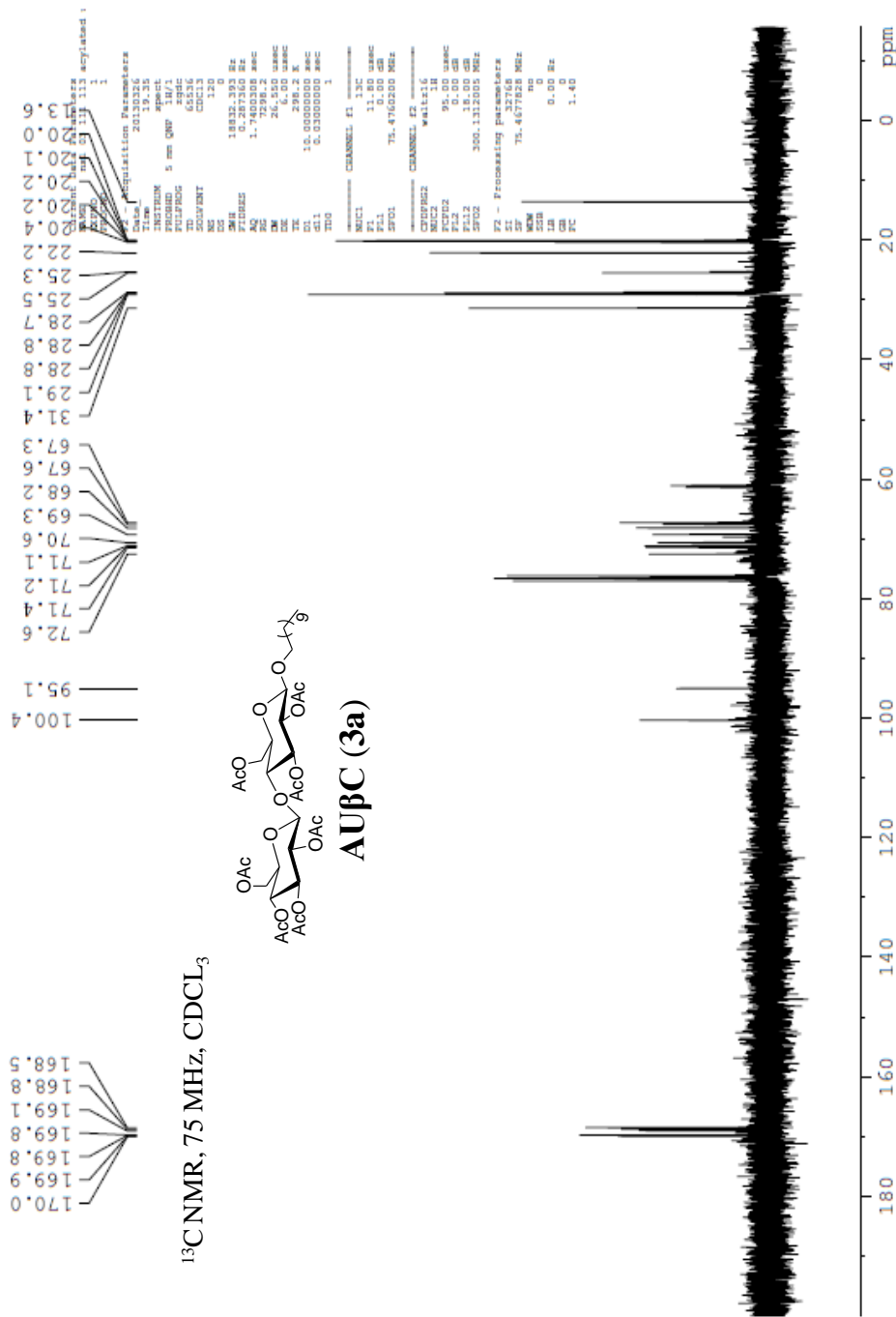
ns1.03.111.115.F5-88 acetylated undecyl cellobioside

¹H NMR, 300 MHz, CDCl₃

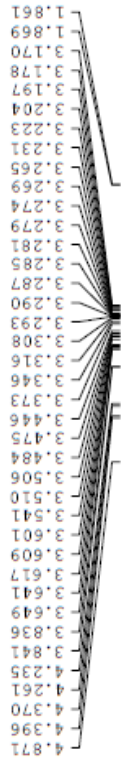


AUβC (3a)

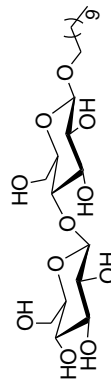
1s1 03 111 113 acylated undecyl cellobioside CNMR_2



nsl.03.112.116. undecyl b cellobioside



¹H NMR, 300 MHz, CD₃OD



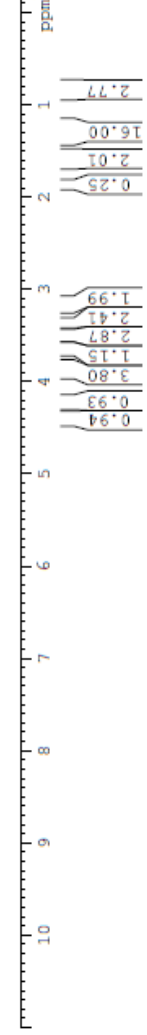
UPC (3)

Current Data Parameters
NAME nsl.03.112.116.
EXPNO 1
PROCNO 1

F2 - Acquisition Parameters
Date_ 20120904
Time 9.25
INSTRUM spect
PROBHD 5 mm QNP 1H/1
PULPROG zg
TD 32768
SOLVENT D2O
NS 16
DS 0
SWH 4789.272 F
FIDRES 0.146157 F
AQ 3.4210291 s
RG 80.6
DW 104.400 μs
DE 54.00 μs
TE 295.2 K
D1 1.00000000 s
TD0 1

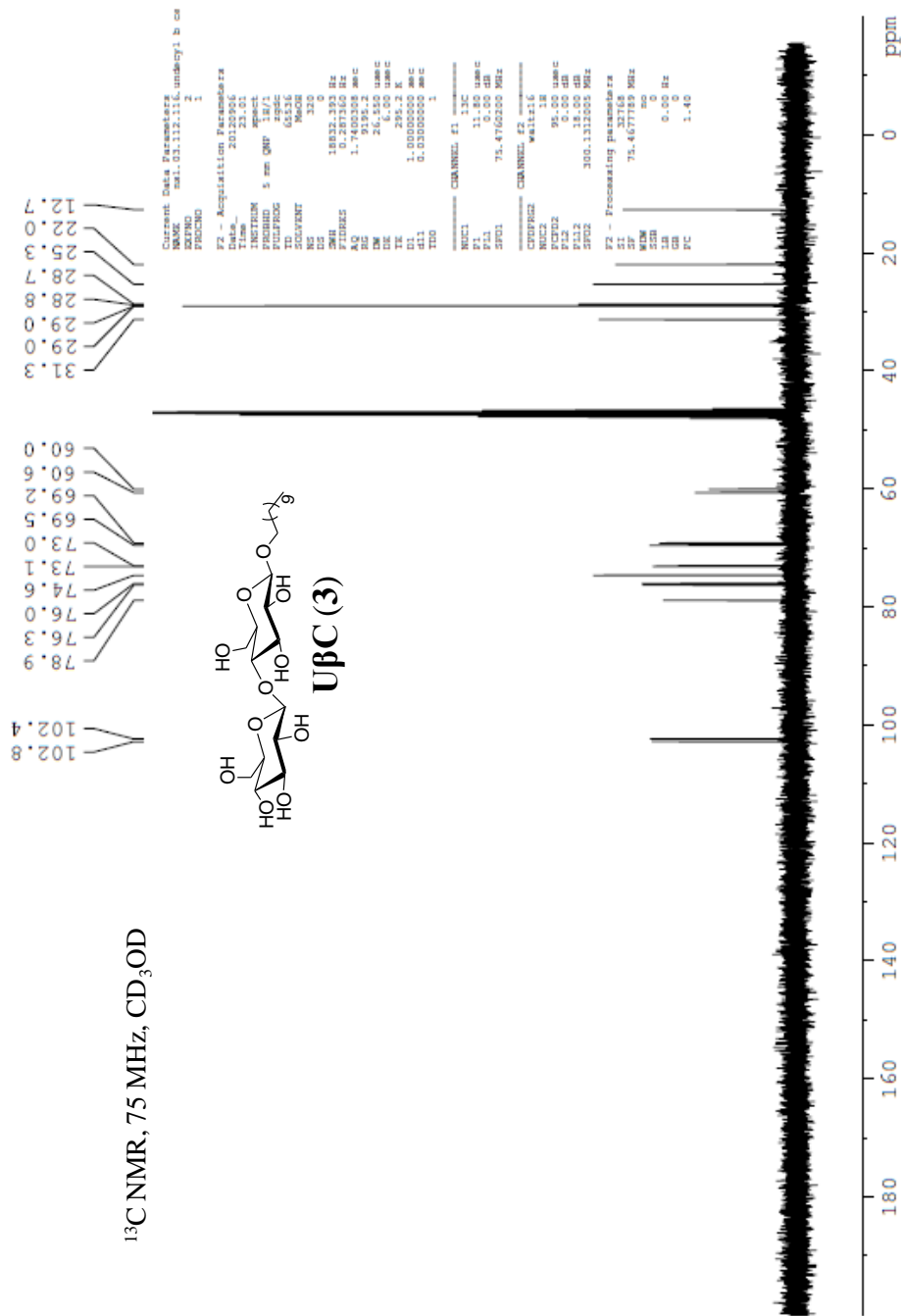
CHANNEL f1
NUC1 1H
P1 9.75 μs
PL1 0.00 dB
SFO1 300.1316507 MHz

F2 - Processing parameters
SI 32768
SF 300.1300141 MHz
WDW no
SSB 0
LB 0.00 Hz
GB 0
PC 1.00

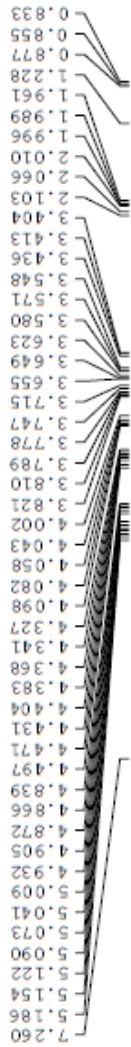


ns1.03.112.116.undecyl b cellobioside CNMR

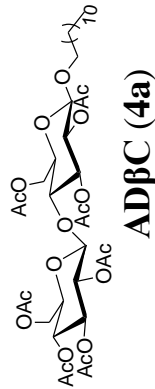
¹³C NMR, 75 MHz, CD₃OD



nsl.03.96.101.F3.acetylated b dodecyl cellobioside again



¹H NMR, 300 MHz, CDCl₃



Current Data Parameters
NAME nsl.03.96.101.F3.ac
EXPNO 1
PROCNO 1

F2 - Acquisition Parameters
Date_ 20120905
Time 20.47
INSTRUM spect
PROBHD 5 mm QNP 1H/1
PULPROG zg
ID 32768
SOLVENT CDCl3
NS 8
DS 0
SWH 4789.272 Hz
FIDRES 0.146157 Hz
AQ 3.4210291 sec
RG 71.8
DW 104.400 usec
DE 54.00 usec
TE 295.2 K
IE 3.0000000 sec
D1 1
ID0 1

CHANNEL f1
NUC1 1H
P1 9.75 usec
PL1 0.00 dB
SFO1 300.1316507 MHz

F2 - Processing parameters
SI 32768
SF 300.1300053 MHz
WDW no
SSB 0
LB 0.00 Hz
GB 0
PC 1.00

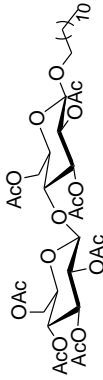
ns1.03.96.101.F3.acetylated beta dodecyl cellobioside CNMR



Current Data Parameters
 NAME ns1.03.96.101.F3.
 EXPNO 2
 PROCNO 1

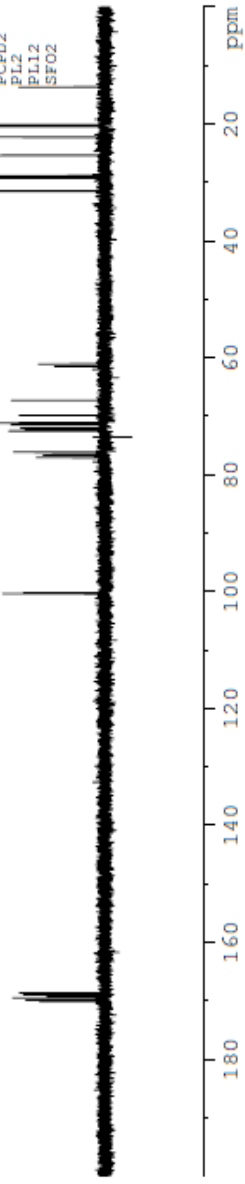
¹³C NMR, 75 MHz, CDCl₃

F2 - Acquisition Parameters:
 Date_ 20120905
 Time 21.05
 INSTRUM spect
 PROBEID 5 mm QNP 1H/1
 PULPROG zgpg30
 TD 65536
 SOLVENT CDCl3
 NS 320
 DS 0
 SWH 18632.393 Hz
 FIDRES 0.287360 Hz
 AQ 1.7400308 sec
 RG 2298.8
 DW 26.550 usec
 DE 6.00 usec
 TE 295.2 K
 D1 1.00000000 sec
 d11 0.03000000 sec
 TD0 1



ADβC (4a)

----- CHANNEL f1 -----
 NUC1 ¹³C
 P1 11.80 usec
 PL1 0.00 dB
 SFO1 75.4760200 MHz
 ----- CHANNEL f2 -----
 CPDPRG2 waltz16
 NUC2 ¹H
 PCPD2 95.00 usec
 PL2 0.00 dB
 PL12 18.00 dB
 SFO2 300.1312005 MHz



ns1.03.97.102. deacetylate b-dodecyl cellobioside

4.870
4.402
4.377
4.269
4.242
3.920
3.850
3.804
3.663
3.609
3.579
3.451
3.401
3.349
3.290
3.252
3.156
1.654
1.600
1.579
1.541
1.409
1.274
1.218
0.905
0.882
0.859

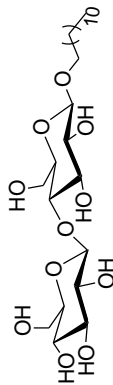
Current Data Parameters
NAME ns1.03.97.102. deacetyl1
EXPNO 1
PROCNO 1

F2 - Acquisition Parameters
Date_ 20120525
Time 14.03
INSTRUM spect
PROBHD 5 mm QNP 1H/1
PULPROG zg
ID 32768
SOLVENT MeOH
NS 16
DS 0
SWH 4789.272 Hz
FIDRES 0.146157 Hz
AQ 3.4210291 sec
RG 3228.1
DW 104.400 usec
DE 54.00 usec
TE 683.2 K
D1 3.0000000 sec
TD0 1

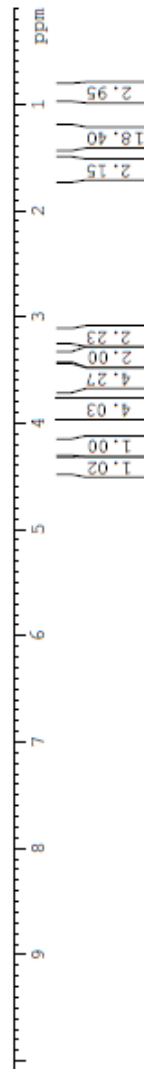
CHANNEL f1
NUC1 1H
P1 9.75 usec
PL1 0.00 dB
SFO1 300.1316507 MHz

F2 - Processing parameters
SI 32768
SF 300.1300108 MHz
WDW EM
SSB 0
LB 1.00 Hz
GB 0
PC 1.00

¹H NMR, 300 MHz, CD₃OD



DβC (4)



ns1.03.110.114. dodacyl b cellobioside CNMR

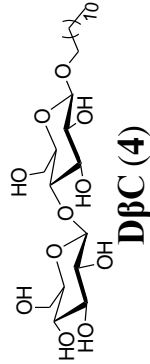
102.8
102.4
78.9
76.3
76.0
74.6
73.1
73.0
69.5
69.2
60.6
60.0
31.3
29.0
29.0
28.8
28.7
25.3
21.9
12.7

Current Data Parameters
NAME ns1.03.110.114. dodac
EXPNO 2
PROCNO 1

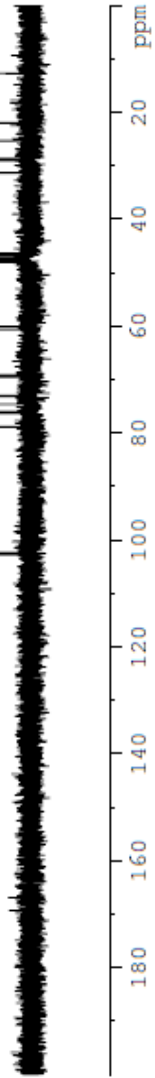
¹³C NMR, 75 MHz, CD₃OD

F2 - Acquisition Parameters

Date_ 20120906
Time 22.06
INSTRUM spect
PROBHD 5 mm QNP 1H/1
PULPROG zgdc
TD 65536
SOLVENT CDCl3
NS 1280
DS 0
SWH 18832.393 Hz
FIDRES 0.267360 Hz
AQ 1.7400308 sec
RG 5160.6
DW 26.550 usec
DE 6.00 usec
TE 295.2 K
D1 1.00000000 sec
d11 0.03000000 sec
ID0 1



----- CHANNEL f1 -----
NUC1 13C
P1 11.80 usec
PL1 0.00 dB
SFO1 75.4760200 MHz
----- CHANNEL f2 -----
CPDPRG2 waltz16
NUC2 1H
PCPD2 95.00 usec
PL2 0.00 dB
PL12 18.00 dB
SFO2 300.1312005 MHz
F2 - Processing parameters
SI 32768
SF 75.4677789 MHz
WDW no
SSB 0
LB 0.00 Hz

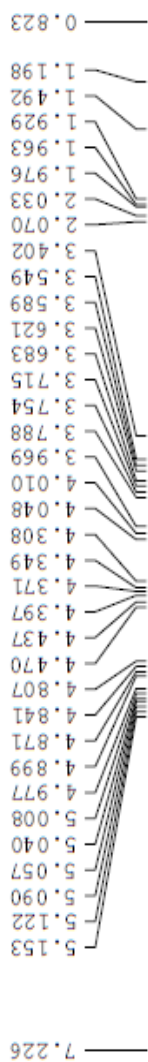


nsl.03.113.117. acetylated tridecyl cellobioside G_90_107

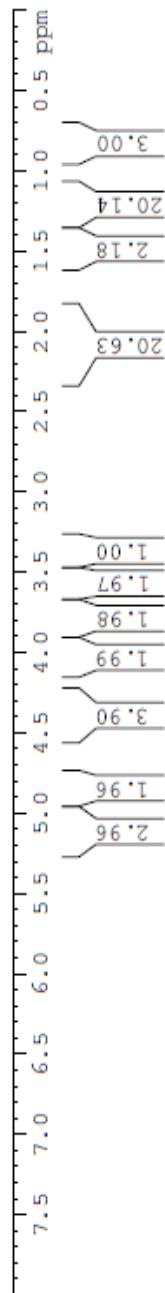
```

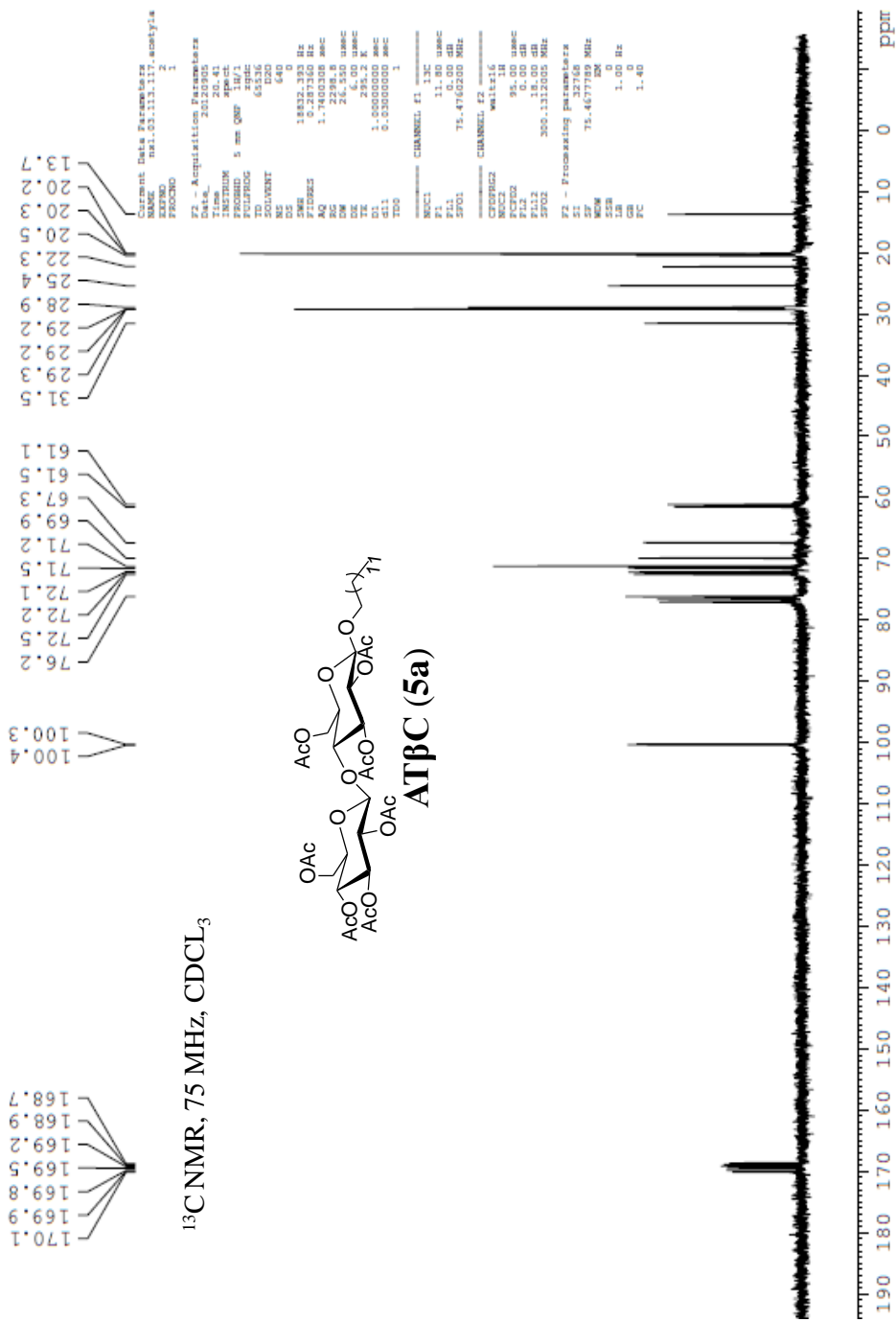
NAME: nsl.03.113.117. acetylated tridecyl
EXPNO: 1
PROCNO: 1
PROCPS: 1
F2 - Acquisition Parameters
Date_ 20120908
Time 14.41
INSTRUM: spect
PROBHD: 5 mm QNP
PULPROG: zgpg30
AQ: 0.20000000
SOLVENT: CDCl3
NS: 6552
DS: 4
SWH: 131.271517 MHz
FIDRES: 0.17116 MHz
AQRES: 171.16 MHz
SFO: 100.6261260 MHz
SI: 32768
SF: 3.00000000 GHz
=====
NAME: CHOLERA 01
EXPNO: 1
PROCNO: 1
PROCPS: 1
F2 - Processing parameters
Date_ 20120908
Time 14.41
INSTRUM: spect
PROBHD: 5 mm QNP
PULPROG: zgpg30
AQ: 0.20000000
SOLVENT: CDCl3
NS: 6552
DS: 4
SWH: 131.271517 MHz
FIDRES: 0.17116 MHz
SFO: 100.6261260 MHz
SI: 32768
SF: 3.00000000 GHz
=====

```



¹H NMR, 300 MHz, CDCl₃





ns1.03.114.118. tridecyl b cellobioside Sep 7 new

4.427
4.401
4.292
4.266
3.897
3.867
3.889
3.672
3.650
3.632
3.597
3.574
3.544
3.535
3.518
3.505
3.476
3.403
3.378
3.347
3.321
3.309
3.263
3.251
3.235
3.225
3.208
3.197
1.891
1.643
1.620
1.597
1.290
0.900
0.877

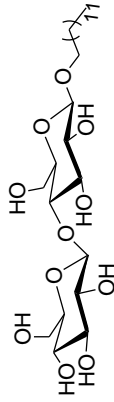
Current Data Parameters
NAME ns1.03.114.118.
EXPNO 1
PROCNO 1

F2 - Acquisition Parameters
Date_ 20120907
Time 19.10
INSTRUM spect
PROBHD 5 mm QNP 1H/1
PULPROG zg
TD 32768
SOLVENT MeOH
NS 16
DS 0
SWH 4789.272 F
FIDRES 0.146157 F
AQ 3.4210291 s
RG 114
DW 104.400 u
DE 54.00 u
TE 295.2 K
D1 3.00000000 s
TD0 1

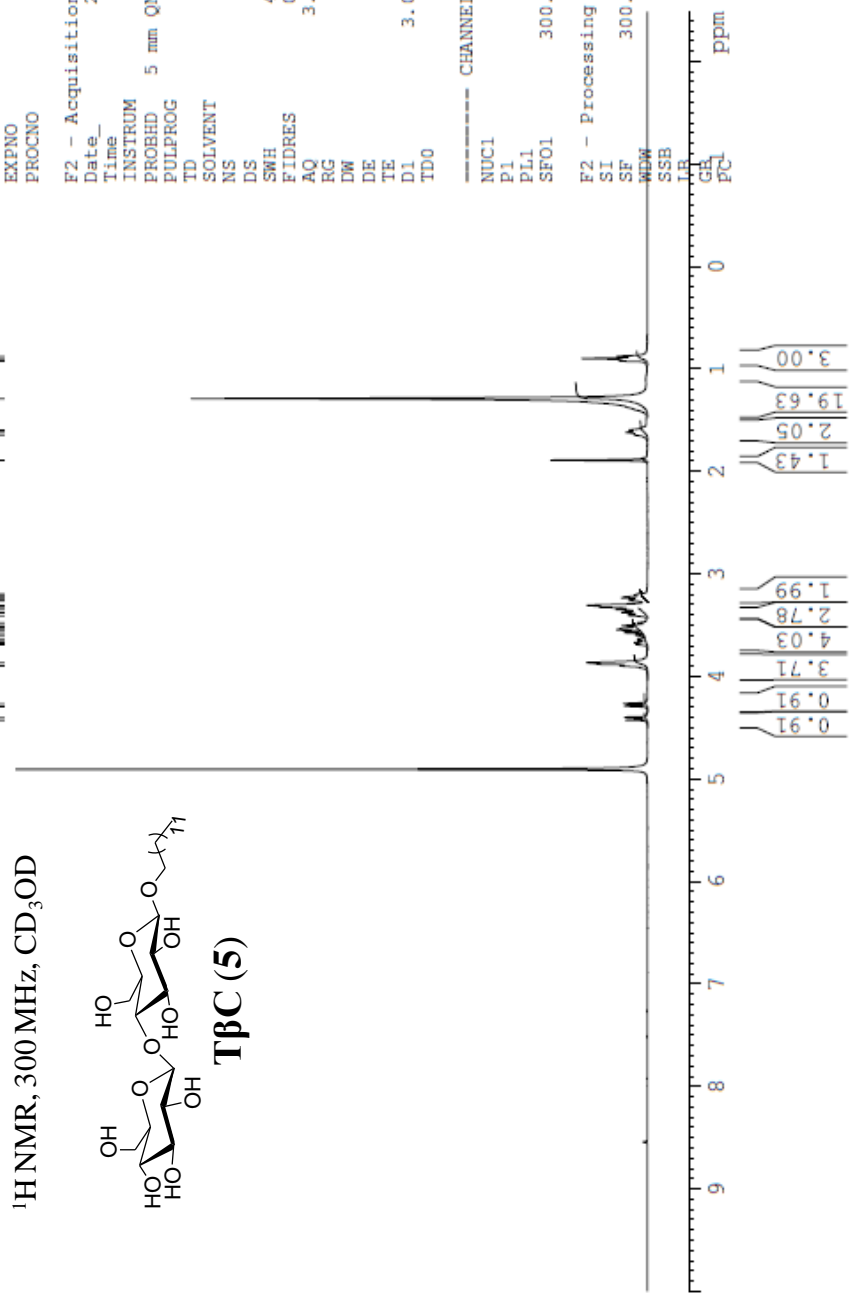
----- CHANNEL f1 -----
NUC1 1H
P1 9.75 u
PL1 0.00 c
SFO1 300.1316507 M

F2 - Processing parameters:
SI 32768
SF 300.1300050 M
WDW no
SSB 0
GB 0.00 F
PC 1.00

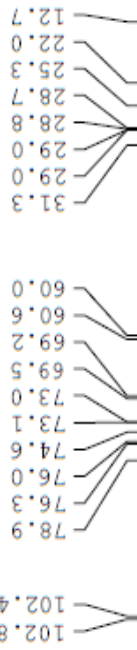
¹H NMR, 300 MHz, CD₃OD



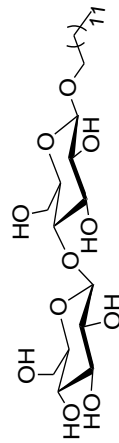
TBC (5)



nsl.03.114.118. tridecyl b cellobioside CNMR



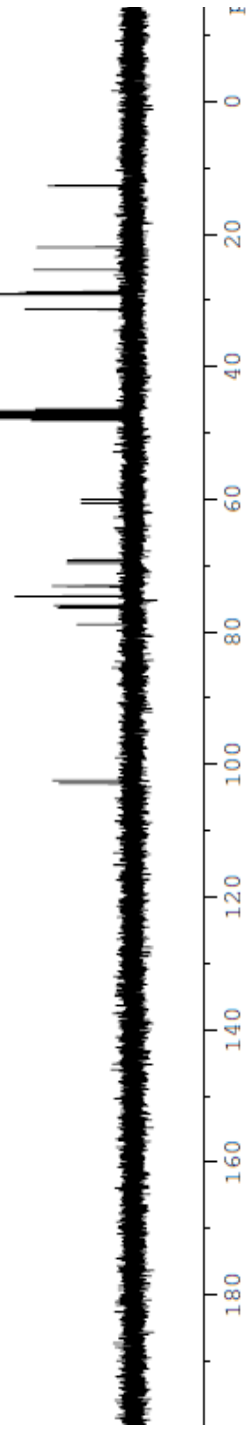
¹³C NMR, 75 MHz, CD₃OD



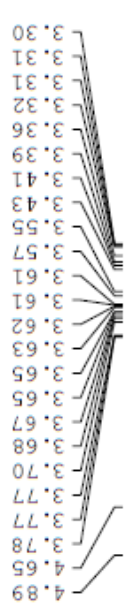
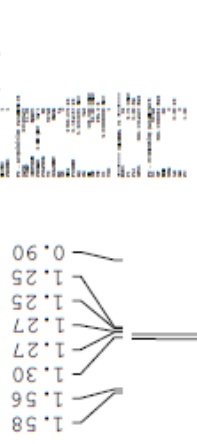
TPC (5)

```

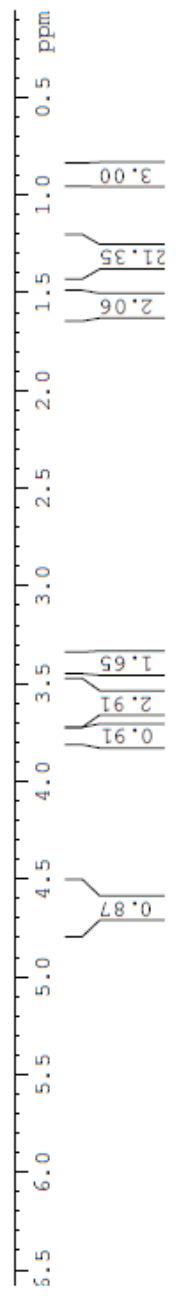
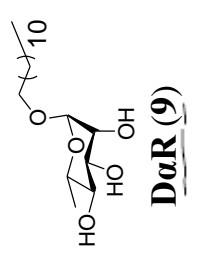
Current Data Parameters
NAME      nsl.03.114.118. tridecyl b
EXPNO    2
PROCNO    1
F2 - Acquisition Parameters
Date_     20120907
Time      19.22
INSTRUM   spect
PROBHD    5 mm QNP 1H/1
PULPROG   zgpg30
TD         65536
SOLVENT   CD3OD
NS         512
DS         0
SWH        18323.70 Hz
AQ         1.7400398 sec
RG         1625.5
DE         26.000000 umsec
TE         285.2 K
D1         1.00000000 sec
d11        0.10000000 sec
DELTA     0.10000000 sec
TD0
===== CHANNEL F1 =====
NUC1       13C
P1         11.80 umsec
PL1        0.00 dB
SFO1       75.4760250 MHz
===== CHANNEL F2 =====
CPDPRG2    waltz16
NUC2       13C
P2         95.00 umsec
PL2        0.00 dB
SFO2       300.1312005 MHz
===== CHANNEL F3 =====
F2 - Processing parameters
SI         32768
SF         75.4677189 MHz
WDW        EM
SSB        0
LB         0.00 Hz
GB         0
PC         1.40
  
```



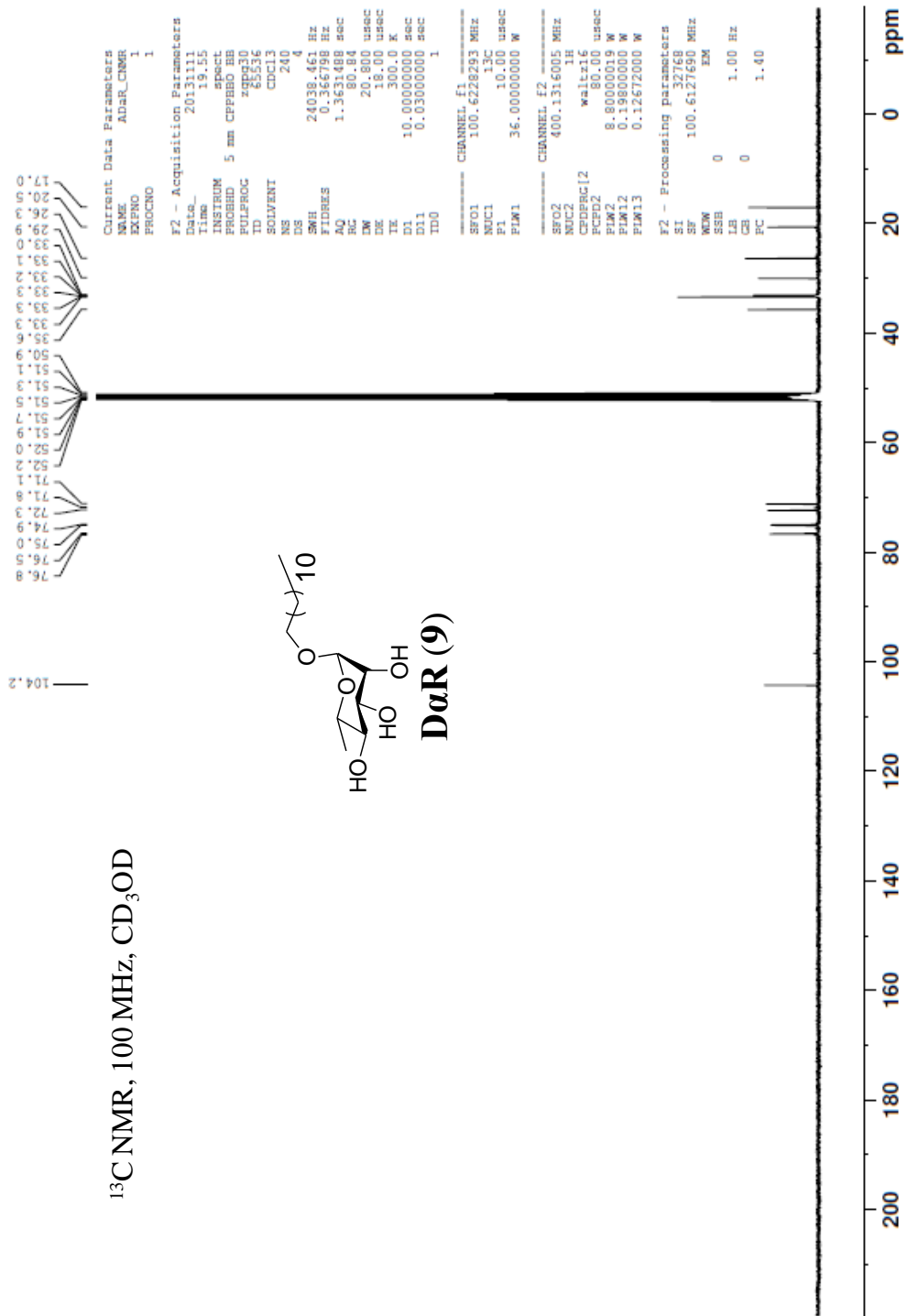
ns1.03.99.104.deacetylated dodecyl rhamnoside F2



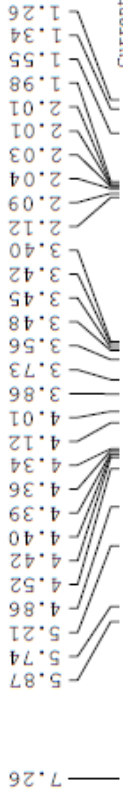
¹H NMR, 300 MHz, CD₃OD



¹³C NMR, 100 MHz, CD₃OD



ns1.03.120.130 undecylene acetylated cellobioside



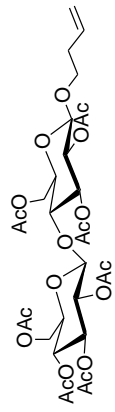
Current Data Parameters
NAME ns1.03.120.130 undecy
EXPNO 1
PROCNO 1

F2 - Acquisition Parameters
Date_ 20120928
Time_ 10.01
INSTRUM spect
PROBHD 5 mm QNP 1H/1
PULPROG zgpg

ID 32768
SOLVENT CDCl3
NS 8
DS 0
SWH 4789.272 Hz
FIDRES 0.146157 Hz
AQ 3.4210291 sec
RG 812.7
DW 104.400 usec
DE 54.00 usec
TE 295.2 K
D1 1.00000000 sec
D10 1

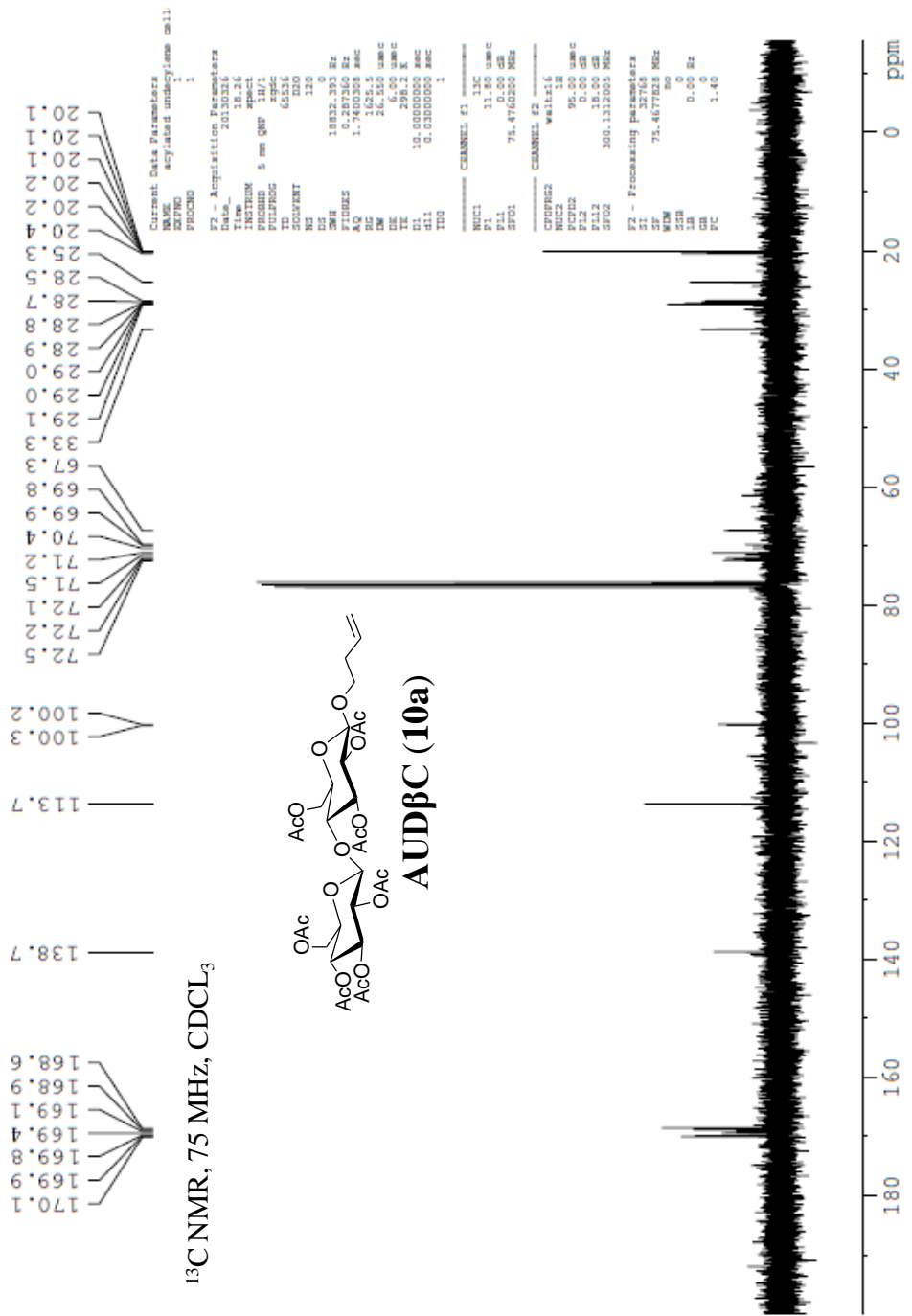
CHANNEL f1
NUC1 1H
P1 9.75 usec
PL1 0.00 dB
SFO1 300.1316507 MHz

F2 - Processing parameters
SI 32768
SF 300.1300062 MHz
WDW EM
SSB 0

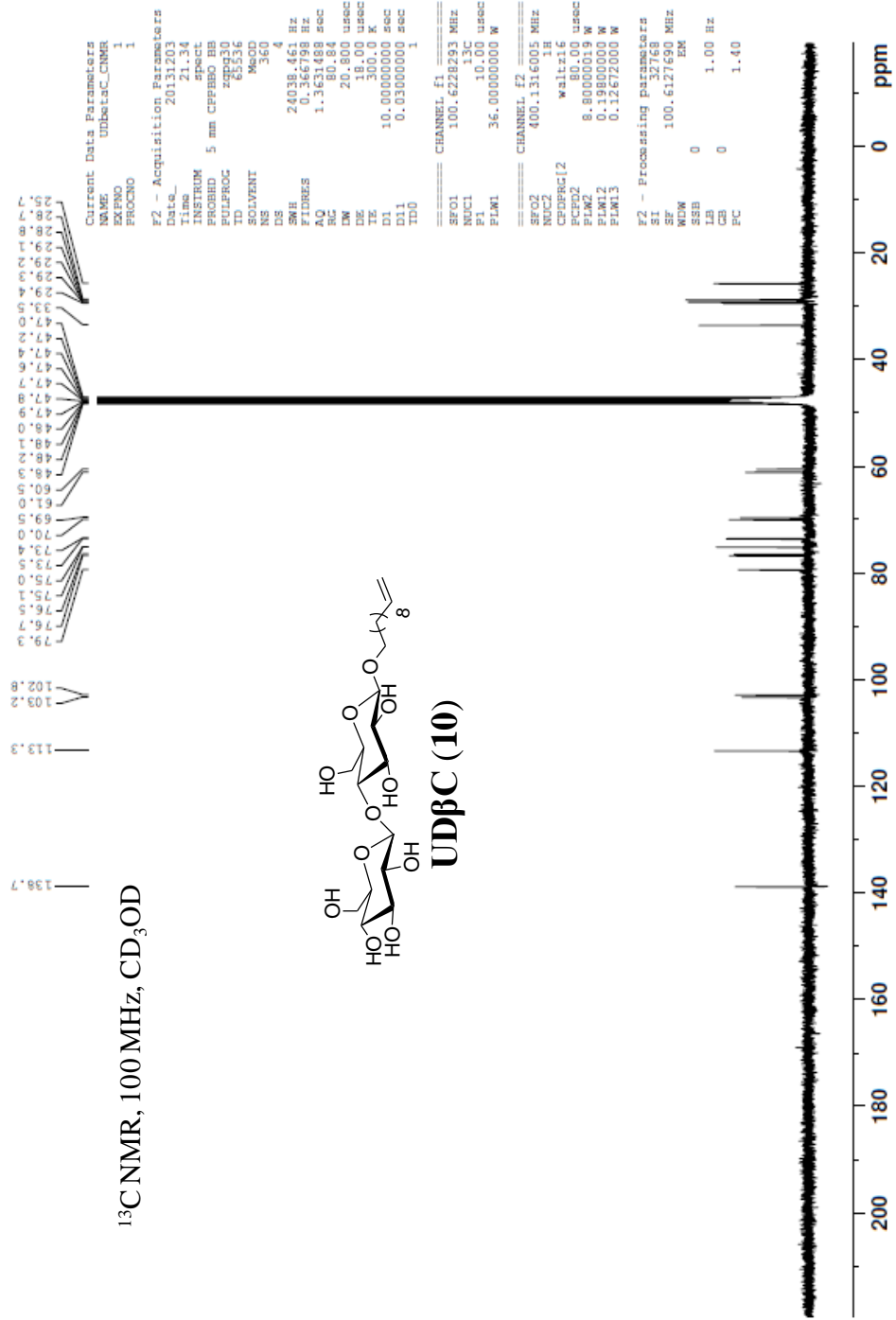


AUDβC (10a)

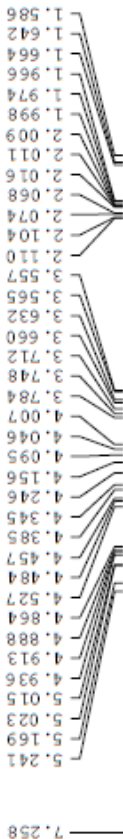
acylated undecylene cellobioside CNMR_2



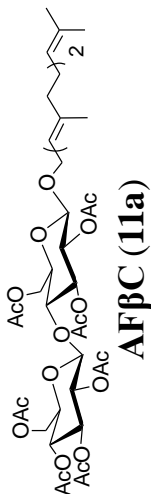
¹³C NMR, 100 MHz, CD₃OD



ns1.03.129.144 F42_46_Acylated Farnesy1 DC



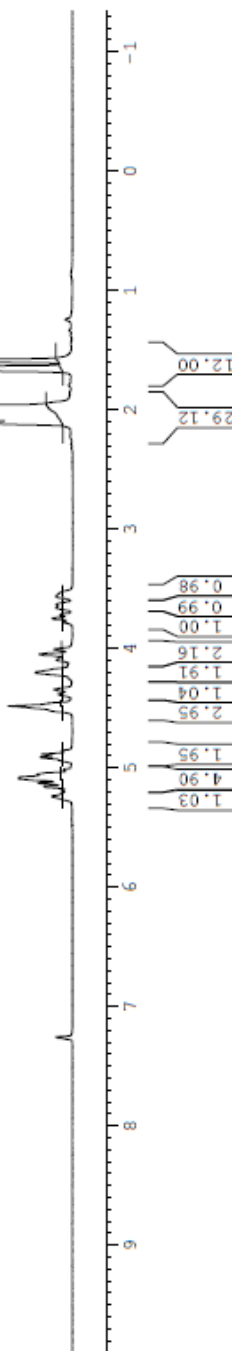
¹H NMR, 300 MHz, CDCl₃

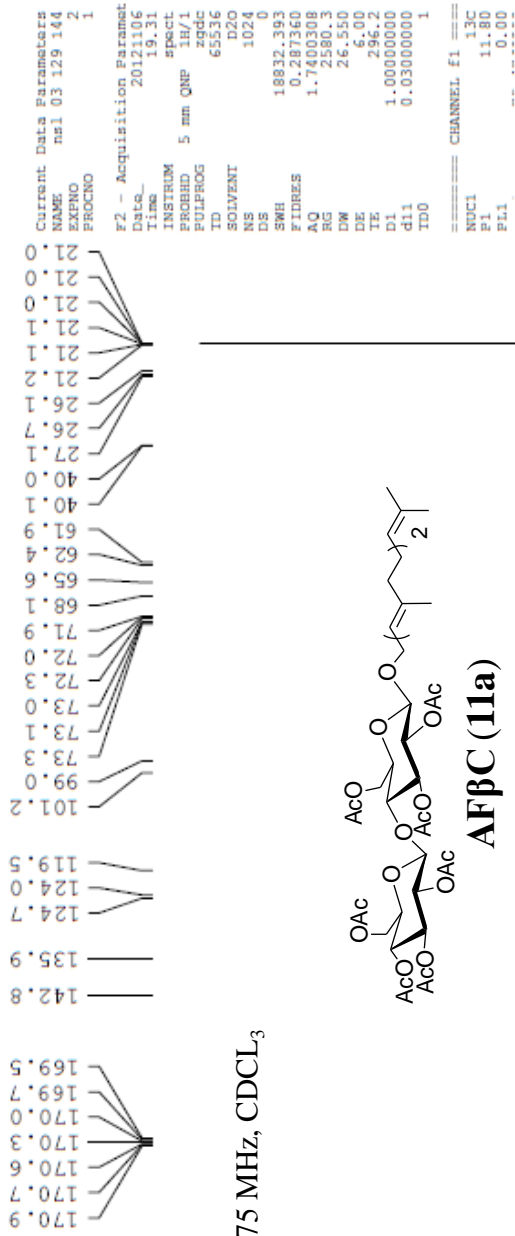


Current Data Parameters
NAME ns1.03.129.144 F42_46.J
EXPNO 1
PROCNO 1

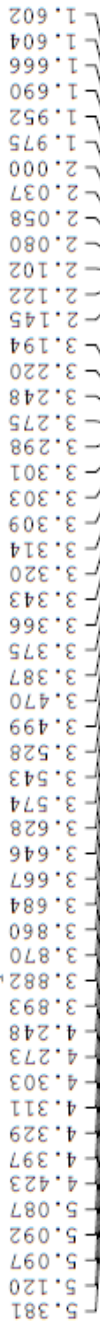
F2 - Acquisition Parameters
Date_ 20121106
Time 18.37
INSTRUM spect
PROBHD 5 mm QNP 1H/1
PULPROG zg
TD 32768
SOLVENT CDCl3
NS 16
DS 0
SWH 4789.272 Hz
FIDRES 0.146157 Hz
AQ 3.4210291 sec
RG 71.8
DW 104.400 usec
DE 54.00 usec
TE 296.2 K
D1 1.0000000 sec
TD0 1

CHANNEL f1
NUC1 1H
P1 9.75 usec
PL1 0.00 dB
SFO1 300.1316507 MHz
F2 - Processing parameters
SI 32768
SF 300.1300553 MHz
WDW EM
SSB 0
GB 0.00 Hz
PC 1.00

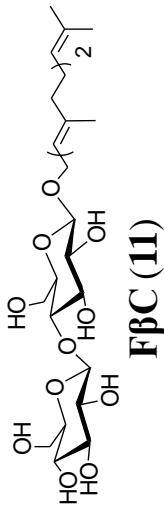




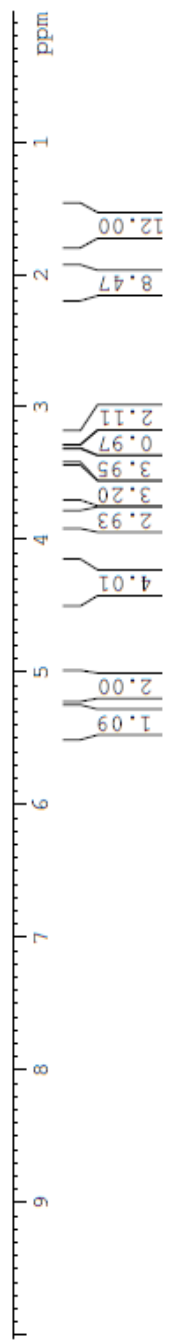
ns1.03.130.147. farnesyl cellobioside 2



¹H NMR, 300 MHz, CD₃OD



Channel Data Parameters
NAME: ns1.03.130.147. farnesyl cellobioside 2
PROCNO: 1
Date_ Time: 2011.03.14 11:24
INSTRUM: spect
PROBHD: 5 mm QNP
PULPROG: zgpg30
TD: 65536
AQ: 1.00000000
RG: 327.5
ORIG: 0.00000000
F2 - Acquisition Parameters
Date_ Time: 2011.03.14 11:24
INSTRUM: spect
PROBHD: 5 mm QNP
PULPROG: zgpg30
TD: 65536
AQ: 1.00000000
RG: 327.5
ORIG: 0.00000000
F2 - Processing parameters
Date_ Time: 2011.03.14 11:24
INSTRUM: spect
PROBHD: 5 mm QNP
PULPROG: zgpg30
TD: 65536
AQ: 1.00000000
RG: 327.5
ORIG: 0.00000000
F2 - Processing parameters
Date_ Time: 2011.03.14 11:24
INSTRUM: spect
PROBHD: 5 mm QNP
PULPROG: zgpg30
TD: 65536
AQ: 1.00000000
RG: 327.5
ORIG: 0.00000000




```

Current Data Parameters
NAME      ns1.03.130.147  farrh
EXPNO     2
PROCNO    1

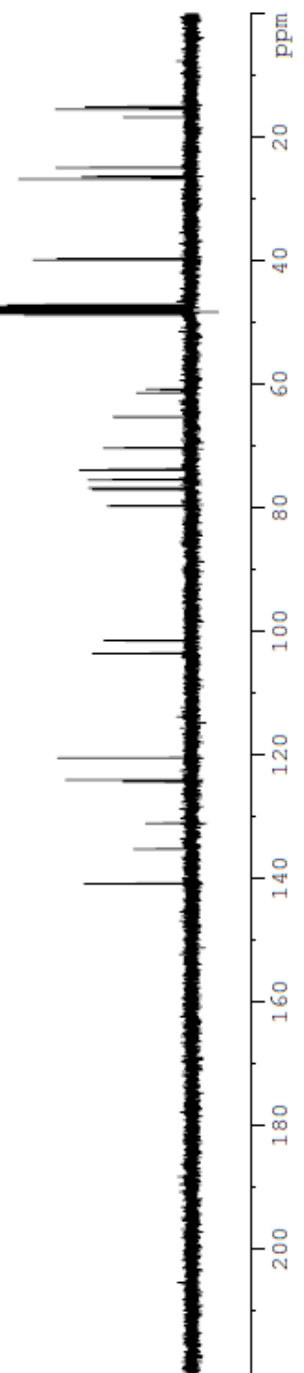
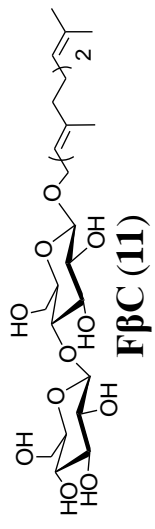
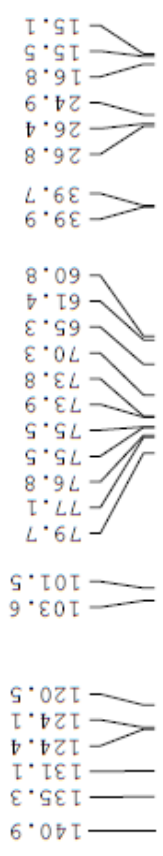
F2 - Acquisition Parameters
Date_     20121108
Time      17.59
INSTRUM   spect
PROBHD    5 mm QNP 1H/1
PULPROG   zgpgc
TD         65536
SOLVENT   CDCl3
NS         640
DS         0
SWH        18832.393 Hz
FIDRES     0.287360 Hz
AQ         1.7400308 sec
RG         2896.3
DM         26.550 usec
DE         6.00 usec
TE         295.2 K
D1         1.00000000 sec
d11        0.03000000 sec
TD0        1

===== CHANNEL F1 =====
NUC1       13C
P1         11.80 usec
PL1        0.00 dB
SFO1       75.4760200 MHz

===== CHANNEL F2 =====
CPDPRG2    waitz16

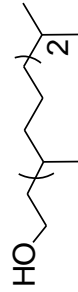
```

¹³C NMR, 75 MHz, CD₃OD

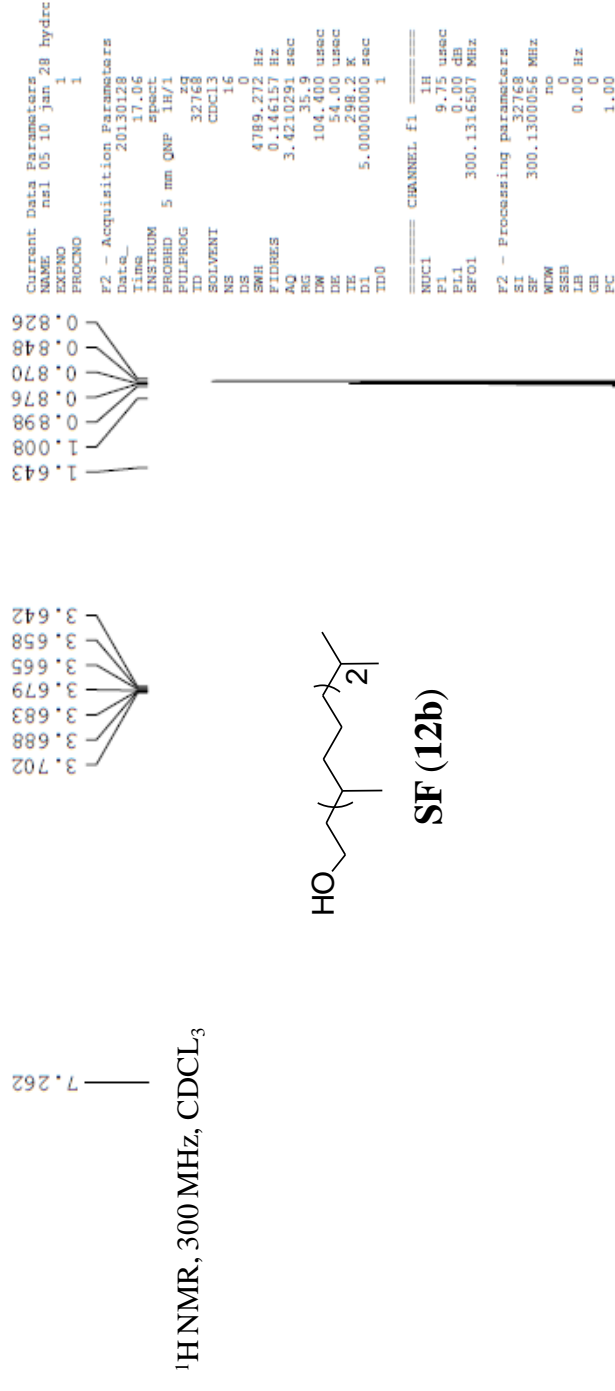


ns1 05 10 jan 28 hydrogenated farnesol F2_18_27

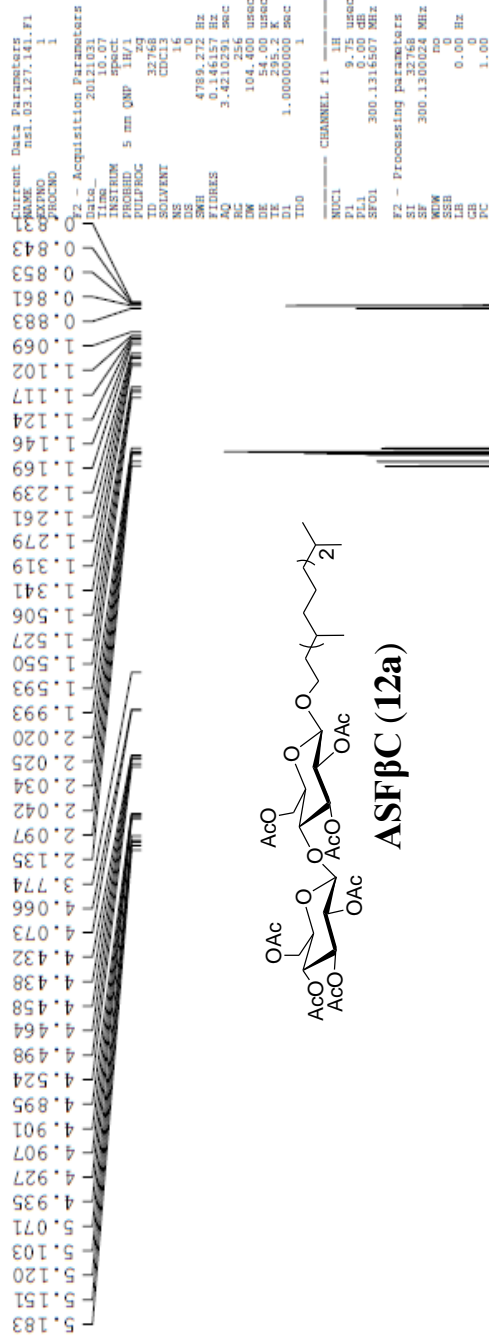
¹HNMR, 300 MHz, CDCl₃



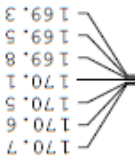
SF (12b)



nsl.03.127.141.F1



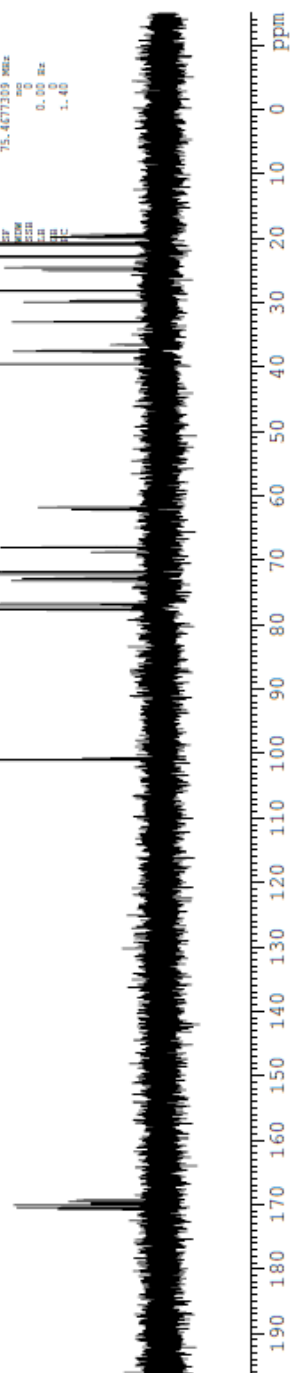
nsl.03.127.141 F1 CNMR



¹³C NMR, 75 MHz, CDCl₃



Current Data Parameters
NAME nsl.03.127.141 F1 CNMR
EXPNO 2
PROCNO 1
F2 - Acquisition Parameters
Date_ 20121101
Time 19.28
INSTRUM spect
PROBHD 5 mm QNP 1H/1
PULPROG zgpg30
TD 65536
SOLVENT DMSO
NS 1440
DS 4
AQ 1893.310 Hz
FIDRES 0.287370 Hz
PDERES 1.7400368 sec
RG 1324.6
DE 26.700 umax
TE 298.2 K
SI 1.0000000 sec
SF 101.625361 MHz
FREQ 101.625361 MHz
NUC1 13C
P1 11.80 umax
PL1 0.00 dB
SFO1 75.4763200 MHz
C2PROG2 waltz16
NUC2 13C
P2 11.80 umax
PL2 0.00 dB
SFO2 75.4763200 MHz
F2 - Processing parameters
SI 32768
SF 75.4673189 MHz
WDW EM
SSB 0.00 Hz
GC 1.40



ns1 05 11 12 b BHFC

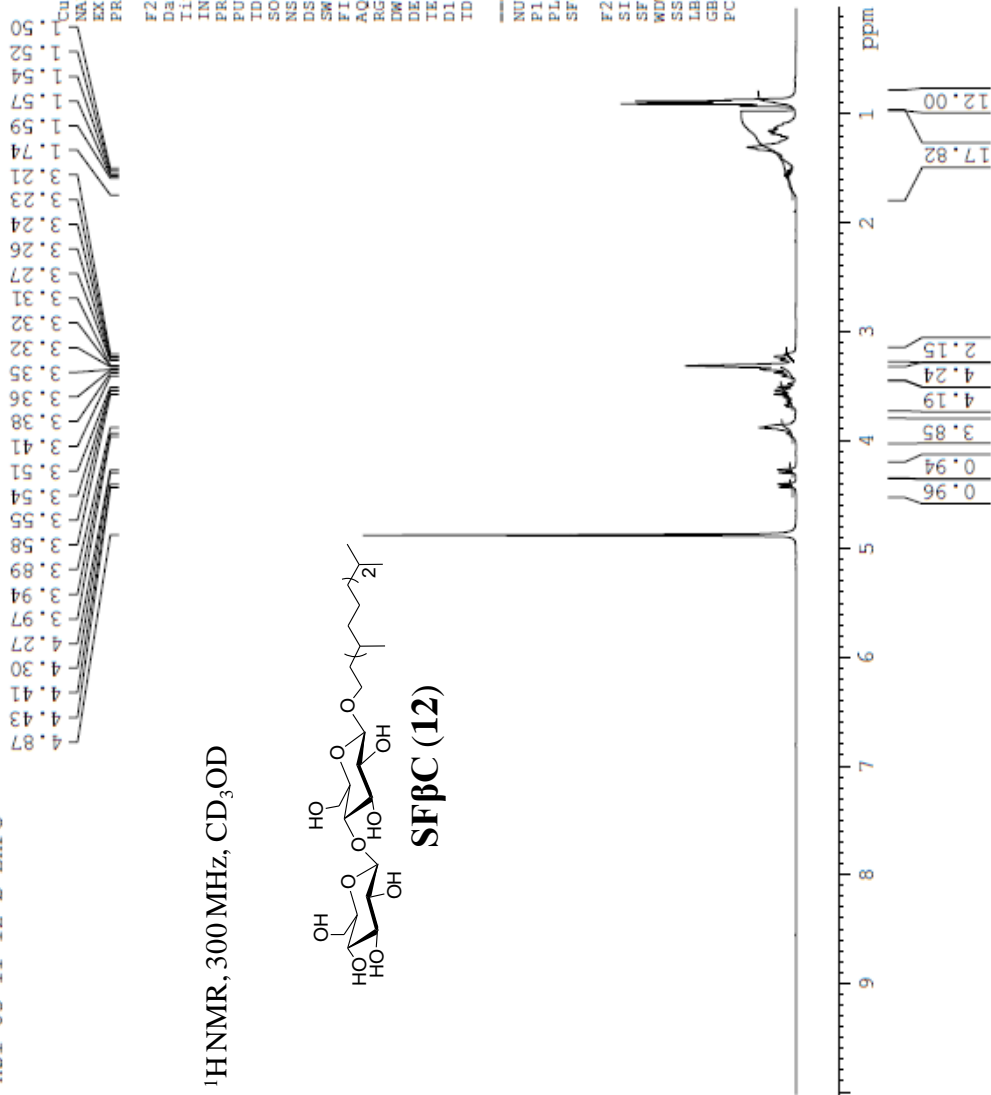
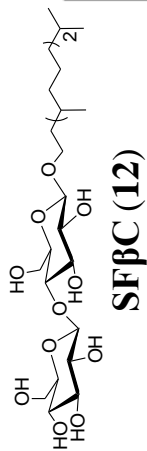
50
52
54
57
59
74
21
23
24
26
27
31
32
32
35
36
38
41
51
54
55
58
89
94
97
27
30
41
43
87

Current Data Parameters
NAME ns1 05 11 12 b BHFC
EXPNO 1
PROCNO 1

F2 - Acquisition Parameters
Date_ 20130201
Time 16.42
INSTRUM spect
PROBHD 5 mm QNP 1H/1
PULPROG zg
ID 32768
SOLVENT MeOH
NS 16
DS 0
SWH 4789.272 Hz
FIDRES 0.146157 Hz
AQ 3.4210291 sec
RG 322.5
DW 104.400 usec
DE 54.00 usec
TE 327.2 K
D1 3.00000000 sec
TD0 1

CHANNEL f1
NUC1 1H
P1 9.75 usec
PL1 0.00 dB
SFO1 300.1316507 MHz
F2 - Processing parameters
SI 32768
SF 300.1300024 MHz
WDW EM
SSB 0
LB 1.00 Hz
GB 0
PC 1.00

¹H NMR, 300 MHz, CD₃OD



Current Data Parameters
 EXPNO 2
 F2 - Acquisition Parameters
 Date_ 2012103
 Time 12.23
 PROBRW 5 mm QNP 1H/1
 PULPROG zgpg30
 PROCNT 4
 SFO1 103.6
 SFO2 75.476200 MHz
 AQ 1.7400000 sec
 DE 26.000 uV
 TE 300.2 K
 SI 1
 TD 1

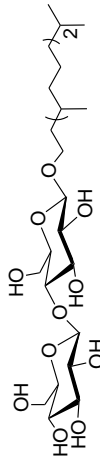
===== CHANNEL f1 =====
 NUC1 13C
 P1 11.00 usec
 SFO1 75.476200 MHz

===== CHANNEL f2 =====
 NUC2 1H
 P2 18.00 usec
 SFO2 400.131005 MHz

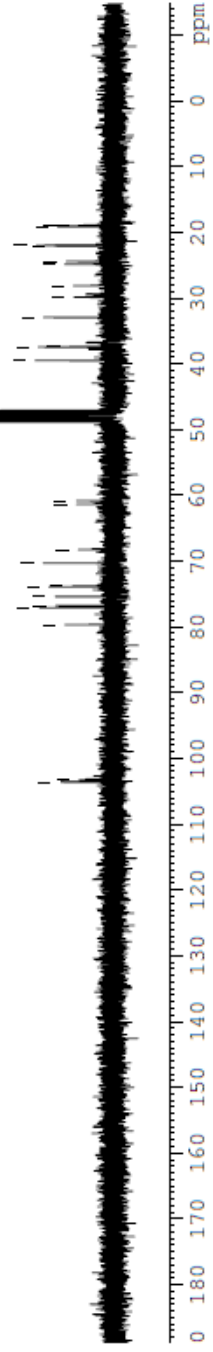
F2 - Processing parameters
 SI 32768
 SF 75.457700 MHz
 DS 4
 SSB 0
 LB 0.00 Hz
 GB 0
 PC 1.40

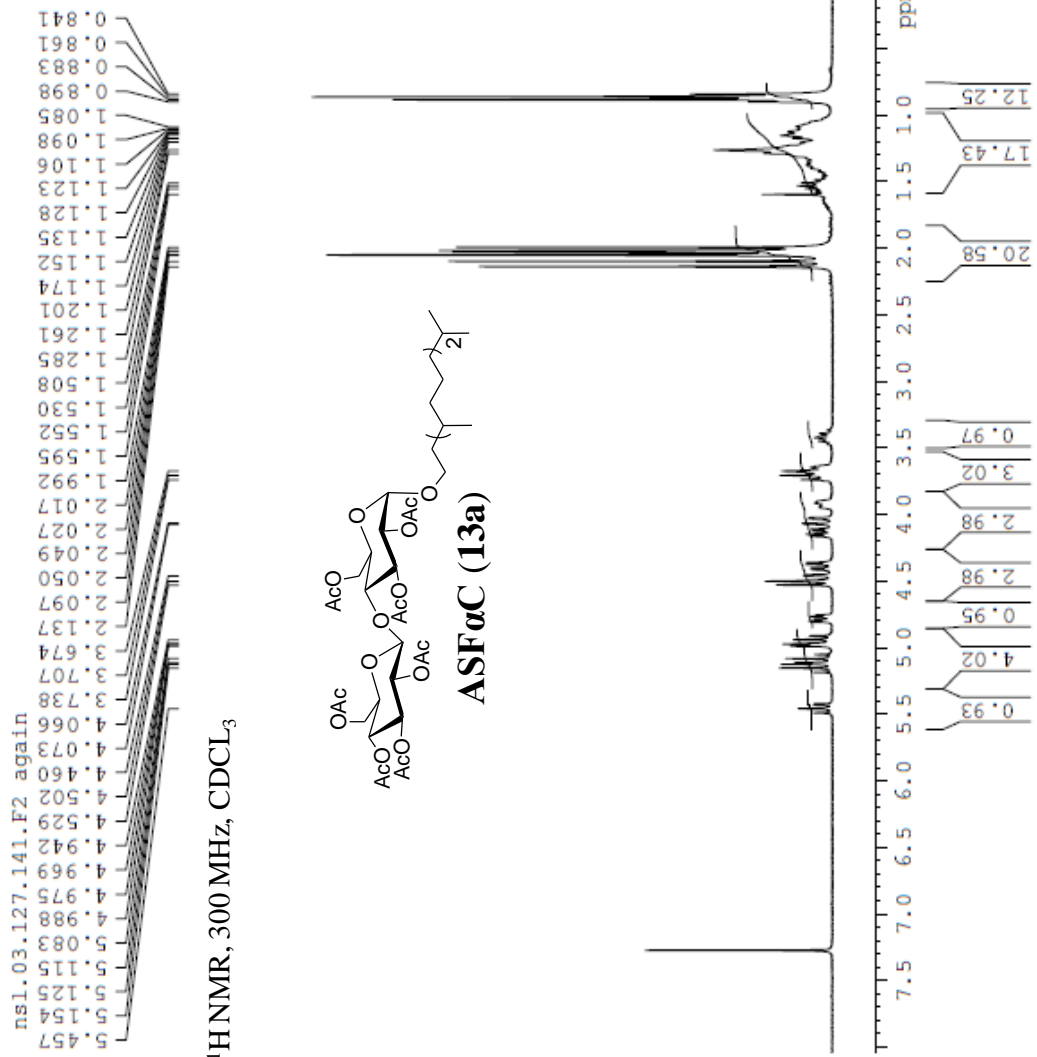
103.6
103.3
79.7
77.1
76.8
75.4
73.9
73.8
70.3
68.3
61.4
60.8
39.5
37.7
37.5
37.4
33.0
29.9
28.1
24.9
24.5
22.1
22.0
19.2
19.1
19.0
18.9

¹³C NMR, 75 MHz, CD₃OD

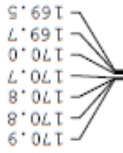


SFBC (12)





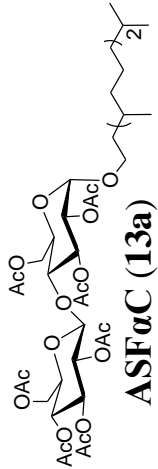
msl.03.127.141 F2 CNMR



¹³C NMR, 75 MHz, CDCl₃

Current Data Parameters
NAME msl.03.127.141 F2 CNMR
EXPNO 2
PROCNO 1

F2 - Acquisition Parameters
Date_ 2012.03
Time 21.05
INSTRUM spect
PROBHD 5 mm QNP 1H/1
PULPROG zgpg30
TD 65536
SOLVENT D2O
NS 640
DS 4

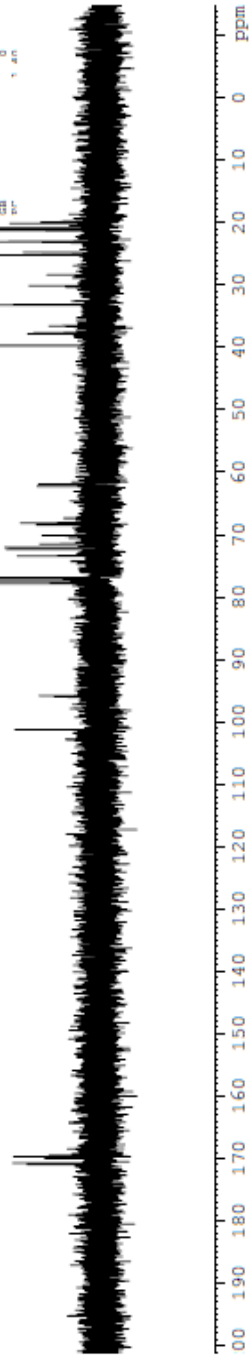


SWH 18832.393 Hz
FIDRES 0.287160 Hz
AQ 1.746039 sec
RG 409.6
DM 26.530 usec
DE 6.00 usec
TE 300.2 K
D1 1.00000000 sec
d11 0.03000000 sec
D10 1.00000000 sec

===== CHANNEL f1 =====
NUC1 ¹³C
P1 1.00 usec
PL1 0.00 dB
SFO1 75.476200 MHz

===== CHANNEL f2 =====
CPDPRG2 waltz16
NUC2 ¹H
PCPD2 95.00 usec
PL2 19.00 dB
PL12 18.00 dB
SFO2 300.1312005 MHz

F2 - Processing parameters
SI 32768
SF 75.457790 MHz
WDW EM
SSB 0
LB 0.00 Hz
GB 0
CB 0
B0 1.40

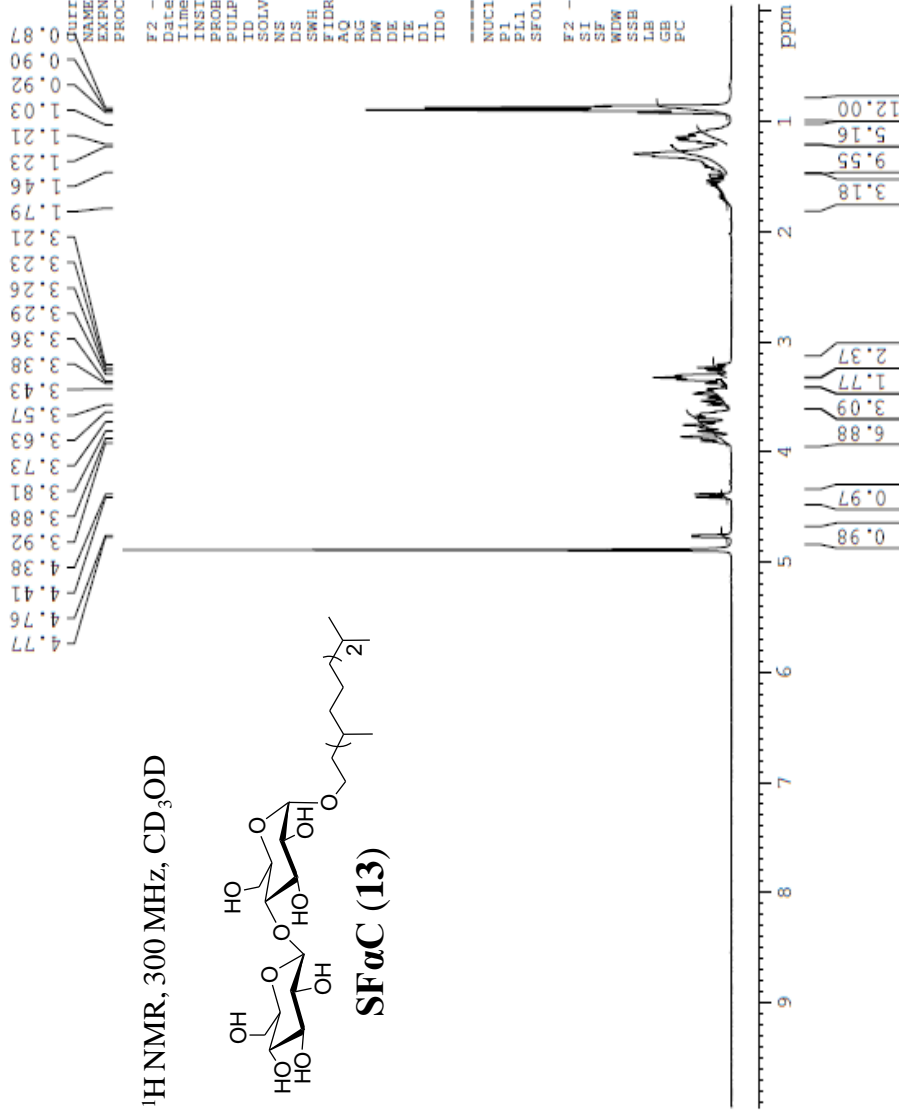


ns1.03.128.143. hydrogenated alpha farnesyl DC 2

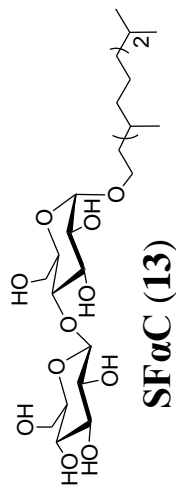
Current Data Parameters
NAME ns1.03.128.143. hydrog
EXPNO 1
PROCNO 1

F2 - Acquisition Parameters
Date_ 2011103
Time_ 11:03
INSTRUM spect
PROBHD 5 mm QNP 1H/1
PULPROG zgpg30
TD 3279
SOLVENT MeOH
NS 16
DS 1
SWH 4789.272 Hz
FIDRES 0.134157 Hz
AQ 3.4210391 SEC
RG 71.8
CW 104.400 usec
DE 5.400 usec
TE 296.2 K
D1 1.00000000 SEC
TD0 1

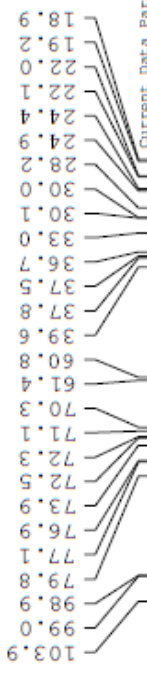
CHANNEL f1
NUC1 1H
P1 9.5 usec
PL1 0.0 dB
SFO1 300.1316507 MHz
F2 - Processing parameters
SI 32796
SF 300.1300053 MHz
WDW no
SSB 0
LB 0.00 Hz
GB 0
PC 1.00



¹H NMR, 300 MHz, CD₃OD

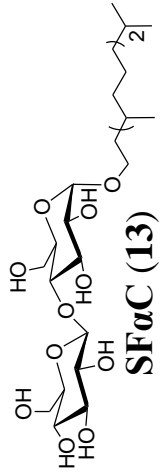


s1.03.128.143. hydrogenated alpha farnesyl DC CNM



Current Data Parameters
NAME s1.03.128.143. hydrogenat
EXPNO 2
PROCNO 1

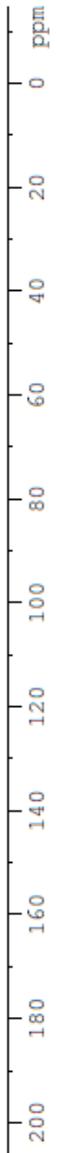
F2 - Acquisition Parameters
Date_ 201210
Time 13.38
INSTRUM spect
PROBHD 5 mm QNP 1H/1
PULPROG zgpg30
ID zgpg30
SOLVENT CDCl3
NS 1024
DS 4
SWH 18832.303 Hz
FIDRES 0.287360 Hz
AQ 1.740502 sec
RG 327.5
RG2 327.5
RG3 327.5
DW 26.566 usec
DE 6.00 usec
TE 296.2 K
SFO1 100.626130 MHz
d11 1.00000000 sec
TD0 1



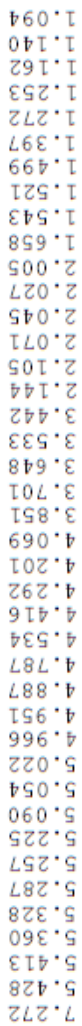
CHANNEL f1
NUC1 13C
P1 1.80 usec
PL1 0.00 dB
SFO1 75.4760200 MHz

CHANNEL f2
CPDPRG2 waltz16
NUC2 1H
PCPD2 95.00 usec
PL2 0.00 dB
PL12 18.00 dB
SFO2 300.1312005 MHz

F2 - Processing parameters
SI 32768
SF 75.4677190 MHz
WDW HO
SSB 0
LB 0.00 Hz
GB 0
PC 1.40



ns1 05 36 41_57_72



¹H NMR, 300 MHz, CDCl₃

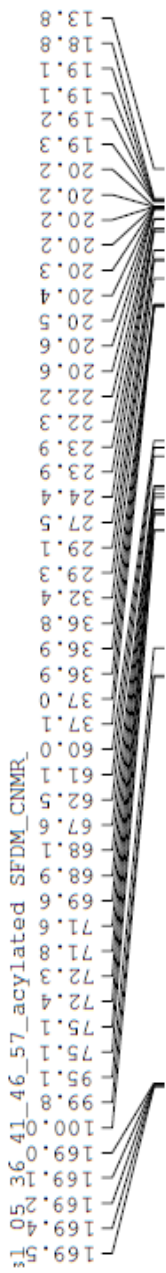
Current Data Parameters
NAME ns1 05 36 41_57_72
EXPNO 1
PROCNO 1

F2 - Acquisition Parameters
Date_ 20130605
Time 10.19
INSTRUM spect
PROBHD 5 mm QNP 1H/1
PULPROG zg
TD 32768
SOLVENT CDCl3
NS 8
DS 0
SWH 4789.272 Hz
FIDRES 0.146157 Hz
AQ 3.4210291 sec
RG 101.6
DM 104.400 usec
DE 54.00 usec
TE 295.2 K
D1 1.0000000 sec
TD0 1

CHANNEL f1
NUC1 1H
P1 9.75 usec
PL1 0.00 dB
SFO1 300.1316507 MHz
F2 - Processing parameters
SI 32768
SF 300.1300024 MHz
WDW EM
SSB 0
LB 1.00 Hz
GB 0
PC 1.00



ASFβM (14a)



¹³C NMR, 75 MHz, CDCl₃



ASFBM (14a)

```

Current Data Parameters
NAME      ns1_05_36_41_46_57_scy
EXPNO     2
PROCNO    1

F2 - Acquisition Parameters
Date_     20130703
Time      17.27
INSTRUM   spect
PROBHD    5 mm QNP 1H/1
PULPROG   zgpg30
SOLVENT   MeOH
NS         240
DS         0
SWH        18832.393 Hz
FIDRES     0.287360 Hz
AQ         1.7400308 sec
RG         3849.1
DW         26.550 usec
DE         6.00 usec
TE         429.2 K
d1         10.00000000 sec
d11        0.03000000 sec
TD0        1

===== CHANNEL F1 =====
NUC1       13C
P1         11.80 usec
PL1        0.00 dB
SFO1       75.4760200 MHz

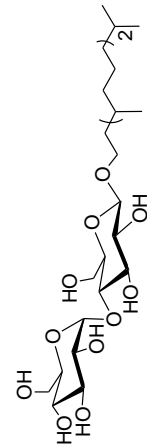
===== CHANNEL F2 =====
CPDPRG2   waitz16
NUC2       1H
PCPD2     95.00 usec
PL2        0.00 dB
PL12       18.00 dB
SFO2       300.1312005 MHz

F2 - Processing parameters
SI         32768
SF         75.4677189 MHz
WDW        EM
SSB        0
GB         0.00 Hz
PC         1.40
  
```

ns1 05 39 43_BetaSFDM



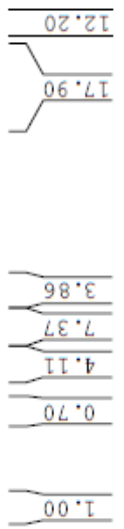
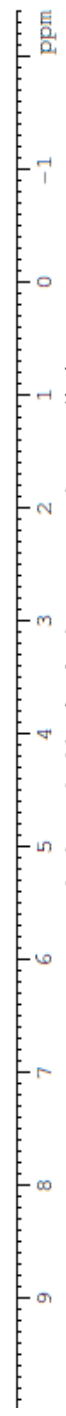
¹H NMR, 300 MHz, CD₃OD



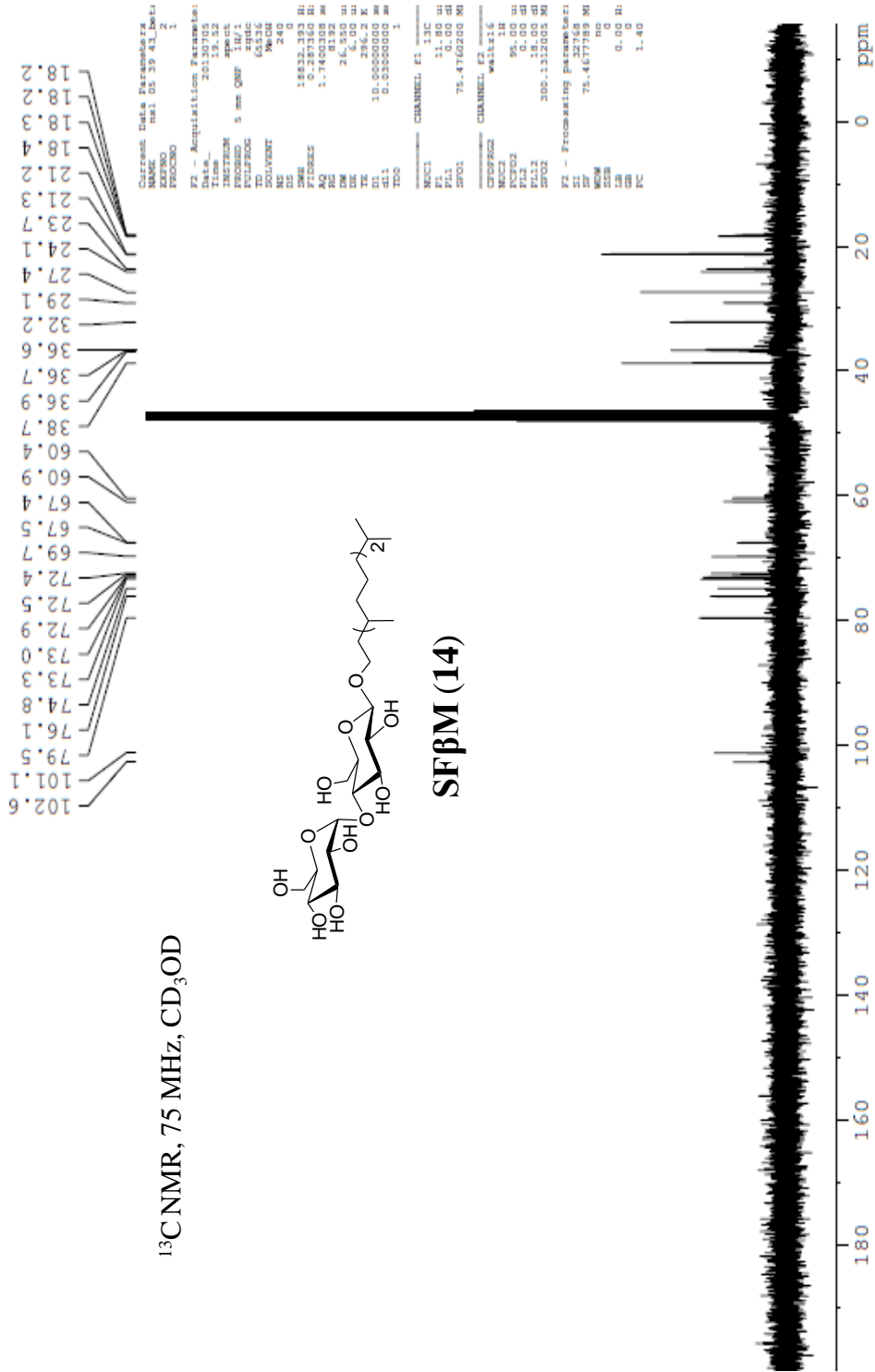
Current Data Parameters
NAME ns1 05 39 43_B
EXPNO 1
PROCNO 1

F2 - Acquisition Parameters
Date_ 20130705
Time 9.46
INSTRUM spect
PROBHD 5 mm QNP 1H/1
PULPROG zg
TD 32768
SOLVENT MeOH
NS 16
DS 5
SWH 4789.272
FIDRES 0.146157
AQ 3.4210291
RG 101.6
DW 104.400
DE 54.00
TE 334.2
D1 3.0000000
TD0 1

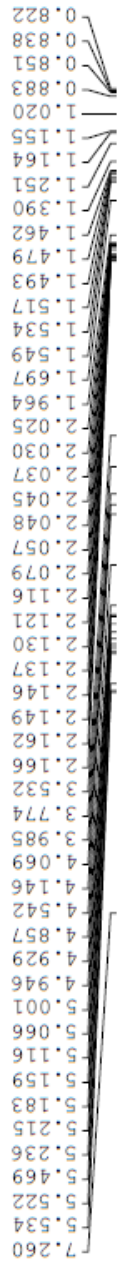
==== CHANNEL f1 ====
NUC1 1H



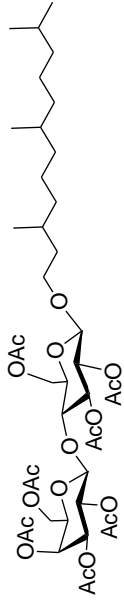
¹³C NMR, 75 MHz, CD₃OD



ASFDL_HNMR



¹H NMR, 300 MHz, CDCl₃



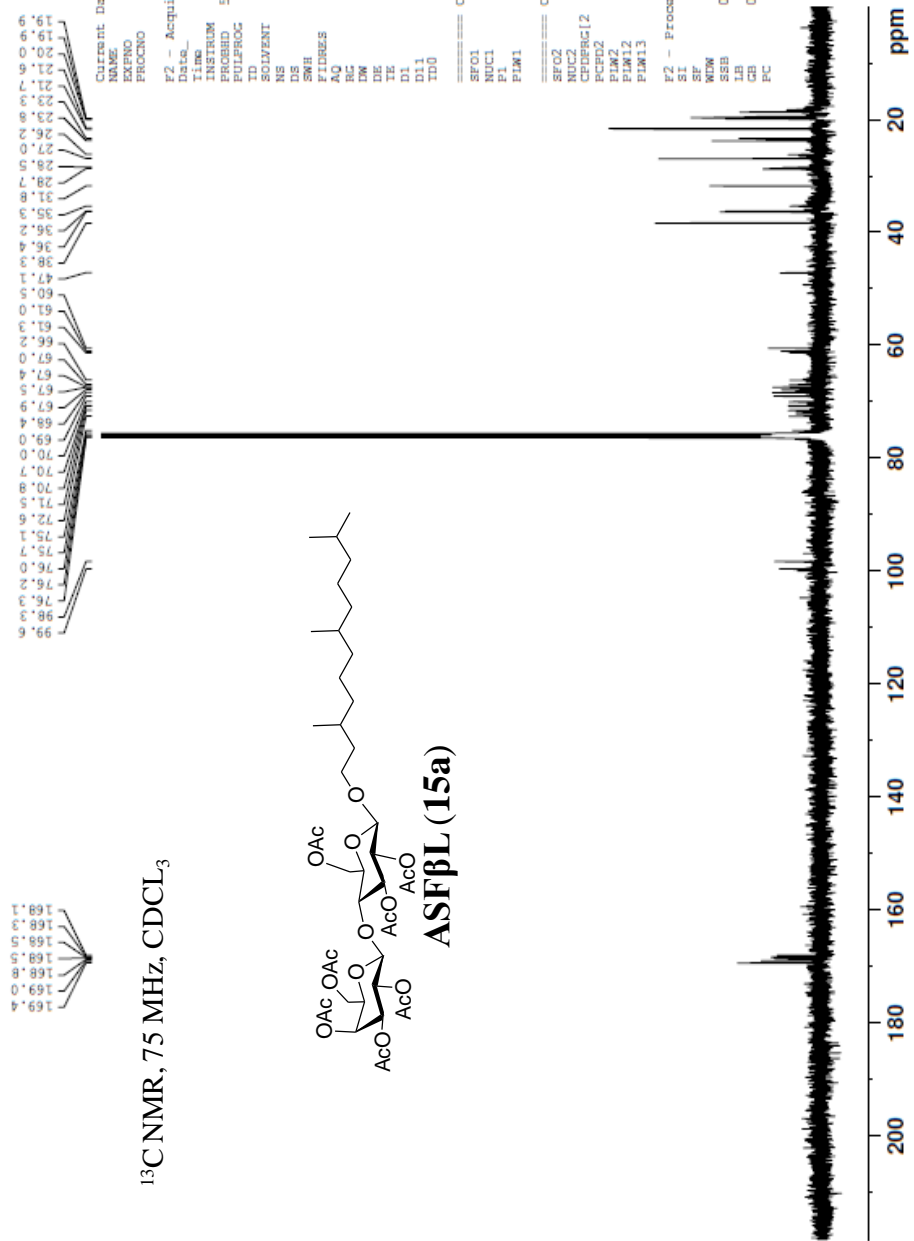
ASFBL (15a)

Current Data Parameters
NAME ASDL_19_21_400
EXPNO 1
PROCNO 1

F2 - Acquisition Parameters
Date_ 20131028
Time 17.44
INSTRUM spect
PROBHD 5 mm CPYBBO BB
PULPROG zg30
TD 65536
SOLVENT CDCl3
DS 12
SWE 8012.820 Hz
FIDRES 0.122266 Hz
AQ 4.0894465 sec
RG 327.440
DM 62.400 USMC
DE 10.00 USMC
TE 298.0 K
D1 1.00000000 sec
TD0 1

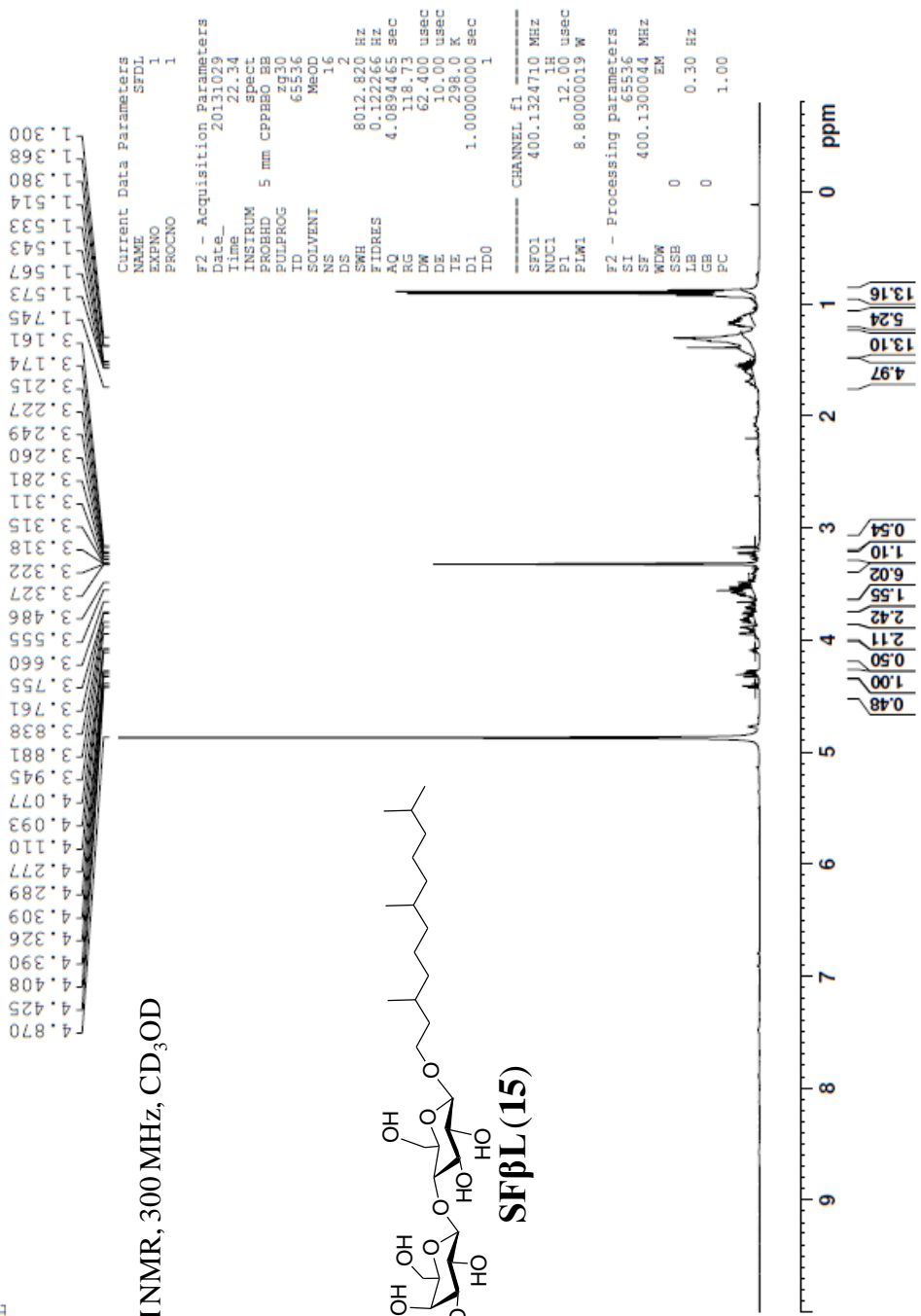
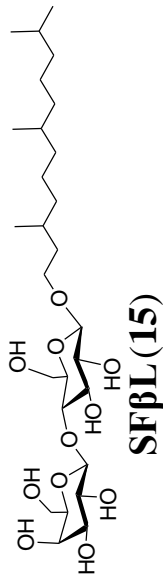
===== CHANNEL f1 =====
SF01 400.1324710 MHz
NUC1 1H
P1 12.00 USMC
PL1 8.80000019 W
F2 - Processing parameters
SI 65536
SF 400.1300105 MHz
WDW EM
SSB 0
LB 0.30 Hz
GB 0
PC 1.00

ASDL_CNMR



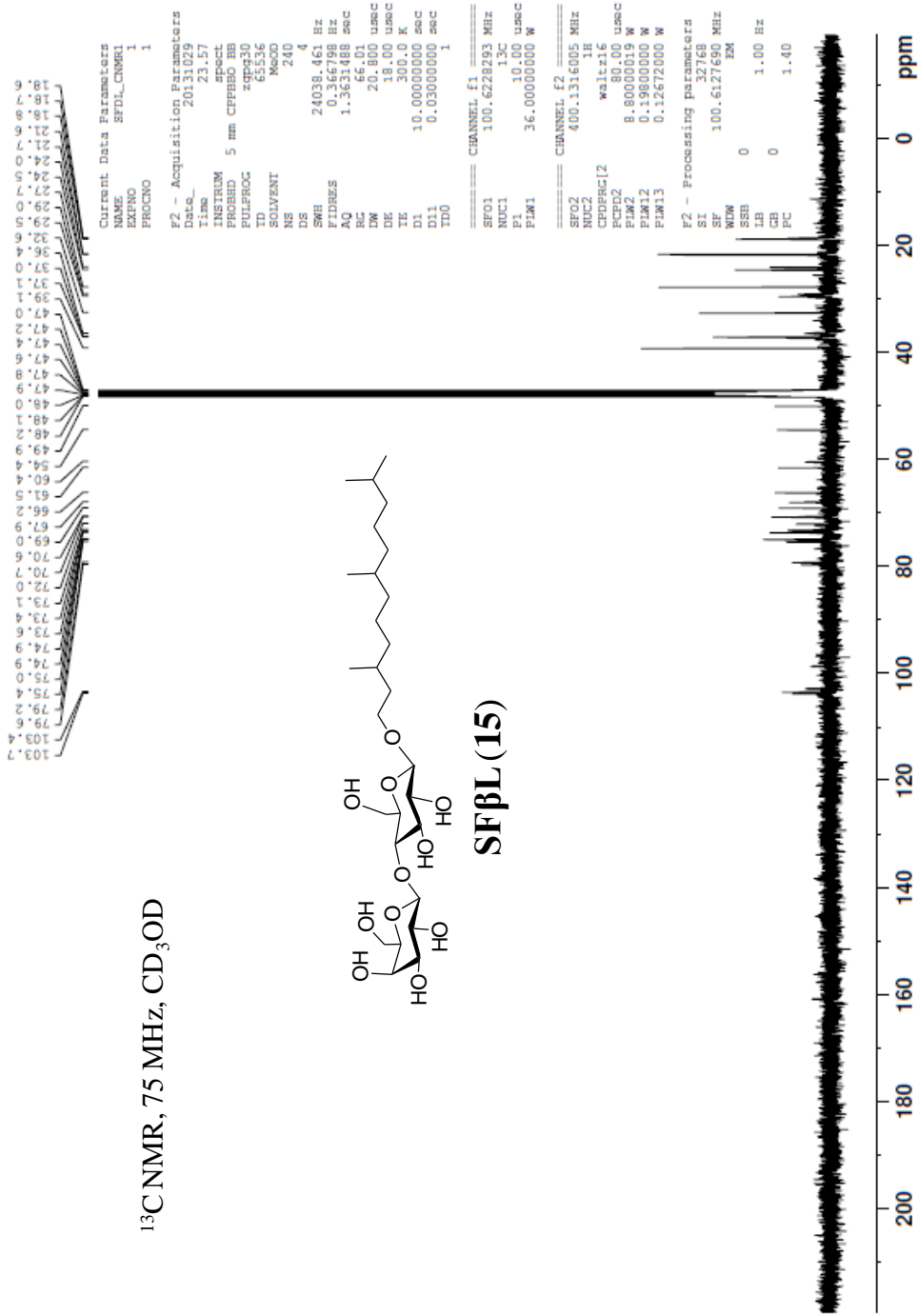
SFDL

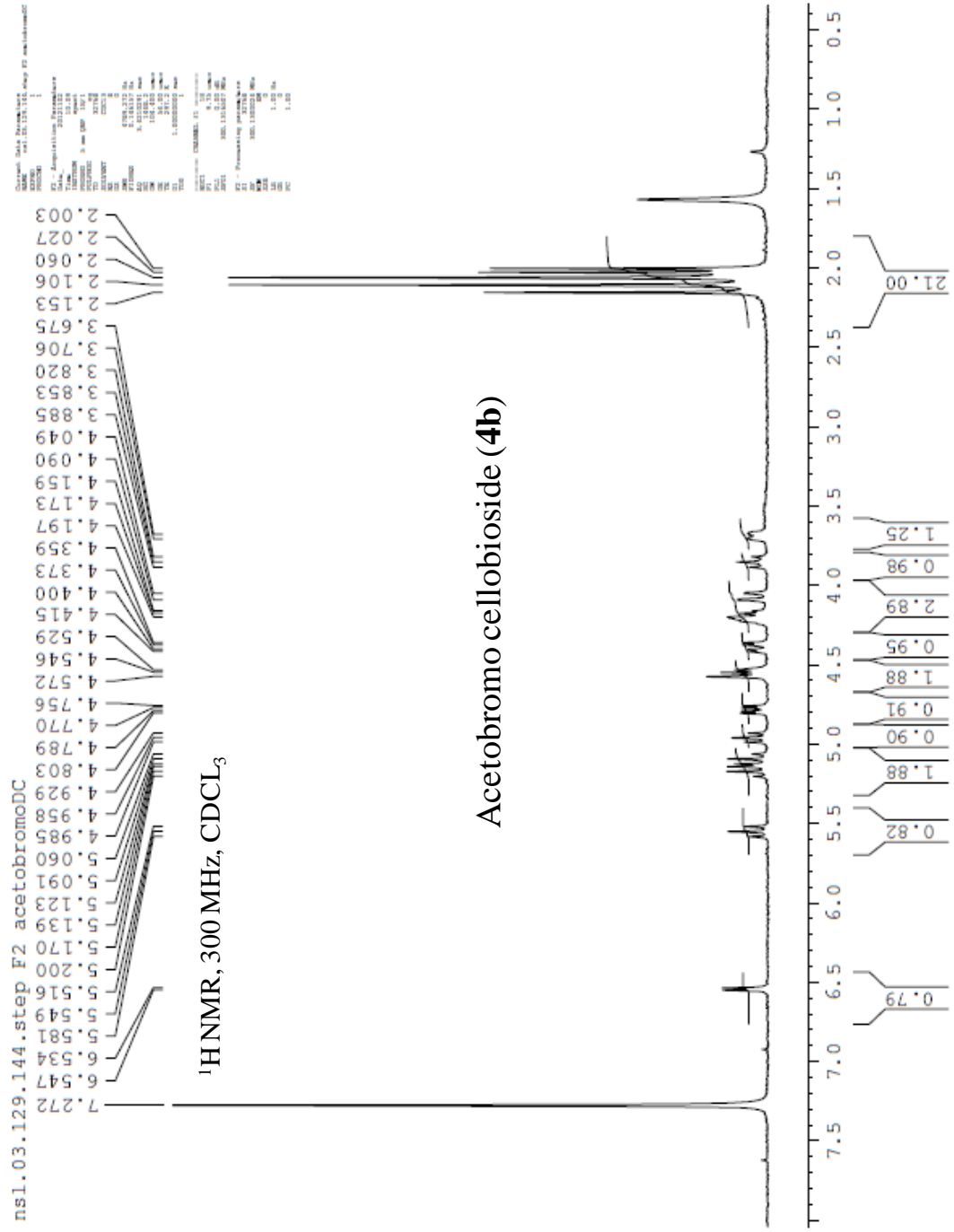
¹H NMR, 300 MHz, CD₃OD



SFDL_CNMR1

^{13}C NMR, 75 MHz, CD_3OD

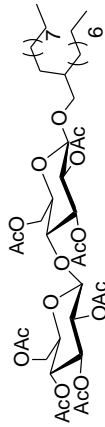




ns1 05 08 09_73_91 acetyl 2_octyl dodecyl cellbioside

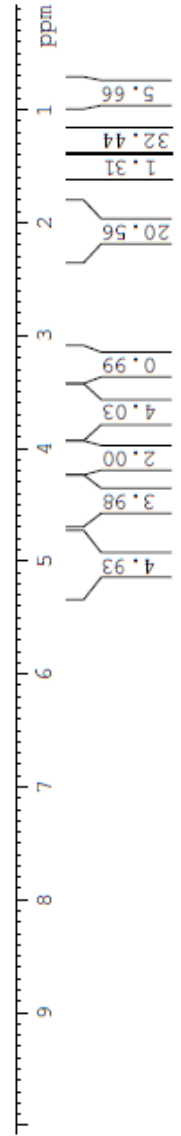
7.28
5.21
5.18
5.15
5.12
5.09
5.06
4.96
4.93
4.91
4.88
4.85
4.82
4.80
4.77
4.74
4.72
4.68
4.64
4.59
4.56
4.52
4.49
4.46
4.42
4.39
4.36
4.33
4.30
4.27
4.24
4.21
4.18
4.15
4.12
4.09
4.06
4.03
4.00
3.97
3.94
3.91
3.88
3.85
3.82
3.79
3.76
3.73
3.70
3.67
3.64
3.61
3.58
3.55
3.52
3.49
3.46
3.43
3.40
3.37
3.34
3.31
3.28
3.25
3.22
3.19
3.16
3.13
3.10
2.09
2.06
2.03
2.00
1.97
1.94
1.91
1.88
1.85
1.82
1.79
1.76
1.73
1.70
1.67
1.64
1.61
1.58
1.55
1.52
1.49
1.46
1.43
1.40
1.37
1.34
1.31
1.28
1.25
1.22
1.19
1.16
1.13
1.10
0.98
0.95
0.92
0.89
0.86
0.83
0.80
0.77
0.74
0.71
0.68
0.65
0.62
0.59
0.56
0.53
0.50
0.47
0.44
0.41
0.38
0.35
0.32
0.29
0.26
0.23
0.20
0.17
0.14
0.11
0.08
0.05
0.02
0.00

¹H NMR, 300 MHz, CDCl₃



2-AODβC (16a)

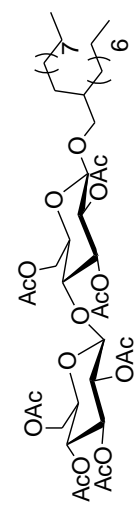
Current Data Parameters
NAME ns1 05 08 09_73
EXPNO 1
PROCNO 1
F2 - Acquisition Paramet
Date_ 20130115
Time 9.36
INSTRUM spect
PROBHD 5 mm QNP 1H/1
PULPROG zg
TD 32768
SOLVENT CDCl3
NS 16
DS 0
SWH 4789.272
FIDRES 0.146157
AQ 3.4210291
RG 90.5
DW 104.400
DE 54.00
TE 297.2
D1 1.00000000
TDO 1
----- CHANNEL f1 -----
NUC1 1H
P1 9.75
PL1 0.00
SFO1 300.1316307
F2 - Processing paramete
SI 32768
SF 300.1300003
WDW no
SSB 0
LB 0.00
GB 0
PC 1.00



170.5
170.3
170.2
169.8
169.4
169.3
169.0

100.9
100.8
77.4
77.2
77.0
76.7
76.6
73.0
72.9
72.6
72.5
71.9
71.6
71.6
67.8
61.9
61.6
37.9
37.9
31.9
31.9
30.8
30.8
30.1
30.0
29.7
29.7
29.6
29.6
29.6
29.3
29.3
26.6
22.6
22.6
20.6
20.6
20.6
20.5
20.5
11

¹³C NMR, 75 MHz, CDCl₃



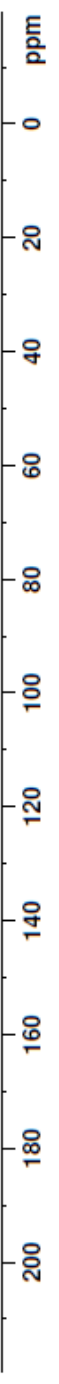
2-AODβC (16a)

===== CHANNEL F1 =====
 SFO1 100.6228293 MHz
 NUC1 13C
 P1 10.00 usec
 PLW1 36.00000000 W

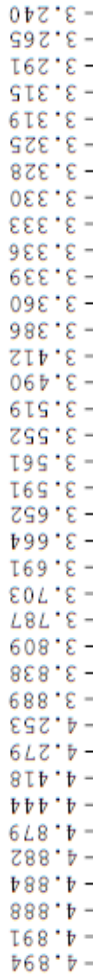
===== CHANNEL F2 =====
 SFO2 400.1316005 MHz
 NUC2 1H
 CFFPRG12 waltz16
 P1 10.00 usec
 PLW2 8.0000010 usec
 PLW3 0.19800000 W
 PLW4 0.12872000 W

F2 - Acquisition Parameters
 Date_ 20131111
 Time_ 19.03
 INSTRUM spect
 PROBD 5 mm CFBBD BB
 PULPROG zgpg30
 ID 65536
 SOLVENT CDCl3
 NS 120
 DS 4
 SWH 24038.461 Hz
 FIDRES 0.366798 Hz
 AQ 1.3631488 sec
 RG 60.00
 DW 206.00 usec
 DE 300.0 usec
 TE 300.2 K
 D1 10.00000000 sec
 D11 0.03000000 sec
 TD0 1

F2 - Processing parameters
 SI 32768
 SF 100.6127690 MHz
 WDW EM
 SSB 0
 LB 1.00 Hz
 GB 0
 PC 1.40

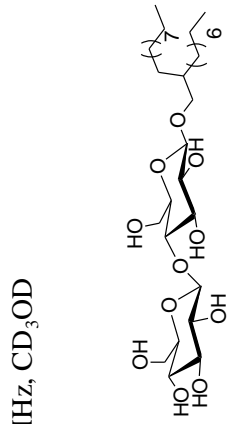


ns1 05 09 11_2_octyl_dodecyl_cellobioside_2



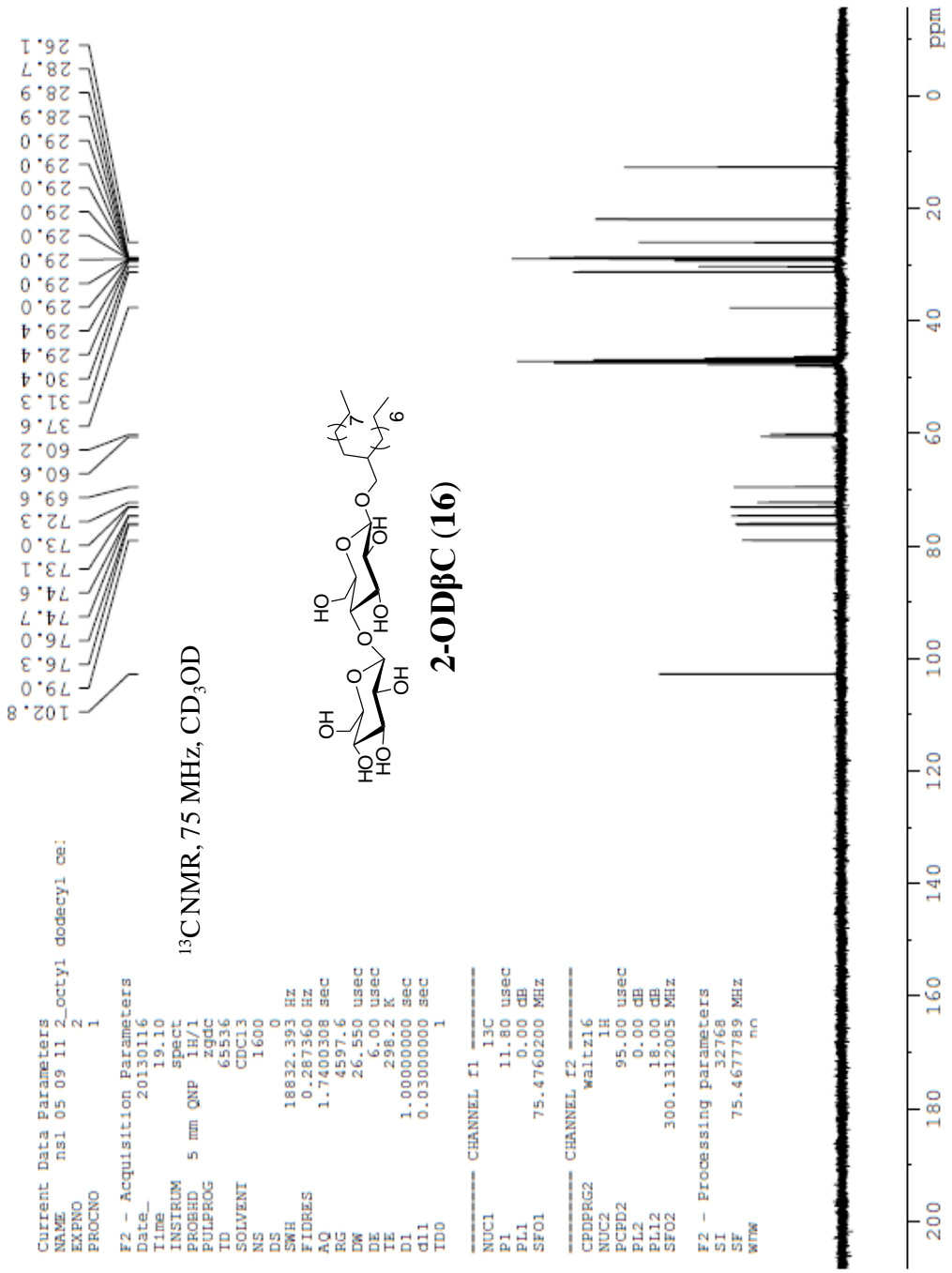
Current Data Parameters
NAME ns1 05 09 11_2_octyl_dodecyl_cellobioside_2
EXPNO 1
PROCNO 1

F2 - Acquisition Parameters
Data_ 20130116
Date_ 1971
INSTRUM spect
PROBHD 5 mm QNP 1H/1
PULPROG zg
TD 32768
SOLVENT MeOH
NS 16
DS 0
SWH 4789.272 Hz
AQ 0.1272 Hz
RG 3.421031 sec
EC 101.6
DW 104.400 usec
DE 54.00 usec
TE 297.2 K
D1 3.0000000 sec
TD0 1



===== CHANNEL f1 =====
NUC1 1H
P1 9.75 usec
PL1 0.00 dB
SFO1 300.1315207 MHz

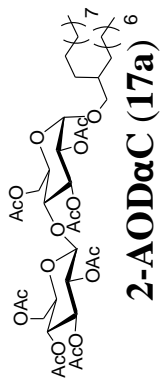
F2 - Processing Parameters
SI 32768
SF 300.1300003 MHz
WDW EM
SSB 0
LB 0.00 Hz
GB 0
PC 1.00



nsl 05 09 11_2_octyl_dodecyl_cellobioside_2_alpha_2



¹H NMR, 300 MHz, CDCl₃

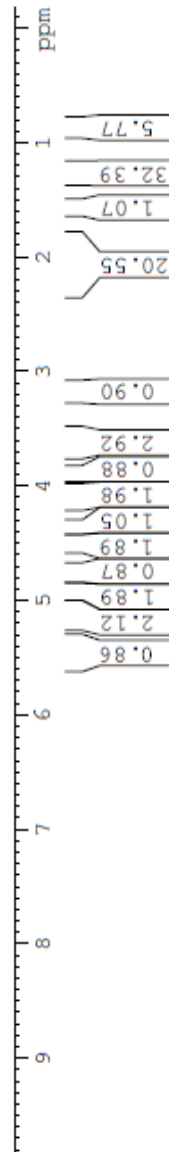


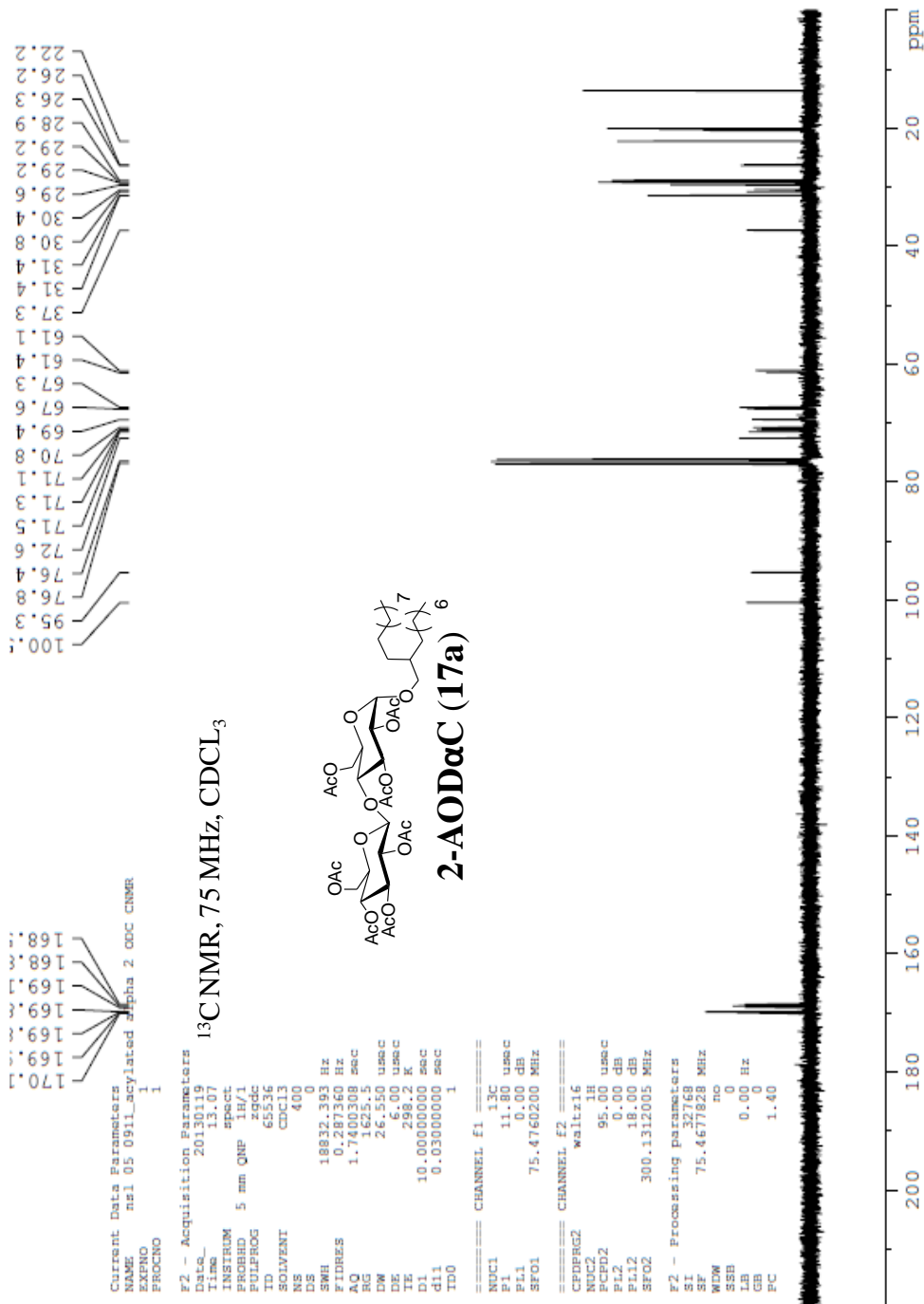
Current Data Parameters
NAME nsl 05 09 11_2_octyl_d
EXPNO 1
PROCNO 1

F2 - Acquisition Parameters
Date_ 20130119
Time 11.22
INSTRUM spect
PROBHD 5 mm QNP 1H/1
PULPROG zg
TD 32768
SOLVENT CDCl3
NS 16
DS 0
SWH 4789.272 Hz
FIDRES 0.146157 Hz
AQ 3.4210291 sec
RG 45.3
DW 104.400 usec
DE 54.00 usec
TE 297.2 K
D1 1.00000000 sec
D10 1

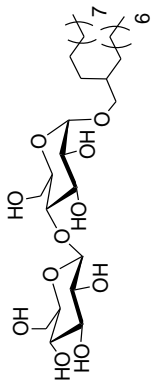
==== CHANNEL f1 =====
NUC1 1H
P1 9.75 usec
PL1 0.00 dB
SFO1 300.1316507 MHz

F2 - Processing parameters
SI 32768
SF 300.1300045 MHz
WDW no
SSB 0
LB 0.00 Hz
GB 0
PC 1.00

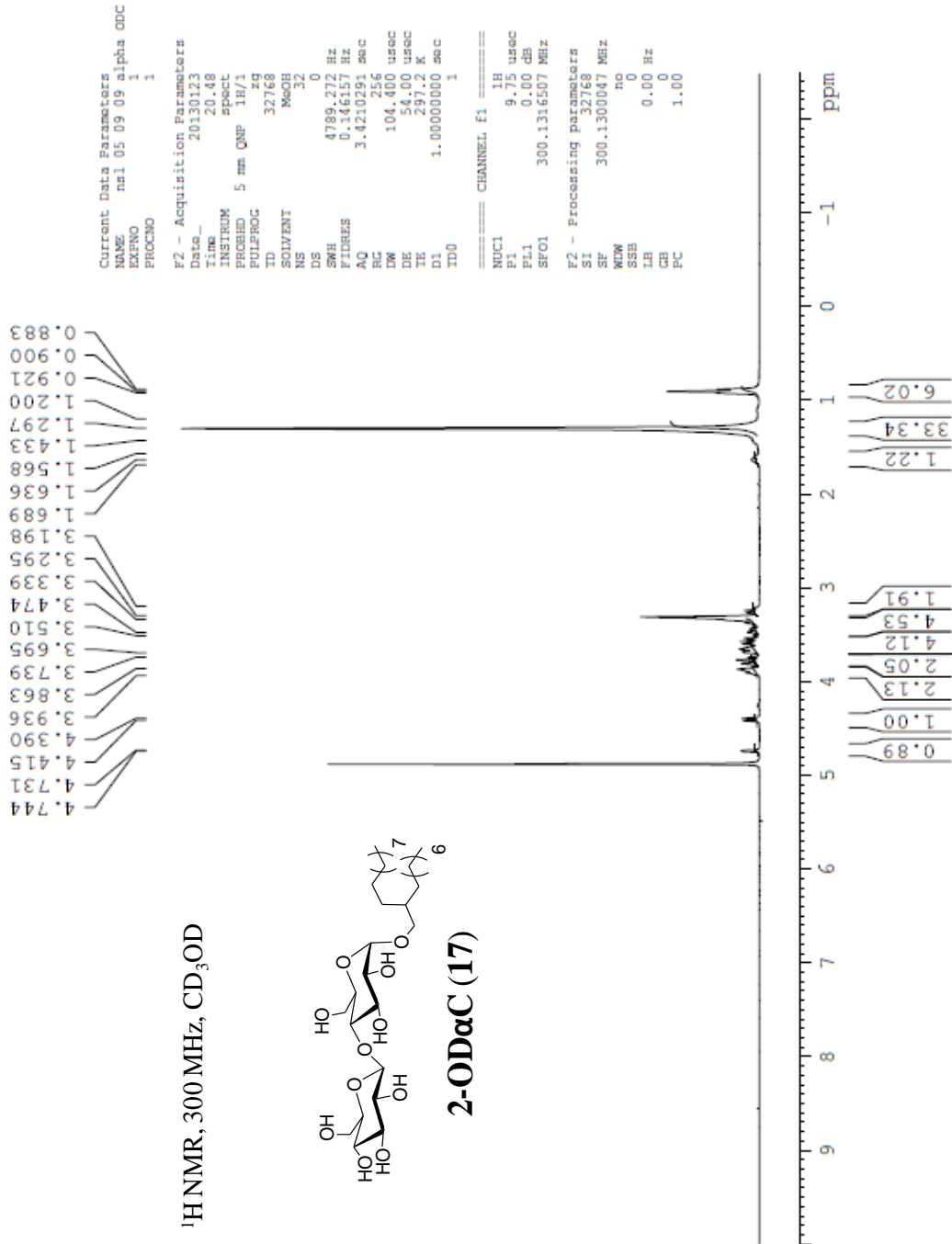




¹H NMR, 300 MHz, CD₃OD



2-ODαC (17)

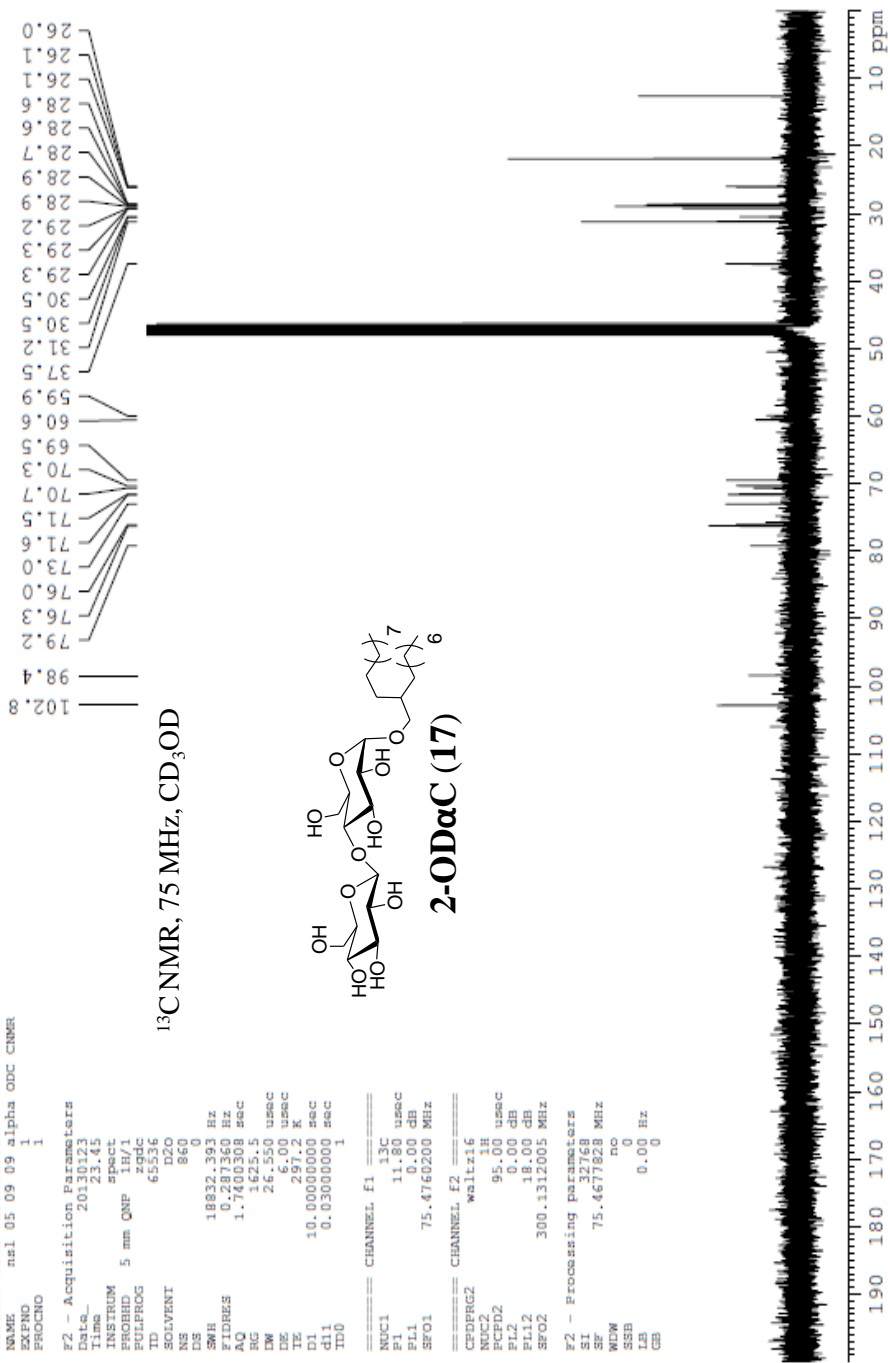


Current Data Parameters
 NAME nsl_05_09_09_alpha_00c_cnmr
 EXPNO 1
 PROCNO 1

F2 - Acquisition Parameters
 Date_ 20130123
 Time 23.45
 INSTRUM spect
 PROBHD 5 mm QNP 1H/1
 PULPROG zgpg30
 TD 65536
 SOLVENT D2O
 NS 860
 DS 4
 SWH 18832.393 Hz
 FIDRES 0.287360 Hz
 AQ 1.7400308 sec
 RG 1625.5
 DW 26.550 usec
 DE 6.00 usec
 TE 300.2 K
 D1 0.000000 sec
 d11 0.0300000 sec
 TD0 1

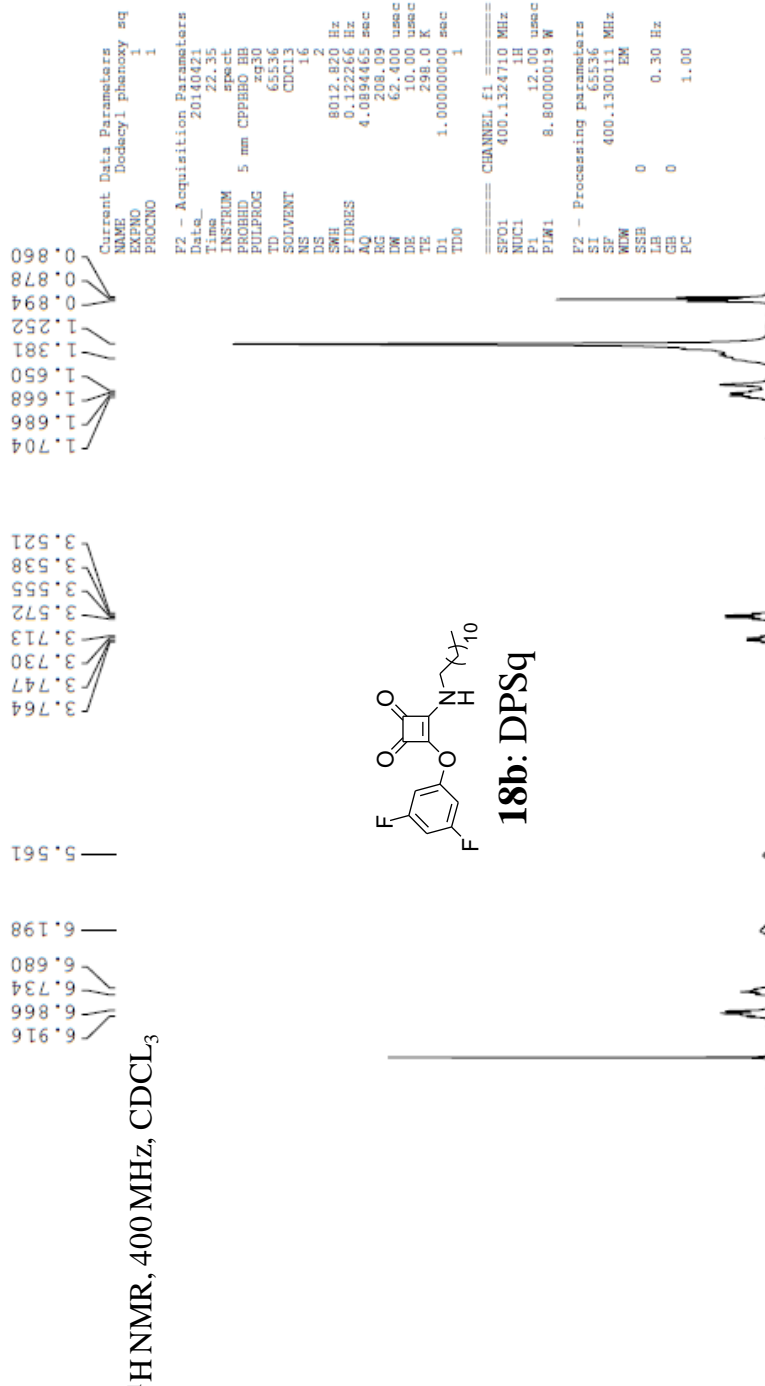
==== CHANNEL F1 =====
 NUC1 13C
 P1 11.80 usec
 PL1 0.00 dB
 SFO1 75.4760200 MHz
 ===== CHANNEL F2 =====
 CPDPRG2 waltz16
 NUC2 1H
 PCPD2 95.00 usec
 PL2 0.00 dB
 PL12 18.00 dB
 SFO2 300.1312005 MHz

F2 - Processing parameters
 SI 32768
 SF 75.467828 MHz
 WDM 16
 SSB 0
 LB 0.00 Hz
 GB 0

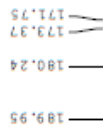


Dodecyl phenoxy sq

¹H NMR, 400 MHz, CDCl₃



Dodecyl phenoxy sq_Cnmr



¹³C NMR, 100 MHz, CDCL₃



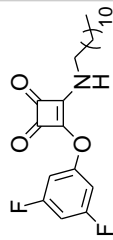
Current Data Parameters
NAME Dodecyl phenoxy sq_Cnmr
EXPNO 1
PROCNO 1

F2 - Acquisition Parameters
Date_ 2010471
Time 21.71
INSTRUM spect
PROBHD 5 mm CPBBO BB
PULPROG zgpg30
TD 65536
SOLVENT CDCl3
NS 240
DS 4
SWH 24038.40 Hz
FIDRES 0.366780 Hz
AQ 1.3631488 sec
RG 80.84
DW 20.800 usec
DE 18.00 usec
TE 300.0 K
D1 5.0000000 sec
D11 0.0300000 sec
D10 1

===== CHANNEL f1 =====
SFO1 100.628293 MHz
NUC1 13C
P1 10.00 usec
PLW1 36.0000000 W

===== CHANNEL f2 =====
SFO2 400.131605 MHz
NUC2 1H
PCPDPRG12 waltz16
PCPD2 80.00 usec
PLW2 0.1980000 W
PLW12 0.1980000 W
PLW13 0.1267200 W

F2 - Processing parameters
SI 32768
SF 100.6127680 MHz
EM
SSB 0
LB 1.00 Hz
GB 0
PC 1.40



18b: DPSq



Chapter 3

Disaccharide derivatives Inhibit and Disperse Biofilm of *P. aeruginosa*

Abstract

Bacterial sessile multicellular lifestyle leads to formation of communities known as biofilms that are highly resistant to the action of antibiotics. Agents that can prevent biofilm formation or alternatively disrupt preformed biofilms are therefore highly desired. Additionally, if such antibiofilm agents are also nonmicrobicidal against bacteria, they will be less likely to invoke resistance over time as compared to antibiotics that are microbicidal.

Here, the ability of certain disaccharide derivatives (DSDs) to inhibit *P. aeruginosa* adhesion, biofilm formation and cause dispersion of existing biofilm via a nonmicrobicidal action was evaluated. The structure activity relationship show that DSDs having disaccharide stereochemistries (cellobiose or maltose) and a bulky aliphatic tail (3, 7, 11-trimethyl-dodecanyl) were potent antibiofilm agents. The half-maximal inhibitory concentrations of few DSDs for biofilm inhibition (IC_{50}) and dispersion (DC_{50}) were comparable to known potent antibiofilm agents against *P. aeruginosa*. One agent, having cellobiose head and 3, 7, 11-trimethyl-dodecanyl tail (**SF β C (12)**) was a more potent antibiofilm agent than the natural ligands, rhamnolipids. The mechanism of action of such DSDs is not via the known *las* or *rhl* quorum sensing systems of *P. aeruginosa*. Results also indicate that the *P. aeruginosa* adhesin protein, pilin maybe a likely target for such DSD molecules.

3.1 Introduction

3.1.1 *P. aeruginosa* is a prominent pathogen associated with medical bacterial infections

The multi-drug resistance (MDR) phenomenon exhibited by a broad range of bacteria is a major health concern, and a prime bacterium in the midst of this grave problem is *P. aeruginosa*. *P. aeruginosa* is a gram negative rod shaped pathogen which is ubiquitously found in soil, water and within humans. *P. aeruginosa* is one of the most common pathogens isolated from hospital acquired infections. This bacterium is also the prime pathogen found in the lungs of patient with chronic respiratory disease, *Cystic fibrosis*. To add to the medical woes associated with *P. aeruginosa* infections, the present day strains isolated from disease organisms display resistance against most antimicrobials including, Penicillins, Ceftazidime, Carbapenems, Aminoglycosides and Ciprofloxacin.

Presently, the primary pharmaceutical approach to fight *P. aeruginosa* infections focuses on finding newer protein targets on the bacteria, against which potent antagonists can be developed and used to disrupt bacterial cellular processes and hence cause bacterial death. The major disadvantage of such a microbicidal approach is that the bacteria will over time acquire resistance against the new drug, and the futile task of finding newer targets and drugs requiring billions of dollars on research and government approvals would have to be repeated over and over again.

Contemporarily newer nonmicrobicidal approaches, that focus on the multicellular behaviors like biofilm formation and swarming (for review on bacterial biofilm formation and swarming see Chapter 1, sections 1.2 and 1.3) are being developed to treat bacterial infections while at the same time limiting the risks of inducing MDR. While no nonmicrobicidal strategy

focusing on bacterial biofilm inhibition has made it to the clinic, there is consensus that for countering MDR the future bacterial therapeutics would have to be centered around this approach. The reasons for this consensus are two; (i) Around 65-80% bacterial infections in humans are biofilm related; (ii) With the use of nonmicrobicidal agents against them, the bacteria would have a lesser or ideally no propensity to acquire resistance. With a distinct hope for a long term and probably a more permanent solution to bacterial infections, the nonmicrobicidal strategies offer some advantages over the existing microbicidal strategies. Therefore, in recent times, there has been a flurry of discoveries primarily focused on inhibiting and disrupting bacterial biofilms with agents that do not kill the microbe. A brief summary of many such nonmicrobicidal strategies has been reviewed in Chapter 1 (Section 1.3.4).

*3.1.2 Motile and sessile multicellular behaviors in *P. aeruginosa* are inversely regulated*

When bacteria land on a surface, they make a calculated choice between forming a sessile community or moving further ahead on the surface in search of more conducive microenvironments for colony formation (Figure 3.1). It is therefore conceived that both these multicellular processes, sessile (biofilm formation) and motile (swarming) are controlled by a common set of genes, whose expression inversely regulates the two bioprocesses. Many such genes and gene products have been identified in *P. aeruginosa* whose role is to make that calculated choice between motile and sessile life styles. In *P. aeruginosa*, the presence of surface attachment defective (SadB) protein is critical for both biofilm formation and swarming motility. While SadB protein was shown to be critical for progression from reversible to irreversible attachment during biofilm formation, this cytoplasmic protein was also shown to be important for sensing rhamnolipids, which are crucial virulence factors necessary during swarming. O' Toole *et al* created a mutant (WT/pSadB) strain of type *P. aeruginosa* by inserting a plasmid

(pSadB⁺) that caused overexpression of SadB protein. When the biofilm formation of such a mutant strain was quantified and compared to the biofilm content of wild type, there was a 3 fold increase in biofilm formation. Contrary to the enhanced biofilm formation, the swarming motility of such a SadB overexpressing mutant was reduced by 2.5 fold. When the gene encoding for SadB was deleted, the resulting mutant strain was hyperswarming. These results by O'Toole *et al* alluded to the notion that the *sadB* gene inversely regulates biofilm formation and swarming in *P. aeruginosa*. Further studies by O'Toole *et al* showed that another gene known as *sadC*, which expresses the membrane-localized diguanylate cyclase protein inversely regulated biofilm formation and swarming motility in *P. aeruginosa*. Later studies by O'Toole *et al* identified another gene *bifA* that can also inversely regulate swarming and biofilm formation, and they tentatively assigned the gene product of this gene, BifA as functioning upstream to the previously identified SadB protein.

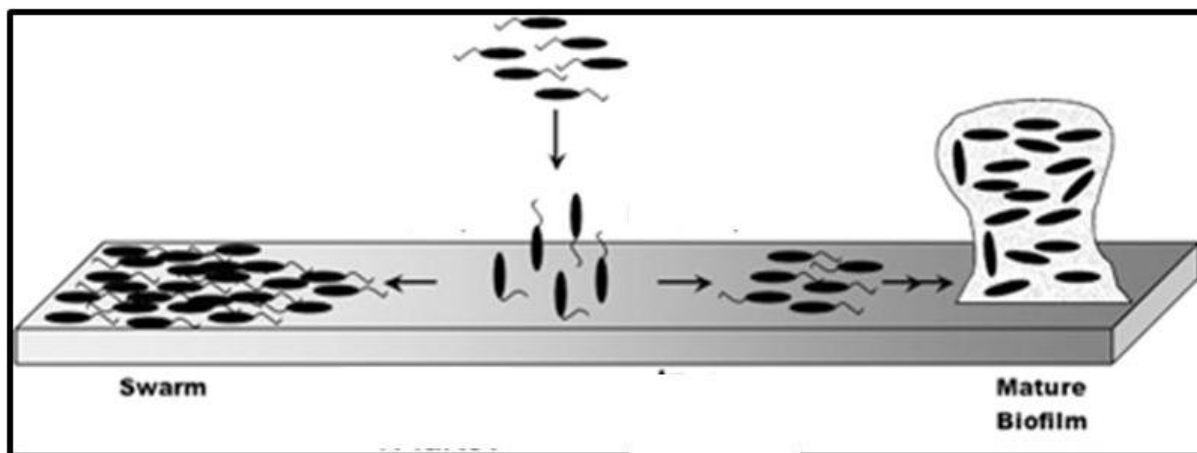


Figure 3.1 Inverse regulation of swarming and biofilm formation. [Modified and Reprinted with permission from Citation:⁴⁵ Caiazza *et al*, Inverse regulation of biofilm formation and swarming motility by *Pseudomonas aeruginosa* PA14, *J. Bacteriol.* **2007**, 189, 3603-3612]

3.1.3 Apart from being critical during swarming, rhamnolipids are important biomolecules secreted by P. aeruginosa during biofilm formation

The biosynthetic pathway for the secretion of rhamnolipids by *P. aeruginosa* has been discussed in Chapter 2, section 2.1.5.4. Also, the biological importance of rhamnolipids secretion by *P. aeruginosa* with respect to swarming motility has been discussed in chapter 2, section 2.1.5.4.1. Secretion of rhamnolipids is also associated with the sessile mode of living, i.e biofilm. The biofilm architecture is quite complex and the component of its matrix varies from species to species. However, it is well documented that most biofilm architectures are "mushroom" shaped that contain voids and channels. The voids and channel are critical elements of biofilm architecture and it is thought that such inter connected channels are important for supplying nutrients, oxygen and water throughout the community.²¹⁵ Davey *et al* showed using fluorescence microscopy that while both the wild type and the *rhlA* mutant strain of *P. aeruginosa* were able to form a biofilm architecture containing macrocolonies separated by voids, only the wild type strain was able to maintain the voids over six days, where as the *rhlA* mutant could not. In comparison to wild type, the critical element that the *rhlA* mutant cannot secrete are rhamnolipids, hence they concluded that secretion of rhamnolipids during biofilm formation of *P. aeruginosa* is necessary for ensuring formation of sturdy biofilm. Apart from the role in maintaining voids in the biofilm, Gilbert *et al* showed that over production of rhamnolipids by *P. aeruginosa* could lead to dispersal of bacteria from the biofilm.²¹⁶

3.1.4 Bacteria employ surface proteins known as adhesins to recognize and bind carbohydrate epitopes found on host cells

The initiation of many infections begin with adherence of bacteria to a host surface with the use of certain surface-exposed bacterial proteins known as adhesins. These bacterial adhesin proteins initiate adherence by recognizing many different kinds of carbohydrate epitopes present on host surfaces. The adhesin proteins used by bacteria may be present either on the cell surface (lectins)²¹⁷ or on specialized appendages (pili and fimbriae). Four different kinds of fimbriae present on *E. Coli* (P, type 1, S, and F1C) are known to exhibit affinity for galabiose (Gal α -(1-4)-Gal), mannose, sialic acid ligands, and GalNAc β (1-4)Gal, respectively.²¹⁸⁻²²² Galabiose epitope is also known to be recognized by *Streptococcus suis* (*S. suis*), a gram positive bacteria that causes meningitis in human.^{219,223} It has also been reported that *H. pylori*, a common stomach bacterium recognizes a prominent carbohydrate epitope (2'3-sialyllactose, Neu5Aca(2-3)Gal β (1-4)Glc) found on human cells.^{219,224}

Pseudomonas aeruginosa use surface proteins as well as adhesins to interact with carbohydrates moieties on host surfaces. Proteins used by *Pseudomonas aeruginosa* for surface adhesion include flagellin (on flagella), pilin (on pili) and lectins (LecA and LecB).²²⁵ While the flagella proteins on *P. aeruginosa* can bind to carbohydrate epitopes found on mucin protein and to glycolipids (asialo-GM₁) on mammalian cells, pilin protein has a specificity for D-GalNac- β -(1 \rightarrow 4)D-Gal- β disaccharide moiety found on glycosphingolipids.²²⁶ The *P. aeruginosa* lectins, LecA and LecB, on the other hand are known to be specific for binding to galactose^{197,227} and fucose moieties, respectively. Molecular intervention of bacterial adhesion process via the use of synthetic carbohydrate ligands also known as the "antiadhesive strategy" is therefore viable therapeutic approach for preventing infection. Reymond and co-workers have demonstrated that

multivalent fucosyl-peptide dendrimers targeting LecB could be used as molecular intervention to inhibit and disperse *P. aeruginosa* biofilm on steel coupons.²²⁸

In *P. aeruginosa*, pilin protein is known to mediate up to ~90 % of the adhesion events. The pili assisted epithelial cell binding domain is located between residues 128-144 on the C-terminal region of PilA, the pili structural protein.²²⁹ Irwin and co-workers have demonstrated that the presence of Type IV pili is critical for adherence of *P. aeruginosa* to steel coupons. Also, synthetic pili peptide sequence (residues 128-144) can also bind to polyvinyl chloride (PVC) and polystyrene (PS) surfaces.²³⁰ The binding specificity of D-GalNac- β -(1 \rightarrow 4)- β -D-Gal disaccharide ligand with minimum binding amino acid sequence of *P. aeruginosa* pili (peptide sequence PAK₍₁₂₈₋₁₄₄₎) was also studied and it was determined that increasing the hydrophobicity of disaccharide side chain increased the binding to the PAK₍₁₂₈₋₁₄₄₎ pili peptide.²³¹

Here, the three key points to summarize are; (i) Swarming and biofilm formation in *P. aeruginosa* are inversely regulated; (ii) Rhamnolipids secretion by *P. aeruginosa* is important for building sturdy biofilms; (iii) *P. aeruginosa* is able to recognize and hence bind with ligands that offer various saccharide stereochemistries. In Chapter 2, the use of certain saccharide derivatives (SDs) to modulate *P. aeruginosa* swarming was shown. Also, the results show that the modulation of swarming by such SDs was probably a result of them mimicking the functions of rhamnolipids. Since, SDs mimicked rhamnolipids during swarming of *P. aeruginosa*, and since swarming and biofilm formation in *P. aeruginosa* are inversely regulated, the potencies of such nonmicrobicidal agents (i.e SDs) to inhibit *P. aeruginosa* surface adhesion and biofilm formation and cause dispersal of preformed biofilm was evaluated in this chapter. As *P. aeruginosa* has many surface proteins that can recognize different saccharide epitopes, a preliminary study to identify the putative target protein of such SDs was also carried out.

3.2 Results and Discussion

The rationale of synthesizing the chemical structures in Figure 3.2 is the same as mentioned in Chapter 2 (Section 2.2.1). In summary, saccharide derivatives (SDs) comprising of different saccharide stereochemistries and various aliphatic structures were included in the study. The structure-activity relationship between structural details and corresponding effects on biofilm inhibition and bacterial adhesion was investigated.

The antibiofilm activities (biofilm inhibition and dispersion) of the SDs and rhamnolipids were screened by using the crystal violet (CV) based static biofilm assay. In this assay, wild type *Pseudomonas aeruginosa* (PAO1) was grown in LB-media with or without 160 μ M SDs or rhamnolipids at 37 °C in the wells of microtiter plates for 24 hours. After the initial incubation period of 24 hours, the biofilm formed on the bottom of the wells was stained with crystal-violet dye and quantified by measuring the absorbance at 600 nm (OD_{600}) (for procedure see Materials and Methods).^{115,213} Comparing the content of biofilm in control wells (no added SD) to that of wells containing various SDs, gave the percent inhibition. The initial analysis of the SDs' antibiofilm (both inhibition and dispersion) activities were assessed at a concentration of ~ 160 μ M. In the dispersion assay, the SDs or rhamnolipids were added after the initial incubation period of 24 hours and then the plates were incubated for additional 24 hours before quantification with CV-dye. Those agents that exhibited >50% antibiofilm activities were further analyzed in a concentration dependent manner to obtain half-maximal inhibitory concentrations for biofilm inhibition (IC_{50}) and dispersion (DC_{50}). Additionally, the antibiofilm activities of a few SDs were also examined via fluorescence based biofilm assay (for procedure see Materials and Methods).

Further, the ability of SDs to prevent initial bacterial adhesion to polystyrene surface was analyzed using a fluorescence based adhesion assay. Here a strain of *P. aeruginosa* that constitutively expresses green fluorescent protein (PAO1-EGFP) was inoculated in the wells of a microtiter plate for 2 hours with LB media as the nutrition source along with (160 μ M) or without various SDs or rhamnolipids. After the initial adhesion period, the amount of fluorescent bacteria (PAO1-EGFP) on the surface of the microtiter plate was quantified by measuring the fluorescence at 510 nm. The ability of pili peptide (minimum binding segment of pilin protein) to reduce the potency of a SD was also analyzed.

The quantitative values of all bioassays (biofilm inhibition & dispersion, IC₅₀, DC₅₀ and bacterial adhesion inhibition) are the average obtained from four identical wells. Each experiment was repeated at least 3 times, each time giving similar results (repeat results are not shown).

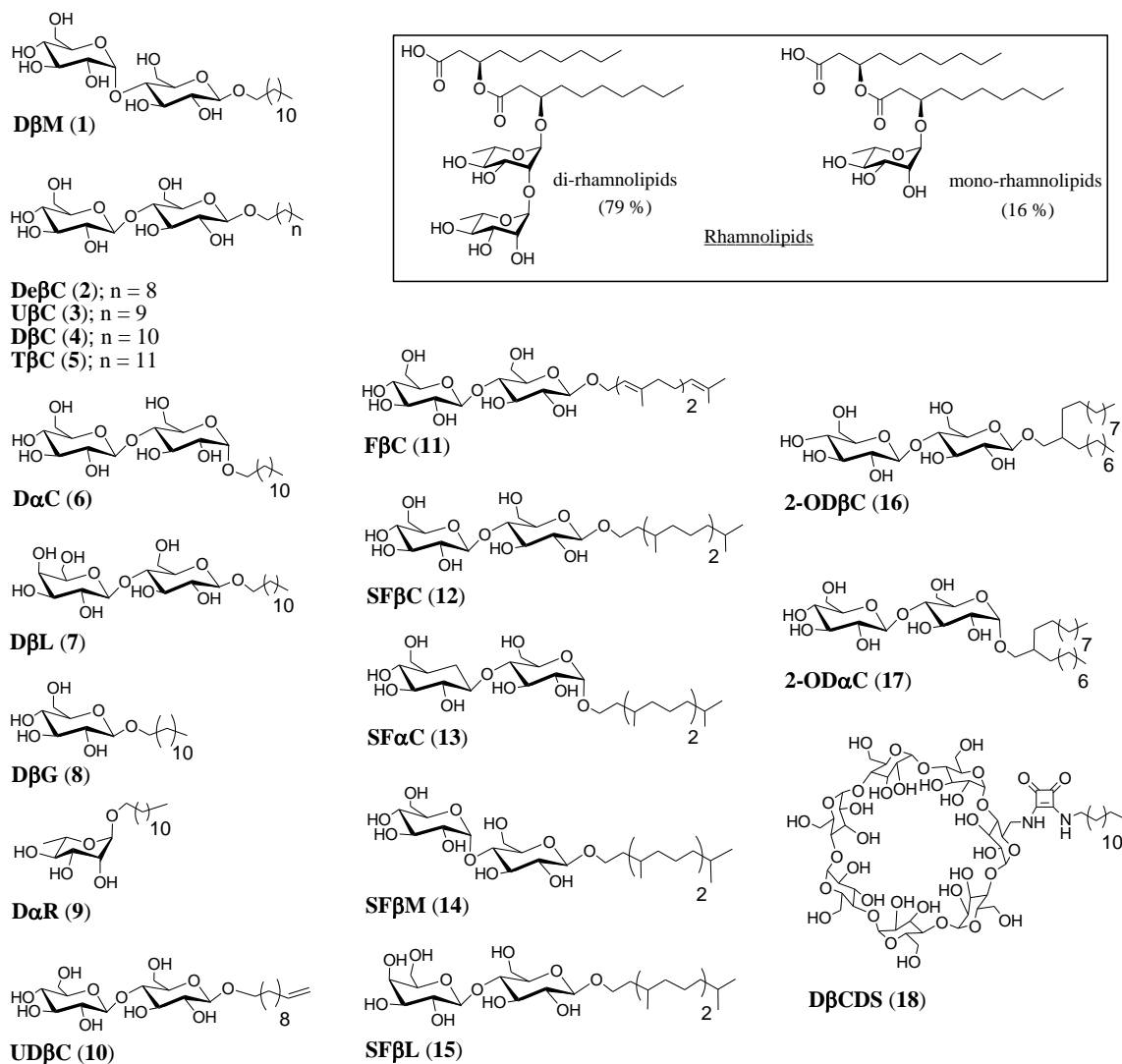


Figure 3.2. Structures of synthetic saccharide based derivatives that include maltose, cellobiose, lactose, glucose, rhamnose, and β-cyclodextrin stereochemistries; and hydrocarbons derived from farnesyl and “saturated” farnesyl molecules. The structures of di-rhamnolipid and mono-rhamnolipid are also shown.

3.2.1 Effect of generic surfactants on biofilm formation

Swarming motility had exhibited no correlation with the surface activity of the molecule (see Chapter 2, Section 2.2.3). The preliminary screening of four generic surfactants (dodecyl- β -maltoside, **DBM (1)**; tetra-(ethylene glycol) monododecyl ether, **C₁₂EG₄OH**; sodium dodecyl sulfate, **SDS**; and dodecyl trimethyl ammonium chloride, **DTAC**) for the ability to reactivate the swarming of the *rhlA* mutant (see Chapter 2, Section 2.2.3), showed that only **DBM (1)** alone was able to exhibit reactivation, similar to the natural ligand, rhamnolipids while other surfactants could not. Further, to assess whether surfactant action had an effect on biofilm formation, the four generic surfactants were also tested for the ability to inhibit *P. aeruginosa* biofilm. The biofilm inhibition assay in presence of 110 μ M of various generic surfactants showed that only one molecule, **DBM (1)** exhibited significant reduction in biofilm content (Figure 3.3).

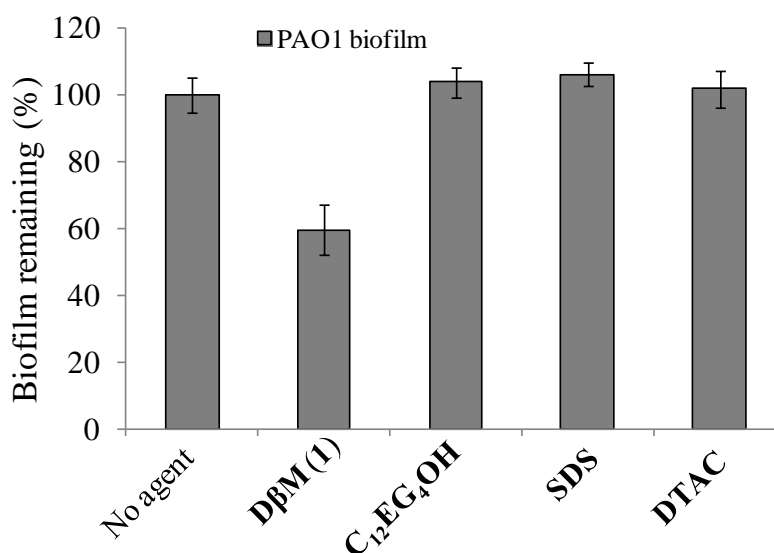


Figure 3.3 Inhibition of *P. aeruginosa* (PAO1) biofilm by 110 μ M of generic surfactants; Dodecyl- β -maltoside (DBM, 1**, -ionic surfactant); tetra (ethylene glycol) monododecyl ether**

(**C₁₂EG₄OH**, nonionic surfactant); sodium dodecyl sulphate (**SDS**, anionic surfactant); dodecyl trimethyl ammonium chloride, (**DTAC**, cationic surfactant). Only **DβM** exhibited antibiofilm activity at tested concentration. Percent PAO1 biofilm remaining after 24 hours of inoculation with (110 μM) or without various generic surfactant. The percentages were obtained by comparing biofilm content of control (no agent) to biofilm content in presence of an agent. Bacteria were cultured in LB-media. Error bar is standard error of the mean from 4 replicates.

3.2.2 Structure-activity relationship (SAR) for biofilm inhibition

(a) Structure and size of sugar head group is critical for biological activity

Initial screening of saccharide derivatives (SDs) at a concentration of 160 μM brought forward following SARs. Saccharide derivatives with a monosaccharide moiety and having a aliphatic chain of twelve carbons (glucose; **DβG (8)** and mono-rhamnoside; **DαR (9)**) had poor antibiofilm activities (Figure 3.4). In contrast to the poor potencies of monosaccharide derivatives (MSDs), a SD having a disaccharide stereochemistry (maltose) and a twelve carbon aliphatic chain **DβM (1)** reduced the biofilm content by ~50% (Figure 3.4). Saccharide derivative with a large cyclicheptasaccharide moiety (β-cyclodextrin) and a twelve carbon aliphatic chain (**DβCDS (18)**) was incapable of exhibiting any biofilm inhibition, in fact this agent seemed to increase the biofilm content slightly (Figure 3.4). Therefore, amongst the various tested SDs, the one with a disaccharide stereochemistry seemed to work best at inhibiting the biofilm of *P. aeruginosa* at a concentration of 160 μM.

(b) Inhibition of Pseudomonas aeruginosa (PA) biofilm by disaccharide derivatives (DSDs) is sensitive to stereochemistry of the sugar head group

Antibiofilm potencies of three different disaccharide derivatives (DSDs) each bearing a twelve carbon aliphatic chain with either lactose (Gal β (1 \rightarrow 4)Glc, **D β L (7)**; poor solubility in water), cellobiose (Glc β (1 \rightarrow 4)Glc, **D β C (4)**) or maltose (Glc α (1 \rightarrow 4)Glc, **D β M (1)**) head group revealed that cellobiose stereochemistry, Glc β (1 \rightarrow 4)Glc out-performed other stereochemistries (Figure 3.4). While lactose stereochemistry severely compromised the antibiofilm activity, cellobiose stereochemistry exhibited ~ 62% biofilm inhibition. In general, cellobiose derived DSD compared better than those of maltose derived DSD having similar aliphatic chains (~46% biofilm inhibition activity).

(c) Chain length of twelve carbons is optimum for observing maximum biofilm inhibition

In order to evaluate the importance of aliphatic chain length, the aglycone moiety of SDs with cellobiose stereochemistry was systematically altered from 10 to 13 carbons. On comparing the effect of carbon chain length on biofilm inhibition activity, DSD with an aliphatic chain length of ten carbons, **De β C (2)** was inactive, where as those with eleven **U β C (3)**, and twelve **T β C (5)** carbons had moderate activity (29 % and 40 %, respectively), while DSD with twelve carbons **D β C (4)** exhibited best activity (62 %) (Figure 3.4). This reliance of activity on aliphatic chain length of the chemical signal is also observed during quorum sensing, when each species is able to produce, secrete and recognize its own chemical signal based on the length of the aliphatic chain.^{167,232} In Gram-Negative bacteria, different species are able to distinguish their own chemical signal from that of others by recognizing the difference in the length of acyl side chain of acyl-homoserine lactone (AHL) auto inducers (chemical signals).²³³⁻²³⁶ Not surprisingly,

the AHL cognate receptor (LuxR type protein) is homologous amongst different species.^{167,233}

The optimization of DSD antibiofilm activity with aliphatic chain length of twelve carbons is therefore an indication of a ligand-receptor type of phenomenon.

(d) Introducing short methyl branches off the main aliphatic chain enhanced the antibiofilm activity of DSDs greatly with low IC₅₀ values (as low as ~9.9 μM)

The effect of aglycone part of the DSD was further evaluated by introducing short methyl branches coming off the main aliphatic chain. This aliphatic chain was obtained by hydrogenating farnesol molecule (3,7,11-trimethyldodeca-2,6,10-trien-1-ol) to obtain saturated farnesol (3, 7, 11-trimethyl-dodecanyl) group. At 160 μM, DSDs with saturated farnesyl aliphatic chain and cellobiose head group, **SFβC (12)** and **SFαC (13)** were strong inhibitors (up to ~ 80%) of *P. aeruginosa* biofilm (Figure 3.4). In an attempt to further optimize antibiofilm activity, DSDs bearing saturated farnesyl aliphatic chain and either maltose or lactose groups were synthesized (**SFβM (14)** and **SFβL (15)**, respectively). Synthetic lactose analog exhibited poor solubility in water and hence was not tested for antibiofilm activity. But **SFβM (14)** at a concentration of 160 μM exhibited antibiofilm activity of around 60 % (Figure 3.4). Contrary to the enhanced antibiofilm activities of DSDs with saturated farnesyl chain, the antibiofilm activity of cellobiose based DSD with unsaturated farnesyl aliphatic chain **FβC (11)** was a meager ~12% (Figure 3.4). This decrease in antibiofilm activity when unsaturation is introduced into the aliphatic chain (leading to less bulky chain structure) was also consistent for another set of DSDs; i.e **DβC (4)** (62% inhibition) and **UDβC (10)** (13% inhibition) (Figure 3.4). Also, the effect of anomeric position of the aliphatic chain (from β to α) on biofilm activities was difficult to predict; for example at 160 μM, **DβC (4)** gave 62% inhibition where as to **DαC (6)** gave only

28% inhibition, but on comparing another set of anomers, i.e **SFβC (12)** and **SFαC (13)**, **SFβC (12)** gave 76 % inhibition where as **SFαC (13)** gave 82 % inhibition (Figure 3.4).

(e) Polyol-derivatized hydrocarbons with the alkyl chain having lipid-like structure are not potent antibiofilm agents

Aliphatic chain with methyl branches seemed to enhance bioactivity, therefore the bulkiness of the aliphatic chain was further increased by attaching a 2-octyldodecyl chain, forming two lipid-like DSDs (**2-ODβC (16)** and **2-ODαC (17)**). However, when tested at a concentration of 160 μM, this modifications lead to structures with poor antibiofilm activities (33% and 15%, respectively) (Figure 3.4).

(f) At a concentration of 160 μM, rhamnolipids seemed to enhance biofilm production

Since, SDs were able to mimic the swarming biofunction of rhamnolipids, and since rhamnolipids also help maintain biofilm architecture, a comparative study between antibiofilm activities of SDs and rhamnolipids was also performed. At 160 μM of rhamnolipids the biofilm content seemed to increase (Figure 3.4).

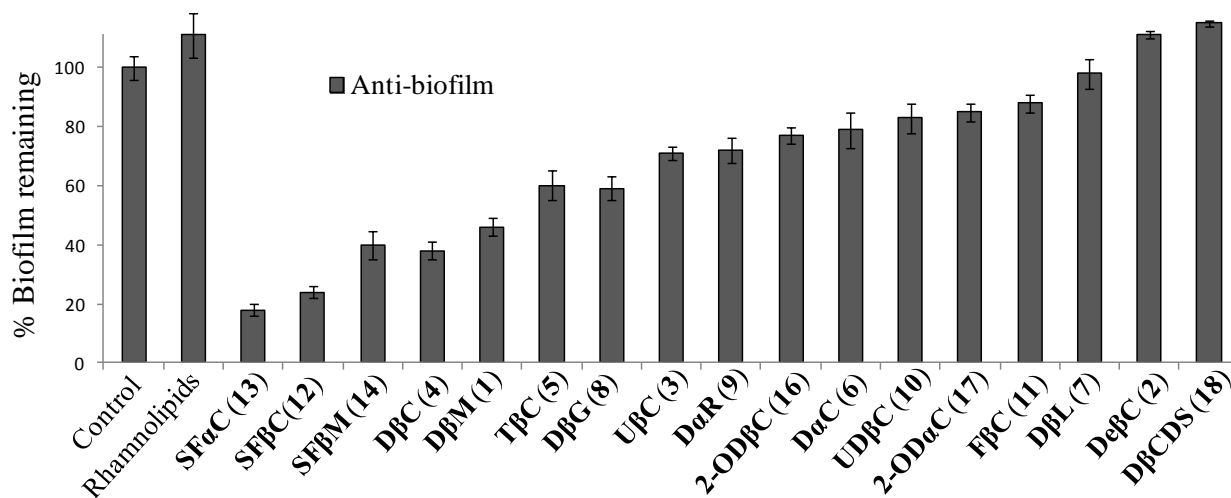


Figure 3.4 Biofilm inhibition potencies of DSDs and rhamnolipids quantified by CV-dye based assay. Percent PAO1 biofilm remaining after 24 hours of inoculation with bacterial culture supplemented with (160 μ M) or without various DSDs or with rhamnolipids. The percentages were obtained by comparing biofilm content of control (no agent) to biofilm content in presence of an agent. Bacteria were cultured in LB-media. Error bar is standard error of the mean from 4 replicates.

3.2.3 Antibiofilm ability of certain DSDs were qualitatively assessed by performing a confocal microscopy assay

The antibiofilm activities of five DSDs, **SF β C (12)**, **SF α C (13)**, **D β C (4)**, **De β C (2)** and **D β L (7)** were also qualitatively validated by using confocal laser scanning microscopy (CLSM) to measure the amount of fluorescent bacteria, PAO1-EGFP adhered on stainless steel coupons grown in LB-media for 24-h supplemented with either of the five DSDs.²³⁷ The CLSM micrographs (Figure 3.5) showed that 160 μ M of **SF β C (12)**, **SF α C (13)** and **D β C (4)** decreased the fluorescence signal significantly as compared to the steel coupon placed in just LB-media. This decrease in fluorescence signal by three DSDs indicated a lesser bacterial cell density on the surface of the steel coupons as compared to control steel coupon. The mean thickness of biofilm obtained from Z-stacked images showed a much thinner biofilm coverage on steel coupons placed in media containing 160 μ M of **SF β C (12)**, **SF α C (13)** and **D β C (4)**. In contrast, with 160 μ M of **De β C (2)** or **D β L (7)**, biomass surface coverage had similar thickness as that of control without the agents. These fluorescence results were consistent with the results of CV-dye based assays for biofilm inhibition.

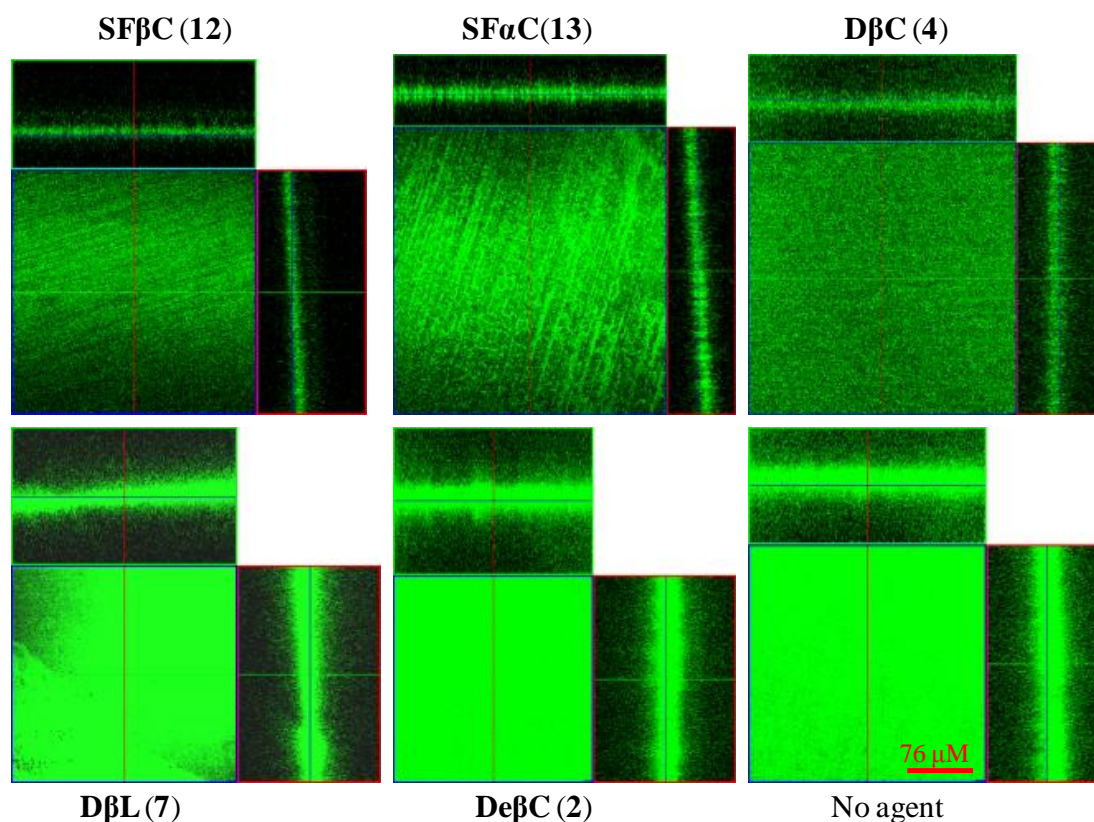


Figure 3.5 Biofilm inhibition activities of DSDs was also validated qualitatively by a confocal fluorescence based biofilm assay. Steel coupons inoculated with PAO1/EGFP for 24 h with ($\sim 160 \mu\text{M}$) or without various disaccharides derivatives (DSDs). After 24-h, the steel coupons with biofilms were viewed under confocal laser scanning microscope (CLSM). Scale bar $\sim 76 \mu\text{M}$. Reduced fluorescence due to the presence of DSDs (in comparison to the Control) indicates lesser amount of biofilm on the steel coupons.

3.2.4 Rhamnolipids antibiofilm activity increases and then decreases with increasing doses exhibiting an “activity reversal”

The antibiofilm activities of those DSDs that exhibited $>50\%$ inhibition at $160 \mu\text{M}$ along with rhamnolipids extract were further probed in a concentration dependent manner to obtain the half-maximal inhibitory concentrations (IC_{50}) of these agents (Figure 3.6). As concentration of

rhamnolipids were increased, the antibiofilm activity initially increased and then declined sharply tracing a bell shaped or an “activity reversal” profile. The antibiofilm activity of rhamnolipids increased gradually to a maximum value of ~65% at a concentration of 42 μM followed by decrease to 46% at 85 μM and then to -14% at 160 μM with respect to biofilm formed in control. The unusual “activity reversal” profile of rhamnolipids observed during antibiofilm assays was also observed during a dose dependent study with many SDs and rhamnolipids itself during swarming assays. The unusual dose dependent bell shaped graph of rhamnolipids prevented calculation of its IC_{50} . Rhamnolipids is a glycolipids and another lipid-like molecule included in this study was **2-OD β C**. Consistently, the antibiofilm activities of both these lipid-like structures at relatively higher concentration (160 μM) is rather low. However, unlike the bell-shaped profile of swarming dose-dependence, none of the four DSDs, **SF β C (12)**, **SF α C (13)**, **SF β M (14)** and **D β C (4)** exhibited any "activity reversal". Instead, the biofilm inhibition of these four DSDs increased over a concentration range and then leveled off at a particular maximum value. The calculated half maximum inhibitory concentrations (IC_{50} s) of the four DSDs were; ~9.9 μM for **SF β C (12)**; ~ 32 μM for **SF α C (13)**; ~72 μM for **D β C (4)**; and ~102 μM for **SF β M (14)**. The dose-dependence study demonstrates **SF β C (12)** is more potent antibiofilm agent than rhamnolipids at all the tested concentrations. This antibiofilm dominance over rhamnolipids is also shown by the other three DSDs, **SF α C (13)**, **SF β M (14)** and **D β C (4)** but only at concentrations higher than 42 μM . The low IC_{50} values of the four DSDs are comparable to some of the most powerful synthetic agents that have been reported to nonmicrobically inhibit *P. aeruginosa* biofilm.^{115,213}

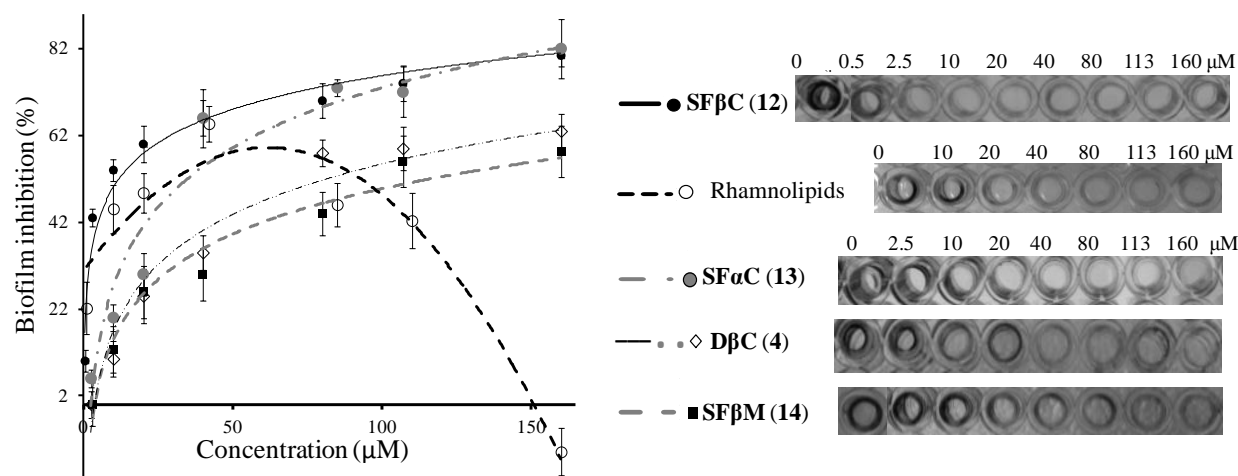


Figure 3.6 Disaccharide derivatives' (DSDs) and rhamnolipids' dose-response curves for *P. aeruginosa* (PAO1) biofilm inhibition. The biofilm was allowed to form with increasing concentrations or without agents for 24-h old biofilm and then quantified by staining with crystal violet (CV) dye. The images on the right show the CV-dye stained biofilms formed on the wells of the microtiter plate for each agent and each concentration tested. Error bar is standard error of the mean from 4 replicates.

3.2.5 Strong biofilm inhibitors were also good biofilm dispersers

Both in industrial and medical settings one commonly encounters biofilms that have already formed and dispersing these preformed biofilms is usually a daunting task. Therefore, while discovering agents that prevent onset of biofilm formation is important, identifying agents that are able to disperse preformed biofilms is more critical from application standpoint.^{80,115,238,239} With this objective in mind, the ability of DSDs to disperse 24-h old PAO1 biofilm was evaluated. In general (with a few exceptions), the dispersing activities of the DSDs displayed an overall similar trend as the SAR for biofilm inhibition (Figure 3.7). When tested at a concentration of 160 μM against 24-h old biofilms, the agents with good antibiofilm activities, **SF β C (12)**, **SF α C (13)**, **SF β M (14)** and **D β C (4)** also displayed good biofilm dispersing abilities

(>60% dispersion as compared to control). At 160 μ M, the rest of the DSDs barring **D β CDS (18)** had biofilm dispersion activities ranging between 20-60%. The saccharide derivative, **D β CDS (18)** was unique as it was the only tested agent that seemed to increase biofilm content when it was added to a 24-h old biofilm.

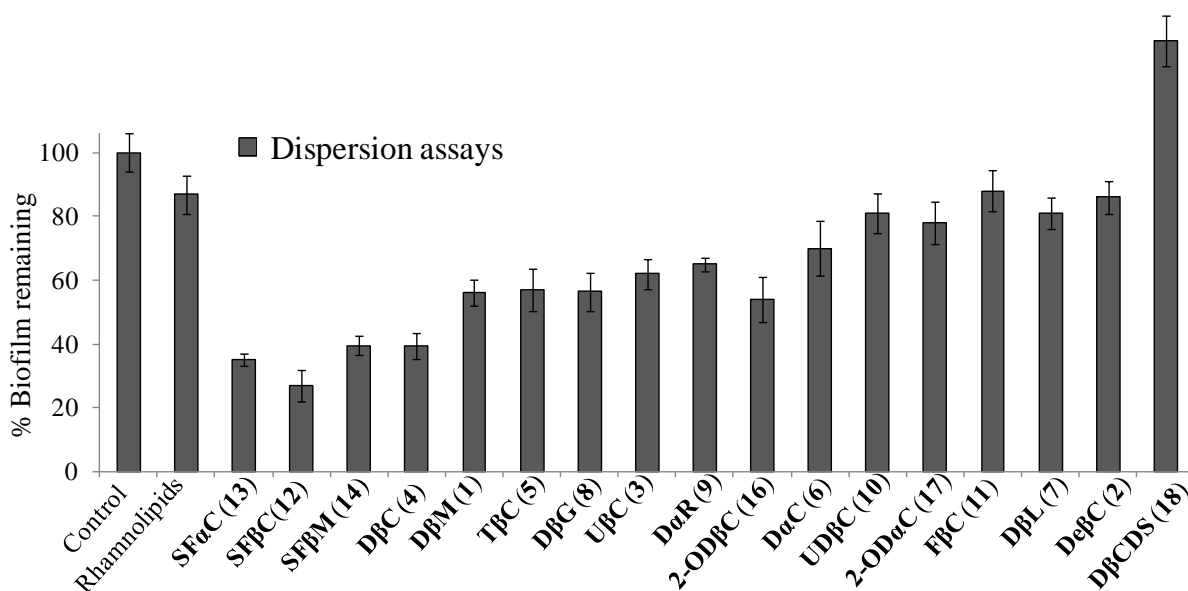


Figure 3.7 Biofilm dispersion potencies of DSDs and rhamnolipids quantified by CV-dye based assay. PAO1 biofilms were grown in microtiter plates without agents for 24-h in LB-media and then fresh LB-media supplemented with various DSDs or rhamnolipids (160 μ M) was added. The percent PAO1 biofilm remaining after inoculating for another 24 hours with (160 μ M) or without various DSDs or rhamnolipids were calculated by comparing biofilm content of control (no agent) to biofilm content in presence of an agent. Error bar is standard error of the mean from 4 replicates.

3.2.6 The potent DSDs strongly dispersed the preformed biofilm of *P. aeruginosa* while rhamnolipids could not

The moderately active antibiofilm rhamnolipids were not able to display much dispersing ability against 24-h old biofilms. The highest biofilm dispersion activity of 34% displayed by

rhamnolipids was at a concentration of 42 μM beyond which the activity continuously dropped (only 17% dispersion at 85 μM) (Figure 3.8). Contrasting the poor dispersive bioactivity of rhamnolipids, the dispersion dose-response curve of three active DSDs, **SF β C (12)**, **SF α C (13)** and **SF β M (14)** brought forward structures that exhibited half-maximal dispersion concentration (DC_{50}) values that compare favorably to known dispersive agents of *Pseudomonas aeruginosa* biofilm.^{80,115} The DC_{50} s calculated for **SF β C (12)** was ~ 44 μM , for **SF α C (13)** was ~ 89 μM and for **SF β M (14)** was ~ 126 μM .

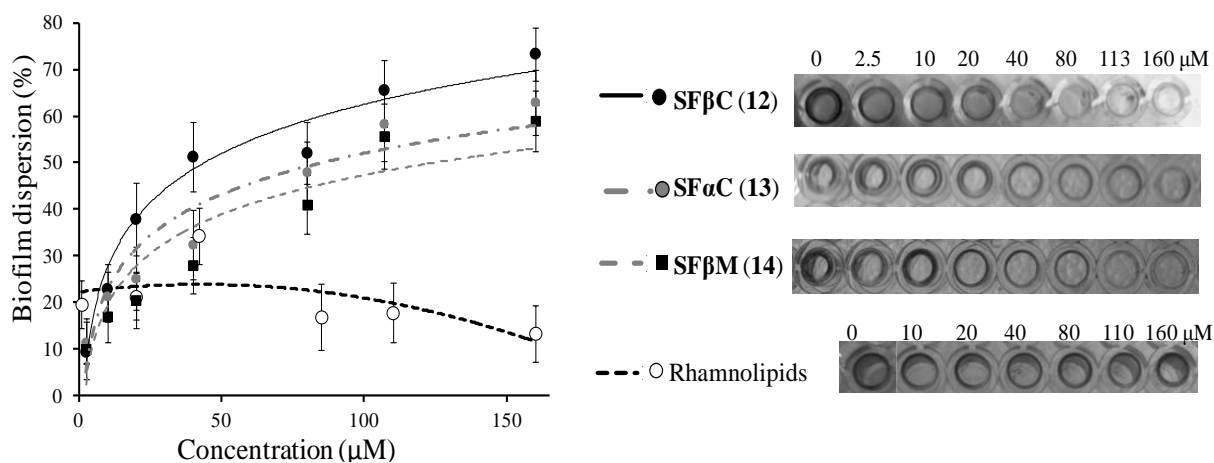


Figure 3.8 Disaccharide derivatives' (DSDs) and rhamnolipids' dose-response curves for dispersion of 24-h old *P. aeruginosa* (PAO1) biofilms. PAO1 biofilms were grown in microtiter plates without agents for 24-h in LB-media and then fresh LB-media supplemented with various DSDs or rhamnolipids was added at different concentrations. The percent PAO1 biofilm remaining after inoculating for additional 24 hours with or without various DSDs or rhamnolipids was calculated by comparing biofilm content of control (no agent) to biofilm content in presence of an agent. Error bar is standard error of the mean from 4 replicates.

3.2.7 Some DSDs and even rhamnolipids reduce the initial adhesion of bacteria to a polystyrene surface

Adhesion of bacteria to biotic surfaces is usually the first step of infection; the first step of biofouling on abiotic surfaces is also the initial attachment of bacteria. Therefore, agents that prevent this initial attachment of bacteria to surfaces offer potential therapeutic and industrial benefits. To evaluate the DSDs' bacterial adhesion inhibition potencies, a mutant strain of *P. aeruginosa* that constitutively expresses green fluorescent protein (PAO1-EGFP) was inoculated for 2 hours in LB media with (160 μ M) or without various SDs or rhamnolipids. After the initial adhesion period, the amount of fluorescent bacteria (PAO1-EGFP) adhered on the surface was quantified by measuring the fluorescence at 510 nm. With the exception of two DSDs, **D α R (9)** and **D β CDS**, the overall SAR trend of bacterial adhesion inhibition was consistent with the trend obtained from biofilm inhibition (Figure 3.9). Another disparity between biofilm inhibition and bacterial adhesion inhibition was the activity of rhamnolipids, while at 160 μ M exhibited negative biofilm inhibition, it showed 39% inhibition of bacterial adhesion. The DSDs that had good biofilm inhibition and dispersion activities, also displayed good bacterial adhesion inhibition potencies including 77% for **SF α C (13)**, 66% for **SF β C (12)**, and 70% for **SF β M (14)**.

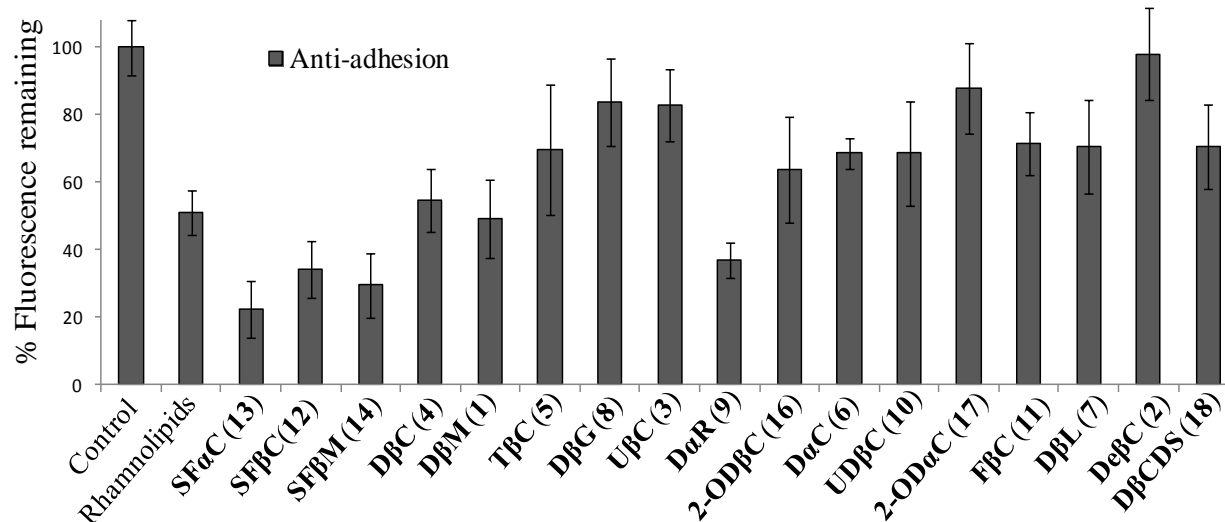


Figure 3.9 Percent bacterial adhesion inhibition potencies of the various DSDs and rhamnolipids. Percent PAO1-EGFP remaining adhered on the wells of polystyrene microtiter plate after 2 hours from inoculation with bacterial culture supplemented with (160 μ M) or without various DSDs or with rhamnolipids. Fluorescent signal emitted by the bacteria (PAO1-EGFP) at 510 nm was quantified to measure the amount of bacteria on the surface. The percentages were obtained by comparing PAO1-EGFP content of control (no agent) to PAO1-EGFP content in presence of an agent. Error bar is standard error of the mean from 4 replicates.

3.2.8 Bioactivities of DSDs depend on structural details

Important results from activation of swarming (Chapter 2), inhibition (IC_{50}) and dispersion (DC_{50}) of biofilm (Chapter 3) are summarized in Table 3.1. Analyzing this data reveals that potent antibiofilm DSDs (**SFβC (12)** & **SFβM (14)** having low IC_{50} and DC_{50}) generally activated the swarming of the *rhlA* mutant at a relatively lower concentration than DSD that had poor antibiofilm activities (**TβC (5)** and **DβG (8)**). Also, the potent antibiofilm DSDs were the only agents that exhibited dominance over rhamnolipids during swarming motilities. While others have shown that under natural settings, rhamnolipids help maintain biofilm architecture of

P. aeruginosa,²⁴⁰ the results in this study showed that adding low concentration of rhamnolipids externally inhibits biofilm formation. The addition of rhamnolipids externally into the growing media could add to the *in situ* secreted rhamnolipids that the bacteria secretes, hence the local concentration of this biosurfactant may increase dramatically, leading to a possible washing effect on the biofilm. The dose-response curves of rhamnolipids depicts "activity reversal" for both swarming activation and biofilm inhibition. This a first documentation for the effect of different concentrations of rhamnolipids on biofilm formation and swarming. The "activity reversal" phenomenon has been noticed earlier by others while studying concentration effects of bacterial signalling molecules on light simulation (another bacterial multicellular behavior). The reversal in antibiofilm activity at higher doses of rhamnolipids underscores the chances of this being a physical phenomenon because the surface activity should only increase with higher doses.

3.2.9 A more stringent structural requirement on DSD is needed for controlling biofilm formation than for controlling swarming motility

Some structures that activated *rhlA* swarming motility including **DeβC (2)**, **UβC (3)**, **DβG (8)** and **TβC (5)** exhibited poor antibiofilm activities. On the contrary some structures including **2-ODβC (16)** and **DαR (9)** had poor antibiofilm capabilities but seemed to effectively inhibit the swarming process of wild type PAO1. However, the DSDs that had good antibiofilm activities like **SFβC (12)**, **SFαC (13)** and **SFβM (14)**, were generally strong inhibitors of PAO1 swarming. Thus, the structure-activity relationships (SAR) indicate that poor antibiofilm agents do not have a predictive effect on swarming, whereas effect of good antibiofilm agents on swarming was generally predictive. The SAR also revealed that combination of certain glycone and aglycone elements generally generated DSDs with poor capabilities to modulate both swarming and

biofilm formation. These elements include short aliphatic chain, **DeβC (2)**, aliphatic chains with unsaturation, **UDβC (10)** and **FβC (11)**, sugar head groups that are either small monosaccharides, **DβG (8)** and **DaR (9)** or large cyclic oligosaccharide, **DβCDS (18)**. Together, these results suggest that the swarming motility, bacterial adhesion and biofilm formation are intertwined together, and designs of disaccharide derivatives can control selectively some or all of these three biological activities.

Table 3.1. Transition concentrations of DSDs that exhibit activity reversal from activating to inhibiting swarming motilities of the *rhlA* mutant and PAO1, and IC₅₀ and DC₅₀ of DSDs for PAO1 biofilm inhibition and dispersion. Antibiofilm activities (inhibition & dispersion) at 160 μM of various agents.

Compound	^a Transition concentration (<i>rhlA</i>)	^b Transition concentration (PAO1)	IC ₅₀ (PAO1)	DC ₅₀ (PAO1)	Antibiofilm activity 160 μM (PAO1) Inhibition Dispersion	
Rhamnolipids	~10 μM	~20-30 μM	^c --	^d --	-14%	13%
SFβM (14)	~10 μM	~7.5 μM	~102 μM	~126 μM	60%	60%
SFβC (12)	~8 μM	~10-20 μM	~9.9 μM	~44 μM	76%	60%
DβC (4)	^e ~45-56 μM	~20-30 μM	~72 μM	^d --	62%	60%
TβC (5)	~40 μM	~20-30 μM	^d --	^d --	40%	43%
DβG (8)	~35-50 μM	~50-60 μM	^d --	^d --	46%	50%
SFαC (13)	^d --	^d --	~32 μM	~89 μM	82%	77%

^aFrom activating to inhibiting swarming motility of the *rhlA* mutant. ^bFrom promoting to inhibiting swarming motility of PAO1; ^crhamnolipids exhibits “activity reversal,” IC₅₀ was not calculated; ^dnot determined, weak antibiofilm activities

3.2.10 DSDs do not interfere with the known *las* and *rhl* quorum sensing circuits of *P.aeruginosa*

The onset of multicellularity in bacteria is controlled by quorum sensing.³⁹ For this quorum sensing process, bacteria use small molecule chemical signals to communicate with one another. Therefore, one effective antibiofilm strategy is to make use of chemical mimics of quorum sensing molecules that interfere with cellular communication and hence disrupt biofilm formation.^{115,213,241} To identify antagonists for the two quorum sensing circuits of *P. aeruginosa*, *las* and *rhl*, gene reporter assays were constructed for reporting activation or suppression of such systems.¹⁷¹ In this assay, the plasmids, *plasI*-LVAgfp and *prhII*-LVAgfp were transformed into the wild type strain PAO1^{115,242} to report activity against the *las* and *rhl* systems, respectively. Natural autoinducers N-3-(oxododecanoyl)-L-homoserine lactone (PAI-1) and N-(butyryl)-L-homoserine lactone (PAI-2) bind the *las* and *rhl* gene product, respectively, resulting in expression of green fluorescent protein (GFP) encoded by the plasmids. Agents that antagonise the *las* or *rhl* system, will have to compete with the naturally secreted autoinducers and as such cause a decrease in the expression of GFP.¹⁶⁷ When two potent antibiofilm agents, **SFβC (12)** and **SFαC (13)** were tested for antagonistic activity against the two reporter strains, PAO1/*plasI*-LVAgfp and PAO1/*prhII*-LVAgfp, both agents did not seem to change the expression of GFP (Figure 3.10). Hence, these agents do not interfere with either the *las* or the *rhl* quorum sensing circuit of *P. aeruginosa*.

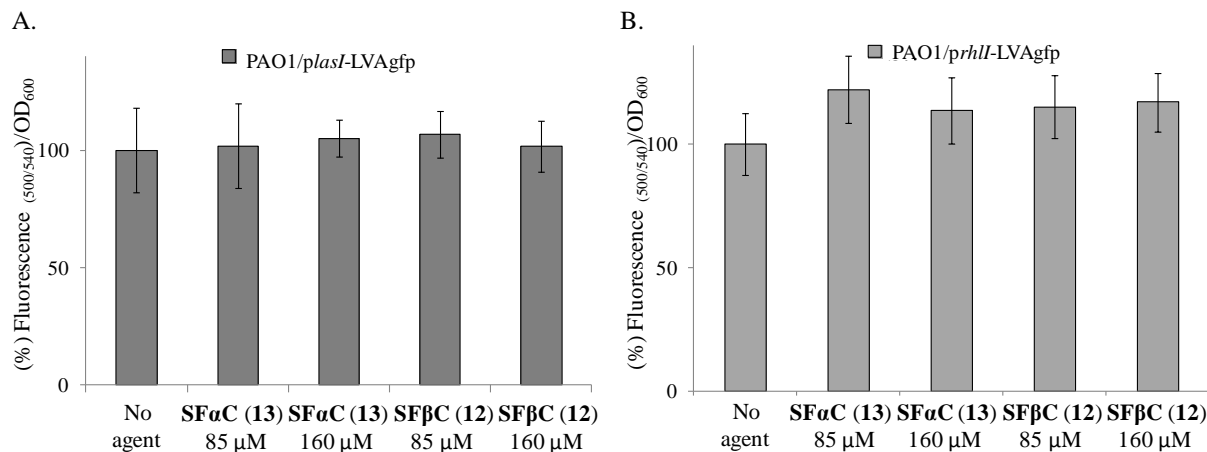


Figure 3.10 Gene-reporter assay with two reporter strains of *Pseudomonas aeruginosa*, PAO1/plasI-LVAgfp and PAO1/prhII-LVAgfp, showed that DSDs did not interfere with either the las or the rhl quorum sensing systems. Fluorescence (GFP) signal by PAO1 having plasmid; (A) *plasI*LVAgfp and (B) *prhII*LVAgfp in the absence and in the presence of SF α C (13) and SF β C (12). Fluorescence signals were corrected for cell density by dividing with OD₆₀₀ of bacterial cell culture. Error bar is a standard error of the mean of the readings from 4 replicate wells.

3.2.11 Competitive biofilm inhibition assay with one DSD and synthetic pili peptide reduced antibiofilm potency of the DSDs

The involvement of pili in promoting the swarming motility of *P. aeruginosa* has been documented by Kohler and coworkers.¹²³ Randall and coworkers have shown that the receptor domain on pilin protein that recognizes carbohydrate moieties on tissues cells is a 17-amino acid residue on the C-terminal region (residues 128-144). This 17-amino acid residue has been shown to be semi-conserved amongst various strains of *P. aeruginosa* with two specific conserved cysteines (at position 129 and 142) in all strains being oxidized to form a di-sulfide loop.²²⁹ Randall and workers have also shown that both the pilin receptor domain and its synthetic

peptide is also critical for enabling bacteria to adhere onto abiotic surface.^{183,225,243} To date the minimum binding carbohydrate epitope that binds both the pilin receptor domain and its synthetic peptide has been shown to be D-GalNac(1→4)-β-D-Gal moiety.^{199,244} The pili assisted epithelial cell binding domain is located between residues 128-144 on the C-terminal region of PilA, the pili structural protein.²²⁹ To explore the identity of the putative receptor for such DSDs and rhamnolipids, the minimum seventeen amino acids residues receptor domain (N¹-Ac-ACKSTQDPMFTPCKGCDN-OH-C¹)^{245,246} of *P. aeruginosa* strain PAO was synthesized via a solid phase strategy. In order to replicate the disulfide loop formed by natural receptor domain, the synthesized pili peptide was subjected to oxidizing conditions to oxidize the cysteines at positions 129 and 142 to form an intra-molecular disulfide loop (called as pili peptide henceforth). To serve as a control a scrambled (N-Ac-AAKSTQDPMFTPCKGADN-OH-C¹) version of the pili peptide was also synthesized where in the cysteines at positions 129 and 142 position were exchanged to alanines (here in referred to as scrambled pili peptide). Both the synthetic peptides were tested along with a potent antibiofilm DSD, **SFαC (13)** at concentration of 85 μM in a competitive antibiofilm assay against wt *P. aeruginosa* (PAO1) (see Figure 3.11). The DSD, **SFαC (13)** by itself exhibited ~70% biofilm inhibition, but when 85 μM of pili peptide was added along with 85 μM of **SFαC (13)**, the antibiofilm activity of the DSD dropped to only ~30% inhibition. Contrary to the effect of pili peptide, when 85 μM of both **SFαC (13)** and the scrambled pili were added to the culture, DSD still seemed to inhibit close to 65% of the biofilm. These results suggest that the synthetic pili peptide likely interferes with the binding between the the DSD **SFαC (13)** and the natural pili receptor domain on the bacteria, whereas the scrambled version of the synthetic pili peptide had little interference.

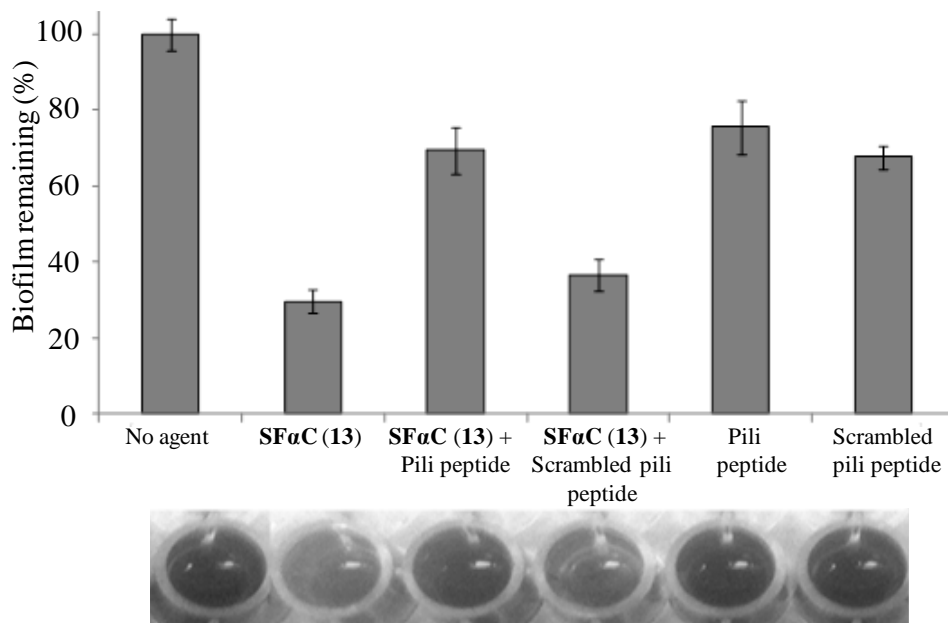


Figure 3.11 Crystal violet (CV) stained PAO1 biofilm within the wells of the microtiter plate after biofilm was allowed to develop for 24 hours in LB-media without any agents and in LB-media that is supplemented with SFαC (13) ~85 μM; SFαC (13) ~85 μM + Pili peptide ~ 85 μM; SFαC (13) ~85 μM + Scrambled pili peptide ~ 85 μM; Pili peptide ~ 85 μM; Scrambled pili peptide ~ 85 μM.

3.2.12 Mechanistic understanding

Biofilm inhibition and swarming results brought forward some key mechanistic points. Rhamnolipids are amphiphilic molecules and their role in biofilm formation and swarming has always been debated to either be biological or physical.²⁰⁴ Similarly, the effects on biofilm formation and swarming by various DSDs, which are amphiphilic in structure could have been hypothesized to either mere washing effect due to surfactant properties (physical) or biological in which a receptor on bacterial surface may bind to these molecules leading to either an antagonistic or an agonistic signaling event. However, few results in this study clearly suggested

that the effects by both rhamnolipids and DSDs on the various bioactivities of *P. aeruginosa* are probably of biological nature. Firstly, generic surfactants that lacked amphiphilic structure with sugar head group (**C₁₂EG₅OH**, **DTAC** and **SDS**) exhibited no effects on biofilm formation and swarming, but **DβM (1)** possessing a maltose head group activated swarming as well as inhibited biofilm formation.²⁴⁷ Secondly, bioactivities of each DSD were sensitive to its structural details. Thirdly, swarming activation reversal caused by increasing concentrations of both rhamnolipids and the active DSDs indicated a trait of a cell-signaling molecule. A similar concentration dependent activity reversal has been reported before for N-(3-oxohexanoyl)-3-aminodihydro-2(3H)-furanone molecule, which was eventually identified as a bacterial signaling molecule.¹²⁰

The gene reporter assays showed that neither of the two quorum sensing circuits of *P. aeruginosa* were perturbed by the two most active DSDs, **SFβC (12)** and **SFαC (13)**. Preliminary studies indicate that the receptor of such DSDs and also rhamnolipids maybe the cell surface adhesins, pilin protein.

3.3 Conclusion

The SAR brought forward specific structural elements that were important for imparting potent bioactivities to disaccharide derivatives (DSDs). The DSDs with either cellobiose or maltose stereochemistries having a bulky aliphatic tail, 3, 7, 11-trimethyl-dodecanyl were both good inhibitors of *P. aeruginosa* adhesion and biofilm formation and also potent dispersers of pre-formed (1-day old) biofilm. Making structural changes on DSDs revealed that alteration in the disaccharide stereochemistry produced lesser variation in bioactivity than changes made to the aglycone part of the molecule. From previous chapter (Chapter 2), it was evident that the most active DSDs and also rhamnolipids caused a swarming activation at lower concentrations followed by a reversal in swarming activation at higher concentrations for the *rhlA* mutant.

Contrary to the effect on swarming, the concentration studies with most active DSDs for biofilm inhibition and dispersion showed that the bioactivities plateaued off at higher concentrations with no indication of reversal. However, in a dose-dependent study with the naturally secreted molecule rhamnolipids being added externally for dispersion assay showed an activity reversal phenomenon. Surfactant action associated with amphiphilic structures like DSDs and rhamnolipids was shown to be less likely to cause such biological events. These DSDs did not perturb the known *las* and *rhl* quorum sensing circuits of *P. aeruginosa*. Therefore, the mode of action of such amphiphilic molecules is through a yet to be identified pathway. Preliminary studies showed that these molecules could be recognizing the adhesin protein pilin present on *P. aeruginosa* pili appendage. The search for putative receptor/s for such DSDs molecules and also rhamnolipids is ongoing. Importantly, the ability of such DSDs molecules to control *P. aeruginosa* motile lifestyle, i.e adhesion, biofilm formation and dispersion and also motile behavior, i.e swarming, while at the same time being nonmicrobicidal to the growth of the bacteria offers a viable alternative strategy to fight bacteria related problems with lower propensity to cause multi-drug resistance (MDR).

3.4 Materials and methods

Bacterial strains and plasmids. *Pseudomonas aeruginosa* strains PAO1 and PAO1-EGFP were obtained from Dr. Guirong Wang (Upstate Medical University). *Pseudomonas aeruginosa* transposon mutant strain PW6886 (rh1A-E08::ISphoA/hah) was obtained from two-allele library.²⁰² PAO1 (*plasI*-LVAgfp), PAO1 (*prhII*-LVAgfp) strains were prepared by literature reported protocol.²¹⁴ The plasmid *plasI*-LVAgfp and *prhII*-LVAgfp were obtained from Dr. Hiroaki Suga (The University of Tokyo) and were maintained by adding 300 µg/mL of carbenicillin in culture media. Freezer stocks of all strains were stored at -80 °C in LB media

with ~20% glycerol. All strains were grown at 37 °C in a rotary-shaker (at 250 rpm) in Luria Bertini (LB) media (10 g/L tryptone, 5 g/L yeast extract, and 10 g/L NaCl). All biofilm inhibition, dispersion and adhesion assays were performed in LB-media and plates were incubated at 37 °C under static conditions.

Stock solution and delivery of disaccharide derivatives (DSDs). All but three saccharide derivatives were water-soluble. For the water soluble DSDs, no organic solvents were used to assist the mixing and delivery for all biological assays. Stock solution (~11.5 mM) of DSDs were prepared in autoclaved water and further sterilized by filtering through cellulose acetate syringe filter (0.2 µm pore size, GVS filter technology) into sterilized vials. The sterilized DSDs stock solutions were stored at -20 °C and thawed prior to each use. Aliquots of DSD stock solutions were added to the cultures in wells. Sterile water (same volume as the DSD stock solution used) was used as positive controls (no agents) in all assays to eliminate the effect of water from the stock solution. Three agents **DβL (7)**, **SFβL (15)** and **2-ODαC (17)** exhibited low water solubility, and were prepared in mixed solution of sterile water (90%) and 200 proof EtOH (10%). Controls for these agents consisted of the same mixed water-ethanol solution.

Crystal violet (CV) dye based-biofilm inhibition assay.^{213,214} Overnight culture of PAO1 were sub-cultured in LB media to obtain an OD₆₀₀ of 0.01, and further cultured to reach an OD₆₀₀ of ~0.1. The bacterial culture (200 µL) was added into the wells of a microtiter plate, followed by predetermined volumes from DSDs stocks. The microtiter plate was then wrapped in GLAD Press n' Seal® (Saran wrap) and further incubated under stationary conditions for 24 h at 37 °C. After incubation, the culture media was discarded by careful pipetting, and the wells were washed once with 200 µL sterile water and the plate was dried at 37 °C in the incubator for 30 mins. Surface attached biofilms in the wells were then stained with 200 µL of 0.1% aqueous

solution of crystal violet (CV) for 30 mins at ambient temperature. The CV stain was then removed by pipetting, and each well was washed with 200 μ L sterile water. The resulting surface attached CV stain in the wells was then solubilized by adding 100 μ L of 30 % AcOH solution (in water) and mixing gently by pipetting. Adding 100 μ L of 30% AcOH solution only solubilizes the biofilm attached to the bottom of the well surface (termed as “surface attached biofilm”)¹¹⁵ and not the “liquid-air interface” biofilm that is formed at the interface of culture media (200 μ L) and air. The amount of biofilms were inferred and quantified by measuring absorption at 600 nm (OD_{600}) of the AcOH solution. A negative control that contained only the media without bacterial inoculum and without agents was also stained. The OD_{600} values of the negative control were subtracted from the OD_{600} values of the wells containing bacteria and treated with DSDs. The difference in OD_{600} values of wells with DSDs and wells with no agent (positive controls) was divided by the OD_{600} value of control to obtain percent biofilm inhibition.

Antiadhesion assay.²⁴⁷ Overnight culture of PAO1-GFP (supplemented with 300 μ g/mL of carbenicillin) in LB medium was sub-cultured (250 rpm and 37 °C) to an OD_{600} of 0.01. When the OD_{600} of the sub-culture reached \sim 0.1, 200 μ L aliquot of the sub-culture was transferred to the wells of 96-well black microtiter plate, followed by designated volumes of DSD stock solutions to achieve desired concentrations of DSD. Positive controls used sterile water in place of DSD stock solution. The black microtiter plate was wrapped by Saran wrap (GLAD Press n’ Seal®) and incubated at 37 °C for 2 h. The bacterial culture was then discarded by pipetting, and each well was washed once with saline water (0.85 w/v% aqueous NaCl). Aliquot of fresh LB medium (200 μ L) was then added into the wells and the fluorescence was measured at an excitation wavelength of 500 nm and an emission wavelength of 540 nm by using Synergy 2

multi-mode microplate reader with Gen5 data analysis software. The absorption from wells containing just LB medium was subtracted from wells treated with DSDs.

Confocal laser scanning microscopy (CLSM) based biofilm inhibition assay. Steel coupons (316L, thickness 0.012', 1 in. × 1 in.) were washed with EtOH, dried under a stream of nitrogen and then sterilized in an autoclave. Overnight culture of PAO1/EGFP ($OD_{600} \sim 1.0$) grown in LB media (supplemented with 300 $\mu\text{g}/\text{mL}$ of carbenicillin), was sub-cultured to $OD_{600} \sim 0.01$, and further cultured to an OD_{600} of ~ 0.1 . Aliquots of 600 μL PAO1/EGFP subculture was added into the wells of a 24-well microtiter plate, followed by 9 μL of stock solutions of DSDs to obtain the concentration of 160 μM . Bacterial sub-culture with no agent served as positive controls. Sterile steel coupons were then placed into the wells and the plates were wrapped with Saran wrap and incubated for 24 h at 37 ° C under static conditions. The steel coupons were then removed and washed by dipping in PBS buffer twice and then gently dabbed on a bleached paper (KIM wipes) to remove the excess solution. The dried steel coupons were viewed under a confocal laser scanning microscope (CLSM). Images were taken at 4 random locations on each steel coupon. The Z-stacked images were also taken to determine the relative thickness of the biofilm.

Biofilm dispersion assays. Crystal violet dye-based assay for quantifying dispersion of 1-day old PAO1 biofilms were similar to the biofilm inhibition assay. Wells of the microtiter plate were inoculated with 200 μL PAO1 subculture ($OD_{600} \sim 0.1$). The plates were incubated at 37 °C for 24 hours to allow biofilm formation. After 24 hours, bacterial culture was gently pipetted out and predetermined volumes of DSDs were added followed by addition of 200 μL of fresh LB medium. The microtiter plate was then incubated for an additional 24 hours at 37 °C. The amount

of the biofilm in the wells was measured using the same procedures for biofilm inhibition assays with the same control solutions.

Dose dependence assays for biofilm inhibition and dispersion. Disaccharide derivatives (DSDs) that were most potent at 160 μM (exhibiting > 60 % biofilm inhibition and dispersion) were selected for determining the dose dependence. For both biofilm inhibition and dispersion assays, predetermined volumes of DSD stock solutions were added to the assigned wells to achieve a concentration between 0.5 to 170 μM . Percent biofilm inhibition or dispersion was calculated by dividing the difference in biofilm content (absorbance at 600 nm, OD_{600}) between wells with DSDs and control wells (no agents) by biofilm content of controls. The percent biofilm inhibition or dispersion was plotted versus the concentrations of DSDs. The graph was curve fitted using equation $y = \ln(x) + C$, where y is % of inhibition (or % dispersion) and x is the concentration. The half maximal inhibitory concentration for both biofilm inhibition and dispersion (IC_{50} and DC_{50}) were obtained by solving for $y = 50$.

Synthesis of oxidized pili peptide $\text{PAO}_{(128-144)\text{ox}}$ and scrambled pili peptide

$\text{PAO}_{(\text{C129A/C142A})\text{Scrambled}}$. Synthesis of the peptides were done according to previously reported procedure.¹⁹⁹ Fmoc-based solid phase peptide synthesis was used and the purification was done by reversed-phase high performance liquid chromatography (HPLC). Air oxidation was employed to oxidize the two cysteines residues in $\text{PAO}_{(128-144)}$ sequence to generate a di-sulfide linkage. For this a dilute solution (6mg/ 4mL) of unoxidized pili peptide was made PBS buffer (pH ~7.8) containing 10 % DMSO, and solution was stirred in air and monitored by reversed phase HPLC and MALDI-TOF. Following the oxidation of pili peptide, purification was done over reverse phase HPLC. $\text{PAO}_{(128-144)\text{ox}}$ sequence is N' Ac-A-C-K-S-T-Q-D-P-M-F-T-P-K-G-C-D-N-OH-C'. While for generating scrambled pili peptide, cysteines at positions 129 and 142

were replaced with alanines to generate the following sequence; PAO_{(C129A/C142)Scrambled}; N⁷Ac-
A-A-K-S-T-Q-D-P-M-F-T-P-K-G-A-D-N-OH-C.

Chapter 4

Synthetic Disaccharide Derivatives Inhibit the Biofilm Formation of *Candida albicans* by Preventing Hyphal Adhesion

Abstract

Disaccharide derivatives (DSDs) with either cellobiose or maltose head groups and having either n-alkyl, farnesyl, hydrogenated farnesyl or 2-octyl dodecyl aliphatic chains were used to nonmicrobically inhibit biofilm formation of *Candida albicans*. The tested DSDs did not inhibit the growth of either fungal blastospores or hyphae. Microscopic evaluation showed that none of the tested DSDs (except **FβC (1)** prevented hyphal germination. The DSDs were only effective at inhibiting the biofilm of *Candida albicans* when applied within five minutes of seeding the test surface with fungal cells. The half-maximal inhibitory concentrations (IC₅₀s) of 14.7 and 21.5 μM for some DSDs like saturated farnesyl-β-maltoside (**SFβM, 6**) and 2-octyl dodecyl-β-cellobioside (**2-ODβC, 7**), respectively are comparable to IC₅₀s of known nonmicrobicidal agents that inhibit *Candida albicans*' biofilm. Tri(ethylene glycol) terminated self-assembled monolayers (SAMs) on gold surface are able to resist *Candida albicans* hyphal adhesion where as pentadecanethiol SAMs allow hyphal adhesion. Using a modified gold surface that contained patterns of pentadecanethiol SAMs surrounded by regions of tri(ethylene glycol) terminated SAMs it was shown that in a media that supports hyphae formation (RPMI-1640), addition of one DSD, saturated farnesyl-α-cellobioside (**SFαC, 5**) dramatically reduced the adhesion of *Candida albicans* hyphae onto the pentadecanethiol SAMs. It is therefore predicted that, the DSDs' ability to prevent initial adhesion of *Candida albicans* hyphae translates into their ability to inhibit biofilm formation.

4.1 Introduction

Both bacteria and fungi can reside harmoniously in the same environment including on mucosal surfaces like skin, the oral cavity, and the gastrointestinal tract.²⁴⁸ The co-colonization of bacteria and fungi is particularly common in the respiratory tracts of chronic lung-diseased patients. A number of pathogenic fungi like, *Candida*,²⁴⁹ *Aspergillus*,²⁵⁰ *Cryptococcus*,²⁵¹ *Trichosporon*,²⁵² *Coccidioides*,²⁵³ and *Pneumocystis*²⁵⁴ have been identified as biofilm dwellers. Importantly, the biofilms of these pathogenic fungi have been reported to display severe to mild resistance against the common antifungals like, fluconazole, amphotericin B, nystatin, and voriconazole. In the United States alone, an estimated ~\$2.6 billion dollars is spent being annually to treat fungal related hospital nosocomial infections.²⁵⁵ Unfortunately, the increase in the occurrence of fungal biofilm within medical settings parallels the rapid increase in the use of more number of medical devices and implants. The most common fungal commensal known to infect medical equipments is *Candida albicans*.^{256,257} The opportunistic pathogen *Candida albicans* is the most common fungi associated with hospital acquired infections, particularly on medical devices, implants, tissue surfaces, oral and vaginal mucosal epithelial cells.^{258,259} Presently, the approximate mortality rate for device related *Candida albicans* infections in the United States is about ~30%.

4.1.1 Biofilm development in *Candida albicans* involves morphogenesis

Candida albicans is a dimorphic fungi that exhibits at least two kinds of morphological cells, budding blastospores and filamentateous hyphae. The onset of fungal biofilm progresses through various stages, similar to the step-by-step biofilm formation process exhibited by bacteria. One important difference between bacteria and fungus, is that upon surface attachment fungal cells known as blastospores form filamentous structures known as hyphae that invade into the surface,

where as biofilm dwelling bacterial cells do not show any such morphogenesis. The next step in biofilm progression is secretion of extracellular matrix which coincides with acquisition of drug resistance. Under normal biofilm progression, small oval shaped yeast cells, blastospores first form germ tubes that give rise to pseudohyphae and ultimately tubular hyphae.²⁶⁰ The existence of dimorphic cells (blastospores and hyphae) within fungal biofilms was confirmed via the genetic studies done by Finkel *et al.*²⁵⁵ Douglas *et al*, showed that dimorphic morphogenesis was true under both natural and laboratory settings (Figure 4.1).²⁶¹ The final step in *Candida albicans*' biofilm development is the release of yeast cells to initiate colonization of newer surfaces. It has been reported that the biofilm development in *Candida albicans* is under genetic control and many such genes may display opposite regulation depending upon which step of biofilm is involved i.e. formation or dispersion.²⁵⁵

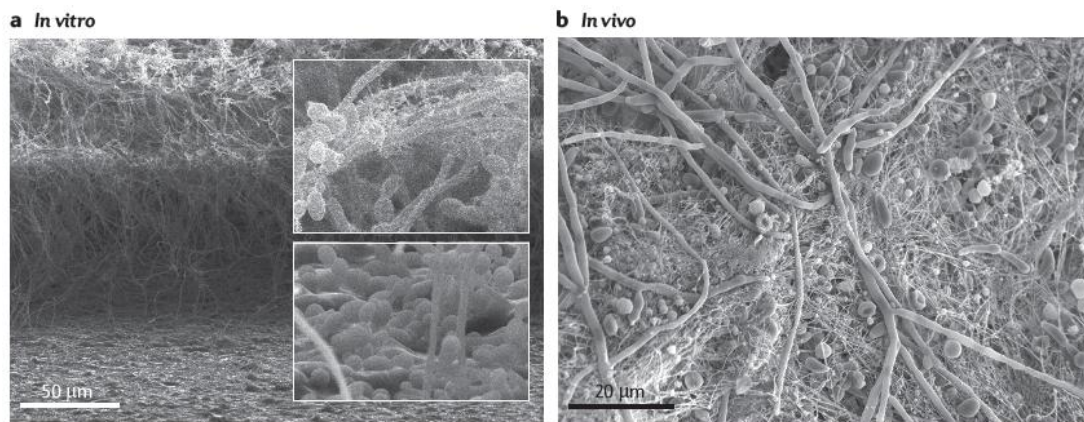


Figure 4.1 Dimorphic nature of *Candida albicans* where both blastospores and hyphae co-exist is evident in both (a) in vitro and (b) in vivo biofilm. The scanning electron microscopic (SEM) micrographs of in vitro biofilm (a) shows lower region comprising of blastospores, middle region containing mainly hyphae and an upper region consisting of both hyphae and blastospores. The in vivo biofilm sample obtained from a rat catheter model (b) shows a mixture of blastospores and hyphae. [Reprinted with permission from Citation:⁸ Finkel, J. S.; Mitchell, A.

P., Genetic control of *Candida albicans* biofilm development. *Nature Reviews Microbiology* **2011**, 9, (2), 109-118].

4.1.2 Farnesol is the key quorum sensing molecule

The occurrence of cell-to-cell communication via secretion of various chemical signals during biofilm formation by bacteria has been well documented.^{41,155-157,166,167,262,263} Similar cellular communication process through the use of chemical signals has also been reported in many fungal species.²⁶⁴ The first autoregulatory molecule that was identified to play a crucial role in *Candida albicans* signaling process was 3,7,11-trimethyl-2,6,10-dodecatrienoate (farnesoic acid).²⁶⁵ By adding the farnesoic acid into the growth media, Oh and coworkers showed that 3,7,11-trimethyl-2,6,10-dodecatrienoate was able to prevent the morphological differentiation from yeast to hyphae.²⁶⁶ After the discovery of the farnesyl based autoregulatory signal, Ramage and coworkers employed trans-trans farnesol molecule for effective inhibition of *Candida albicans* biofilm. The biofilm inhibition ability of farnesol was mediated through its ability to prevent yeast to hyphae morphogenesis.²⁶⁷ Later, Alem and coworkers discovered a second QS molecule secreted by *Candida albicans*. This, second QS chemical signal was an alcohol derived from tyrosine.²⁶⁸ Apart from these two chemical signals, many small molecules like, phenylethyl alcohol, dodecanol and nerodiol have been identified as autoregulators secreted by *Candida albicans* during QS and biofilm formation²⁶⁴ The later three molecules are also known inhibitors of hyphal formation therefore, these agents have good biofilm dispersion properties.²⁶⁹ Similar to genetic regulation of virulence genes in bacteria, the secretion of many extracellular factors responsible for both intercellular and cell-to-substrate adhesion by *Candida albicans* are controlled by a set of genes.²⁷⁰ Two such *Candida albicans* genes regulate the expression of hyphal wall proteins (Hwp1) and adhesin Eap1. While the expression of *hwp1* is

critical for formation of hyphal wall protein, adhesin Eap1 mediates binding of fungal cells to other cells and to surfaces.²⁷¹ Both, hyphal wall proteins (Hwp1) and adhesin Eap1 have become targets for effective therapeutics against *Candida albicans*.

4.1.3 Interspecies interactions between fungus and bacteria can be cooperative as well as uncooperative

From clinical perspective, the mixed biofilm formed by bacteria and fungi probably has more adverse effects than biofilm formed by a single species alone. One work consistent with the medical perspective about mixed biofilms was done by Azoulay, E. *et al* in which they showed that the risk of contracting ventilator associated pneumonia (VAP) caused by *Pseudomonas aeruginosa* was increased when the patients respiratory tract was colonized with *Candida spp*. Therefore, exploring ways to treat mixed biofilms is important primarily because dual infection by bacteria and fungus are known to lead to increased mortality rates.²⁷² Mechanistically, co-existence of bacteria and fungi can exhibit many diverse interactions, that affect either microbial physiology or growth or both, and of these interactions some are symbiotic but most are inhibitory.^{273,274} The autoregulatory signal farnesol secreted by *Candida albicans* has been reported to inhibit the formation of biofilm by *Staphylococcus aureus*.^{275,276} Likewise, the autoinducers secreted by *Pseudomonas aeruginosa* have been shown to prevent *Candida albicans* hyphal formation and hence inhibit biofilm formation.²⁷⁷

4.1.4 Three broad classes of fungicidal agents against Candida albicans

Overall antifungal agents can be classified into three broad classes; echinocandins, polyenes and azoles. The mode of action for all the three types of antifungal agents is via blocking some fungal metabolic activity or by targeting an important structural element on yeast cells. Apart from these traditional antifungal agents, Cheng *et al* isolated and characterized

Flocculosin (octadecyl cellobiosides) which is a class of cellobiose-based lipids from a fungus, *Pseudozyma flocculosa* and reported that such agents possessed antifungal activities.²⁷⁸ Mimee et al used flocculosin isolated from *Pseudozyma flocculosa* for effective antibacterial activity.²⁷⁹ Cellobiose based molecule isolated from *Trichosporon porosum* by Nifantiev and co-worker was shown to have antifungal activity too.²⁸⁰

4.1.5 Antibiofilm strategies developed so far

Farnesol is the cell-signalling molecule of *Candida albicans* and its secretion controls induction of hyphal phase. Ramage *et al* demonstrated that biofilm formation could be prevented when farnesol was applied in the early stages of biofilm formation.²⁶⁷ As farnesol prevented biofilm formation via blocking germ tube formation, Nickerson *et al* performed a comprehensive structure activity relationship (SAR) study with farnesol analogues to understand how structural changes affected germ tube formation in *Candida albicans*.²⁸¹ In that study, a chemical library of forty molecules that differed from farnesol either in head group, or aliphatic chain structure, or in chain unsaturation, or in occurrence of hetero atoms in the backbone were studied for their effect on germ tube formation. Of the forty molecules, only twenty two molecules inhibited the germ tube formation by >50%, and the rest did not even come close to the activity of farnesol. Amongst the better twenty two molecules, the activity of the most potent agent was only ~7% of the activity exhibited by farnesol. The extracellular factors of both bacteria and fungi can affect the physiology and morphology of each other and vice-versa. The prime example of this inhibitory relationship between bacteria and fungus was reported by Hogan *et al* when they showed that two auto inducers secreted by *Pseudomonas aeruginosa*, 3-oxo-C12 homoserine lactone (HSL) and C12-acyl homoserine lactone (AHL) can inhibit hyphal germination in *Candida albicans*.²⁷⁷ Inhibitory relationship was further elucidated by Holcombe *et al* who

showed that supernatants taken from *Pseudomonas aeruginosa* cultures could decrease the ability of *Candida albicans* to form biofilms on silicone.²⁸² Dispersion of *Candida albicans* biofilms by an amphiphilic molecule, dodecyl glucoside was reported by Dusane *et al.* Apart from the antibiofilm agents mentioned here, many other small molecules have also been applied to prevent biofilm formation and disperse existing biofilms of *Candida albicans*.²⁸³⁻²⁸⁵ Amongst these, the antibiofilm activities of a class of small molecules isolated from natural sources by Cichewicz *et al.* against *Candida albicans* are the the most potent reported to date.^{286,287}

In the previous chapters (2&3), the effective use of disaccharide derivatives (DSDs) for modulating multiple multicellular behaviors of bacteria *Pseudomonas aeruginosa* was reported. Here, these synthetic DSDs were functional mimics of a class of amphiphilic molecules, rhamnolipids secreted by *Pseudomonas aeruginosa*. Since external factors secreted by both bacteria and fungus have been shown to impact the morphology and physiology of one another, it was but logical to test the effect of DSDs on *Candida albicans*. Since certain DSDs were potent inhibitors of *Pseudomonas aeruginosa* biofilm, their corresponding effect on *Candida albicans* biofilms formation was evaluated. Second compelling reason to test DSDs on *Candida albicans* stemmed from their structural details. The most potent DSDs against *Pseudomonas aeruginosa* biofilm were composed of cellobiose head group and a farnesyl aliphatic tail. The effect of both farnesyl based molecules and cellobiose based molecules on *Candida albicans* has been document earlier. Primarily, many fungicidal agents have been shown to posses cellobiose moieties while farnesol is a known cell-signalling molecule secreted by *Candida albicans*. But a study to understand the effect of structures possessing both the farnesyl and cellobiose moieties on *Candida albicans* morphology and physiology had never been done before.

4.2 Results and Discussions

4.2.1 Structural design of disaccharide derivatives (DSDs) selected for biofilm inhibition of *Candida albicans*

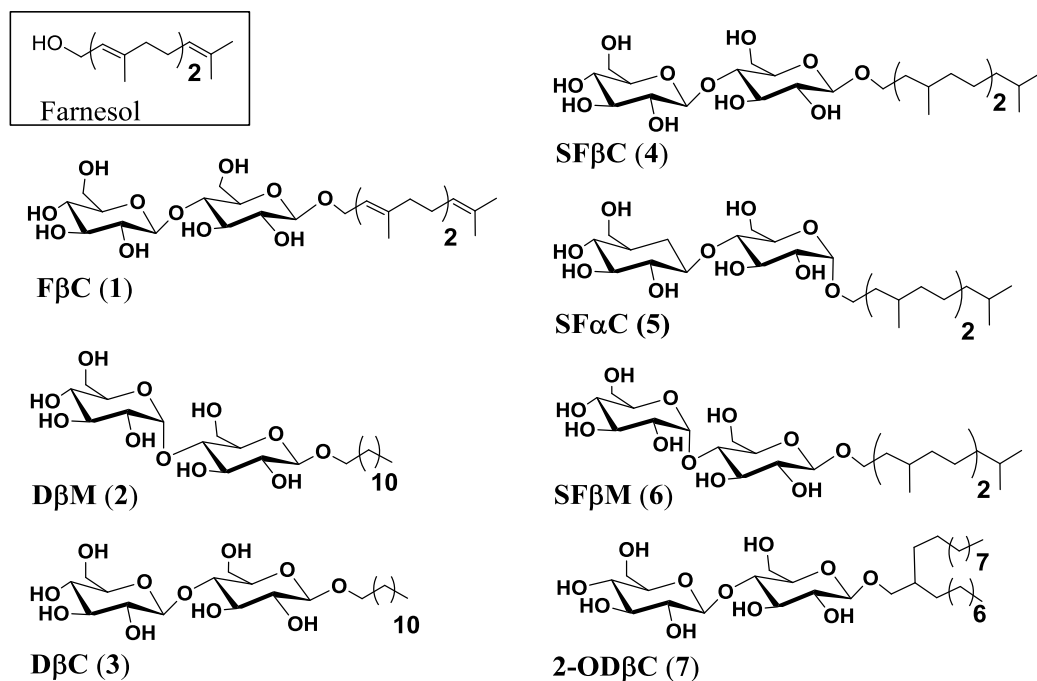


Figure 4.2 Synthetic disaccharide derivatives (DSD) used in this study. Inset: Structure of *Candida albicans* quorum sensing molecule (QSM), farnesol.

The structural design of the agents incorporated disaccharide head group (either cellobiose or maltose) and an aliphatic tail (either n-alkyl, or farnesyl, or saturated farnesyl, or lipid). The DSDs that had cellobiose stereochemistry include, farnesyl-β-cellobioside, **FβC (1)**; dodecyl-β-cellobioside, **DβC (3)**; saturated farnesyl-β-cellobioside, **SFβC (4)**; saturated farnesyl-α-cellobioside, **SFαC (5)** and 2-octyl-dodecyl-β-cellobioside, **2-ODβC (7)**; and those with maltose stereochemistry included, dodecyl-β-cellobioside, **DβC (3)**; saturated farnesyl-β-maltoside, **SFβM (6)** (Figure 4.2). The DSDs could also be classified via their aliphatic tail; having a farnesyl tail; **FβC (1, cellobiose based)**; or those having a saturated farnesyl tail; **SFβC**

(**4**, cellobiose based); **SF α C** (**5**, cellobiose based) and **SF β M** (**6**, maltose based); or those having n-alkyl tail; **D β M** (**2**, maltose based); and **D β C** (**3**, cellobiose based); or the one having a branched lipid tail; **2-OD β C** (**7**, cellobiose based); Since farnesol is a known QSM secreted by *Candida albicans* that has been shown to inhibit biofilm formation, it was also included in the chemical library as a control. Synthesis of all DSDs molecules was done according to previously reported route and the synthetic procedures and characterizations are mentioned in Chapter 2 (Materials & Methods).

4.2.2 None of the DSDs were toxic to the growth of *Candida albicans* blastospores

At the onset it was necessary to establish whether the effect on *Candida albicans* biofilm formation by these DSDs did not originate from their ability to impede growth. For this, the toxic effect of DSDs was evaluated on the growth of *Candida albicans* blastospores grown in yeast-peptone-dextrose (YPD) media. The concentration of DSDs selected 340 μ M, was higher or equal to the highest concentration at which all the other bioassays were done (fungal susceptibility assay, biofilm inhibition assay, adhesion assay etc). The growth of blastospores with or without 340 μ M of various DSDs in YPD media was monitored by observing absorbance at 600 nm (OD_{600}).^{288,289} The growth curves (Figure 4.3) so generated over 24 hours revealed none of the tested DSDs impeded the growth of *Candida albicans* blastospores at 340 μ M.

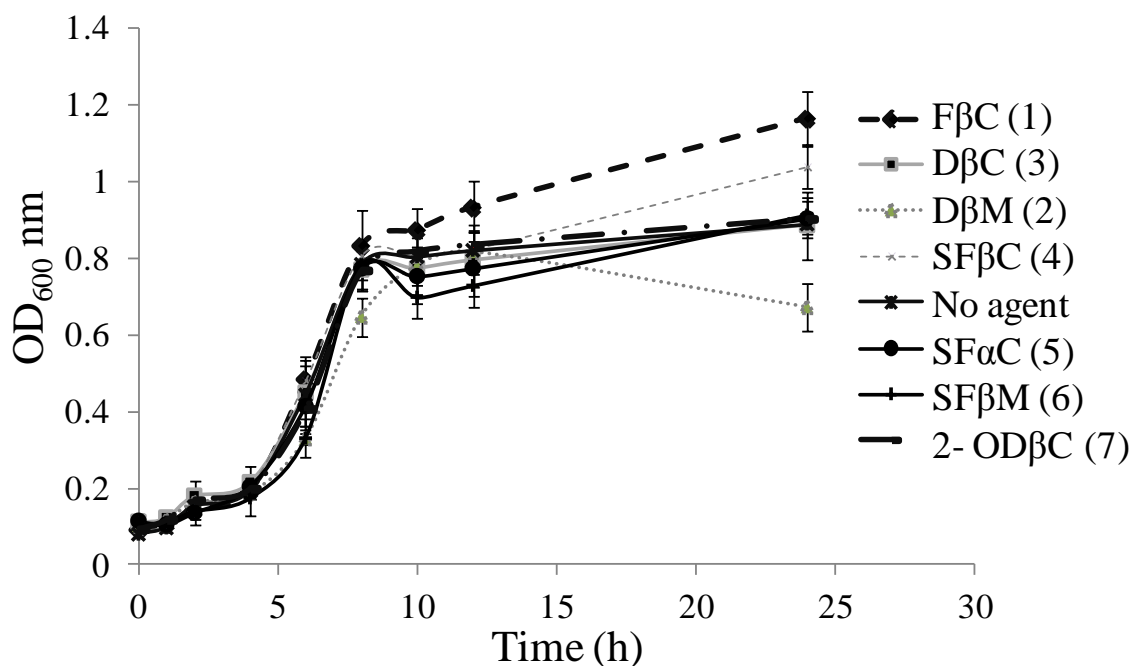


Figure 4.3 *Candida albicans* growth curves in YPD medium. Growth was monitored in the presence (340 μM) or in absence of various DSDs by measuring the optical density of the culture at 600 nm (OD₆₀₀) over 24 hours.

4.2.3 The disaccharide derivatives (DSDs) were not fungicidal

The fungicidal activity of the DSDs on *Candida albicans* was done according to the standard protocol outlined in the NCCLS 2002 CLSI M27-A2 method (micro-broth dilution assay).²⁹⁰ The fungal susceptibility assay was done in RPMI-1640 media and the highest concentration of the DSDs (340 μM) were serially diluted to obtain a minimum inhibitory concentration (MIC₉₀). Here again, like the growth studies with blastospores, the highest concentration tested was either higher than or equal to the concentrations at which biofilm inhibition studies were done. Images of the micro-broth dilution assay results after 24 hours (Figure 4. 4) shows that all the DSDs did not inhibit the growth of *Candida albicans* in the tested concentration range. With no effect on growth of blastospores and no fungicidal activity, the

subsequent effect of these DSDs on the biofilm formation of *Candida albicans* cannot be attributed to the inhibitory effect on growth.

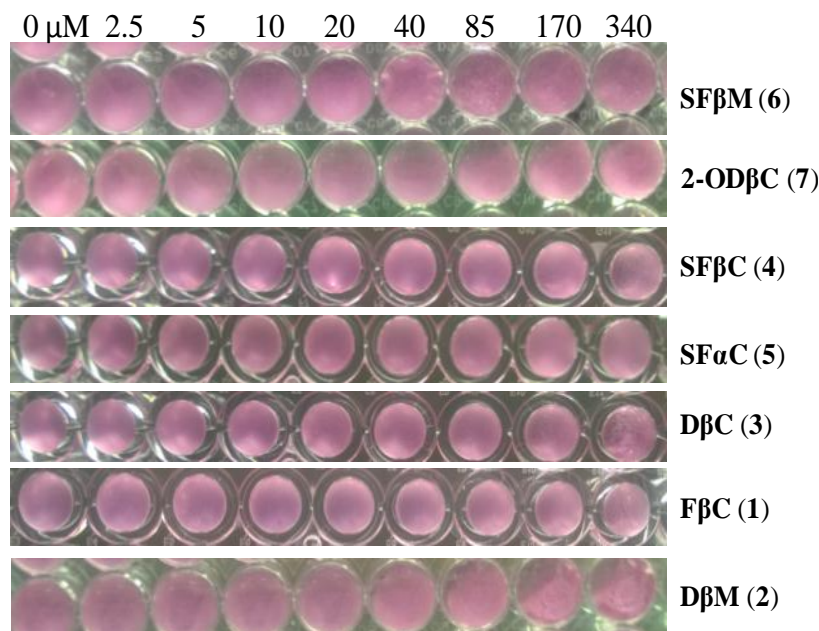


Figure 4.4 Microbroth

dilution antifungal

susceptibility assays. Images

of micotiter plate wells

inoculated with *Candida*

albicans in 1640-RPMI media

YPD supplemented with

various concentrations of

different DSDs. The images

were taken 48 hours after

4.2.4 Most DSDs did not inhibit *Candida albicans* hyphae formation

Although, the DSDs were not fungicidal nor had any inhibitory effect on the growth of blastospores, it was also necessary to establish whether such agents affected the germination of hyphae. Aliquots from the microbroth dilution susceptibility assays after 48 hours of inoculation (Section 4.2.3) with few of the DSDs were viewed under a microscope to physically characterize the fungal morphology. Two concentrations of DSDs selected for being viewed under the microscope were 340 and 40 μM and the fungal morphology within cultures containing these concentrations were compared to that of control (observed with 0 μM concentration of the agent). The content of the cultures with the mentioned concentrations was aspirated and then a drop of the culture was gently dispensed atop a microscope slide and viewed under the microscope. The optical micrograph images of some of these DSDs obtained at the two

concentrations (340 and 40 μM) and at 0 μM (control) in RPMI-1640 media are shown in Figure 4.5. Amongst the four tested DSDs, **F β C (1)**, **D β C (2)**, **SF β C (4)** and **SF α C (5)** none (except one, **F β C (1)**) seemed to inhibit the hyphal formation of *Candida albicans* at both the selected concentrations. However, **F β C (1)** did seem to prevent hyphae formation at 340 μM . Therefore, overall, it could be concluded that all DSDs were nonfungicidal at tested concentration range and one DSD prevented hyphal formation at 340 μM .

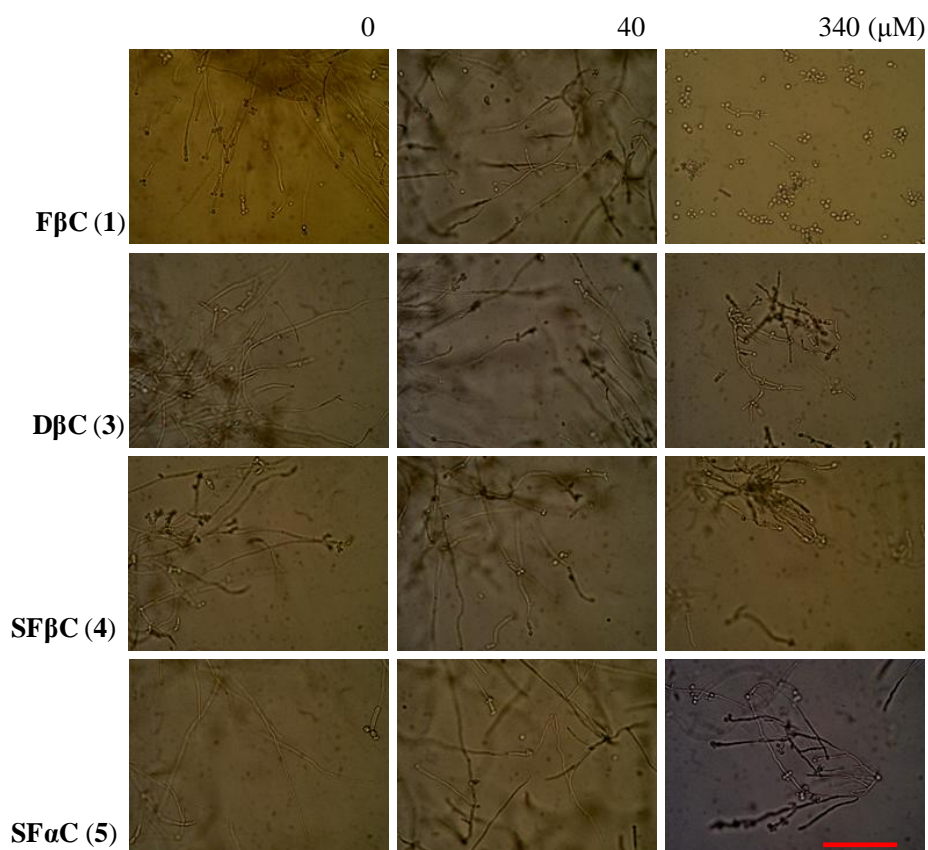


Figure 4.5 Optical micrograph images of *Candida albicans* grown in RPMI-1640 media with (at 340 or 40 μM) or without (0 μM ; control) DSDs. The aliquots were obtained from microbroth dilution antifungal susceptibility assays after 48 hours of inoculation. Scale bar ~ 76 μm

4.2.5 DSDs were screened for biofilm inhibition potencies at 170 μ M using a semi-quantitative XTT-dye based assay^{291,292}

The quantification of *Candida albican* biofilm was done by using a XTT-based semi-quantitative analysis. Since, *Candida albican* undergoes yeast to hyphae morphogenesis over time, therefore, it was important to establish what stage of biofilm development did the DSDs inhibit. Therefore, *Candida albican* cells were allowed to adhere for two different time-frames (seeding of cells), 5 minutes and 4-hours (see Materials and Methods for detailed procedure). After the seeding time, wells were washed with PBS buffer and fresh media containing 170 μ M of various DSDs was introduced in experimental wells whereas no agent was added to control wells. The biofilm was allowed to form for 24 hours, following which quantification was done by adding XTT dye, then storing the microtiter plates in the dark for 3 hours followed by measuring the absorbance of the culture at 490nm.^{267,286,292} The results of the XTT-dye based quantification are shown in Figure 4.6. When the initial seeding time of 4 hours is allowed, none of the DSDs were able to inhibit biofilm formation of *Candida albicans*. However, when the *Candida albicans* cells were seeded for only 5 minutes followed by addition of fresh media and 170 μ M of various DSDs, the percent biofilm inhibited by all agents was > 60 %. The biofilm inhibition potency of two DSDs, **SF β C (4)** and **SF β M (6)** at 170 μ M was particularly high, >85 %.

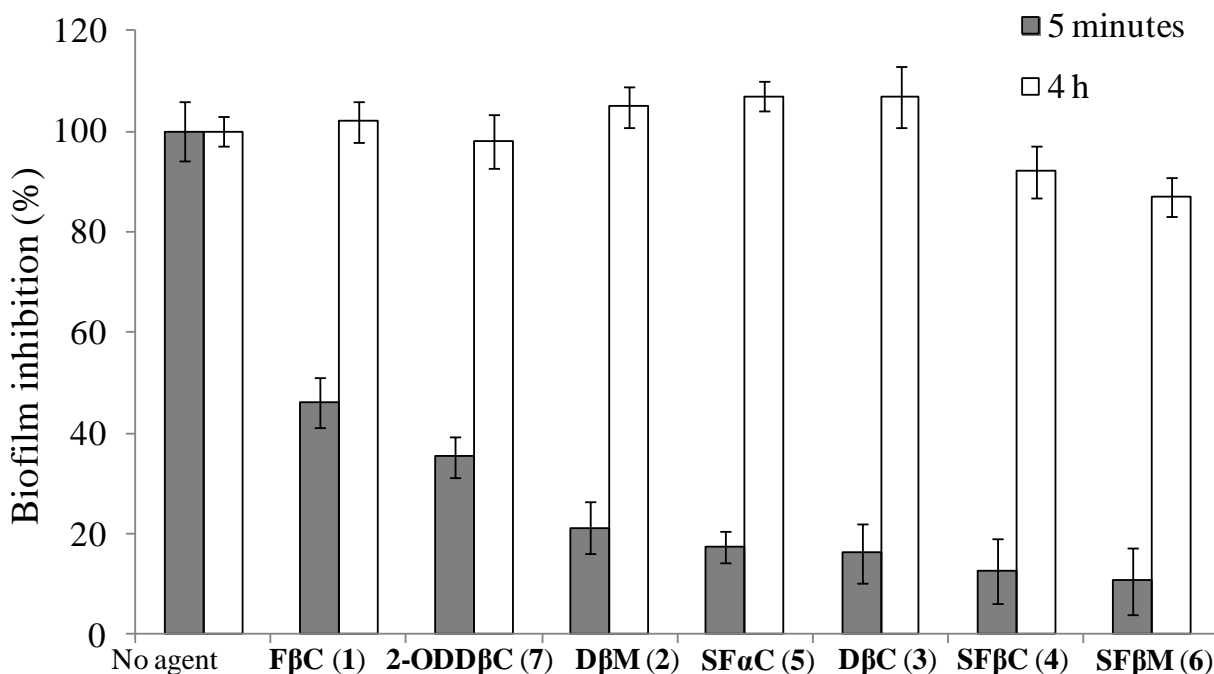


Figure 4.6 *Candida albicans* percent biofilm inhibition caused by various DSDs with two different seeding times (5 minutes & 4-hours). The biofilm was allowed to form for 24 hours in RPMI-1640 media with or without the agent and then the quantification was done using XTT-dye assay. Error bars are the mean standard deviation of biofilm inhibition from 4-replicate wells.

4.2.6 Dose response assays brought forward potent DSDs

After getting preliminary evidence that with initial seeding time of five minutes, 170 μM of the most DSDs could effectively inhibit *Candida albicans* biofilm, a dose-response curve for all agents was plotted to obtain the half-maximal inhibitory concentrations (IC_{50}) for inhibition of *Candida albicans* biofilm. The IC_{50} values of DSDs for inhibiting *Candida albicans* biofilm are shown in Table 4.1. The corresponding dose-response curves have also been plotted (see Materials and Methods). The dose-response study brings forward highly potent antibiofilm agents with SFβM (6) having $\text{IC}_{50} \sim 14.7 \mu\text{M}$ and 2-ODβC (7) having $\text{IC}_{50} \sim 21.5 \mu\text{M}$ (Table

4.1). We note that structure activity study reveals that DSDs with bulky aliphatic and branched aliphatic chains were generally more potent than DSDs with n-alkyl or unsaturated chains. The activity of **FβC (1)** with $IC_{50} \sim 129 \mu M$ was lesser than all of the DSDs having hydrogenated farnesol aliphatic chain **SFβC (4)**, **SFαC (5)** and **SFβ M (6)**. Therefore, reducing the number of double bonds in the aliphatic chain from three to zero increased the potency and lowered the IC_{50} for **SFβC (4)** to $\sim 14.7 \mu M$ (31 % reduction in IC_{50} value as compared to **FβC (1)**). Apart from inhibition, none of the DSDs exhibited any ability to disperse the pre-formed (24-hours old) biofilm of *Candida albicans*.

Agents	IC_{50}
SFβM (6)	14.7 μM
2-ODβC (7)	21.5 μM
SFβC (4)	71.5 μM
DβC (3)	73.6 μM
SFαC (5)	82.8 μM
DβM (2)	122.0 μM
FβC (1)	129.0 μM

Table 4.1. Half-maximal inhibitory concentrations (IC_{50}) for inhibition of *Candida albicans* biofilm by various DSDs. DSDs were immediately added after seeding the microtiter plate wells with *Candida albicans* cells (1×10^5 cell/mL) for 5 minutes.

4.2.7 DSD prevent surface adhesion of *Candida albicans* hyphae

The next step was to understand the mechanism of action of such DSDs on *Candida albicans* biofilm. Results had indicated that the DSDs did not inhibit growth of *Candida albicans* blastospores or hyphae but yet they were effective at inhibiting its biofilm when applied within five minutes of seeding the wells with cells. As, DSDs had exhibited good antiadhesion property against bacteria *P. aeruginosa* (Chapter 3), the antiadhesive ability against fungus *Candida*

albicans was therefore evaluated. For this, a surface-study was employed where firstly, a modified gold surface was created by micro-contact printing the patterns of alkane terminated self-assembled monolayers (SAMs) surrounded by regions of tri-(ethylene glycol) terminated SAMs on gold. Secondly, the adherence of *Candida albicans* blastospores and hyphae on such a modified gold surface in presence and in absence of a DSD was studied. In a study performed by Luk and workers previously, it was shown that SAMs with tri(ethylene glycol) termination resist attachment of *C. albicans* hyphae but not blastospores, whereas SAMs terminating with alkyl groups allow adherence of both blastospores and hyphae.²⁸⁹ Using the adhesion assay, the effect of a DSD, **SFaC (5)** on adhesion of *C. albicans* blastospores and hyphae to modified gold surface was evaluated. For observing the effect of **SFaC (5)** on attachment of blastospores, the *C. albicans* cells were grown in yeast-peptone-dextrose (YPD) growth media whereas for analyzing the effect on hyphal attachment, the cells were grown in a media that supports hyphae i.e RPMI-1640 media. The control contained no agent whereas the experimental well contained 170 μ M of DSD, **SFaC (5)**. The adhesion of *C. albicans* blastospores and hyphae to microcontact printed gold surface in presence and in absence of 170 μ M **SFaC (5)** was observed at two different time points 3 and 6 hours (Figure 4.7). *C. albicans* grown on gold slides under these conditions was viewed under phase contrast microscope. The phase contrast micrographs are reported in Figure 4.7. From the micrographs, it is evident that at 6 hours, both in presence and in absence of 170 μ M of **SFaC (5)** blastospores appear to adhere everywhere on the microcontact printed gold surface. At 6 hours, under a condition that supports hyphae, dense square patterns were formed on alkane terminated SAMs for control experiment. Whereas, addition of 170 μ M of **SFaC (5)** caused significant reduction in hyphal adhesion onto alkane terminated SAM surface as compared to control. The reduction in adherence of hyphae to

modified gold surface in presence of **SFaC (5)** could be due to either microbicidal action of such an agent on *C. albicans* cells or prevention of blastospores to hyphae morphogenesis or such an agent preventing hyphae adhesion. From growth studies in presence of 340 μM of **SFaC (5)**, it is evident that the DSD neither inhibits the growth of blastospores (Figure 4.3) nor the growth of hyphae (Figure 4.4 & 4.5). Therefore, **SFaC (5)** inhibits surface adhesion of hyphae which possibly leads to inhibition of surface attached biofilm.

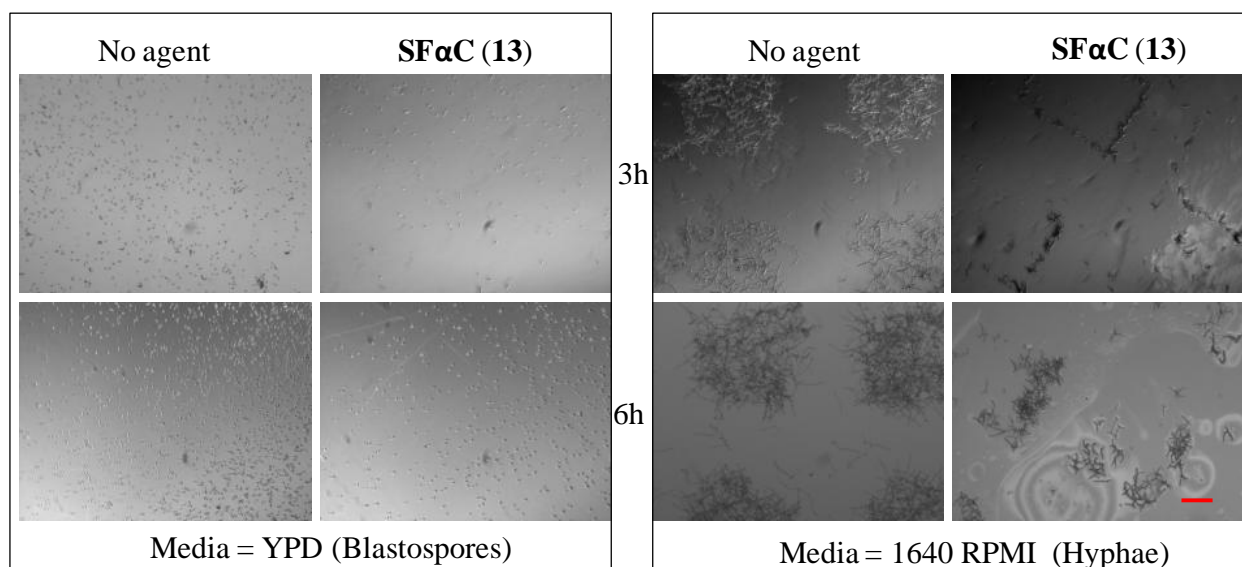


Figure 4.7. Analysis of antiadhesive property of DSD, SFaC (5) against *Candida albicans* blastospores and hyphae. Phase contrast optical micrographs of *Candida albicans* grown in medium supporting either blastospores (left box) or hyphae (right box) growth in presence (170 μM) or in absence of DSD, SFaC (5). *Candida albicans* were grown on gold slides having squares patterns of pentadecanethiol SAMs surrounded by regions of tri-(ethylene glycol) terminated SAMs. Scale bar $\sim 76 \mu\text{m}$. *Candida albicans* cells were inoculated for mentioned time-frame and then viewed under phase contrast microscope.

4.3 Conclusion

This study brought forward a new way to inhibit biofilm formation of fungus *Candida albicans* by making use of DSDs. The growth assays indicated that such DSDs do not inhibit the growth of both blastospores and hyphal cells. Adhesion assay using modified gold surface showed that one DSD, **SF α C (5)** prevented surface adherence of hyphae. The antibiofilm activity of DSDs against *Candida albicans* was only apparent when these agents were applied within 5 minutes of seeding the surface with fungus cells. Results suggest that the DSDs are not effective antibiofilm agent when applied after 4-hours because longer seeding times would allow hyphae to form and adhere to the surface. Therefore, the antibiofilm activity of such DSDs is probably due to their ability to prevent initial adhesion of hyphae to the surface. Some agents like, **SF β M (6)** and **2-OD β C (7)** exhibited potent antibiofilm activities with IC₅₀s of 14.7 and 21.5 μ M, respectively. The “antihyphal adhesion” property of such DSDs could be used as an approach to design new therapeutics that prevent *C. albicans* colonization.

4.4 Materials and Methods

General experimental information for synthesis. Synthesis of a DSDs used here are reported in Chapter 2 under Materials and Methods. Fluconazole and trans-trans-farnesol were bought from Sigma Aldrich.

General information for biological assays

Chemicals. Phosphate buffer saline (PBS), 1-Pentadecanethiol, sulfuric acid (95-98%), (3-*N*-morpholino) propane sulfonic acid (MOPS) were purchased from Sigma-Aldrich. The piranha cleaning reagents, hydrogen peroxide (30%) and methanol were purchased from Fisher chemical (Fair Lawn, NJ). 200-proof ethanol used for washing and cleaning glass-slides were purchased

from Pharmaco-Aaper (Shelbyville, KY). Gold deposition was done on piranha cleaned Fisher's finest premium microscope slides (Pittsburgh, PA). For preparing yeast peptone dextrose (YPD) media to support growth of blastospores, yeast extract was purchased from Fulka (St. Louis, MO), bacto peptone was purchased from BD and Co (Sparks, MD) and dextrose was purchased from Sigma (St. Louis, MO). Media supporting hyphae was prepared from commercially available RPMI-1640 media containing glutamine and NaHCO_3 by buffering with 0.165 M MOPS to a pH (~6.9-7.1). Flat bottom 96-well microtiter plates (untreated) (Costar 3370) and U-bottom 96-well microtiter plates (nontissue culture, BD-falcon) were used for biofilm inhibition and fungicidal assays respectively. For assays involving patterned gold slides 24-well plate were purchased from Nunc (Thermofisher Scientific, Pittsburgh, PA). Synthesis of tri(ethylene glycol)-terminated undecanethiol was done by previous group member.

Fungal strains and growth media condition. Clinical isolate of *C. albicans* SC5314 were obtained from Dr. Dacheng Ren (Syracuse University). To culture blastospores, a loopful of *C. albicans* SC5314 glycerol stock maintained at -80°C was cultured in 5mL yeast peptone dextrose (YPD) media (1%, w/v yeast extract; 2%, w/v of peptone, 2%, w/v of dextrose in autoclaved water) overnight in orbital shaker (250 rpm) overnight at 35°C to produce phase of budding blastospores. For experiments involving surface adhesion, working stocks of blastospores were prepared by subculturing overnight culture to an optical density $\text{OD}_{600} \sim 0.05$ as measured by Biotek ELx800 absorbance plate reader which uses Gen 5™ data analysis software. Hyphal induction was achieved by harvesting cells from 5 mL of overnight YPD culture by centrifugation at $3000g$ for 5min at room temperature, followed by discarding supernatant, resuspending yeast cells in 20 mL of sterile PBS buffer (pH ~7.4) twice followed by addition of prewarmed (37°C) RPMI 1640 media (20 mL) buffered to pH 7.04 with 0.165M MOPS. From

this suspension, a working cell suspension containing 1×10^5 cell mL^{-1} of *C. albicans* was obtained by doing a 1:100-fold dilution with buffered RPMI 1640 media followed by counting cells with a hemacytometer.

Effect of disaccharide derivatives on growth of *Candida albicans*. Yeast cells were grown overnight in yeast-dextrose peptone (YPD) media at 35 °C with constant shaking (250 rpm). The overnight culture was subcultured to an initial optical density at 600 nm (OD_{600}) of ~0.05 measured by Biotek ELx800 absorbance plate reader which uses Gen 5™ data analysis software. The sub culture was then grown in presence (340 μM) or in absence of various DSDs to a final OD_{600} of ~1.0 under constant rotatory conditions (250 rpm) at 35 °C. The OD_{600} at various time intervals were plotted to obtain a growth curve (Figure 4.3).

Micro-broth based anti fungal susceptibility assay

Preparing the microtiter plates and delivering agents. The DSD agents were prepared as 11.5 mM stock solution in sterile water. To the wells of 96-wells microtiter plate was added 100 μL of RPMI-1640 media (buffered to pH ~7.00 by adding MOPs buffer). To the wells in column 11 was added additional 100 μL of RPMI-1640 media. Aliquots of various DSD stock solutions were added to wells in column number 11 at double the required concentration. The media in column 11 wells was aspirated ~ six times with the use of a pipette set at withdrawing 100 μL of solution. After mixing the DSD stock solution six times with the RPMI-1640 media, 100 μL of the mixture was withdrawn and added into the adjoining wells on the left (i.e column 10). The contents were aspirated and again 100 μL was removed and added to wells of column nine and so on. Following this serial dilution of DSD, the extra 100 μL of solution remaining after last the dilution was discarded away. Appropriate amount of water was added into wells serving as

positive controls. The micro-titer plate containing RPMI-1640 media with serially diluted DSD agent was now ready to receive 100 μ L of *Candida albicans* working culture stock.

Culturing C. albicans for fungicidal studies. Yeast cells were grown in YPD media (5mL) at 35 °C with constant shaking (250 rpm) for ~16 hours. After 16 hours the yeast cells were harvested by centrifuging at 3000g for 5 mins at room temperature. The harvested cells were washed twice (20 mL) with PBS buffer solution (pH ~ 7.4, 10 mM). After washing, the yeast cells were suspended in 20 mL of RPMI-1640 media to obtain the culture stock. The stock culture was diluted 100 times and cells were counted using a hemacytometer to a final cell count of 2×10^5 cells/mL to obtain a working stock of culture. Aliquots (100 μ L) of the working culture stock were then added into each well of the microtiter plate having serial dilution of the DSD agent. The resultant culture in each well was mixed gently by swirling the solution with clean pipette tips. The plates were then covered with lids and placed at 35 °C for 48 hours. After 48 hours, the amount of cellular growth in each well was visually inspected and compared to the wells having no agent (positive control). Images of the wells after 48 hours of growth were taken with a camera. Micro-titer plate containing serially diluted fluconazole was also optimized to serve as a control.

Inspecting for hyphal growth. For observing the growth inhibition of hyphae in presence of various DSDs, 3 μ L of culture from the wells (340, 60 and 0 μ M) of the micro-broth dilution experiments were spotted on a microscope slide and viewed under a microscope (Olympus BX51 microscope) and images were taken under 10X zoom using a mounted Olympus wide zoom camera.

XTT-based biofilm inhibition assays.

Preparation of the reagents for the assay. A semi-quantitative XTT [2, 3-bis(2-methoxy-4-nitro-5-sulfo-phenyl)-2H-tetrazolium-5-carboxanilide]-reduction assay was used to quantify biofilm formed by *C. albicans* SC5314. For this, XTT was prepared as 0.5 mg/mL solution in 10 mM sterile PBS buffer (pH ~7.4) and filtered through 0.22 µm filter, aliquoted (5 mL) into vials wrapped with aluminum foil and stored at -80 ° C in the dark. A solution of menadione (5 mM) in acetone was also prepared, aliquoted as 50 µL working stock into eppendorf tubes and stored at -80 ° C. During the day of quantitative measurement for biofilm, a freezer aliquot of both XTT and menadione was removed, thawed to room temperature prior to use. Leftover solution was never reused for a subsequent assay. Stock solutions of all antibiofilm agents were prepared in sterile water (11.5 mM), filtered through a 0.22 µm filter and stored at -20 ° C. A stock solution of trans-trans-farnesol was also prepared (11 mM) in MeOH to serve as a control for biofilm assay.

Serial dilution of DSDs for dose-response assay. Aliquots (100 µL) of *C. albicans* (1×10^5 cell mL⁻¹) from a working culture stock prepared in RPMI-1640 media were seeded into the wells of a 24-well microtiter plate. Two different seeding times, 5 mins and 4 hours were chosen. After the seeding time, the culture was removed and the wells were washed and aspirated with 200 µL of PBS buffer (10 mM, pH~7.4) to remove nonadherent cells. Following this, fresh media (RPMI-1640) (200 µL) containing the highest concentration of agent (340 µM) was added to wells in column number 11. Fresh media (100 µL) was also added to the remaining wells (column 2-10). Serial dilution of the agent was performed by mixing with pipette the content of column 11 gently, then removing 100 µL of culture media and adding to wells in column 10. Again the contents of column 10 were mixed gently and 100 µL was removed and added to the

next column (9) and so on. After serial dilution of column 3, the extra 100 μL was discarded. Column 2 served as positive control. Column 12 content only RPMI-1640 media to serve as a negative control. Following the serial dilution of agent, the microtiter plate was wrapped in GLAD press (saran wrap) and incubated at 37 $^{\circ}\text{C}$ under static conditions for 24 hours.

XTT-reduction assay. Prior to each assay, 1 μL of thawed menadione was added to the thawed XTT solution (5 mL). After 24 hours incubation, the culture was removed and the wells of the microtiter plates were gently washed and aspirated twice with 100 μL of PBS buffer solution to remove nonadherent and planktonic cells. Following this 100 μL of XTT/menadione solution was added into the wells and the plates were incubated in the dark for 3 hour at 37 $^{\circ}\text{C}$. The surface attached metabolically active cells can reduce XTT into a water soluble orange dye, formazan. A semi-quantitative measurement of surface attached biofilm was therefore made by measuring the absorbance from different wells at 490 nm and comparing the A_{490} to the readings obtained from the wells without any agent.

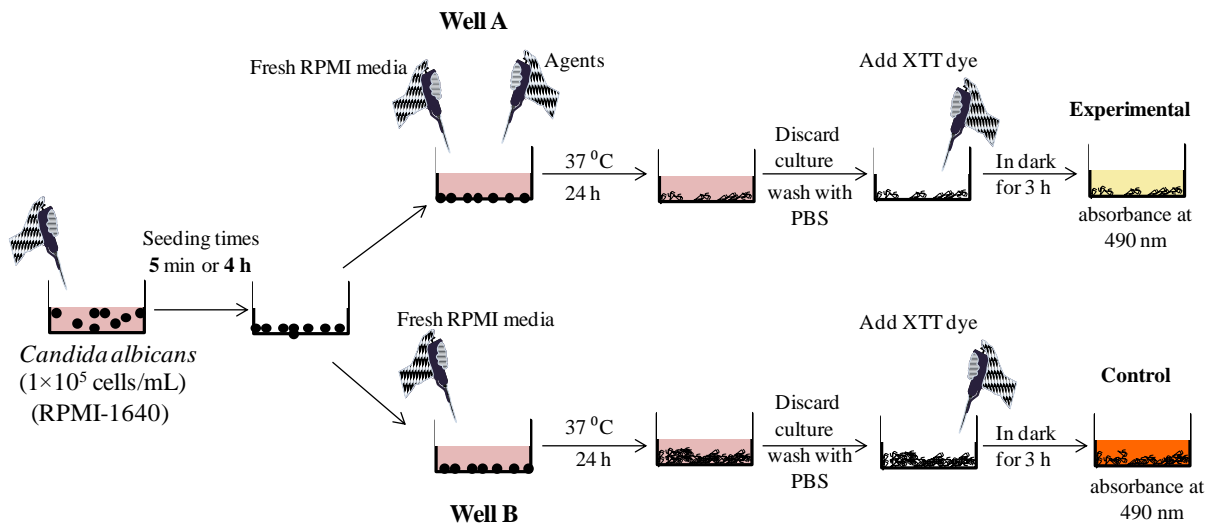


Figure S1. Schematic depicting XTT-dye based biofilm assay for *Candida albicans* with two different seeding times (5 minutes and 4 hours).

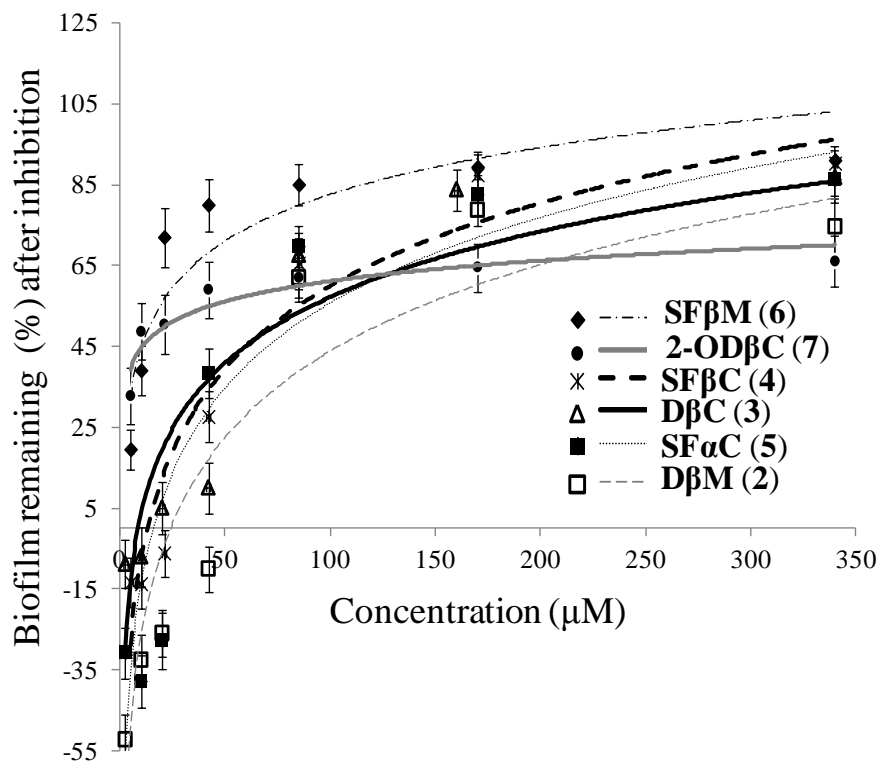


Figure S2. Dose-response curves for inhibition of *Candida albicans* biofilms by various disaccharide derivatives (DSDs).

Adhesion studies with a modified gold surface

Piranha Cleaning of Glass Substrates. Piranha solution (7 parts of concentrated sulfuric acid and 3 parts of hydrogen peroxide (30 % in water)) was used to clean glass substrates prior to gold deposition. For this, the glass substrates were first washed with 200-proof ethanol and dried under a stream of nitrogen, followed by dipping the slides for 45 min in a piranha solution maintained at 70 °C. Following this, the piranha solution was allowed to cool to room temperature and slowly poured off. Multiple washes (~20 times) of the slides was done with deionized water, followed by 10 washes with ethanol and 10 washes with methanol. The slides

were dried off by placing under a stream of nitrogen gas and then kept in the oven overnight at 100 °C. The dried slides were subsequently used for gold deposition.

Gold deposition on gold slides. An electron beam evaporator system (Thermionics, Port Townsend, WA) was used to deposit a semi-transparent film of gold on the piranha cleaned glass slides. Deposition of titanium followed by gold was done by placing the glass slides in a holder such that the deposition angle was 45° to the glass surface. The first coating applied on glass to enhance adhesion of gold was that of titanium (~70 Å). Following deposition by titanium, gold was deposited on the surface at a rate of 0.1 Å/s to achieve a final gold thickness of ~280 Å.

Micropatterning of pentadecanethiol SAMs surrounded by tri(ethylene glycol) terminated alkanethiols. Previous protocol reported by Luk *et al.* was used to create micropatterned regions of pentadecanethiol SAMs surrounded by tri(ethylene glycol) terminated alkanethiols. Briefly, the gold deposited glass slides were cut into 1 cm x 1 cm squares and washed with 200 proof ethanol followed by drying under a stream of nitrogen gas. A polydimethylsiloxane (PDMS) stamp having size (380 X 380 μm²) washed with 200 proof of ethanol and dried under nitrogen gas. The clean PDMS stamp was dabbed with a thin film of 2 mM ethanolic solution of pentadecanethiol and later stamped for 20 seconds on the gold slides. Following the stamping the glass slide was rinsed with ethanol, dried under nitrogen and then immersed in 2mM ethanolic solution of tri(ethylene glycol) terminated undecanethiol for 18h. After 18 h, the micropatterned gold slides (called gold slides henceforth) were removed from the solution, rinsed with ethanol and dried under a stream of nitrogen gas.

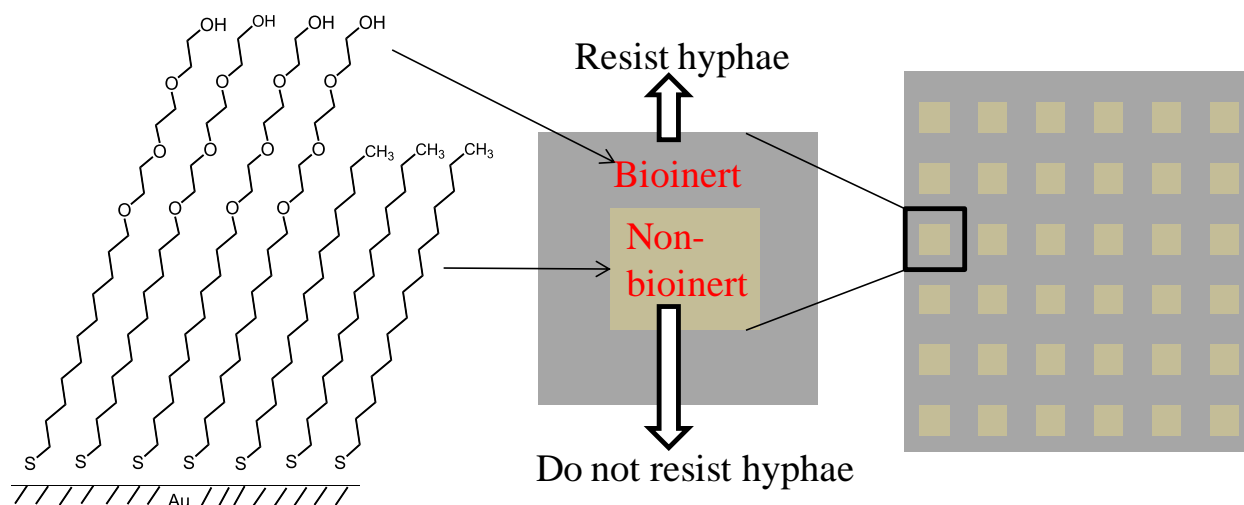


Figure S3. Schematic representation of a micropatterned gold slide containing regions of pentadecanethiol SAMs surrounded by SAMs formed by tri(ethylene glycol)-terminated undecanethiol.

Adhesion of blastospores and hyphae on micropatterned gold slides.

Three separate 24-well microtiter plates were prepared such that each plate contained four micropatterned gold slides in the inner four wells. Two wells in each plate was inoculated with YPD culture containing blastospores ($OD_{600} \sim 0.05$; 600 μ L), while in the remaining two wells were inoculated with *C. albicans* (1×10^5 cell mL^{-1}) in RPMI-1640 media (600 μ L). In each plate, one well with YPD yeast inoculum was supplemented with **SFaC (5; 170 μ M)** and one well with RPMI inoculum was also supplemented with **SFaC (5; 170 μ M)**. The remaining wells containing no agents served as controls for YPD and RPMI conditions, respectively. In the remaining outer wells, sterile water (600 μ L) was added to limit evaporation and drying from the inner wells. The microtiter plates containing the gold slides and culture media were then wrapped in GLAD Press n' Seal® (saran wrap) and further incubated under stationary conditions at 37 °C. The time of incubation was noted and for observation. The gold slides were removed from the media after three, six and twenty four hours and washed gently by slowly dipping in

sterile water once followed by dabbing the edge of the gold slide on a kim wipe to remove excess water. The gold slides were viewed under phase contrast microscope (Motic, AE31, equipped with Infinity 2 Camera) under 4X magnification.

Chapter 5

Future directions

One future direction of the *Pseudomonas aeruginosa* project (chapters 2 & 3) would be to create activity based probes to identify the target protein. Results in this thesis have indicated that the three bioactivities, i.e biofilm inhibition, adhesion inhibition and swarming modulation associated with the saccharide derivatives are less sensitive to the sugar stereochemistry in comparison to the aliphatic structure. Hence, making chemical modifications like epoxides on the sugar head groups are less likely to reduce the molecule's activity when compared to the same change done to the aliphatic chain. In future, sugar derivatives having epoxide modification could serve as good activity based probes for making covalent linkage with the active site.

Once the receptor protein has been identified, the next goal would be target validation, identification of the active site and ultimately performing binding studies. Structure of active site and identification of key interactions will be important for creating more optimized saccharide structures.

Rhamnolipids and its aliphatic chain variants are produced by a few bacteria including *Pseudomonas aeruginosa*, *Burkholderia glumae* and *Burkholderia pseudomallei*,²³ and such secreted rhamnolipids have also been used to inhibit the biofilm formation for a wide range of other bacterial species, including *Rhodococcus erythropolis*, *L. monocytogenes*, *Staphylococcus aureus*, *Bacillus pumilus*.²⁴ These findings call for a deeper understanding of how rhamnolipids function with respect to their specific biological activities that other generic surfactants and biosurfactants cannot perform. Because of the versatile bioactivities, this class of secreted

molecules has the potential to be developed as nonmicrobicidal therapeutic agents that can control bacterial behaviors without invoking drug resistance.

References

- (1) Talbot, G. H.; Bradley, J.; Edwards, J. E.; Gilbert, D.; Scheld, M.; Bartlett, J. G. Bad bugs need drugs: an update on the development pipeline from the Antimicrobial Availability Task Force of the Infectious Diseases Society of America, *Clinical Infectious Diseases*, **2006**, *42*, 657.
- (2) Boyce, J. M.; Opal, S. M.; Chow, J. W.; Zervos, M. J.; Potter-Bynoe, G.; Sherman, C. B.; Romulo, R.; Fortna, S.; Medeiros, A. A. Outbreak of multidrug-resistant *Enterococcus faecium* with transferable vanB class vancomycin resistance, *Journal of Clinical Microbiology*, **1994**, *32*, 1148.
- (3) Spellberg, B.; Guidos, R.; Gilbert, D.; Bradley, J.; Boucher, H. W.; Scheld, W. M.; Bartlett, J. G.; Edwards, J., Jr. The epidemic of antibiotic-resistant infections: a call to action for the medical community from the Infectious Diseases Society of America, *Clin Infect Dis*, **2008**, *46*, 155.
- (4) Bukholm, G.; Tannæs, T.; Kjelsberg, A. B. B.; Smith-Erichsen, N. An outbreak of multidrug-resistant *Pseudomonas aeruginosa* associated with increased risk of patient death in an intensive care unit, *Infection control and hospital epidemiology*, **2002**, *23*, 441.
- (5) Foster, T. J. The *Staphylococcus aureus* “superbug”, *Journal of clinical Investigation*, **2004**, *114*, 1693.
- (6) Spellberg, B.; Bartlett, J. G.; Gilbert, D. N. The future of antibiotics and resistance, *New England Journal of Medicine*, **2013**, *368*, 299.
- (7) Spellberg, B. New antibiotic development: barriers and opportunities in 2012, **2012**.
- (8) Bozdogan, B.; Appelbaum, P. C. Oxazolidinones: activity, mode of action, and mechanism of resistance, *International journal of antimicrobial agents*, **2004**, *23*, 113.

- (9) Diekema, D. J.; Jones, R. N. Oxazolidinone antibiotics, *The Lancet*, **2001**, 358, 1975.
- (10) Steenbergen, J. N.; Alder, J.; Thorne, G. M.; Tally, F. P. Daptomycin: a lipopeptide antibiotic for the treatment of serious Gram-positive infections, *Journal of antimicrobial Chemotherapy*, **2005**, 55, 283.
- (11) Alekshun, M. N.; Levy, S. B. Molecular mechanisms of antibacterial multidrug resistance, *Cell*, **2007**, 128, 1037.
- (12) Nikaido, H. Multidrug resistance in bacteria, *Annual review of biochemistry*, **2009**, 78, 119.
- (13) Higgins, C. F. Multiple molecular mechanisms for multidrug resistance transporters, *Nature*, **2007**, 446, 749.
- (14) Filloux, A. A variety of bacterial pili involved in horizontal gene transfer, *Journal of bacteriology*, **2010**, 192, 3243.
- (15) Dzidic, S.; Bedeković, V. Horizontal gene transfer-emerging multidrug resistance in hospital bacteria, *Acta Pharmacologica Sinica*, **2003**, 24, 519.
- (16) Warnes, S. L.; Highmore, C. J.; Keevil, C. W. Horizontal transfer of antibiotic resistance genes on abiotic touch surfaces: implications for public health, *MBio*, **2012**, 3, e00489.
- (17) Barlow, M. In *Horizontal Gene Transfer*; Springer: 2009, p 397.
- (18) Coates, A.; Hu, Y. Novel approaches to developing new antibiotics for bacterial infections, *British journal of pharmacology*, **2007**, 152, 1147.
- (19) Kohanski, M. A.; Dwyer, D. J.; Collins, J. J. How antibiotics kill bacteria: from targets to networks, *Nature Reviews Microbiology*, **2010**, 8, 423.
- (20) Walsh, C. Molecular mechanisms that confer antibacterial drug resistance, *Nature*, **2000**, 406, 775.

- (21) Benveniste, R.; Davies, J. Mechanisms of antibiotic resistance in bacteria, *Annual review of biochemistry*, **1973**, *42*, 471.
- (22) Davies, J.; Davies, D. Origins and evolution of antibiotic resistance, *Microbiology and Molecular Biology Reviews*, **2010**, *74*, 417.
- (23) Arias, C. A.; Murray, B. E. Antibiotic-resistant bugs in the 21st century—a clinical super-challenge, *New England Journal of Medicine*, **2009**, *360*, 439.
- (24) Fernebro, J. Fighting bacterial infections—future treatment options, *Drug Resistance Updates*, **2011**, *14*, 125.
- (25) McDonnell, G.; Russell, A. D. Antiseptics and disinfectants: activity, action, and resistance, *Clinical microbiology reviews*, **1999**, *12*, 147.
- (26) Yeaman, M. R.; Yount, N. Y. Mechanisms of antimicrobial peptide action and resistance, *Pharmacological reviews*, **2003**, *55*, 27.
- (27) Drenkard, E.; Ausubel, F. M. Pseudomonas biofilm formation and antibiotic resistance are linked to phenotypic variation, *Nature*, **2002**, *416*, 740.
- (28) Olson, M. E.; Ceri, H.; Morck, D. W.; Buret, A. G.; Read, R. R. Biofilm bacteria: formation and comparative susceptibility to antibiotics, *Canadian Journal of Veterinary Research*, **2002**, *66*, 86.
- (29) Bassler, B. L.; Losick, R. Bacterially speaking, *Cell (Cambridge, MA, U. S.)*, **2006**, *125*, 237.
- (30) Shapiro, J. A. Thinking about bacterial populations as multicellular organisms, *Annual Reviews in Microbiology*, **1998**, *52*, 81.

- (31) Hooshangi, S.; Bentley, W. E. From unicellular properties to multicellular behavior: bacteria quorum sensing circuitry and applications, *Current Opinion in Biotechnology*, **2008**, *19*, 550.
- (32) Hall-Stoodley, L.; Costerton, J. W.; Stoodley, P. Bacterial biofilms: From the natural environment to infectious diseases, *Nat. Rev. Microbiol.*, **2004**, *2*, 95.
- (33) Michod, R. E. Evolution of individuality during the transition from unicellular to multicellular life, *Proceedings of the National Academy of Sciences*, **2007**, *104*, 8613.
- (34) Shapiro, J. A. Bacteria as multicellular organisms, *Scientific American*, **1988**, *258*, 82.
- (35) Claessen, D.; Rozen, D. E.; Kuipers, O. P.; Søgaard-Andersen, L.; van Wezel, G. P. Bacterial solutions to multicellularity: a tale of biofilms, filaments and fruiting bodies, *Nature Reviews Microbiology*, **2014**, *12*, 115.
- (36) Davey, M. E.; O'toole, G. A. Microbial biofilms: from ecology to molecular genetics, *Microbiology and Molecular Biology Reviews*, **2000**, *64*, 847.
- (37) Engelberg-Kulka, H.; Amitai, S.; Kolodkin-Gal, I.; Hazan, R. Bacterial programmed cell death and multicellular behavior in bacteria, *PLoS genetics*, **2006**, *2*, e135.
- (38) Verstraeten, N.; Braeken, K.; Debkumari, B.; Fauvart, M.; Fransaer, J.; Vermant, J.; Michiels, J. Living on a surface: swarming and biofilm formation, *Trends in microbiology*, **2008**, *16*, 496.
- (39) Caiazza, N. C.; Merritt, J. H.; Brothers, K. M.; O'Toole, G. A. Inverse regulation of biofilm formation and swarming motility by *Pseudomonas aeruginosa* PA14, *Journal of bacteriology*, **2007**, *189*, 3603.
- (40) Bordi, C.; de Bentzmann, S. Hacking into bacterial biofilms: a new therapeutic challenge, *Annals of intensive care*, **2011**, *1*, 1.

- (41) Taga, M. E.; Bassler, B. L. Chemical communication among bacteria, *Proc. Natl. Acad. Sci. U. S. A.*, **2003**, *100*, 14549.
- (42) Lowery, C. A.; Dickerson, T. J.; Janda, K. D. Interspecies and interkingdom communication mediated by bacterial quorum sensing, *Chem. Soc. Rev.*, **2008**, *37*, 1337.
- (43) Ng, W.-L.; Bassler, B. L. Bacterial quorum-sensing network architectures, *Annual review of genetics*, **2009**, *43*, 197.
- (44) Whiteley, M.; Bangera, M. G.; Bumgarner, R. E.; Parsek, M. R.; Teitzel, G. M.; Lory, S.; Greenberg, E. Gene expression in *Pseudomonas aeruginosa* biofilms, *Nature*, **2001**, *413*, 860.
- (45) Caiazza, N. C.; Merritt, J. H.; Brothers, K. M.; O'Toole, G. A. Inverse regulation of biofilm formation and swarming motility by *Pseudomonas aeruginosa* PA14, *J. Bacteriol.*, **2007**, *189*, 3603.
- (46) Costerton, J. W.; Lewandowski, Z.; Caldwell, D. E.; Korber, D. R.; Lappin-Scott, H. M. Microbial biofilms, *Annual Reviews in Microbiology*, **1995**, *49*, 711.
- (47) Stoodley, P.; Sauer, K.; Davies, D. G.; Costerton, J. W. Biofilms as complex differentiated communities, *Annu. Rev. Microbiol.*, **2002**, *56*, 187.
- (48) Watnick, P.; Kolter, R. Biofilm, city of microbes, *Journal of bacteriology*, **2000**, *182*, 2675.
- (49) Abdel-Aziz, S. M.; Aeron, A. Bacterial Biofilm: Dispersal and Inhibition Strategies, *SAJ Bio-technol*, **2014**, *1*, 105.
- (50) Donlan, R. M.; Costerton, J. W. Biofilms: survival mechanisms of clinically relevant microorganisms, *Clinical microbiology reviews*, **2002**, *15*, 167.
- (51) Monds, R. D.; O'Toole, G. A. The developmental model of microbial biofilms: ten years of a paradigm up for review, *Trends in microbiology*, **2009**, *17*, 73.

- (52) Flemming, H.-C.; Wingender, J. The biofilm matrix, *Nat Rev Micro*, **2010**, 8, 623.
- (53) Costerton, J.; Lewandowski, Z.; DeBeer, D.; Caldwell, D.; Korber, D.; James, G. Biofilms, the customized microniche, *Journal of bacteriology*, **1994**, 176, 2137.
- (54) Monroe, D. Looking for chinks in the armor of bacterial biofilms, *PLoS Biol.*, **2007**, 5, 2458.
- (55) Sutherland, I. W. Biofilm exopolysaccharides: a strong and sticky framework, *Microbiology*, **2001**, 147, 3.
- (56) Sutherland, I. W. The biofilm matrix—an immobilized but dynamic microbial environment, *Trends in microbiology*, **2001**, 9, 222.
- (57) Bura, R.; Cheung, M.; Liao, B.; Finlayson, J.; Lee, B.; Droppo, I.; Leppard, G.; Liss, S. Composition of extracellular polymeric substances in the activated sludge floc matrix, *Water Science and Technology*, **1998**, 37, 325.
- (58) Jiao, Y.; Cody, G. D.; Harding, A. K.; Wilmes, P.; Schrenk, M.; Wheeler, K. E.; Banfield, J. F.; Thelen, M. P. Characterization of extracellular polymeric substances from acidophilic microbial biofilms, *Applied and environmental microbiology*, **2010**, 76, 2916.
- (59) Davies, D. G.; Parsek, M. R.; Pearson, J. P.; Iglewski, B. H.; Costerton, J. W.; Greenberg, E. P. The involvement of cell-to-cell signals in the development of a bacterial biofilm, *Science (Washington, D. C.)*, **1998**, 280, 295.
- (60) Pearson, J. P.; Gray, K. M.; Passador, L.; Tucker, K. D.; Eberhard, A.; Iglewski, B. H.; Greenberg, E. P. Structure of the autoinducer required for expression of *Pseudomonas aeruginosa* virulence genes, *Proc. Natl. Acad. Sci. U. S. A.*, **1994**, 91, 197.

- (61) Pearson, J. P.; Passador, L.; Iglewski, B. H.; Greenberg, E. P. A second N-acylhomoserine lactone signal produced by *Pseudomonas aeruginosa*, *Proc. Natl. Acad. Sci. U. S. A.*, **1995**, *92*, 1490.
- (62) Waters, C. M.; Bassler, B. L. Quorum sensing: Cell-to-cell communication in bacteria, *Annu. Rev. Cell Dev. Biol.*, **2005**, *21*, 319.
- (63) Camilli, A.; Bassler, B. L. Bacterial Small-Molecule Signaling Pathways, *Science (Washington, DC, U. S.)*, **2006**, *311*, 1113.
- (64) Davies, D. G.; Parsek, M. R.; Pearson, J. P.; Iglewski, B. H.; Costerton, J. W.; Greenberg, E. P. The involvement of cell-to-cell signals in the development of a bacterial biofilm, *Science*, **1998**, *280*, 295.
- (65) Kierek-Pearson, K.; Karatan, E. Biofilm development in bacteria, *Adv. Appl. Microbiol.*, **2005**, *57*, 79.
- (66) Davey, M. E.; O'Toole, G. A. Microbial biofilms: From ecology to molecular genetics, *Microbiol. Mol. Biol. Rev.*, **2000**, *64*, 847.
- (67) Hogan, D.; Kolter, R. Why are bacteria refractory to antimicrobials? , *Curr. Opin. Microbiol.*, **2002**, *5*, 472.
- (68) Nikolaev, Y. A.; Plakunov, V. K. Biofilm-"City of microbes" or an analogue of multicellular organisms? , *Microbiology (N. Y., NY, U. S.)*, **2007**, *76*, 125.
- (69) Stewart, P. S. Diffusion in biofilms, *Journal of bacteriology*, **2003**, *185*, 1485.
- (70) Mikkelsen, H.; Duck, Z.; Lilley, K.; Welch, M. Interrelationships between colonies, biofilms, and planktonic cells of *Pseudomonas aeruginosa*, *Journal of bacteriology*, **2007**, *189*, 2411.

- (71) Costerton, J.; Stewart, P. S.; Greenberg, E. Bacterial biofilms: a common cause of persistent infections, *Science*, **1999**, *284*, 1318.
- (72) Kaplan, J. á. Biofilm dispersal: mechanisms, clinical implications, and potential therapeutic uses, *Journal of dental research*, **2010**, *89*, 205.
- (73) McDougald, D.; Rice, S. A.; Barraud, N.; Steinberg, P. D.; Kjelleberg, S. Should we stay or should we go: mechanisms and ecological consequences for biofilm dispersal, *Nature Reviews Microbiology*, **2011**, *10*, 39.
- (74) Webb, J. S. Differentiation and dispersal in biofilms, *The biofilm mode of life: mechanisms and adaptations*, **2007**, 165.
- (75) Richards, J. J.; Melander, C. Controlling bacterial biofilms, *ChemBioChem*, **2009**, *10*, 2287.
- (76) Davies, D. Understanding biofilm resistance to antibacterial agents, *Nat Rev Drug Discov*, **2003**, *2*, 114.
- (77) Richards, J. J.; Melander, C. Small molecule approaches toward the non-microbicidal modulation of bacterial biofilm growth and maintenance, *Anti-Infect. Agents Med. Chem.*, **2009**, *8*, 295.
- (78) Evans, R. C.; Holmes, C. J. Effect of vancomycin hydrochloride on *Staphylococcus epidermidis* biofilm associated with silicone elastomer, *Antimicrobial agents and chemotherapy*, **1987**, *31*, 889.
- (79) Mah, T.-F. C.; O'Toole, G. A. Mechanisms of biofilm resistance to antimicrobial agents, *Trends in microbiology*, **2001**, *9*, 34.

- (80) Richards, J. J.; Ballard, T. E.; Melander, C. Inhibition and dispersion of *Pseudomonas aeruginosa* biofilms with reverse amide 2-aminoimidazole oroidin analogues, *Org Biomol Chem*, **2008**, *6*, 1356.
- (81) Richards, J. J.; Melander, C. Controlling bacterial biofilms, *ChemBioChem*, **2009**, *10*, 2287.
- (82) Ren, D.; Sims, J. J.; Wood, T. K. Inhibition of biofilm formation and swarming of *Bacillus subtilis* by (5Z)-4-bromo-5-(bromomethylene)-3-butyl-2(5H)-furanone, *Lett. Appl. Microbiol.*, **2002**, *34*, 293.
- (83) Richards, J. J.; Huigens, R. W., III; Ballard, T. E.; Basso, A.; Cavanagh, J.; Melander, C. Inhibition and dispersion of proteobacterial biofilms, *Chem. Commun. (Cambridge, U. K.)*, **2008**, 1698.
- (84) Harper, D. R.; Parracho, H. M.; Walker, J.; Sharp, R.; Hughes, G.; Werthén, M.; Lehman, S.; Morales, S. Bacteriophages and Biofilms, *Antibiotics*, **2014**, *3*, 270.
- (85) Donlan, R. M. Preventing biofilms of clinically relevant organisms using bacteriophage, *Trends in microbiology*, **2009**, *17*, 66.
- (86) O'Flaherty, S.; Ross, R.; Meaney, W.; Fitzgerald, G.; Elbreki, M.; Coffey, A. Potential of the polyvalent anti-*Staphylococcus* bacteriophage K for control of antibiotic-resistant staphylococci from hospitals, *Applied and environmental microbiology*, **2005**, *71*, 1836.
- (87) Slopek, S.; Weber-Dabrowska, B.; Dabrowski, M. Results of bacteriophage treatment of suppurative bacterial infections in the years 1981–1986, *Arch Immunol Ther Exp*, **1987**, *35*, 569.
- (88) Cornelissen, A.; Ceysens, P.-J.; T'syen, J.; Van Praet, H.; Noben, J.-P.; Shaburova, O. V.; Krylov, V. N.; Volckaert, G.; Lavigne, R. The T7-related *Pseudomonas putida* phage ϕ 15 displays virion-associated biofilm degradation properties, *PLoS One*, **2011**, *6*, e18597.

- (89) Hanlon, G. W.; Denyer, S. P.; Olliff, C. J.; Ibrahim, L. J. Reduction in exopolysaccharide viscosity as an aid to bacteriophage penetration through *Pseudomonas aeruginosa* biofilms, *Applied and environmental microbiology*, **2001**, *67*, 2746.
- (90) Hughes, K. A.; Sutherland, I. W.; Jones, M. V. Biofilm susceptibility to bacteriophage attack: the role of phage-borne polysaccharide depolymerase, *Microbiology*, **1998**, *144*, 3039.
- (91) Bandyopadhyay, D.; Prashar, D.; Luk, Y.-Y. Anti-Fouling Chemistry of Chiral Monolayers: Enhancing Biofilm Resistance on Racemic Surface, *Langmuir*, **2011**, *27*, 6124.
- (92) Bandyopadhyay, D.; Prashar, D.; Luk, Y.-Y. Anti-fouling chemistry of chiral monolayers: enhancing biofilm resistance on racemic surface, *Langmuir*, **2011**, *27*, 6124.
- (93) Burton, E. A.; Simon, K. A.; Hou, S.; Ren, D.; Luk, Y.-Y. Molecular Gradients of Bioinertness Reveal a Mechanistic Difference between Mammalian Cell Adhesion and Bacterial Biofilm Formation, *Langmuir*, **2009**, *25*, 1547.
- (94) Hou, S.; Burton, E. A.; Wu, R. L.; Luk, Y.-Y.; Ren, D. Prolonged control of patterned biofilm formation by bio-inert surface chemistry, *Chem. Commun. (Cambridge, U. K.)*, **2009**, 1207.
- (95) Mansouri, J.; Harrisson, S.; Chen, V. Strategies for controlling biofouling in membrane filtration systems: challenges and opportunities, *Journal of Materials Chemistry*, **2010**, *20*, 4567.
- (96) Antoci Jr, V.; Adams, C. S.; Parvizi, J.; Davidson, H. M.; Composto, R. J.; Freeman, T. A.; Wickstrom, E.; Ducheyne, P.; Jungkind, D.; Shapiro, I. M. The inhibition of *Staphylococcus epidermidis* biofilm formation by vancomycin-modified titanium alloy and implications for the treatment of periprosthetic infection, *Biomaterials*, **2008**, *29*, 4684.
- (97) Chen, M.; Yu, Q.; Sun, H. Novel strategies for the prevention and treatment of biofilm related infections, *International journal of molecular sciences*, **2013**, *14*, 18488.

- (98) Bandyopadhyay, D.; Prashar, D.; Luk, Y.-Y. Anti-Fouling Chemistry of Chiral Monolayers: Enhancing Biofilm Resistance on Racemic Surface, *Langmuir*, **2011**, *27*, 6124.
- (99) Boks, N. P.; Kaper, H. J.; Norde, W.; van der Mei, H. C.; Busscher, H. J. Mobile and immobile adhesion of staphylococcal strains to hydrophilic and hydrophobic surfaces, *Journal of colloid and interface science*, **2009**, *331*, 60.
- (100) Tang, H.; Cao, T.; Liang, X.; Wang, A.; Salley, S. O.; McAllister, J.; Ng, K. Influence of silicone surface roughness and hydrophobicity on adhesion and colonization of *Staphylococcus epidermidis*, *Journal of Biomedical Materials Research Part A*, **2009**, *88*, 454.
- (101) Truong, V. K.; Lapovok, R.; Estrin, Y. S.; Rundell, S.; Wang, J. Y.; Fluke, C. J.; Crawford, R. J.; Ivanova, E. P. The influence of nano-scale surface roughness on bacterial adhesion to ultrafine-grained titanium, *Biomaterials*, **2010**, *31*, 3674.
- (102) Harris, L.; Tosatti, S.; Wieland, M.; Textor, M.; Richards, R. *Staphylococcus aureus* adhesion to titanium oxide surfaces coated with non-functionalized and peptide-functionalized poly (l-lysine)-grafted-poly (ethylene glycol) copolymers, *Biomaterials*, **2004**, *25*, 4135.
- (103) Kostakioti, M.; Hadjifrangiskou, M.; Hultgren, S. J. Bacterial biofilms: development, dispersal, and therapeutic strategies in the dawn of the postantibiotic era, *Cold Spring Harbor perspectives in medicine*, **2013**, *3*, a010306.
- (104) Schaeffer, A. J.; Amundsen, S. K.; Jones, J. M. Effect of carbohydrates on adherence of *Escherichia coli* to human urinary tract epithelial cells, *Infection and immunity*, **1980**, *30*, 531.
- (105) Bouckaert, J.; Berglund, J.; Schembri, M.; De Genst, E.; Cools, L.; Wuhrer, M.; Hung, C. S.; Pinkner, J.; Slättegård, R.; Zavialov, A. Receptor binding studies disclose a novel class of

high-affinity inhibitors of the Escherichia coli FimH adhesin, *Molecular microbiology*, **2005**, *55*, 441.

(106) Sperling, O.; Fuchs, A.; Lindhorst, T. K. Evaluation of the carbohydrate recognition domain of the bacterial adhesin FimH: design, synthesis and binding properties of mannoside ligands, *Organic & biomolecular chemistry*, **2006**, *4*, 3913.

(107) Kaplan, J. B.; Ragunath, C.; Velliyagounder, K.; Fine, D. H.; Ramasubbu, N. Enzymatic detachment of Staphylococcus epidermidis biofilms, *Antimicrobial agents and chemotherapy*, **2004**, *48*, 2633.

(108) Izano, E. A.; Amarante, M. A.; Kher, W. B.; Kaplan, J. B. Differential roles of poly-N-acetylglucosamine surface polysaccharide and extracellular DNA in Staphylococcus aureus and Staphylococcus epidermidis biofilms, *Applied and environmental microbiology*, **2008**, *74*, 470.

(109) Chaignon, P.; Sadovskaya, I.; Ragunah, C.; Ramasubbu, N.; Kaplan, J.; Jabbouri, S. Susceptibility of staphylococcal biofilms to enzymatic treatments depends on their chemical composition, *Applied microbiology and biotechnology*, **2007**, *75*, 125.

(110) Kolodkin-Gal, I.; Romero, D.; Cao, S.; Clardy, J.; Kolter, R.; Losick, R. D-amino acids trigger biofilm disassembly, *Science*, **2010**, *328*, 627.

(111) Kolodkin-Gal, I.; Cao, S.; Chai, L.; Böttcher, T.; Kolter, R.; Clardy, J.; Losick, R. A self-produced trigger for biofilm disassembly that targets exopolysaccharide, *Cell*, **2012**, *149*, 684.

(112) Barraud, N.; J Kelso, M.; A Rice, S.; Kjelleberg, S. Nitric oxide: a key mediator of biofilm dispersal with applications in infectious diseases, *Current pharmaceutical design*, **2015**, *21*, 31.

(113) Römling, U.; Kjelleberg, S.; Normark, S.; Nyman, L.; Uhlin, B.; Åkerlund, B. Microbial biofilm formation: a need to act, *Journal of internal medicine*, **2014**.

- (114) Kishikawa, H.; Ebberyd, A.; Römling, U.; Brauner, A.; Lüthje, P.; Lundberg, J. O.; Weitzberg, E. Control of pathogen growth and biofilm formation using a urinary catheter that releases antimicrobial nitrogen oxides, *Free Radical Biology and Medicine*, **2013**, *65*, 1257.
- (115) Frei, R.; Breitbach, A. S.; Blackwell, H. E. 2-Aminobenzimidazole Derivatives Strongly Inhibit and Disperse *Pseudomonas aeruginosa* Biofilms, *Angew. Chem., Int. Ed.*, **2012**, *51*, 5226.
- (116) Geske Grant, D.; Mattmann Margrith, E.; Blackwell Helen, E. Evaluation of a focused library of N-aryl L-homoserine lactones reveals a new set of potent quorum sensing modulators, *Bioorg Med Chem Lett*, **2008**, *18*, 5978.
- (117) Harshey, R. M. Bacterial motility on a surface: many ways to a common goal, *Annual Reviews in Microbiology*, **2003**, *57*, 249.
- (118) Schauder, S.; Bassler, B. L. The Languages of Bacteria, *Genes Dev.*, **2001**, *15*, 1468.
- (119) Caiazza, N. C.; Shanks, R. M. Q.; O'Toole, G. A. Rhamnolipids modulate swarming motility patterns of *Pseudomonas aeruginosa*, *J. Bacteriol.*, **2005**, *187*, 7351.
- (120) Eberhard, A.; Burlingame, A.; Eberhard, C.; Kenyon, G.; Nealson, K.; Oppenheimer, N. Structural identification of autoinducer of *Photobacterium fischeri* luciferase, *Biochemistry*, **1981**, *20*, 2444.
- (121) Tremblay, J.; Richardson, A.-P.; Lepine, F.; Deziel, E. Self-produced extracellular stimuli modulate the *Pseudomonas aeruginosa* swarming motility behavior, *Environ. Microbiol.*, **2007**, *9*, 2622.
- (122) Kearns, D. B. A field guide to bacterial swarming motility, *Nat. Rev. Microbiol.*, **2010**, *8*, 634.

- (123) Kohler, T.; Curty, L. K.; Barja, F.; Van, D. C.; Pechere, J.-C. Swarming of *Pseudomonas aeruginosa* is dependent on cell-to-cell signaling and requires flagella and pili, *J. Bacteriol.*, **2000**, *182*, 5990.
- (124) Tremblay, J.; Deziel, E. Gene expression in *Pseudomonas aeruginosa* swarming motility, *BMC Genomics*, **2010**, *11*, 587.
- (125) Chevance, F. F.; Hughes, K. T. Coordinating assembly of a bacterial macromolecular machine, *Nature Reviews Microbiology*, **2008**, *6*, 455.
- (126) Henrichsen, J. Bacterial surface translocation: a survey and a classification, *Bacteriological reviews*, **1972**, *36*, 478.
- (127) Mattick, J. S. Type IV pili and twitching motility, *Annual Reviews in Microbiology*, **2002**, *56*, 289.
- (128) Mignot, T. The elusive engine in *Myxococcus xanthus* gliding motility, *Cellular and Molecular Life Sciences*, **2007**, *64*, 2733.
- (129) Matsuyama, T.; Kaneda, K.; Nakagawa, Y.; Isa, K.; Hara-Hotta, H.; Yano, I. A novel extracellular cyclic lipopeptide which promotes flagellum-dependent and-independent spreading growth of *Serratia marcescens*, *Journal of bacteriology*, **1992**, *174*, 1769.
- (130) Kinsinger, R. F.; Kearns, D. B.; Hale, M.; Fall, R. Genetic requirements for potassium ion-dependent colony spreading in *Bacillus subtilis*, *Journal of bacteriology*, **2005**, *187*, 8462.
- (131) Murray, T. S.; Kazmierczak, B. I. *Pseudomonas aeruginosa* exhibits sliding motility in the absence of type IV pili and flagella, *Journal of bacteriology*, **2008**, *190*, 2700.
- (132) Lowe, G.; Meister, M.; Berg, H. C. Rapid rotation of flagellar bundles in swimming bacteria, **1987**.
- (133) Berg, H. C.; Anderson, R. A. Bacteria swim by rotating their flagellar filaments, **1973**.

- (134) Fraser, G. M.; Hughes, C. Swarming motility, *Current opinion in microbiology*, **1999**, 2, 630.
- (135) Tremblay, J.; Déziel, E. Improving the reproducibility of *Pseudomonas aeruginosa* swarming motility assays, *Journal of basic microbiology*, **2008**, 48, 509.
- (136) Rashid, M. H.; Kornberg, A. Inorganic polyphosphate is needed for swimming, swarming, and twitching motilities of *Pseudomonas aeruginosa*, *Proceedings of the National Academy of Sciences*, **2000**, 97, 4885.
- (137) Kearns, D. B.; Losick, R. Swarming motility in undomesticated *Bacillus subtilis*, *Molecular microbiology*, **2003**, 49, 581.
- (138) Harshey, R. M.; Matsuyama, T. Dimorphic transition in *Escherichia coli* and *Salmonella typhimurium*: surface-induced differentiation into hyperflagellate swarmer cells, *Proceedings of the National Academy of Sciences*, **1994**, 91, 8631.
- (139) Shinoda, S.; Okamoto, K. Formation and function of *Vibrio parahaemolyticus* lateral flagella, *Journal of bacteriology*, **1977**, 129, 1266.
- (140) Alberti, L.; Harshey, R. M. Differentiation of *Serratia marcescens* 274 into swimmer and swarmer cells, *Journal of bacteriology*, **1990**, 172, 4322.
- (141) Merino, S.; Shaw, J. G.; Tomás, J. M. Bacterial lateral flagella: an inducible flagella system, *FEMS microbiology letters*, **2006**, 263, 127.
- (142) Schneider, W. R.; Doetsch, R. Effect of viscosity on bacterial motility, *Journal of bacteriology*, **1974**, 117, 696.
- (143) Berg, H. C.; Turner, L. Movement of microorganisms in viscous environments, **1979**.

- (144) Kirov, S. M.; Tassell, B. C.; Semmler, A. B.; O'Donovan, L. A.; Rabaan, A. A.; Shaw, J. G. Lateral flagella and swarming motility in *Aeromonas* species, *Journal of bacteriology*, **2002**, *184*, 547.
- (145) Eberl, L.; Molin, S.; Givskov, M. Surface motility of *Serratia liquefaciens* MG1, *Journal of bacteriology*, **1999**, *181*, 1703.
- (146) Matsuyama, T.; Bhasin, A.; Harshey, R. M. Mutational analysis of flagellum-independent surface spreading of *Serratia marcescens* 274 on a low-agar medium, *Journal of bacteriology*, **1995**, *177*, 987.
- (147) Miller, M. B.; Bassler, B. L. Quorum sensing in bacteria, *Annu. Rev. Microbiol.*, **2001**, *55*, 165.
- (148) Nakano, M. M.; Xia, L.; Zuber, P. Transcription initiation region of the *srfA* operon, which is controlled by the *comP-comA* signal transduction system in *Bacillus subtilis*, *Journal of bacteriology*, **1991**, *173*, 5487.
- (149) Young, G. M.; Smith, M. J.; Minnich, S. A.; Miller, V. L. The *Yersinia enterocolitica* motility master regulatory operon, *flhDC*, is required for flagellin production, swimming motility, and swarming motility, *Journal of bacteriology*, **1999**, *181*, 2823.
- (150) Copeland, M. F.; Flickinger, S. T.; Tuson, H. H.; Weibel, D. B. Studying the dynamics of flagella in multicellular communities of *Escherichia coli* by using biarsenical dyes, *Applied and environmental microbiology*, **2010**, *76*, 1241.
- (151) Jones, B. V.; Young, R.; Mahenthiralingam, E.; Stickler, D. J. Ultrastructure of *Proteus mirabilis* swarmer cell rafts and role of swarming in catheter-associated urinary tract infection, *Infection and immunity*, **2004**, *72*, 3941.

- (152) Rauprich, O.; Matsushita, M.; Weijer, C. J.; Siegert, F.; Esipov, S. E.; Shapiro, J. A. Periodic phenomena in *Proteus mirabilis* swarm colony development, *Journal of bacteriology*, **1996**, *178*, 6525.
- (153) McCarter, L. The multiple identities of *Vibrio parahaemolyticus*, **1999**.
- (154) Ragatz, L.; Jiang, Z.-Y.; Bauer, C. E.; Gest, H. Macroscopic phototactic behavior of the purple photosynthetic bacterium *Rhodospirillum rubrum*, *Archives of microbiology*, **1995**, *163*, 1.
- (155) Waters, C. M.; Bassler, B. L. Quorum sensing: Cell-to-cell communication in bacteria, *Annu. Rev. Cell Dev. Biol.*, **2005**, *21*, 319.
- (156) Schaefer, A. L.; Val, D. L.; Hanzelka, B. L.; Cronan, J. E., Jr.; Greenberg, E. P. Generation of cell-to-cell signals in quorum sensing: acyl homoserine lactone synthase activity of a purified *Vibrio fischeri* LuxI protein, *Proc. Natl. Acad. Sci. U. S. A.*, **1996**, *93*, 9505.
- (157) Whitehead, N. A.; Barnard, A. M. L.; Slater, H.; Simpson, N. J. L.; Salmond, G. P. C. Quorum-sensing in Gram-negative bacteria, *FEMS Microbiol. Rev.*, **2001**, *25*, 365.
- (158) Rutherford, S. T.; Bassler, B. L. Bacterial quorum sensing: its role in virulence and possibilities for its control, *Cold Spring Harbor perspectives in medicine*, **2012**, *2*, a012427.
- (159) Jayaraman, A.; Wood, T. K. Bacterial quorum sensing: signals, circuits, and implications for biofilms and disease, *Annu. Rev. Biomed. Eng.*, **2008**, *10*, 145.
- (160) Pearson, J. P.; Gray, K. M.; Passador, L.; Tucker, K. D.; Eberhard, A.; Iglewski, B. H.; Greenberg, E. P. Structure of the autoinducer required for expression of *Pseudomonas aeruginosa* virulence genes, *Proc. Natl. Acad. Sci. U. S. A.*, **1994**, *91*, 197.

- (161) Solomon, J. M.; Lazazzera, B. A.; Grossman, A. D. Purification and characterization of an extracellular peptide factor that affects two different developmental pathways in *Bacillus subtilis*, *Genes & development*, **1996**, *10*, 2014.
- (162) Håvarstein, L.; Coomaraswamy, G.; Morrison, D. A. An unmodified heptadecapeptide pheromone induces competence for genetic transformation in *Streptococcus pneumoniae*, *Proceedings of the National Academy of Sciences*, **1995**, *92*, 11140.
- (163) Ji, G.; Beavis, R. C.; Novick, R. P. Cell density control of staphylococcal virulence mediated by an octapeptide pheromone, *Proceedings of the National Academy of Sciences*, **1995**, *92*, 12055.
- (164) Chater, K. F.; Horinouchi, S. Signalling early developmental events in two highly diverged *Streptomyces* species, *Molecular microbiology*, **2003**, *48*, 9.
- (165) Parsek, M. R.; Greenberg, E. P. Quorum sensing signals in development of *Pseudomonas aeruginosa* biofilms, *Methods Enzymol.*, **1999**, *310*, 43.
- (166) Williams, P. Quorum sensing, communication and cross-kingdom signalling in the bacterial world, *Microbiology (Reading, U. K.)*, **2007**, *153*, 3923.
- (167) Fuqua, C.; Winans, S. C.; Greenberg, E. P. Census and consensus in bacterial ecosystems: the LuxR-LuxI family of quorum-sensing transcriptional regulators, *Annual Reviews in Microbiology*, **1996**, *50*, 727.
- (168) More, M. I.; Finger, L. D.; Stryker, J. L.; Fuqua, C.; Eberhard, A.; Winans, S. C. Enzymic synthesis of a quorum-sensing autoinducer through use of defined substrates, *Science (Washington, D. C.)*, **1996**, *272*, 1655.
- (169) Kaplan, H. B.; Greenberg, E. Diffusion of autoinducer is involved in regulation of the *Vibrio fischeri* luminescence system, *Journal of bacteriology*, **1985**, *163*, 1210.

- (170) Stevens, A. M.; Dolan, K. M.; Greenberg, E. Synergistic binding of the *Vibrio fischeri* LuxR transcriptional activator domain and RNA polymerase to the lux promoter region, *Proceedings of the National Academy of Sciences*, **1994**, *91*, 12619.
- (171) Pesci, E.; Pearson, J. P.; Seed, P. C.; Iglewski, B. H. Regulation of las and rhl quorum sensing in *Pseudomonas aeruginosa*, *J. Bacteriol.*, **1997**, *179*, 3127.
- (172) De, K. T. R.; Gillis, R.; Marx, S.; Brown, C.; Iglewski, B. H. Quorum-sensing genes in *Pseudomonas aeruginosa* biofilms: their role and expression patterns, *Appl. Environ. Microbiol.*, **2001**, *67*, 1865.
- (173) Hentzer, M.; Eberl, L.; Nielsen, J.; Givskov, M. Quorum sensing: a novel target for the treatment of biofilm infections, *BioDrugs*, **2003**, *17*, 241.
- (174) Ochsner, U. A.; Fiechter, A.; Reiser, J. Isolation, characterization, and expression in *Escherichia coli* of the *Pseudomonas aeruginosa* rhlAB genes encoding a rhamnolipid biosurfactant synthesis, *J. Biol. Chem.*, **1994**, *269*, 19787.
- (175) Bodey, G. P.; Bolivar, R.; Fainstein, V.; Jadeja, L. Infections caused by *Pseudomonas aeruginosa*, *Rev Infect Dis*, **1983**, *5*, 279.
- (176) Imundo, L.; Barasch, J.; Prince, A.; Al-Awqati, Q. Cystic fibrosis epithelial cells have a receptor for pathogenic bacteria on their apical surface, *Proc. Natl. Acad. Sci. U. S. A.*, **1995**, *92*, 3019.
- (177) Shawar, R. M.; MacLeod, D. L.; Garber, R. L.; Burns, J. L.; Stapp, J. R.; Clausen, C. R.; Tanaka, S. K. Activities of tobramycin and six other antibiotics against *Pseudomonas aeruginosa* isolates from patients with cystic fibrosis, *Antimicrob. Agents Chemother.*, **1999**, *43*, 2877.
- (178) Davies, J. C. *Pseudomonas aeruginosa* in cystic fibrosis: pathogenesis and persistence, *Paediatr Respir Rev*, **2002**, *3*, 128.

- (179) Wagner, V. E.; Iglewski, B. H. P. aeruginosa biofilms in CF infection, *Clin. Rev. Allergy Immunol.*, **2008**, 35, 124.
- (180) Overhage, J.; Bains, M.; Brazas, M. D.; Hancock, R. E. Swarming of *Pseudomonas aeruginosa* is a complex adaptation leading to increased production of virulence factors and antibiotic resistance, *Journal of bacteriology*, **2008**, 190, 2671.
- (181) Déziel, E.; Lépine, F.; Milot, S.; Villemur, R. rhlA is required for the production of a novel biosurfactant promoting swarming motility in *Pseudomonas aeruginosa*: 3-(3-hydroxyalkanoyloxy) alkanolic acids (HAAs), the precursors of rhamnolipids, *Microbiology*, **2003**, 149, 2005.
- (182) Burrows, L. L. *Pseudomonas aeruginosa* twitching motility: type IV pili in action, *Annual review of microbiology*, **2012**, 66, 493.
- (183) Giltner, C. L.; van, S. E. J.; Audette, G. F.; Kao, D.; Hodges, R. S.; Hassett, D. J.; Irvin, R. T. The *Pseudomonas aeruginosa* type IV pilin receptor binding domain functions as an adhesin for both biotic and abiotic surfaces, *Mol. Microbiol.*, **2006**, 59, 1083.
- (184) Overhage, J.; Lewenza, S.; Marr, A. K.; Hancock, R. E. W. Identification of genes involved in swarming motility using a *Pseudomonas aeruginosa* PAO1 mini-Tn5-lux mutant library, *J. Bacteriol.*, **2007**, 189, 2164.
- (185) Brint, J. M.; Ohman, D. E. Synthesis of multiple exoproducts in *Pseudomonas aeruginosa* is under the control of RhlR-RhlI, another set of regulators in strain PAO1 with homology to the autoinducer-responsive LuxR-LuxI family, *Journal of bacteriology*, **1995**, 177, 7155.
- (186) Pearson, J. P.; Passador, L.; Iglewski, B. H.; Greenberg, E. P. A second N-acylhomoserine lactone signal produced by *Pseudomonas aeruginosa*, *Proc. Natl. Acad. Sci. U. S. A.*, **1995**, 92, 1490.

- (187) Pearson, J. P.; Pesci, E. C.; Iglewski, B. H. Roles of *Pseudomonas aeruginosa* las and rhl quorum-sensing systems in control of elastase and rhamnolipid biosynthesis genes, *J. Bacteriol.*, **1997**, *179*, 5756.
- (188) Bjarnsholt, T.; Jensen, P. O.; Jakobsen, T. H.; Phipps, R.; Nielsen, A. K.; Rybtke, M. T.; Tolker-Nielsen, T.; Givskov, M.; Hoeiby, N.; Ciofu, O. Quorum sensing and virulence of *Pseudomonas aeruginosa* during lung infection of cystic fibrosis patients, *PLoS One*, **2010**, *5*, No pp. given.
- (189) Ochsner, U. A.; Reiser, J. Autoinducer-mediated regulation of rhamnolipid biosurfactant synthesis in *Pseudomonas aeruginosa*, *Proc Natl Acad Sci U S A*, **1995**, *92*, 6424.
- (190) Jarvis, F. G.; Johnson, M. J. A glycolipide produced by *Pseudomonas aeruginosa*, *J. Am. Chem. Soc.*, **1949**, *71*, 4124.
- (191) Davey, M. E.; Caiazza, N. C.; O'Toole, G. A. Rhamnolipid surfactant production affects biofilm architecture in *Pseudomonas aeruginosa* PAO1, *J. Bacteriol.*, **2003**, *185*, 1027.
- (192) Rahim, R.; Ochsner, U. A.; Olvera, C.; Graninger, M.; Messner, P.; Lam, J. S.; Soberon-Chavez, G. Cloning and functional characterization of the *Pseudomonas aeruginosa* rhlC gene that encodes rhamnosyltransferase 2, an enzyme responsible for di-rhamnolipid biosynthesis, *Mol. Microbiol.*, **2001**, *40*, 708.
- (193) Miyashiro, T.; Ruby, E. G. Shedding light on bioluminescence regulation in *Vibrio fischeri*, *Molecular microbiology*, **2012**, *84*, 795.
- (194) Shetye, G. S.; Singh, N.; Jia, C.; Nguyen, C. D. K.; Wang, G.; Luk, Y.-Y. Specific Maltose Derivatives Modulate the Swarming Motility of Nonswarming Mutant and Inhibit Bacterial Adhesion and Biofilm Formation by *Pseudomonas aeruginosa*, *ChemBioChem*, **2014**, *15*, 1514.

- (195) Imberty, A.; Wimmerova, M.; Mitchell, E. P.; Gilboa-Garber, N. Structures of the lectins from *Pseudomonas aeruginosa*: insights into the molecular basis for host glycan recognition, *Microbes Infect.*, **2004**, *6*, 221.
- (196) Pieters, R. J. Intervention with bacterial adhesion by multivalent carbohydrates, *Med. Res. Rev.*, **2007**, *27*, 796.
- (197) Chevlot, Y.; Zhang, J.; Meyer, A.; Goudot, A.; Rouanet, S.; Vidal, S.; Pourceau, G.; Cloarec, J.-P.; Praly, J.-P.; Souteyrand, E. Multiplexed binding determination of seven glycoconjugates for *Pseudomonas aeruginosa* Lectin I (PA-IL) using a DNA-based carbohydrate microarray, *Chemical Communications*, **2011**, *47*, 8826.
- (198) Funken, H.; Bartels, K.-M.; Wilhelm, S.; Brocker, M.; Bott, M.; Bains, M.; Hancock, R. E.; Rosenau, F.; Jaeger, K.-E. Specific association of lectin LecB with the surface of *Pseudomonas aeruginosa*: role of outer membrane protein OprF, *PLoS one*, **2012**, *7*, e46857.
- (199) Sheth, H. B.; Lee, K. K.; Wong, W. Y.; Srivastava, G.; Hindsgaul, O.; Hodges, R. S.; Paranchych, W.; Irvin, R. T. The pili of *Pseudomonas aeruginosa* strains PAK and PAO bind specifically to the carbohydrate sequence β GalNAc(1–4) β Gal found in glycosphingolipids asialo-GM1 and asialo-GM2, *Molecular Microbiology*, **1994**, *11*, 715.
- (200) Koto, S.; Hirooka, M.; Tashiro, T.; Sakashita, M.; Hatachi, M.; Kono, T.; Shimizu, M.; Yoshida, N.; Kurasawa, S.; Sakuma, N.; Sawazaki, S.; Takeuchi, A.; Shoya, N.; Nakamura, E. Simple preparations of alkyl and cycloalkyl α -glycosides of maltose, cellobiose, and lactose, *Carbohydr. Res.*, **2004**, *339*, 2415.
- (201) Prashar, D.; Cui, D.-W.; Bandyopadhyay, D.; Luk, Y.-Y. Modification of Proteins with Cyclodextrins Prevents Aggregation and Surface Adsorption and Increases Thermal Stability, *Langmuir*, **2011**, *27*, 13091.

- (202) Jacobs, M. A.; Alwood, A.; Thaipisuttikul, I.; Spencer, D.; Haugen, E.; Ernst, S.; Will, O.; Kaul, R.; Raymond, C.; Levy, R. Comprehensive transposon mutant library of *Pseudomonas aeruginosa*, *Proceedings of the National Academy of Sciences*, **2003**, *100*, 14339.
- (203) Deziel, E.; Lepine, F.; Milot, S.; Villemur, R. rhlA is required for the production of a novel biosurfactant promoting swarming motility in *Pseudomonas aeruginosa*: 3-(3-hydroxyalkanoyloxy)alkanoic acids (HAAs), the precursors of rhamnolipids, *Microbiology* **2003**, *149*, 2005.
- (204) Caiazza, N. C.; Shanks, R. M. Q.; O'Toole, G. A. Rhamnolipids modulate swarming motility patterns of *Pseudomonas aeruginosa*, *J. Bacteriol.*, **2005**, *187*, 7351.
- (205) Kearns, D. B. A field guide to bacterial swarming motility, *Nat. Rev. Microbiol.*, **2010**, *8*, 634.
- (206) Lenz, P.; Søgaard-Andersen, L. Temporal and spatial oscillations in bacteria, *Nature Reviews Microbiology*, **2011**, *9*, 565.
- (207) Bubb, W. A. NMR spectroscopy in the study of carbohydrates: Characterizing the structural complexity, *Concepts in Magnetic Resonance Part A*, **2003**, *19*, 1.
- (208) Koto, S.; Hirooka, M.; Tashiro, T.; Sakashita, M.; Hatachi, M.; Kono, T.; Shimizu, M.; Yoshida, N.; Kurasawa, S.; Sakuma, N.; Sawazaki, S.; Takeuchi, A.; Shoya, N.; Nakamura, E. Simple preparations of alkyl and cycloalkyl α -glycosides of maltose, cellobiose, and lactose, *Carbohydr. Res.*, **2004**, *339*, 2415.
- (209) Kasuya, M. C. Z.; Ikeda, M.; Hashimoto, K.; Sato, T.; Hatanaka, K. Effect of anomeric linkage on the sialylation of glycosides by cells, *Journal of carbohydrate chemistry*, **2005**, *24*, 705.

- (210) Zhang, Z.; Wang, P.; Ding, N.; Song, G.; Li, Y. Total synthesis of cleistetroside-2, partially acetylated dodecanyl tetra-rhamnoside derivative isolated from *Cleistopholis patens* and *Cleistopholis glauca*, *Carbohydr. Res.*, **2007**, *342*, 1159.
- (211) Bennett, C. J.; Caldwell, S. T.; McPhail, D. B.; Morrice, P. C.; Duthie, G. G.; Hartley, R. C. Potential therapeutic antioxidants that combine the radical scavenging ability of myricetin and the lipophilic chain of vitamin E to effectively inhibit microsomal lipid peroxidation, *Bioorg. Med. Chem.*, **2004**, *12*, 2079.
- (212) Prashar, D.; Cui, D.-W.; Bandyopadhyay, D.; Luk, Y.-Y. Modification of Proteins with Cyclodextrins Prevents Aggregation and Surface Adsorption and Increases Thermal Stability, *Langmuir*, **2011**, *27*, 13091.
- (213) Huigens, R. W.; Richards, J. J.; Parise, G.; Ballard, T. E.; Zeng, W.; Deora, R.; Melander, C. Inhibition of *Pseudomonas aeruginosa* biofilm formation with bromoageliferin analogues, *Journal of the American Chemical Society*, **2007**, *129*, 6966.
- (214) Shetye, G. S.; Singh, N.; Gao, X.; Bandyopadhyay, D.; Yan, A.; Luk, Y.-Y. Structures and biofilm inhibition activities of brominated furanones for *Escherichia coli* and *Pseudomonas aeruginosa*, *MedChemComm*, **2013**.
- (215) Lawrence, J.; Korber, D.; Hoyle, B.; Costerton, J.; Caldwell, D. Optical sectioning of microbial biofilms, *Journal of bacteriology*, **1991**, *173*, 6558.
- (216) Schooling, S. R.; Charaf, U. K.; Allison, D. G.; Gilbert, P. A role for rhamnolipid in biofilm dispersion, *Biofilms*, **2004**, *1*, 91.
- (217) Tielker, D.; Hacker, S.; Loris, R.; Strathmann, M.; Wingender, J.; Wilhelm, S.; Rosenau, F.; Jaeger, K.-E. *Pseudomonas aeruginosa* lectin LecB is located in the outer membrane and is involved in biofilm formation, *Microbiology*, **2005**, *151*, 1313.

- (218) Sharon, N. Carbohydrates as future anti-adhesion drugs for infectious diseases, *Biochimica et Biophysica Acta (BBA)-General Subjects*, **2006**, 1760, 527.
- (219) Pieters, R. J. Intervention with bacterial adhesion by multivalent carbohydrates, *Medicinal Research Reviews*, **2007**, 27, 796.
- (220) Moch, T.; Hoschützky, H.; Hacker, J.; Kröncke, K.; Jann, K. Isolation and characterization of the alpha-sialyl-beta-2, 3-galactosyl-specific adhesin from fimbriated *Escherichia coli*, *Proceedings of the National Academy of Sciences*, **1987**, 84, 3462.
- (221) Khan, A.; Mühldorfer, I.; Demuth, V.; Wallner, U.; Korhonen, T.; Hacker, J. Functional analysis of the minor subunits of S fimbrial adhesin (SfaI) in pathogenic *Escherichia coli*, *Molecular and General Genetics MGG*, **2000**, 263, 96.
- (222) Khan, A. S.; Kniep, B.; Oelschlaeger, T. A.; Van Die, I.; Korhonen, T.; Hacker, J. Receptor structure for F1C fimbriae of uropathogenic *Escherichia coli*, *Infection and immunity*, **2000**, 68, 3541.
- (223) Arends, J.; Zanen, H. Meningitis caused by *Streptococcus suis* in humans, *Review of Infectious Diseases*, **1988**, 10, 131.
- (224) Mysore, J. V.; Wigginton, T.; Simon, P. M.; Zopf, D.; Heman-Ackah, L. M.; Dubois, A. Treatment of *Helicobacter pylori* infection in rhesus monkeys using a novel antiadhesion compound, *Gastroenterology*, **1999**, 117, 1316.
- (225) Irvin, R. T. In *Pseudomonas*; Wiley-VCH Verlag GmbH & Co. KGaA: 2008, p 45.
- (226) Sheth, H.; Lee, K.; Wong, W.; Srivastava, G.; Hindsgaul, O.; Hodges, R.; Paranchych, W.; Irvin, R. The pili of *Pseudomonas aeruginosa* strains PAK and PAO bind specifically to the carbohydrate sequence β GalNAc (1–4) β Gal found in glycosphingolipids asialo-GM1 and asialo-GM2, *Molecular microbiology*, **1994**, 11, 715.

- (227) Chen, C.-P.; Song, S.-C.; Gilboa-Garber, N.; Chang, K. S.; Wu, A. M. Studies on the binding site of the galactose-specific agglutinin PA-IL from *Pseudomonas aeruginosa*, *Glycobiology*, **1998**, *8*, 7.
- (228) Johansson, E.; Crusz, S. A.; Kolomiets, E.; Buts, L.; Kadam, R. U.; Cacciarini, M.; Bartels, K.-M.; Diggle, S. P.; Cámara, M.; Williams, P. Inhibition and Dispersion of *Pseudomonas aeruginosa* Biofilms by Glycopeptide Dendrimers Targeting the Fucose-Specific Lectin LecB, *Chemistry & biology*, **2008**, *15*, 1249.
- (229) Irvin, R.; Doig, P.; Lee, K.; Sastry, P.; Paranchych, W.; Todd, T.; Hodges, R. Characterization of the *Pseudomonas aeruginosa* pilus adhesin: confirmation that the pilin structural protein subunit contains a human epithelial cell-binding domain, *Infection and immunity*, **1989**, *57*, 3720.
- (230) Giltner, C. L.; Van Schaik, E. J.; Audette, G. F.; Kao, D.; Hodges, R. S.; Hassett, D. J.; Irvin, R. T. The *Pseudomonas aeruginosa* type IV pilin receptor binding domain functions as an adhesin for both biotic and abiotic surfaces, *Molecular microbiology*, **2006**, *59*, 1083.
- (231) Schweizer, F.; Jiao, H.; Hindsgaul, O.; Wong, W. Y.; Irvin, R. T. Interaction between the pili of *Pseudomonas aeruginosa* PAK and its carbohydrate receptor β -D-GalNAc (1- \rightarrow 4) β -D-Gal analogs, *Canadian journal of microbiology*, **1998**, *44*, 307.
- (232) Reading, N. C.; Sperandio, V. Quorum sensing: the many languages of bacteria, *FEMS Microbiol. Lett.*, **2006**, *254*, 1.
- (233) Davies, D. G.; Parsek, M. R.; Pearson, J. P.; Iglewski, B. H.; Costerton, J. W.; Greenberg, E. P. The involvement of cell-to-cell signals in the development of a bacterial biofilm, *Science*, **1998**, *280*, 295.

- (234) Pearson, J. P.; Gray, K. M.; Passador, L.; Tucker, K. D.; Eberhard, A.; Iglewski, B. H.; Greenberg, E. P. Structure of the autoinducer required for expression of *Pseudomonas aeruginosa* virulence genes, *Proc. Natl. Acad. Sci. U. S. A.*, **1994**, *91*, 197.
- (235) Dubern, J.-F.; Diggle, S. P. Quorum sensing by 2-alkyl-4-quinolones in *Pseudomonas aeruginosa* and other bacterial species, *Mol. BioSyst.*, **2008**, *4*, 882.
- (236) Riedel, K.; Hentzer, M.; Geisenberger, O.; Huber, B.; Steidle, A.; Wu, H.; Hoiby, N.; Givskov, M.; Molin, S.; Eberl, L. N-acylhomoserine-lactone-mediated communication between *Pseudomonas aeruginosa* and *Burkholderia cepacia* in mixed biofilms, *Microbiology (Reading, U. K.)*, **2001**, *147*, 3249.
- (237) Han, Y.; Hou, S.; Simon, K. A.; Ren, D.; Luk, Y.-Y. Identifying the important structural elements of brominated furanones for inhibiting biofilm formation by *Escherichia coli*, *Bioorg. Med. Chem. Lett.*, **2008**, *18*, 1006.
- (238) Musk, D. J.; Banko, D. A.; Hergenrother, P. J. Iron Salts Perturb Biofilm Formation and Disrupt Existing Biofilms of *Pseudomonas aeruginosa*, *Chem. Biol.*, **2005**, *12*, 789.
- (239) Junker, L. M.; Clardy, J. High-throughput screens for small-molecule inhibitors of *Pseudomonas aeruginosa* biofilm development, *Antimicrobial Agents and Chemotherapy*, **2007**, *51*, 3582.
- (240) Davey, M. E.; Caiazza, N. C.; O'Toole, G. A. Rhamnolipid surfactant production affects biofilm architecture in *Pseudomonas aeruginosa* PAO1, *J. Bacteriol.*, **2003**, *185*, 1027.
- (241) Geske, G. D.; Wezeman, R. J.; Siegel, A. P.; Blackwell, H. E. Small molecule inhibitors of bacterial quorum sensing and biofilm formation, *J Am Chem Soc*, **2005**, *127*, 12762.
- (242) Smith, K. M.; Bu, Y.; Suga, H. Library Screening for Synthetic Agonists and Antagonists of a *Pseudomonas aeruginosa* Autoinducer, *Chem. Biol.*, **2003**, *10*, 563.

- (243) Doig, P.; Todd, T.; Sastry, P. A.; Lee, K.; Hodges, R. S.; Paranchych, W.; Irvin, R. Role of pili in adhesion of *Pseudomonas aeruginosa* to human respiratory epithelial cells, *Infection and immunity*, **1988**, *56*, 1641.
- (244) Campbell, A. P.; Wong, W. Y.; Irvin, R. T.; Sykes, B. D. Interaction of a bacterially expressed peptide from the receptor binding domain of *Pseudomonas aeruginosa* pili strain PAK with a cross-reactive antibody: conformation of the bound peptide, *Biochemistry*, **2000**, *39*, 14847.
- (245) Schweizer, F.; Jiao, H.; Hindsgaul, O.; Wong, W. Y.; Irvin, R. T. Interaction between the pili of *Pseudomonas aeruginosa* PAK and its carbohydrate receptor β -D-GalNAc(1->4) β -D-Gal analogs, *Can. J. Microbiol.*, **1998**, *44*, 307.
- (246) Wong, W. Y.; Irvin, R. T.; Paranchych, W.; Hodges, R. S. Antigen-antibody interactions: Elucidation of the epitope and strain-specificity of a monoclonal antibody directed against the pilin protein adherence binding domain of *Pseudomonas aeruginosa* strain K, *Protein Science*, **1992**, *1*, 1308.
- (247) Shetye, G. S.; Singh, N.; Luk, Y.-Y. Specific Maltose Derivatives Modulate the Swarming Motility of Nonswarming Mutant and Inhibit Bacterial Adhesion and Biofilm Formation by *Pseudomonas aeruginosa*, *ChemBioChem* (Under Revision).
- (248) Pierce, C. G.; Srinivasan, A.; Uppuluri, P.; Ramasubramanian, A. K.; López-Ribot, J. L. In *Antibiofilm Agents*; Springer: 2014, p 273.
- (249) Finkel, J. S.; Mitchell, A. P. Genetic control of *Candida albicans* biofilm development, *Nature Reviews Microbiology*, **2010**, *9*, 109.
- (250) Kaur, S.; Singh, S. Biofilm formation by *Aspergillus fumigatus*, **2013**.

- (251) Martinez, L. R.; Casadevall, A. Cryptococcus neoformans biofilm formation depends on surface support and carbon source and reduces fungal cell susceptibility to heat, cold, and UV light, *Applied and environmental microbiology*, **2007**, *73*, 4592.
- (252) Di Bonaventura, G.; Pompilio, A.; Picciani, C.; Iezzi, M.; D'Antonio, D.; Piccolomini, R. Biofilm formation by the emerging fungal pathogen Trichosporon asahii: development, architecture, and antifungal resistance, *Antimicrobial agents and chemotherapy*, **2006**, *50*, 3269.
- (253) Davis, L. E.; Cook, G.; Costerton, J. W. Biofilm on ventriculo-peritoneal shunt tubing as a cause of treatment failure in coccidioidal meningitis, *Emerging infectious diseases*, **2002**, *8*, 376.
- (254) Cushion, M. T.; Collins, M. S.; Linke, M. J. Biofilm formation by Pneumocystis spp, *Eukaryotic cell*, **2009**, *8*, 197.
- (255) Finkel, J. S.; Mitchell, A. P. Genetic control of Candida albicans biofilm development, *Nature Reviews Microbiology*, **2011**, *9*, 109.
- (256) Kojic, E. M.; Darouiche, R. O. Candida infections of medical devices, *Clinical microbiology reviews*, **2004**, *17*, 255.
- (257) Ramage, G.; Mowat, E.; Williams, C.; Ribot, J. L. In *Pathogenic Yeasts*; Ashbee, R., Bignell, E. M., Eds.; Springer Berlin Heidelberg: 2010, p 121.
- (258) Dongari-Bagtzoglou, A.; Kashleva, H.; Dwivedi, P.; Diaz, P.; Vasilakos, J. Characterization of mucosal Candida albicans biofilms, *PloS one*, **2009**, *4*, e7967.
- (259) Harriott, M. M.; Lilly, E. A.; Rodriguez, T. E.; Fidel, P. L.; Noverr, M. C. Candida albicans forms biofilms on the vaginal mucosa, *Microbiology*, **2010**, *156*, 3635.
- (260) Sudbery, P. E. Growth of Candida albicans hyphae, *Nature Reviews Microbiology*, **2011**, *9*, 737.

- (261) Douglas, L. J. < i> Candida</i> biofilms and their role in infection, *Trends in Microbiology*, **2003**, *11*, 30.
- (262) Wood, T. K.; Bentley, W. E. Signaling in Escherichia coli biofilms, *Biofilm Mode Life*, **2007**, 123.
- (263) Suga, H.; Smith, K. M. Molecular mechanisms of bacterial quorum sensing as a new drug target, *Curr. Opin. Chem. Biol.*, **2003**, *7*, 586.
- (264) Kruppa, M. Quorum sensing and Candida albicans, *Mycoses*, **2009**, *52*, 1.
- (265) Hornby, J. M.; Jensen, E. C.; Lisec, A. D.; Tasto, J. J.; Jahnke, B.; Shoemaker, R.; Dussault, P.; Nickerson, K. W. Quorum sensing in the dimorphic fungus Candida albicans is mediated by farnesol, *Applied and environmental microbiology*, **2001**, *67*, 2982.
- (266) Oh, K.-B.; Miyazawa, H.; Naito, T.; Matsuoka, H. Purification and characterization of an autoregulatory substance capable of regulating the morphological transition in Candida albicans, *Proceedings of the National Academy of Sciences*, **2001**, *98*, 4664.
- (267) Ramage, G.; Saville, S. P.; Wickes, B. L.; López-Ribot, J. L. Inhibition of Candida albicans biofilm formation by farnesol, a quorum-sensing molecule, *Applied and environmental microbiology*, **2002**, *68*, 5459.
- (268) Alem, M. A.; Oteef, M. D.; Flowers, T. H.; Douglas, L. J. Production of tyrosol by Candida albicans biofilms and its role in quorum sensing and biofilm development, *Eukaryotic cell*, **2006**, *5*, 1770.
- (269) Martins, M.; Henriques, M.; Azeredo, J.; Rocha, S. M.; Coimbra, M. A.; Oliveira, R. Morphogenesis control in Candida albicans and Candida dubliniensis through signaling molecules produced by planktonic and biofilm cells, *Eukaryotic cell*, **2007**, *6*, 2429.

- (270) Blankenship, J. R.; Mitchell, A. P. How to build a biofilm: a fungal perspective, *Current opinion in microbiology*, **2006**, *9*, 588.
- (271) Li, F.; Palecek, S. P. Distinct domains of the *Candida albicans* adhesin Eap1p mediate cell-cell and cell-substrate interactions, *Microbiology (Reading, U. K.)*, **2008**, *154*, 1193.
- (272) Shirtliff, M. E.; Peters, B. M.; Jabra-Rizk, M. A. Cross-kingdom interactions: *Candida albicans* and bacteria, *FEMS microbiology letters*, **2009**, *299*, 1.
- (273) Adam, B.; Baillie, G. S.; DOUGLAS, L. J. Mixed species biofilms of *Candida albicans* and *Staphylococcus epidermidis*, *Journal of medical microbiology*, **2002**, *51*, 344.
- (274) Bamford, C. V.; d'Mello, A.; Nobbs, A. H.; Dutton, L. C.; Vickerman, M. M.; Jenkinson, H. F. *Streptococcus gordonii* modulates *Candida albicans* biofilm formation through intergeneric communication, *Infection and immunity*, **2009**, *77*, 3696.
- (275) Jabra-Rizk, M.; Meiller, T.; James, C.; Shirtliff, M. Effect of farnesol on *Staphylococcus aureus* biofilm formation and antimicrobial susceptibility, *Antimicrobial Agents and Chemotherapy*, **2006**, *50*, 1463.
- (276) Kuroda, M.; Nagasaki, S.; Ito, R.; Ohta, T. Sesquiterpene farnesol as a competitive inhibitor of lipase activity of *Staphylococcus aureus*, *FEMS microbiology letters*, **2007**, *273*, 28.
- (277) Hogan, D. A.; Vik, Å.; Kolter, R. A *Pseudomonas aeruginosa* quorum-sensing molecule influences *Candida albicans* morphology, *Molecular microbiology*, **2004**, *54*, 1212.
- (278) Cheng, Y.; McNally, D. J.; Labbé, C.; Voyer, N.; Belzile, F.; Bélanger, R. R. Insertional mutagenesis of a fungal biocontrol agent led to discovery of a rare cellobiose lipid with antifungal activity, *Applied and environmental microbiology*, **2003**, *69*, 2595.

- (279) Mimee, B.; Pelletier, R.; Bélanger, R. In vitro antibacterial activity and antifungal mode of action of flocculosin, a membrane-active cellobiose lipid, *Journal of applied microbiology*, **2009**, *107*, 989.
- (280) Kulakovskaya, T.; Golubev, W.; Tomashevskaya, M.; Kulakovskaya, E.; Shashkov, A.; Grachev, A.; Chizhov, A.; Nifantiev, N. Production of antifungal cellobiose lipids by *Trichosporon porosum*, *Mycopathologia*, **2010**, *169*, 117.
- (281) Shchepin, R.; Hornby, J. M.; Burger, E.; Niessen, T.; Dussault, P.; Nickerson, K. W. Quorum Sensing in *Candida albicans*: Probing Farnesol's Mode of Action with 40 Natural and Synthetic Farnesol Analogs, *Chem. Biol.*, **2003**, *10*, 743.
- (282) Holcombe, L. J.; McAlester, G.; Munro, C. A.; Enjalbert, B.; Brown, A. J.; Gow, N. A.; Ding, C.; Butler, G.; O'Gara, F.; Morrissey, J. P. *Pseudomonas aeruginosa* secreted factors impair biofilm development in *Candida albicans*, *Microbiology*, **2010**, *156*, 1476.
- (283) Ramage, G.; Wickes, B. L.; López-Ribot, J. L. Inhibition on *Candida albicans* biofilm formation using divalent cation chelators (EDTA), *Mycopathologia*, **2007**, *164*, 301.
- (284) Zhang, Y.; Cai, C.; Yang, Y.; Weng, L.; Wang, L. Blocking of *Candida albicans* biofilm formation by cis-2-dodecenoic acid and trans-2-dodecenoic acid, *Journal of medical microbiology*, **2011**, *60*, 1643.
- (285) Braga, P. C.; Culici, M.; Alfieri, M.; Dal Sasso, M. Thymol inhibits *Candida albicans* biofilm formation and mature biofilm, *International journal of antimicrobial agents*, **2008**, *31*, 472.
- (286) You, J.; Du, L.; King, J. B.; Hall, B. E.; Cichewicz, R. H. Small-molecule suppressors of *Candida albicans* biofilm formation synergistically enhance the antifungal activity of amphotericin B against clinical *Candida* isolates, *ACS chemical biology*, **2013**, *8*, 840.

(287) Wang, X.; You, J.; King, J. B.; Powell, D. R.; Cichewicz, R. H. Waikialoid A suppresses hyphal morphogenesis and inhibits biofilm development in pathogenic *Candida albicans*, *Journal of natural products*, **2012**, *75*, 707.

(288) Duo, M.; Zhang, M.; Luk, Y.-Y.; Ren, D. Inhibition of *Candida albicans* growth by brominated furanones, *Appl. Microbiol. Biotechnol.*, **2010**, *85*, 1551.

(289) Varghese, N.; Yang, S.; Sejwal, P.; Luk, Y.-Y. Surface control of blastospore attachment and ligand-mediated hyphae adhesion of *Candida albicans*, *Chemical Communications*, **2013**, *49*, 10418.

(290) CLSI (2008a) Reference method for broth dilution antifungal susceptibility testing of yeasts;

approved standard-third edition; CLSI document M27-A3 . Clinical and Laboratory Standards Institute, Wayne

(291) Pierce, C. G.; Uppuluri, P.; Tristan, A. R.; Wormley, F. L.; Mowat, E.; Ramage, G.; Lopez-Ribot, J. L. A simple and reproducible 96-well plate-based method for the formation of fungal biofilms and its application to antifungal susceptibility testing, *Nature protocols*, **2008**, *3*, 1494.

(292) Ramage, G.; Walle, K. V.; Wickes, B. L.; López-Ribot, J. L. Standardized method for in vitro antifungal susceptibility testing of *Candida albicans* biofilms, *Antimicrobial Agents and Chemotherapy*, **2001**, *45*, 2475.

Curriculum Vitae

Name of the Author: Nischal Singh

Date and Place of Birth: May 28, 1985, Dhanbad, India

Language proficiency: English, Hindi, Punjabi

Degrees Awarded

- Ph.D., Chemistry, Advisors: Prof. Yan-Yeung Luk & Prof. Michael B. Sponsler (Degree expected May, 2015)
- M. Phil., Chemistry, Advisors: Prof. Yan-Yeung Luk & Prof. Michael B. Sponsler (Aug 2009-May 2011)
- Master of Science (M.Sc.), Organic Chemistry (Aug 2006-May 2008)
- Bachelor of Science (B.Sc.), Chemistry (Aug 2003-May 2006)

RESEARCH EXPERIENCE

GlaxoSmithKline Pharmaceuticals, Collegeville, PA (May 2014 – May 2015)

PhD Student Scientist Intern, Anti-Bacterial DPU(Medicinal Chemistry),

Infectious Diseases R&D, Line manager: Dr. Haifeng Cui

Syracuse University, Syracuse, NY (Aug 2009 – May 2014)

Research Assistant, Department of Chemistry,

PhD Program, Advisors: Professor Yan-Yeung Luk & Professor Michael B. Sponsler

TEACHING EXPERIENCE

Syracuse University, Syracuse, NY (Aug 2009 – May 2014)

Teaching Assistant, Department of Chemistry, PhD. Program

PUBLICATIONS

1. **Nischal Singh**, Shetye, G. S.; Zhang, H.; Luk, Y.-Y.; Chemical Signals of Synthetic Disaccharide Derivatives Dominate Rhamnolipids at Controlling Multiple Bacterial Activities. (Submitted *Chem. Biol.*, **2015**)
2. **Nischal Singh**, Shetye, G.; S.; Yan-Yeung Luk; Effective Inhibition of *Candida albicans* Biofilm by Disugar-hydrocarbons (Manuscript in preparation)
3. Shetye, G.; S.; **Nischal Singh**, Gao, X.; Bandyopadhyay, D.; Yan, A.; Luk, Y.-Y., Structures and Biofilm Inhibition Activities of Brominated Furanones for *Escherichia coli* and *Pseudomonas aeruginosa*. *MedChemComm* **2013**, 4, (7), 1079-1084.
4. Shetye, G. S.; **Nischal Singh**, Luk, Y.-Y., Specific Maltose Derivatives Modulate the Swarming Motility of Nonswarming Mutant and Inhibit Bacterial Adhesion and Biofilm Formation by *Pseudomonas aeruginosa*, *ChemBioChem*, **2014**, 15, 1514-1523

PATENT

1. Yan-Yeung Luk, **Nischal Singh**, Shetye, G.; S.; Synthetic Disugar Hydrocarbons as Signaling Analogs for Microbial Control

PRESENTATIONS AND CONFERENCE

1. **Nischal Singh**; Gauri S. Shetye; Guirong Wang; Yan-Yeung Luk, Structure-activity study of polyol-derivatized hydrocarbons in inhibition and dispersion of *Pseudomonas aeruginosa* biofilm, Abstracts of Papers, 245th ACS National Meeting, New Orleans, Louisiana, April 7-11, 2013.

2. Gauri S. Shetye; **Nischal Singh**; Xiang Gao; Debjyoti Bandyopadhyay; Aixin Yan; Yan-Yeung Luk, Inhibition of *P.aeruginosa* and *E.coli* biofilm formation by brominated furanones and the interfering of their quorum sensing pathways. Abstracts of Papers, 245th ACS National Meeting, New Orleans, Louisiana, April 7-11, 2013.

3. Gauri S. Shetye; **Nischal Singh**; Guirong Wang; Yan-Yeung Luk, Polyol-derivatized hydrocarbons as a class of nonmicrobicidal agents for inhibition and dispersion of biofilm formed by *Pseudomonas aeruginosa*, Abstracts of Papers, 245th ACS National Meeting, New Orleans, Louisiana, April 7-11, 2013.

4. Gauri S. Shetye; **Nischal Singh**; Guirong Wang; Yan-Yeung Luk, Non-microbicidal inhibition and dispersion of mucoid *Pseudomonas aeruginosa* biofilm by polyol-derivatized hydrocarbons, Abstracts of Papers, 245th ACS National Meeting, New Orleans, Louisiana, April 7-11, 2013.